Spatial risk assessment of threats to Hector's and Māui dolphins (*Cephalorhynchus hectori*)

J.O. Roberts, D.N. Webber, W.D. Roe,
C.T.T. Edwards, I.J. Doonan

TABLE OF CONTENTS

EXECUTIVE SUMMARY

Roberts, J.O.; Webber, D.N.; Roe, W.T.; Edwards, C.T.T.; Doonan, I.J. (2019). Spatial risk assessment of threats to Hector's/Māui dolphins (*Cephalorhynchus hectori*).

New Zealand Aquatic Environment and Biodiversity Report No. 214. **168 p.**

Risk assessment methodology

A spatial risk assessment of threats was undertaken for Hector's dolphins (*Cephalorhynchus hectori*) and their closely-related sub-species Māui dolphin (*Cephalorhynchus hectori maui*), to inform a revised Threat Management Plan (TMP) for the species. A Bayesian spatial risk model was developed using the spatially-explicit fisheries risk assessment (SEFRA) approach. Under this approach, encounters between animals and lethal threats such as fishing are estimated as a function of their overlap in space, and the probability of death per encounter is estimated from fisheries observer data or other observations of deaths.

The SEFRA risk assessment model for Hector's and Māui dolphins estimated annual deaths (D), the Population Sustainability Threshold (PST) (akin to the PBR), and the annual risk ratio (R) (D/PST) for commercial set net and inshore trawl fisheries (fitting to fishery data) and lethal non-fishery threats (fitting to necropsy observations). Bayesian inference was used to propagate uncertainty with respect to model parameters through to posteriors of D, PST and R.

The SEFRA model estimation of D attempts to account for potential differences in the spatial overlap of total fishing effort and the observed portion of that effort with the estimated spatial density of Hector's and Māui dolphins.

The SEFRA model PST assumed a calibration coefficient (ϕ) value of 0.2, a tuning factor chosen such that $R = 1$ would be consistent with population recovery to and/or stabilisation at an equilibrium population size of approximately 90% of the unimpacted level. Annual deaths and risk were explored for all around New Zealand and within several smaller sub-populations.

Spatial density of Hector's and Māui dolphins

As an input to the SEFRA model, the summer and winter spatial densities of Hector's and Māui dolphins were estimated using a habitat model fitted to Hector's dolphin aerial survey observations and using turbidity and prey species presence as habitat-based predictors. Spatial predictions arising from the habitat model were independently validated using public and commercial fisheries observer sightings, i.e., the public sightings of Māui dolphins and fishery observer sightings of Hector's dolphins, almost perfectly matched the Hector's dolphin habitat model spatial prediction. Boat-based public sightings were also used to estimate the relative density of Māui dolphins in harbours of the West Coast North Island; these estimates were low, consistent with prior information from acoustic monitoring devices.

Population growth potential

This assessment updated the estimate of intrinsic rate of population growth ($r^{\max}$) for Hector's dolphins, based on an invariant with optimal generation time observed across vertebrate species including other cetaceans. The revised estimate for Hector's dolphins ($r^{\max} = 0.050$; 95% CI = 0.029–0.071) is consistent with their estimated age at maturity of 6.9 (95% CI = 5.8 – 8.2), given the relationship observed across other mammals. A slightly lower $r^{\max}$ was estimated for the small population of Māui dolphins (median of 0.045), using an individual-based simulation modelling approach that accounted for demographic stochasticity and lethal alleles. Lower values of $r^{\max}$ may result from increased environmental variability and social Allee mechanisms, but were not included in this risk assessment.

Commercial fisheries deaths and risk

Annual deaths and risk were estimated quantitatively for commercial fisheries only, owing to data limitations with respect to capture rates in recreational fishing. For commercial fisheries, capture event observability priors increased the estimate of deaths that would have been obtained from observed captures only (effectively doubled for set nets). When accounting for this cryptic mortality, model

estimates of commercial fishery annual deaths were consistent with previous spatial risk assessment model estimates for this species. For commercial set net fisheries, the upper 95% credible interval of the risk ratio was above 1 for all sub-populations, except the West Coast South Island. However, the median value of risk ratio was below 1 for all except for the east and north coasts of the North Island (risk ratio of 1.61) and was 0.28 for the extent of the west coast of the North Island where Māui dolphin occur.

As such, the best estimates of commercial fishery deaths for all sub-populations would be insufficient to prevent population recovery to 90% of the unimpacted level. However, uncertainty in model inputs, including capture observability rate, pushed the upper estimate of annual deaths above this threshold. Also, greater levels of risk from commercial set netting may be experienced by smaller local populations (i.e., at scales smaller than the identified sub-populations) on the east coast of the South Island, including: the Kaikoura coast, Pegasus Bay north of Banks Peninsula, and the southern Canterbury Bight. For inshore trawl fisheries, the upper 95% credible interval of the risk ratio was below 1 for all sub-populations.

Options for increasing the precision of commercial set net and trawl fisheries risk estimates are discussed, including the development of more informative priors for the probability that capture events were observable, and targeted increases in fishery observer coverage.

Non-fishery deaths and risk

A summary of necropsy records found that toxoplasmosis, caused by infection with *Toxoplasma gondii* oocysts, was the primary non-fishery cause of death for the recovered sample of 55 Hector's and Māui dolphins and seven out of nine cases were mature females. Other non-fishery causes of death included non-infectious diseases, brucellosis, predation and maternal separation. With the exceptions of toxoplasmosis and fishery bycatch, no other anthopogenic causes of death were identified in necropsied individuals.

The SEFRA modelling approach was extended to estimate non-fishery deaths. The model first estimated annual non-fishery deaths based on estimates of population size and non-calf survival. The model then partitioned these based on the proportional causes of death of necropsied individuals. One model run assumed that all non-fishery causes of death had an equal detection probability, whereas the 'predation sensitivity' run assumed a 10-fold reduction in the detection probability of predation deaths, reducing the proportion of non-fishery deaths that were attributed to toxoplasmosis. The coastal spatial density of *Toxoplasma gondii* oocysts was estimated and used to partition toxoplasmosis deaths by sub-population, based on the degree of spatial overlap with Hector's and Māui dolphins.

The median risk ratios for toxoplasmosis exceeded 1 for all sub-populations including Māui dolphins. This was also true for all assessment areas except the North Coast of the South Island for the predation sensitivity run. This suggests that toxoplasmosis has impacted on the status of Māui dolphin and South Island Hector's dolphin populations. However, we stress that model risk ratio estimates for toxoplasmosis and other non-fishery causes of death will be biased if the proportional causes of death of necropsied individuals are not representative of deaths in the wider population. An assessment of potential sources of bias would be informed by increased carcass recovery rate for this species, which would also allow more precise estimates of non-fisheries risks.

Assessment of other threats

Spatial threat intensity was estimated for other anthropogenic threats including recreational netting, oil spill risk and aquaculture. Recreational netting had greatest overlap with Hector's/Māui dolphins along the Taranaki/Kapiti coast; oil spill risk overlap was greatest north of Banks Peninsula; aquaculture overlap was greatest on the north coast of the Sorth Island; and the estimated overlap with *T. gondii* cysts was greatest near to the Waikato River on the west coast of the North Island, overlapping with the known range of Māui dolphins.

Data limitations meant that some potentially key threats, such as the effects of seismic disturbance, and climate change effects on physical habitat and prey availability, were not addressed quantitatively. Future research can address these limitations and others identified by this assessment report.

1. INTRODUCTION

1.1 Background

The Hector's dolphin (*Cephalorhynchus hectori*) is one of four species of small dolphins belonging to the genus *Cephalorhynchus* and is endemic to New Zealand (NZ) (the other related species are: Commerson's dolphin—*C. commersonii*, Chilean dolphin—*C. eutropia* and Heaviside's dolphin—*C. heavisidii*). There are two recognised sub-species of Hector's dolphin: *C. h. hectori*—which is distributed all around the South Island and the genetically distinct *C. h. Māui* (common name Māui dolphin)—which is currently only observed on the west coast of the North Island (Baker et al. 2016a; Hamner et al. 2012; MacKenzie & Clement 2016). The two sub-species are thought to have diverged towards the end of the last ice age, around 15–16 000 years ago (Pichler 2001). The latest population size estimate for South Island Hector's dolphins is 14 849 individuals (95% confidence interval (c.i.) 11 923–18 492) (MacKenzie & Clement 2016), compared to the latest Māui dolphin estimate of 63 individuals excluding calves (95% c.i. 57–75) (Baker et al. 2016a).

The South Island Hector's dolphin (hereafter referred to as 'Hector's dolphin') is currently listed as Nationally Endangered by the NZ Threat Classification System (NZTCS) and as Endangered by the International Union for Conservation of Nature (IUCN) Red List of Threatened Species. These classifications are based on: moderate population size; a population decline exceeding 50% over three generations (39 years) (Baker et al. 2016b; Reeves et al. 2013a), estimated by a population viability analysis (PVA) (Slooten 2007); and ongoing mortality relating to interactions with commercial fisheries. Māui dolphin are currently listed as Nationally Critical by the NZTCS and Critically Endangered by the IUCN Red List on the basis of very small population size and an estimated past and future population decline exceeding 80% over three generations (Baker et al. 2016a; Baker et al. 2016b; Currey et al. 2012; Hamner et al. 2014; Reeves et al. 2013b).

The management of threats to Hector's and Māui dolphins is guided by a Threat Management Plan (TMP), which was last updated for Hector's dolphins in 2007 (MFISH/DOC 2007) and for Māui dolphins in 2012 (MPI/DOC 2012). These TMPs were informed by risk assessments of anthropogenic and natural threats (Currey et al. 2012; MFISH/DOC 2007). The previous multi-threat risk assessment for Māui dolphins used an expert panel to estimate threat-specific annual deaths for a range of perceived key threats to this sub-species, relative to a Potential Biological Removal (PBR) (Currey et al. 2012). The assessment summarised by Currey et al. (2012) estimated that approximately 95% of human-induced Māui dolphin mortalities were caused by fishing (commercial, recreational, customary and illegal fishing combined) with the remainder attributed to non-fishery threats (mining and oil activities, vessel traffic, pollution and human-caused disease). Estimated annual mortalities resulting from commercial fisheries were estimated to have a PBR risk ratio of greater than 50 and, taken together with other human threats, would result in a 96% probability of future population decline (Currey et al. 2012). The 2007 risk assessment addressing Hectors and Māui dolphins considered a range of threats that might potentially impact the three genetic sub-populations (i.e., west coast, south coast and east/north coasts of the South Island) (Hamner et al. 2012), including incidental mortality in commercial and recreational set nets and other human and natural threats and was primarily based on a qualitative review of the available literature and data (DOC/MPI 2007).

The scope and methods of the risk assessment of threats to Hector's and Māui dolphins has evolved with:

- The completion of spatially comprehensive and methodologically rigorous aerial surveys of Hector's dolphins, to estimate both the population size and spatial distribution of the dolphins, and to inform the parameterisation of spatial habitat models (e.g., MacKenzie & Clement 2016).
- Changes in other data availability (e.g., longer time series of fisheries information, more comprehensive necropsy methods, and improvements to habitat-based information);

- Advances in scientific approaches to risk assessment (e.g., the development of the SEFRA method; see below) (Sharp 2018); and
- New information with respect to the key anthropogenic and natural threats (e.g., the relatively recent discovery that toxoplasmosis is a major cause of death for Hector's and Māui dolphins) (Roe et al. 2013).

In addition, the spatial distribution and intensity of threats impacting on Hector's and Māui dolphins has changed, e.g., in response to the implementation of commercial set net and trawl fishery restrictions, and will continue to change with the development of existing and new marine industries, or with climate change effects on prey and the physical habitat. Spatial risk assessment tools are increasingly being used to undertake risk assessment and to inform the potential spatial management of ongoing and emerging threats.

1.2   Spatial risk assessment

Spatial risk assessments can be advantageous when either the threat or the receiving population are heterogenous in space. Assuming that a species' vulnerability per encounter to a particular threat is constant in space, the proportion of their population affected by a threat (or the received threat level for diffuse threats) will vary with the degree of spatial overlap. Assessments that accurately derive the spatial overlap between threats and receiver species are useful for spatial planning.

A further application of spatial risk assessment relates to the estimation of threat impacts. Where the information about mortality rate is spatially-biased (e.g., if commercial fishery observer records are predominantly in areas of low fishing effort relative to the subject species and information from high overlap areas is lacking) then the estimation of threat-specific deaths will ideally account for this (i.e., by attributing greater proportional mortality rate in those locations with greater overlap and *vice versa*).

Previous spatial risk assessments for Hector's and Māui dolphins have focussed on direct commercial fishery-related mortalities. The first spatial commercial fishery risk assessments developed for Hector's and Māui dolphins (e.g. Martien et al. 1999; Burkhart & Slooten 2003; Slooten 2007; Slooten & Dawson 2010) used New Zealand statistical fishery areas as the basic spatial unit (i.e. fishing effort and Hector's/Māui dolphin population size was aggregated within these areas). These assessments estimated the regional (e.g. North Island, East Coast and West Coast) population effects of commercial set net mortality when assuming logistic population growth (for a given intrinsic population growth rate (r^{max}) and carrying capacity (K the derived population size in 1970)). As with later spatial risk assessments, a vulnerability parameter was estimated (called "entanglement rate" or "M" by these studies) from which annual mortalities were estimated by statistical area given annual effort (Martien et al. 1999; Burkhart & Slooten 2003; Slooten 2007; Slooten & Dawson 2010). These assessments estimated the Hector's dolphin population size to be 27% of the 1970 population size (Slooten & Dawson 2010); and 7% of the 1970 population size for the North Island population (including Māui dolphins) (Slooten 2007).

In these earlier spatial assessments, the vulnerability parameter was estimated outside of the model and was based on the relatively short time series of commercial fishery observer reported capture rate that was available at the time; and on historical estimates of Hector's and Māui dolphin population size from a combination of boat and aerial surveys (Dawson et al. 2004; Slooten et al. 2004; Slooten et al. 2006). These historical estimates were much lower than later estimates from aerial surveys, which counted much higher densities of Hector's dolphins and extended further off-shore (e.g., MacKenzie & Clement 2016).

The Bayesian multi-species marine mammal risk assessment by Abraham et al. (2017) used an early adaptation of the spatially-explicit fishery risk assessment (SEFRA) method to estimate commercial fishery-specific annual deaths and risk ratio (deaths relative to a population sustainability threshold (PST)) for an array of marine mammal species occurring around New Zealand, including Hector's and Māui dolphins. Some key differences in the methods and inputs used by Abraham et al. (2017) relative to previous spatial risk assessments for Hector's and Māui dolphins include:

- The calculation of spatial overlap that was continuous in space (though note that the model was fitted to spatially-aggregated dolphin captures and overlap);
- The estimation of the vulnerability parameter during model fitting;
- Updated abundance and spatial density estimates (from aerial surveys reported by MacKenzie & Clement 2016); and
- Updated biological inputs, e.g. $r^{\max}$ (Abraham et al. (2017) used expert knowledge applying the Delphi method) (Linstone & Turoff 2002).

The assessment by Abraham et al. (2017) obtained commercial fishery risk ratios of 0.45 (95% credible interval (CI) = 0.18–0.92) for Hector's dolphins and 0.47 (0.00–1.33) for Māui dolphins across all commercial set net and trawl fisheries between 2012–13 and 2014–15 (i.e. below the PST), primarily driven by deaths in commercial set nets. Note, however, that the multi-species assessment of Abraham et al. (2017) used a default calibration coefficient (ϕ) value of 0.5 in the definition of the PST, corresponding to a median population outcome at 75% of the un-impacted status. Following stakeholder consultation, the default ϕ for this TMP risk assessment was set instead at 0.2, corresponding to a median population outcome at approximately 90% of un-impacted status. The choice of ϕ is a policy decision with a direct scalar effect on the corresponding estimate of PST and risk. As a consequence, for comparison with the risk scores estimated here, the risk scores of Abraham et al. (2017) would need to be multiplied by a factor of 2.5.

1.3 Research objectives

A spatial risk assessment of anthropogenic and natural threats to Hector's and Māui dolphins was undertaken to inform the development of a revised TMP for the species. The primary research objectives for this project were to:

1. Estimate the summer and winter spatial density of Hector's and Māui dolphins;

2. Map spatial fishing effort and estimate spatial threat intensity of potential non-fishery threats to Hector's and Māui dolphins;

3. Calculate the spatial overlap between Hector's and Māui dolphins and spatially resolved non-fishery threats;

4. Estimate the intrinsic population growth rate ($r^{\max}$) for Hector's and Māui dolphins; and

5. Apply the SEFRA method to estimate fisheries and spatially-resolved non-fishery threat risk (with uncertainty) to Hector's and Māui dolphins, using new information from research under the objectives above, including at a regional sub-population level.

The next sections set out the overall risk assessment methodology and detailed methods used to achieve these research objectives.

2. RISK ASSESSMENT METHODOLOGY & SCOPING OF THREATS

2.1 Risk assessment methodology

Threat-specific risk

The risk assessment method varied by threat depending on information available with respect to lethality and the spatial intensity of the threat:

1. **Spatially-explicit risk** was estimated for threats for which there was information available for estimating a spatial intensity <u>and</u> where necropsy information showed that the threat was a verified cause of death;

2. **Relative spatial overlap** was estimated for spatially-resolved threats that <u>were not</u> a verified cause of death from the necropsy information; and
3. **Qualitative literature review** for all other threats within scope.

The risk model used to estimate spatially-explicit risk is an extension of the spatially-explicit fisheries risk assessment (SEFRA) approach, incorporating non-fishery causes of death (Sharp 2018). The SEFRA method is briefly described in the next sub-section with detailed methods in Section 4.5.

SEFRA method

The spatial risk model was based on the SEFRA method (Sharp 2018), in which risk is expressed as a ratio between a threat-specific estimate of deaths in the numerator and a 'Population Sustainability Threshold' (PST) in the denominator. The rate at which animals encounter the threat is estimated as a function of the spatial overlap between the threat intensity and the animal density in space, and the vulnerability (probability of death per encounter), is estimated from observed mortality rates. The PST was inspired by the Potential Biological Removal (PBR) approach used internationally for identifying anthropogenic mortality thresholds for wild marine megafauna populations (Wade 1998). The SEFRA method was deemed by an independent review initiated by Fisheries New Zealand (previously Ministry for Primary Industries) to be a high-quality tool for spatial risk assessment (Lonergan et al. 2017). As with the PBR approach, the SEFRA method estimates annual threat-specific mortalities and relates this to a mortality threshold (PST instead of PBR)—the maximum number of annual deaths that a population unit can sustain without impacting on a population recovery objective. The PBR equation for estimating the PBR annual mortality threshold is

$$PBR = N^{\min} \frac{1}{2} r^{\max} F_R$$

where $N^{\min}$ is the minimum population estimate, $r^{\max}$ is the intrinsic population growth rate (achieved in the absence of density dependent effects), and F_R is the recovery factor, which accounts for uncertainty with respect to the estimation of input parameters and adverse conservation status. The equivalent SEFRA equation for estimating the Population Sustainability Threshold (PST) has the same structure as the PBR calculation

$$PST = N \frac{1}{2} r^{\max} \phi$$

where F_R (in the PBR calculation) is replaced by ϕ, a calibration coefficient that can be tuned to achieve user-specified population-based management goals and account for alternative assumptions of the shape of population growth in response to density dependence; and where $N^{\min}$ is replaced by N, the estimate of total population size.

In addition to the replacement of F_R by ϕ and $N^{\min}$ by N, another key difference from the standard PBR approach is that the estimation of annual deaths (D) by SEFRA models (referred to as "Annual Potential Fatalities" or "APF" by previous SEFRA implementations, e.g. Abraham et al. 2017) is spatially-explicit—i.e., it accounts for spatial overlap when estimating threat-specific threats from information on capture rate. This is desirable when the spatial distribution of total fishing effort and the observed portion of that effort have a different degree of overlap with the assessed species, as may occur when the level of observer coverage is low. This improves on the standard implementation of the PBR approach (e.g. Hayes et al. 2018), which does not routinely account for spatial overlap when using observer data to estimate annual deaths.

The risk ratio (R) is then calculated as

$$R = \frac{D}{PST}$$

where R expresses anthropogenic threat-specific deaths (D) as a proportion of the threshold (PST) and is presented as a posterior probability distribution, propagating uncertainty in both D and the PST.

All SEFRA modelling to date including this assessment has been Bayesian (not typically the case for PBR assessments), such that uncertainty with respect to the estimation of input parameters is propagated through to the estimation of both annual deaths and the PST and, then, through to the risk ratio. For example, PBR assessments take a precautionary approach with respect to population size only, by using a precautionary low value for population size ($N^{\min}$), whereas Bayesian SEFRA models sample from a posterior distribution of N, propagating uncertainty in this quantity through to the risk ratio. The non-Bayesian PBR approach produces a point estimate of risk that does not include information about uncertainty with respect to this value. Bayesian SEFRA model posteriors of risk include uncertainty with respect to D and the PST. This allows users to define a threshold probability of R exceeding 1, given uncertainty with respect to model outputs and the management objectives for the assessed population.

SEFRA inputs

The various information sources used in the SEFRA calculation of risk ratio (R) are shown in Figure 1. Detailed methods for estimating annual threat-specific deaths (D) are given in Section 4.5. This calculation requires information with respect to:

- The spatial abundance of the study species;
- Spatially-resolved mortality rate information (e.g., commercial fisheries observer records) pertaining to a threat; and
- Total spatial intensity of a threat (e.g., all commercial set net fishing effort records, including observed <u>and</u> unobserved), so that mortality rate information from above can be used to estimate the total number of deaths relating to a threat given spatial overlap.

In addition, population size and annual survival rate information can be used to constrain model runs that estimate annual deaths exceeding what is possible given the demographic information.

The derivation of PST requires information with respect to:

- Intrinsic population growth rate ($r^{\max}$)—this assessment has estimated population specific $r^{\max}$ to use for Hector's and Māui dolphin populations (described in Appendices 2 and 3);
- A specified population reference outcome to inform the choice of the calibration coefficient (ϕ). The reference outcome is expressed in terms of recovery to and/or stabilisation of the impacted population at a defined proportion of the un-impacted population state, at equilibrium and; and
- Estimates of total population size (note that this is also used for estimating D).

All of these inputs were estimated/updated by the risk assessment for Hector's and Māui dolphins, with the exception of: total population size (N) for which the latest approved population size estimates were used (e.g. MacKenzie & Clement 2016); and the calibration coefficient (ϕ), for which Fisheries New Zealand specified a base case value (0.2), consistent with population recovery to at least 90% the unimpacted population state under a default assumption of linear density dependence (Darryl MacKenzie unpublished data).

The SEFRA and PBR approaches do not necessarily require information on recent population status and trajectory and are useful when these are poorly understood for a study/species or population.
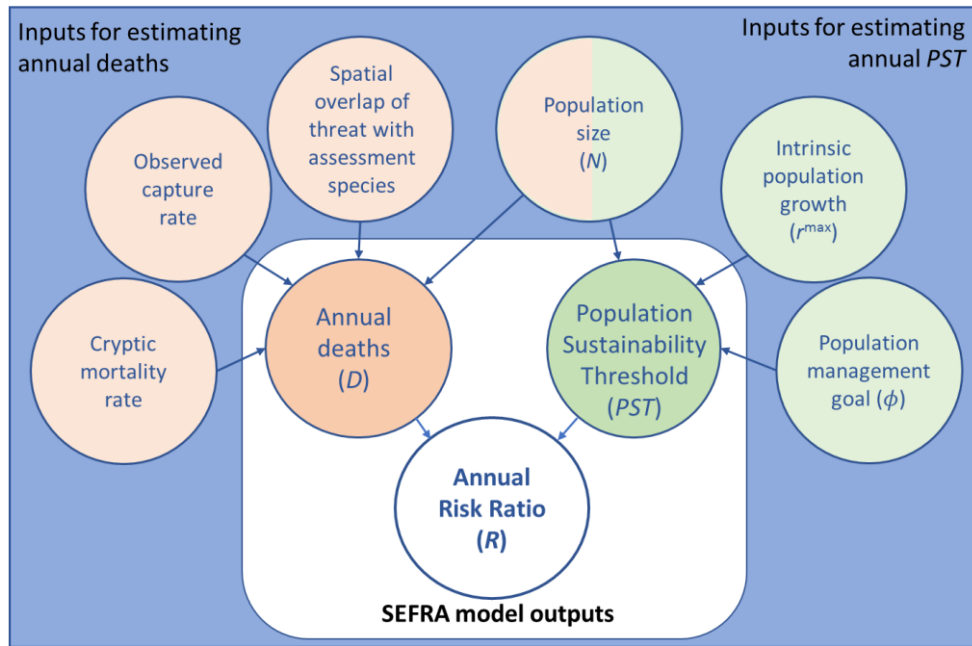
Figure 1: Conceptual diagram of spatially-explicit risk model approach and data inputs. Note that the population size is used in both the derivation of annual deaths and the Population Sustainability Threshold (PST).

Extension of SEFRA to include non-fishery threats

The updated risk assessment for Hector's and Māui dolphins customised the SEFRA approach to incorporate specific non-fishery threats. Detailed methods are given in Section 4.5. Briefly, this was achieved by simulating the total annual deaths (from demographic assessments), subtracting model estimated commercial fisheries deaths, and partitioning the remainder using proportional cause of death information from necropsy records. The total number of necropsied individuals (using consistent methods) was small and the estimation of causes of death relied on the simplifying assumption that relative detection rates for different non-fishery causes of death were equivalent (although a simple sensitivity was trialled to assess relative detection rate effects on model outputs). These deficiencies are noted at the relevant points in the analysis and also with respect to future research needs.

Spatial overlap was also used to estimate the relative proportional causes of death for each subpopulation. Note that spatial threat intensity for non-fishery threats had to be estimated (rather than being assumed known, as it is for commercial fisheries).

Relative spatial overlap

For non-lethal threats (potentially including lethal threats that have not yet appeared in the necropsy records) that can still be resolved spatially, an alternative approach was taken. For these threats, spatial overlap was presented in two different ways:

1. Mapping of relative spatial overlap between spatial dolphin abundance and spatial threat intensity. This will highlight areas with a high density of Hector's/Māui dolphins and high threat intensity (i.e. if the population density is low, as it will be for Māui dolphins given low overall population size then they will be less visible in spatial overlap plots than high density Hector's dolphin areas, given an equivalent threat intensity); and
2. Relative overlap statistic scaling for population size. This will highlight populations for which the threat intensity is high in the locations that dolphins occur (i.e. for the example given above the relative overlap statistic by sub-population will be similar, given equivalent threat levels).

Note that in these instance, since the absolute threat intensity is not used to estimate annual deaths (using overlap) the threat intensity units do not have inherent meaning in this assessment. The degree of spatial overlap is only *relative* and cannot be translated into deaths until information is available to estimate threat-specific vulnerability, i.e., the relationship between threat exposure and probability of death.

Population units

The threat-specific risk ratios estimated by the SEFRA model can be disaggregated at any user-defined spatial scale, e.g. corresponding to a presumed sub-population definition. The SEFRA model can estimate risk ratios across the entire area inhabited by Hector's dolphins, or for a very small sub-population (i.e. for which there is good evidence for demographic independence with neighbouring areas). For this assessment, we estimated SEFRA risk ratios separately for Hector's and Māui dolphins. In addition, we produced area-disaggregated risk ratios and relative spatial overlap statistics for smaller sub-populations of Hector's dolphins, according to the polygons depicted in Figure 2. These areas were agreed with the Aquatic Environment Working Group and with the Expert Panel of the July 2018 workshop for this assessment (Taylor et al. 2018).

Assessment seasonality & timeframe

Spatial model inputs (including spatial abundance of dolphins and spatial threat intensity) were disaggregated into summer and winter periods defined as 1 November to 31 April and 1 May to 31 October, respectively. The defined summer period includes the calving season of Hector's and Māui dolphins, from November to February (Slooten 1991).

The spatial abundance of Hector's and Māui dolphins (and spatial intensity of some threats) were primarily estimated from information collected since 2008 (consistent with the period of comprehensive and consistent necropsy methods). Note that the SEFRA model was used to estimate commercial fishery-specific risk across a wider timeframe (since the early 1990s). No assumptions were made regarding potential changes in the spatial distribution or overall abundance of Hector's or Māui dolphin populations through time.

Process of risk assessment development

All component inputs to this risk assessment were developed separately and evaluated prior to the model being fitted and run, to minimise the potential for bias and ensure independent review of each component set of inputs on its own merits. To this end, inputs were reviewed in three sets: first the biological and demographic input parameters; second the spatial characterisation of threats; and, finally, the estimation of seasonally-resolved spatial dolphin density. All inputs were reviewed on multiple occasions by members of the Aquatic Environment Working Group and at an assessment workshop at which the assessment was reviewed by an independent expert panel (Taylor et al. 2018), and methods revised according to reviewer suggestions. Model estimated risk ratios and relative spatial overlap plots/statistics were not produced until the development of all model inputs was finalised or well-advanced. Subsequently to the review workshop, methods were revised according to reviewer suggestions.

2.2   Scoping of threats

Threats were considered for this risk assessment by the following criteria:

1. Threats shortlisted by 2013 Māui dolphin TMP risk assessment (Currey et al. 2012);
2. Threats screened for management by 2008 Hector's/Māui dolphin TMP risk assessment (MFISH/DOC 2007);
3. Threats that have emerged since the latest TMP risk assessment; and
4. Threats that may have been overlooked by previous TMP risk assessments.

Threats addressed by this risk assessment are listed in Table 1 along with the respective risk assessment method used for that threat.

Table 1: Threats addressed by this risk assessment and respective risk assessment method used.

Threat	Basis for inclusion in risk assessment	Risk assessment method used
Commercial fishing – set net & inshore trawl*	Shortlisted by 2013 TMP risk assessment	Estimation of spatially-explicit deaths and risk ratio using extension of SEFRA method
Toxoplasma gondii infection (Toxoplasmosis)*	Identified since the 2013 TMP risk assessment—the main non-fishery cause of death in the sample of necropsied individuals (Roe et al. 2013)	
Predation mortality	Not an anthropogenic threat, although a known cause of death and a spatially-resolvable threat	
Recreational netting	Shortlisted by 2013 TMP risk assessment	Relative spatial overlap
Aquaculture	Screened for management by 2008 TMP risk assessment	
Oil pollution risk	Shortlisted by 2013 TMP risk assessment	
Oil and gas seismic survey noise disturbance	Shortlisted by 2013 TMP risk assessment	Relative spatial overlap and qualitative assessment of received noise (West Coast North Island, WCNI, only)
Vessel traffic noise disturbance	Shortlisted by 2013 TMP risk assessment	
Climate effects on prey availability	Not addressed explicitly by previous TMP risk assessments for this species, although availability of main prey is known to be temporally dynamic	Qualitative review of the literature
Indirect effects of fishing on prey availability	Not addressed explicitly by previous TMP risk assessments for this species, although availability of main prey is known to be temporally dynamic	
Brucella spp infection (Brucellosis)	A non-fishery cause of death in the sample of necropsied individuals (Roe et al. 2013).	
Ship strike	Screened for management by 2008 TMP risk assessment	
Pollution (pesticides & metals)	Shortlisted by 2013 TMP risk assessment	
Seabed mining (noise & plume)	Shortlisted by 2013 TMP risk assessment	
Coastal development	Screened for management by 2008 TMP risk assessment	
Commercial tourism	Screened for management by 2008 TMP risk assessment	
Scientific research	Screened for management by 2008 TMP risk assessment	
Small population (Allee) effects	Not addressed explicitly by previous TMP risk assessments for this species, though potentially an issue for small sub-populations such as Māui dolphins	Adjustment of spatial model input parameters, informed by individual-based modelling

* Note that separate assessments by Roberts et al. (2019) and Cooke (2019) have assessed the effects of commercial fishing mortality and toxoplasmosis on population trajectory.

3.   STRUCTURE OF ASSESSMENT REPORT

This risk assessment has updated numerous inputs with respect to Hector's and Māui dolphins and their threats, including:

- The life history and spatial abundance of Hector's and Māui dolphins;
- Updated spatially-resolved commercial fisheries effort data and fisheries observer data
- Information with respect to commercial fishery and non-fishery causes of death; and
- The spatial intensity of an array of potential threats.

For many of these, the assessments that generated the respective risk model inputs (including data inputs, methods and results) are provided in appendices at the end of the risk assessment document (see the Table of Contents) and cross-referenced at relevant points in the text.

The details of analyses producing core inputs to the overall risk assessment are described in the main body of the report, including:

- The updated summary of necropsy information with respect to cause of death and maturity stage (Sections 4.1 and 5.1); and
- The estimation of the seasonal spatial abundance of Hector's and Māui dolphins (Sections 4.2 and 5.1).

Methods and results with respect to the estimation of spatial threat intensity and spatial overlap with threats are also presented in the main body of the report (Sections 4.3, 4.4 and 5.2), along with the methods used to develop the spatial risk model (Section 4.5) and risk model outputs (Section 5.3).

All aspects of the assessment including the various risk assessment inputs as well as the risk assessment model and outputs are addressed by the discussion and conclusions (Sections 6 and 6.7).

4.   METHODS

4.1   Necropsy observations

Necropsy results were retrieved from the School of Veterinary Science (SoVS) Pathobiology database, which holds records of necropsy investigations conducted at Massey University. A database search was conducted for Hector's and Māui dolphins received between 2007 and 2018. The provenance and processing of the recovered dolphins is described briefly below.

Recovery of dolphins

The SoVS has an ongoing contract with the New Zealand Department of Conservation (DOC), to conduct pathological investigations on Hector's and Māui dolphins found dead around the New Zealand coastline. Beachcast (stranded) Hector's and Māui dolphins reported to the DOC hotline are located and assessed by regional DOC field staff. If the dolphin is determined to be in a suitably preserved state for necropsy, arrangements are made for transport to the necropsy facility at SoVS. In some cases, due to requirements of the transport company, the dolphin is frozen prior to shipping and, when possible, are processed within 24 hours of receipt at SoVS.

Necropsy protocol

Dolphins are thawed prior to necropsy. Necropsies are conducted by a board-certified veterinary pathologist, according to standard necropsy protocols. The state of preservation (fresh, or mild/moderate/severe decomposition) is noted, along with body condition, based on presence or absence of a 'neck' (dorsal convexity behind the head, indicating loss of muscle mass) and curvature of the lumbar muscles. Dolphins are weighed and a standard set of morphometric measurements are

collected. A small full thickness sample of skin is collected, placed into 70% ethanol and stored for later submission to Auckland University for genetic analysis. Four to five teeth from the middle of the mandibular arcade are excised and saved into 70% ethanol to be stored for subsequent ageing. The external surface of the body is examined for lesions such as net marks, wounds and scavenger damage. Blubber depth is measured (dorsal, lateral and ventral) at an incision made at the level of the cranial aspect of the dorsal fin. The body is flensed and any subcutaneous bruising is noted. The thoracic and abdominal cavities are opened and internal organs are examined for lesions. Representative samples of organs and lesions are preserved in 10% neutral buffered formalin for histopathology. Samples for ancillary testing (e.g. molecular diagnostics) are also collected and frozen at -20ºC.

For the purposes of this project, the following data were extracted from the Pathobiology database: identification numbers ('H' number, post mortem number, MUCIC number), age class, sex, cause of death, standard length, and state of preservation. Location of the body and hence subpopulation was determined from the DOC stranding database. For each case, an 'investigation classification/confidence' level was established to indicate the degree of confidence in the diagnosis. Levels were classified as: 'full' (adequate tissues and state of preservation to allow reliable histological diagnosis and diagnostics sufficient to determine cause of death); 'intermediate' (moderate decomposition hampering diagnostics or adequate range of tissues not examined); and 'poor' (significant scavenging or decomposition making diagnosis unreliable). Animals with a 'poor' level of confidence were excluded from further analysis.

Cause of death

The cause of death recorded in the database for these dolphins was determined by experienced veterinary pathologists based on consideration of the history, gross necropsy findings, and histological evaluations, according to diagnostic convention. Where possible, the underlying cause for animals diagnosed with 'disease' was further investigated using histological, microbiological and/or molecular testing.

Individuals known or suspected to have died as a result of entanglement in fishing gear were classified into one of three categories, using a method based on that described by Jepson et al. (2013):

1. **'known bycatch'**; when a dolphin was reported to DOC as having been found dead in a net;
2. **'probable bycatch'**; animals that had suspected net marks, were in good body condition and had no other likely cause of death.; or
3. **'possible bycatch';** there were no convincing signs of entanglement, no other diagnosed cause of death despite full investigation, and one or more other changes suggestive for (but not diagnostic of) entanglement.

For calves, a diagnosis of **'maternal separation'** was made where no other likely cause of death was apparent; in this case, death was attributed to a combination of metabolic disturbances and hypothermia associated with lack of suckling. The underlying cause of the 'Maternal separation' cannot be further defined, but theoretically could include physical separation of the pair during a storm event, death of the mother, or failure to suckle due to maternal or neonatal factors.

An 'open' diagnosis was assigned when the state of the body (decomposition, scavenging, or a combination of both) precluded diagnosis.

Sex and maturity stage

Determination of sex was based on examination of the reproductive organs. Where decomposition or scavenging made this assessment impossible, sex was recorded as unknown. Age class was established using standard length measurements and examination of the reproductive organs, as described by Slooten (1991). For females, necropsy reports were reviewed to determine the state of the ovaries as either 'smooth' (small ovaries with a smooth external surface and no evidence of corpora lutea or corpora albicantia) or 'active' (corpora present). Females with smooth ovaries were considered to be

sexually immature (subadult). For sexually mature (adult) females, evidence of current or previous pregnancy was established based on presence of an embryo or fetus within the uterus, or the presence of linear striations on the serosal surface of the uterus. For males, age class was established as either subadult or adult, based on summed testicular mass and testicular histology. Animals were defined as 'juveniles' based on immaturity plus morphological features such as non-erupted teeth, fetal folds, lateral papillae on the tongue, and standard length (lengths shorter than 119 cm indicating age less than two years (Slooten, 1991)).

4.2   Spatial abundance of Hector's and Māui dolphins

Methodology for estimating seasonal spatial abundance

The primary spatial abundance information for predicting the coastal abundance of Hector's and Māui dolphins came from a series of seasonal (summer and winter) aerial line-transect surveys for estimating the abundance and spatial distribution of Hector's dolphins, conducted around the South Island of New Zealand between 2010 and 2015 (MacKenzie & Clement 2014; MacKenzie & Clement 2016). A seasonal habitat preference model was then fitted to aerial survey observations for respective survey transect segments related to spatially comprehensive habitat variable layers. Wherever possible, the relationship between dolphin density and habitat conditions was estimated based on time-specific observations at or near the moment of the observation. For example, patterns of turbidity are known to affect dolphin distributions and satellite-derived turbidity estimates can be obtained for any time period since 1997 (e.g., NASA 2019). So, in the model fitting stage, the aerial survey observations could be related to ocean turbidity patterns in or close to the month in which each survey transect was flown. Only subsequently, in the prediction phase, were long-term seasonally-averaged environmental conditions used to predict average dolphin densities over time.

The habitat model was used to generate seasonal (summer or winter) spatial abundance of Hector's and Māui dolphins around all New Zealand, to a bathymetric depth of up to 250 m. This was deeper than the core range of the species (over seafloor ranging from 0–40 m depth) and the deepest locations where Hector's dolphins were observed by aerial surveys (200 m off the west coast and 150 m off the east coast of the South Island) (MacKenzie & Clement 2014; MacKenzie & Clement 2016).

The use of the Hector's dolphin habitat model for predicting the coastal distribution of Māui dolphins and North Island Hector's dolphins assumed that the habitat preference was the same across the wider species. The two sub-species are thought to have diverged towards the end of the last ice age, around 15–16 000 years ago (Pichler 2001), which is a limited timescale for the development of differential habitat preferences. Although based on a very small sample of individuals, the dietary composition of two Māui dolphins were dominated by ahuru (*Auchenoceros punctatus*) and sole (*Pelthoramphus sp.*), which were both also key prey species for Hector's dolphins (Miller et al. 2013)—suggesting that the habitat preferences of the two sub-species are still quite similar.

A habitat-based prediction was preferred to raw or geographically-smoothed spatial abundance because:

- Including a geographic term in the habitat model would have precluded meaningful predictions of Hector's/Māui dolphin density around the North Island, i.e., outside of the spatial extent of the South Island aerial survey (MacKenzie & Clement 2016); and
- The spatial abundance of Hector's dolphins is likely to change through time in response to a temporally-dynamic habitat.

Environmental conditions inside harbours of the WCNI were outside the bounds of habitat conditions spanned by the South Island aerial survey data used to parameterise the habitat model. As such, the relative spatial density of Māui dolphins in the harbours of the WCNI was estimated using a separate habitat preference function fitted to validated public sightings and an aerial survey of spatially-resolved boat density as a proxy for spatial public sighting 'effort' (see below), related to locational/habitat-based variables.

The combined habitat preference-based coastal/harbour spatial abundance prediction for Hector's and Māui dolphins was rescaled using population size estimates for rescaling stratum areas deemed to be most useful for management (Figure 2 and Table 2). The stratum area boundaries and associated population sizes were applied, as advised by the Fisheries New Zealand Aquatic Environment Working Group.
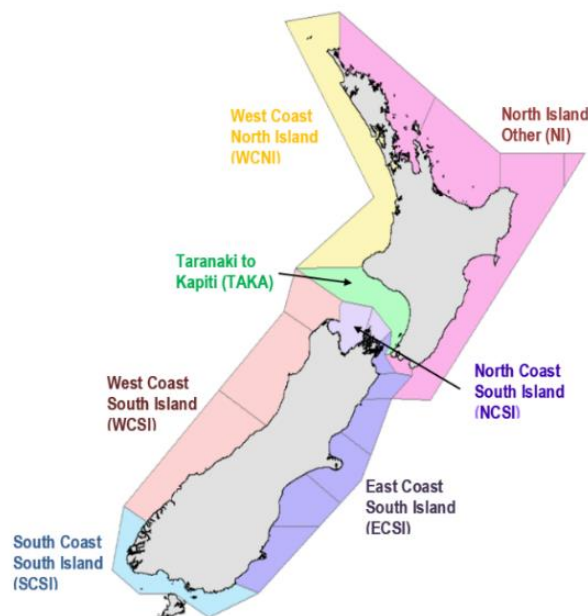
Figure 2: Spatial extent of sub-population areas delineating assessment sub-populations (discrete colours) and strata used to rescale habitat preference-based spatial abundance predictions of Hector's and Māui dolphins (black-edged polygons). Population sizes assumed for each sub-area are shown in Table 2. Note that the spatial abundance of Hector's and Māui dolphins was assumed to be zero at depths greater than 250 m, whereas the sub-population polygons depicted here extended an arbitrary distance from shore.

Table 2: Population size estimates for area strata used to rescale the habitat preference based spatial abundance prediction of Hector's and Māui dolphins. Stratum areas are displayed in Figure 2. Note that there is no evidence of current resident sub-populations in the TAKA (Taranaki to Kapiti) or 'North Island other' areas. Non-zero dolphin densities are assigned to these areas to inform the estimation of risk to dolphins that may be transient in these areas or dispersing from other areas. Because under the SEFRA method risk accrues per individual animal, the estimation or risk in these areas is not sensitive to the choice of hypothetical population sizes assigned here.

Rescaling stratum (label)	Population size (scaling factor)	Rationale
West Coast North Island (WCNI)	65	63 Māui and 2 Hector's
Taranaki to Kapiti (TAKA)	15 Summer 17 Winter	Derives from rescaling of East Coast North Island (ECNI) population to 65 individuals
North Island Other (NI)	10	Arbitrary decision based on few public sightings (will not affect risk ratio)
East Coast South Island (ECSI)	9728	Aerial survey abundance estimates for survey strata
North Coast South Island (NCSI)	214	within respective rescaling stratum boundaries
West Coast South Island (WCSI)	5482	(MacKenzie & Clement 2014; MacKenzie & Clement 2016). Note that the NCSI estimate was based on a single observation from the winter survey, and so will be highly uncertain.
South Coast South Island (SCSI)	332	Summer aerial survey summer abundance estimate for the south coast of the South Island (MacKenzie & Clement unpublished data; Fisheries New Zealand project code PRO2016-09)

A detailed description of methods by which the two habitat preference models were developed is given below, along with the method used for generating a single (seasonal) spatial abundance estimate for Māui dolphin.

Coastal abundance of Hector's and Māui dolphins

Aerial survey observations

Summer and winter aerial survey density estimates were obtained for 1 km transect segments for Hector's dolphin aerial surveys of the West Coast South Island (WCSI), East Coast South Island (ECSI) and South Coast South Island (SCSI) (MacKenzie & Clement 2016). The aerial survey methods and estimates were endorsed for informing management planning by an Intersessional Expert Group of the International Whaling Commission (IWC 2016). The survey adopted an extension of mark-recapture distance sampling (MRDS) techniques and line segment abundance estimates (including calves) accounted for locational/seasonal availability bias (see MacKenzie & Clement 2016 for a detailed summary of survey methods).

Habitat predictors

Aerial survey abundance estimates for line transect were related to an array of habitat variables, summarised to a 1 km grid cell resolution. Static physical habitat variables included: bathymetric depth, bathymetric slope (gradient of the seafloor derived from bathymetry) and distance from shore. Sea surface habitat variables were produced for: sea temperature, turbidity, chlorophyll-a concentration and downwelling light attenuation (K_{PAR}); all of which were derived from satellite ocean colour data (plotted in Appendix 6). The methods for producing satellite-derived habitat variables are described in Pinkerton et al. (2018). Spatial predictions of the relative presence of Hector's and Māui dolphin key prey species (accounting for approximately 80% of their dietary mass) were estimated from trawl survey observations (analysis and spatial predictions shown in Appendix 5). See Table 3 for a description of all habitat variables offered to Hector's and Māui dolphin habitat models.

For the sea surface variables (temperature, turbidity, chlorophyll a concentration and K_{PAR}), location-specific values were extracted for the year and month corresponding to the date of each aerial survey transect (i.e. in the fitting stage Hector's dolphin abundance estimates were related to habitat variables at the time of the survey). Subsequently in the prediction stage, dolphin densities were predicted using seasonally-averaged conditions over the period from 2009–2018.

Seasonal (summer and winter) habitat layers were only produced for satellite-derived habitat variables. Hector's dolphin prey species distributions are known to vary by season (Miller 2015), although the temporal-spatial coverage of the trawl survey used to estimate prey species' distributions was not adequate to produce predictions by season (see Appendix 5).

The degree of spatial correlation between each pair of habitat variables was assessed using the Spearman Rank Correlation Coefficient (Spearman ρ) (Spearman 1904). New terms were not offered to the model if they were strongly correlated with existing terms (less than -0.6 or greater than 0.6). Spatial habitat layers for horizontal gradients in all satellite-derived sea surface variables were also developed (using absolute values), although were all found to have a strong spatial correlation with absolute values for each respective parameter and, so, were not offered to habitat models or described further in this report.

Table 3: Summary of habitat variables used to fit Hector's and Māui dolphins habitat preference models.

Variable	Unit	Description	Source	Seasonality (summer/ winter)
Bathymetric depth	Metres	Depth of seafloor interpolated from contours, generated from echo sounders, satellite gravimetric inversion, and other sources (Mitchell et al., 2012).	National Institute of Water and Atmospheric Research (NIWA) unpublished data	No
Bathymetric slope	Degrees	Bathymetric slope derived from bathymetric depth.		No
Distance from Shore (km)	Kilometres	Using a NIWA-sourced polygon of the New Zealand coastline, distance from shore was calculated using the spatial analysis extension in ArcGIS.	unpublished data	No
Turbidity	Nephelometric Turbidity Unit (NTU)	Loss of transparency due to suspended particulates, derived from satellite ocean colour data.	Methods described in Pinkerton et al. (2018)	Yes
Chlorophyll-a	mg/m^3	A proxy for the amount of photosynthetic plankton, or phytoplankton, present in the ocean, derived from satellite ocean colour data.		Yes
Sea Surface Temperature	Degrees-Celsius	Temperature at the ocean's surface as measured by satellite.		Yes
Downwelling light attenuation (K_{PAR})	K_{PAR}/m	Representative of diffuse attenuation which is influenced by sedimentation close to the coast and chlorophyll in the open ocean, derived from satellite ocean colour data.		Yes
Red Cod (*Pseudophycis bachus*)	Probability of presence	Model predicted probability of presence in survey trawls.	See Appendix 5.	No
Sprat (Sprattus spp.)				No
Giant stargazer (*Crapatalus* sp.)				No
Ahuru (*Auchenoceros punctatus*)				No
Arrow Squid (*Nototodarus* sp.)				No
Sole (*Pelthoramphus* sp.)				No

Habitat model development

Seasonal (summer and winter) habitat preference models were developed using Generalised Additive Models (GAMs) produced using the *mgcv* package in *R* (R Core Team 2018; Wood 2011). Aerial survey density estimates for 1 km line transect segments (i.e., adjusted for locational/seasonal availability bias, see MacKenzie & Clement 2016) were specified as the response variable. The candidate predictor variables were the habitat variables for the respective 1 km grid cell that each transect segment was located within, in the month and year of the survey (for satellite-derived layers).

All GAMs assumed a negative binomial error structure (family = '*nb*'), with the shape parameter (θ) estimated during model fitting to account for over-dispersion in the response variable. A univariate spline was specified for all habitat variables with the smooth basis dimension (k) constrained to prevent complex relationships that lack biological credibility (fixed to equal four for the initial model term, then three for all subsequent terms). Cubic regression splines with shrinkage ("bs = '*cs*'") were specified as the smooth terms in all cases.

Model selection followed the standard Fisheries New Zealand approach used for predictive modelling, in which terms were sequentially added until the addition of a new term explained less than an additional 1% of the model deviance. Standard diagnostics were used to compare models (model Akaike information criterion (AIC) (Akaike 1974) and the percentage of deviance explained) and to check that distributional assumptions were met (quantile-quantile plots).

Generating spatial prediction

The optimal habitat preference model was used to generate seasonal predictions of Hector's and Māui dolphin abundance for the habitat variables in the respective model, aggregated to a 1 × 1 km spatial resolution, with spatial extent from the coast out to a depth of 250 m. With respect to satellite-derived sea surface habitat variables, seasonally-averaged values (consistent with the risk assessment definition of summer from 1 November to 31 April and winter from 1 May to 31 October) were used in the prediction stage, averaged across the period 2009–2018 (consistent with the period for which methodologically consistent and comprehensive necropsies were conducted for Hector's and Māui dolphins). The coefficient of variation (CV) associated with GAM predictions for each 1 km grid cell was obtained by dividing the reported standard error and then dividing this by the model prediction for the respective grid cell.

The seasonal model-predicted abundance of Hector's and Māui dolphins and associated CV of that prediction were plotted across the spatial extent of the habitat grid (from the coast to a depth of 250 m).

Relative abundance of Hector's and Māui dolphins in North Island harbours

Public sighting observations

Public sightings of Hector's and Māui dolphins were extracted from the "Māui and Hector's dolphin sightings database", maintained by DOC (DOC 2018). Sightings consistent with the following subsets were used:

- **Validation category (values of 1–3)**. The description of colouration and dorsal fin shape was consistent with a Māui or Hector's dolphin and may potentially have been observed outside of their known core spatial distribution. The selection of these validation categories was agreed with the AEWG;
- **Date event observed (November to April)**. A subset of sightings in summer months, consistent with the risk assessment definition.
- **Platform (Charter vessel, Private vessel, Tourism vessel, or Other vessel).** A subset of platforms consistent with public-based vessels (i.e. not research or government vessels).
- **Longitude (> 172.539 & < 175.216) and Latitude (> -41.198 & < -33.991)**. The aerial extent of the public sighting effort layer, described below.
- **Depth (< 250 m).** Depth was attributed to public sightings from NIWA's bathymetric depth dataset (Table 3).

The field **Estimated minimum number of animals** gave the number of dolphins assumed to have been observed at a given sighting event. No distinction was made with respect to subspecies (**Vernacular name** in the sightings database).

The selection of only summer months was necessitated by few sighting events in winter months. Consequently, the relative spatial abundance in harbours was based on summer information only, and the relative density in harbour areas was assumed to be the same in summer and winter.

The selection of boat-based public sightings was required because this was the only layer for which a proxy 'sighting effort' layer was readily available with adequate spatial coverage (see below). Other public sighting platforms included non-motorised coastal craft (mainly surfers) and land-based sightings, but these were not used by this assessment. Research vessel sightings were used by the previous TMP risk assessment to estimate the spatial density of Māui dolphins for this sub-species

(Currey et al. 2012). However, research vessel sightings were not used by the current assessment, because this effort was mostly centred on the region of relatively high abundance, and spatial coverage in the harbours was low. Likewise, aerial survey sightings were not used because of a lack of effort in harbour areas.

Public sighting effort proxy

Spatially-resolved information on the spatial density of public sighting effort (i.e., the total number of people present who may see and report a dolphin) were not directly available, so, the spatial distribution of recreational fishing boats was used as a proxy for 'sighting effort' and related only to the boat-based public sightings of Hector's and Māui dolphins. Year-round aerial surveys of coastal recreational fishing craft were conducted between 2004 and 2007 (Fisheries New Zealand project code SEC2007-01), including the north and west coast of the North Island and the north coast of the South Island. Across all surveys, this provided the geospatial coordinates of approximately 50 000 recreational fishing platforms, including around 42 000 in summer months (November to April). The following subsets were applied to this dataset:

- **Boat_type (Charter, Launch, Trailer or Yacht)**. To exclude kayak and scuba-based sightings;
- **Month (November to April).** A subset of boats observed in summer months, consistent with the risk assessment definition.

This created a subset of more than 41 000 vessels, pooled across all aerial surveys.

Details of the recreational fishing aerial survey methods are given by Hartill et al. (2011). The recreational fishing aerial survey flight path was mostly within 1 km of the coastline (figure 11 of Hartill et al. 2011), with wide loops off harbour entrances, towns, around offshore islands, and a number of offshore waypoints were flown off the South Taranaki Bight (Hartill et al. 2011). Planes flew at an altitude between 500 and 1000 feet, at which fishing vessels were clearly visible at a distance of three kilometres, although sightings were made at greater distances. Hartill et al. (2011) estimated that approximately 10% of the recreational fishing boats targeting snapper would have been seaward of the aerial survey coverage along open coast, compared with 1% for the Taranaki area and 6% for the Taranaki Coast. All vessels in harbours were potentially within visual range of the observer.

In order to account for additional sightings effort off-shore of what was visible to the aerial survey, a grid of pseudo-absences was added to the surveyed boat locations, with a 2 km spacing, over water shallower than 250 m depth (and continuing over land). The use of pseudo-absences was required to prevent spurious model predictions seaward of the recreational boat survey coverage and to minimise the extent to which model predictions of dolphin abundance in harbours were influenced by offshore sightings/effort and vice versa.

The recreational boat locations (all assumed to be negative for sightings of Hector's/Māui dolphins) were then pooled with the boat-based public sightings of Hector's/Māui dolphins. Note that the public are not required to conduct regular searches for Māui dolphins, and there may be spatial biases in reporting rate by members of the public, which were not estimated or accounted for by this assessment.

Habitat predictors

The same habitat layers used for the coastal habitat preference model (Table 3) were also used for fitting the public sightings data. Because satellite-derived turbidity estimates were often missing for coastal cells or cells in harbours in which part of the cell covered land instead of water, the turbidity layer was modified by iteratively taking the arithmetic mean of adjacent cells for which there were turbidity estimates until turbidity values were obtained for all cells where recreational boats were located (and all cells seaward of these).

Habitat model development

As with the coastal habitat modelling, GAMs were produced with sighting counts (including pseudo-absences) specified as the response variable. The candidate predictor variables were the habitat variables for the respective 1 km grid cell in which each sighting event was located. GAMs assumed a negative binomial error structure (family = '*nb*'), with the shape parameter (θ) estimated during model fitting. A bivariate spline for latitude and longitude was forced as the first model term for the Māui dolphin habitat model, which meant that the model could not be used to predict outside of the spatial domain of the effort layer. For all additional model terms, univariate splines were specified with the smooth basis dimension (k) constrained to equal 3.

The shape parameter (θ) estimate varied with model run (unlike with the coastal habitat preference models), owing to comparatively fewer positive events (see below). As such, it was not appropriate to use model deviance for model selection, and this was instead achieved by comparison of model AIC (recommended by Simon Wood, the author of the *mgcv* R package). Once the optimal model structure was found, the model was refitted using the habitat layer with flooded harbour cells, to include information from the upper reaches of harbours where cells were otherwise missing (see above). Quantile-quantile plots were produced to check that distributional assumptions were met.

Generating spatial prediction

The optimal habitat preference model was then used to generate the summer only prediction of Hector's/Māui dolphin density, aggregated to a 1 km spatial resolution, with spatial extent from the coast out to a depth of 250 m. All aspects of the prediction were as described for the coastal habitat model (above).

Merging coastal and harbour predictions

The summer spatial density prediction from the public sightings-based habitat model was rescaled for the west coast of the North Island north of Cape Egmont, so that it summed to 65 individuals (see Table 2). This was repeated for the summer and winter predictions from the coastal habitat model (fitted to aerial survey sightings) for the same area. These layers were then merged, using harbour estimates from the public sightings model and estimates for all locations excluding harbours from the aerial survey-parameterised habitat model. The flooded, merged spatial abundance layer was then rescaled so that raster cells again summed to 65 individuals.

The merged spatial density prediction derived from the previous step was then flooded for all remaining coastal 1 km cells around New Zealand that intersected the sea but did not have an associated Hector's/Māui dolphin density estimate (due to habitat variables not being collated for the respective cells). Flooding was achieved by iteratively taking the arithmetic mean of the density estimate for adjacent cells.

4.3 Spatial threat intensity

Commercial set net and inshore trawl

Spatial information on commercial set net and inshore trawl fisheries used in the risk model are described in Section 4.5.

Toxoplasmosis and predation

Methods for the creation of spatial threat intensity layers for predation by broadnose sevengill sharks (*Notorynchus cepedianus*) and exposure to the parasite *Toxoplasma gondii* are described in Appendix 8 and Appendix 9, respectively.

Recreational fishing

The seasonally-resolved relative spatial intensity of recreational netting was produced by Fisheries New Zealand (Andy McKay unpublished data) and includes multiple gear types, including drag, throw and set-netting. Information was collated from surveys conducted by the National Panel Survey of Marine

Recreational Fishers (NPS) over a 12-month period spanning 2011/12 and again in the summer of 2017/18. In this survey, fishing activity was surveyed on a weekly basis across these periods and reported as a general location from which geospatial coordinates were inferred by matching with the New Zealand Place Names database maintained by LINZ. A total of 573 recreational netting locations were collated across the two survey periods and the spatial pattern of effort was consistent between the two survey years. The data were pooled across the two survey years to produce a raster of 1 km grid cells out to 2 nautical miles from the coast. A smoother was applied to take the mean of all cells within a 2-cell circle neighbourhood. The same spatial distribution was applied for both summer and winter recreational netting effort, but 75% of the effort was assigned to the summer period (Andy McKay unpublished data).

Aquaculture

A geodatabase of aquaculture facilities (current and applications) was provided by Fisheries New Zealand (up to date as of May 2018). The aquaculture spatial threat intensity layer used current facilities only and assumed equal intensity across all 1 km grid cells with some spatial overlap with the polygons provided by Fisheries New Zealand (no buffer zone was specified, although some positive 1 km cells will have minimal overlap). No attempt was made to produce separate layers for different aquaculture sectors (e.g., shellfish or finfish) despite probable differences in their effects on Hector's and Māui dolphins.

Oil spill risk

A spatial marine oil spill risk assessment (MOSRA 15) was undertaken by Navigatus Consulting for Marico in 2015 (Navigatus 2015). Oil spill sources in this assessment included: oil production installations (including associated oil pipelines), oil tankers, cargo vessels, passenger vessels and fishing vessels. The assessment accounted for factors affecting the movement of spilt oil (including regional wind and current patterns) as well as factors affecting oil decay and shoreline properties affecting the relative grounding probability of vessels. It was estimated that approximately 99% of the oil spill risk originated from oil tankers, passenger vessels and cargo vessels (Navigatus 2015).

The MOSRA 15 assessment estimated ratings from 1–5 to a log10 scale for 10 km hexagonal open water cells around New Zealand (Navigatus 2015). Accordingly, a 10-fold increase in relative oil spill risk was assumed with each unit increase in risk rating (from 1 to 5). The corresponding oil spill risk value was then derived for 1 km raster cells overlapping MOSRA 15 hexagonal cells.

Seismic survey & vessel noise

An independent underwater noise modelling assessment of vessel traffic (using Automated Identification System (AIS) data) and selected oil and gas seismic surveys was undertaken by JASCO Australia (McPherson et al. 2019) and the outputs were made available to this spatial risk assessment. The noise model created one-month equivalent continuous underwater noise levels (L_{eq}) aggregated across 3 km grid cells from the coast of the west coast North Island to 100 km from the shore. Cumulative noise was estimated for both unweighted and frequency-weighted sound levels to account for the hearing capability of Māui dolphins, which are classified as a high-frequency cetacean species (NMFS 2018). McPherson et al. (2019) also estimated sound fields (unweighted and high-frequency weighted) at 14 receiver locations in the regions of Kaipara, Manakau, Kawhia, New Plymouth, Cape Egmont and the South Taranaki Bight. See McPherson et al. (2019) for detailed methods.

4.4   Overlap for non-commercial fishery threats

Spatial overlap maps

Spatial overlap for non-commercial fishery threats was generated by multiplying the seasonal (summer and winter) relative density rasters for each defined sub-population (p_s^S and p_s^W) by the seasonal non-commercial fishery threat rasters (T_t^S and T_t^W). Because the spatial extent and projection of rasters differed for the spatial abundance of dolphins and the threats, reprojection and resampling of the threat

rasters was done to generate rasters with the same spatial extent and projection. Thus, non-commercial fishery threat overlap maps were calculated for summer and winter as

$$T_t^S p_s^S \text{ and } T_t^W p_s^W$$

respectively, where $\sum\left(p_s^S + p_s^W\right) = 1$.

Relative overlap statistic

A relative overlap statistic was developed for each sub-population by forcing the non-commercial fishery threats to sum to one across all of New Zealand, then forcing the relative density within each sub-population to sum to one, and finally multiplying the two rasters and integrating over each sub-population.

4.5   Spatial risk assessment model

Spatial risk model to assess commercial fishery-related deaths

The SEFRA method is used to estimate commercial fishery-related deaths for Hector's/Māui dolphins. The conceptual and mathematical basis of the SEFRA method, including the format of data inputs and underlying structural assumptions, are described in Sharp (2018).

The following databases were provided by Fisheries New Zealand, on the 6 of August 2018:

1. Spatially-resolved commercial fishing effort data, per fishing event;
2. Fisheries observer data, per fishing event;
3. Fisheries observer-recorded protected species captures, per capture event.

These databases, along with spatio-temporal species distribution maps and priors for all model parameters, inform the SEFRA model. All variables used to describe the model can be found in Table 4.

This implementation of the SEFRA method includes two commercial fishery groups known to pose a risk to Hector's/Māui dolphins—set netting and inshore trawling. Fishing events were either observed (an observer is onboard the fishing vessel at the time of a capture) or unobserved. Hector's dolphin captures recorded by fisheries observers on the observed portion of the fishing effort were used to estimate model parameters by fitting a relationship between this effort and observed dolphin captures. Observed dolphin captures are recorded as being alive or dead and this is also reflected in the model and subsequently used to estimate the number of deaths, assuming that not all animals captured alive and released will die. The combination of observed and unobserved effort, along with the estimated parameters, was used to estimate the total number of commercial fishery related captures, deaths and risk.

Table 4: Variable symbols, support, and descriptions. Estimated parameters are estimated within the model while random variables are simulated from a prior outside the model (i.e., within the generated quantities block of the *Stan* code).

Symbol	Support	Description
Indices		
i	$i = \{1,2,...\}$	A fishing event (e.g. a net is set or a trawl tow begins) that occurs at a time and location
s	$s = \{1,2\}$	Population – Hector's dolphin or Māui dolphin
g	$g = \{1,2\}$	Commercial fishery group – set net (SN) or inshore trawl
k	$k = \{1,2,3\}$	Necropsy type – toxoplasmosis, predation, or other
l	$l = \{1,2,...\}$	A necropsy event
c	$c = \{1,2,...\}$	A cell in a map
Data		
$\left(C_{sg}^{\text{live}}\right)'$	≥ 0	Number of observed live captures
$\left(C_{sg}^{\text{dead}}\right)'$	≥ 0	Number of observed dead captures
η_l	$\{1,2,3\}$	Necropsy observations
Covariates		
a'_{gi}, a_{gi}	≥ 0	Observed fishing intensity and fishing intensity (km of net for set net and number of tows for inshore trawl)
$p_{si}^{\text{S}}, p_{si}^{\text{W}}$	$\in [0,1)$	Relative density during summer and winter
O'_{sg}, O_{sg}	≥ 0	Observed overlap and overlap
Estimated parameters		
v_g	≥ 0	Vulnerability
p_g^{obs}	$\in (0,1)$	Probability that an event is observable
ψ_g	$\in (0,1)$	Probability of an individual being alive given that it is caught
N_s	> 0	Population size for each sub-species
ρ_k	$\in (0,1)$	Proportion of non-fishery deaths for each necropsy type
Random variables		
r_s^{max}	> 0	Intrinsic population growth rate for each sub-species
ω_g	$\in (0,1)$	Live release survival rate
S_s^{1+}	$\in (0,1)$	Non-calf annual survival rate
Fixed parameters		
ϕ	$\in (0,1)$	Calibration coefficient
∂_k	> 0	Necropsy detection scalar
Derived quantities		
$C_{sg}^{\text{live}}, C_{sg}^{\text{dead}}$	≥ 0	Live and dead captures
D_{sg}	≥ 0	Deaths
PST_s	≥ 0	Population sustainability threshold
R_{pg}	≥ 0	Risk ratio
k_g	≥ 0	Cryptic mortality

Estimating key model parameters

Two commercial fishery groups (g) were included in this model: set net (SN) and inshore trawl. Fishing effort is summarised per fishing event (i.e. not aggregated within cells); every fishing event (i) has an associated fishing intensity (a_{gi}) measured in kilometres of net length for set net and number of trawl events for inshore trawl. Observed fishing events are denoted using the prime symbol as a'_{gi} where

$$a'_{gi} \subset a_{gi}$$

meaning that observed effort is a subset of all fishing effort. Note that for a small number of 1 km grid cells, the aggregated fishing intensity for observed fishing events exceded that of the total (observed and unobserved) fishing intensity. The reasons for this discrepancy in the input data were not identified or accounted for by this assessment.

Māui dolphin are a closely related sub-species of Hector's dolphin (Pichler 2001). As such, several key model parameters are assumed to be the same for the whole species and are estimated simultaneously across all subpopulations (i.e. Māui dolphins and four subpopulations of Hector's dolphin). Parameters estimated (at the species level) in this way include vulnerability (i.e., probability of capture or death) in

each commercial fisheries group (v_g), the probability that an event is observable (given that an observer is on watch) for each fisheries group (p_g^{obs}), the probability of an individual being alive (given that it is captured) for each fisheries group (ψ_g), and the live-release survival rate for each fisheries group (ω_g). Population size estimates (N_s) for each sub-species (s) are specified as priors in the model. Vulnerability, the probability that an event is observable, the probability of an individual being alive given that it is captured, and the live release survival rate are all parameters that need to be estimated.

Fisheries observer data (protected species captures on observed fishing events) are used to estimate model parameters. Observed overlap is calculated for each sub-species (s) and commercial fisheries group (g) using data from 1995/96 to 2016/17

$$
O'_{sg} =
\begin{cases}
\sum_i a'_{gi} p^{\text{S}}_{si} & i \in \text{summer} \\
\sum_i a'_{gi} p^{\text{W}}_{si} & i \in \text{winter}
\end{cases}
$$

The probability of an individual being alive given that it is captured (ψ_g) is then used to calculate the expected number of observed alive ($\lambda_{sg}^{\text{live}}$) and dead ($\lambda_{sg}^{\text{dead}}$) captures

$$
\lambda_{sg}^{\text{live}} = O'_{sg} N_s v_g p_g^{\text{obs}} \psi_g
$$
$$
\lambda_{sg}^{\text{dead}} = O'_{sg} N_s v_g p_g^{\text{obs}} (1 - \psi_g)
$$

Using the posterior distribution for the model parameters $N_s v_g p_g^{\text{obs}}$, maps are generated that display the number of predicted observed captures (alive and dead)

$$
C'_{sgc} = \sum_{i \in c} O'_{sgi} \times \mathbb{E}(N_s v_g p_g^{\text{obs}})
$$

where $i \in c$ means that fishing event i is in cell c and $\mathbb{E}(\cdot)$ is the expected value (or mean) of the product of the posterior samples. Note however that because fishing effort and fisheries observer data are utilised at the level of individual fishing events, cell size has no effect on model outcomes; and maps of captures and risk can be re-generated at any user-defined cell size.

Throughout this document reference is made to cryptic mortality rate which is defined as

$$
k_g = \frac{1}{p_g^{\text{obs}}}
$$

Bayesian Inference

Priors and simulated random variables

Priors relate to estimated model parameters. Random variables are simulated (in the generated quantities block in the Stan code) and are therefore not updated by data.

The prior for the Hector's dolphin population size ($N_{s=\text{HDO}}$) is derived from Mackenzie & Clement (2016) who estimated a mean of 14 849 individuals by averaging the summer and winter abundance estimates for each of the ECSI, SCSI, and WCSI then summing these to get the total abundance estimate for the South Island. They provided a CV of 11% which was translated into a standard deviation for a lognormal distribution using

$$
\sigma = \sqrt{\log(CV^2 + 1)} = 0.110
$$

Thus, the prior is

$$N_{s=\text{HDO}} \sim \text{lognormal}(\log(14849)\,, 0.110^2)$$

The prior for Māui dolphin population size ($N_{s=\text{HDM}}$) is derived from Baker et al. (2016a) who estimated a mean of 63 and a CV of 11% also. Thus, the prior is

$$N_{s=\text{HDM}} \sim \text{lognormal}(\log(63)\,, 0.110^2)$$

Both of these priors are illustrated in Figure 3.
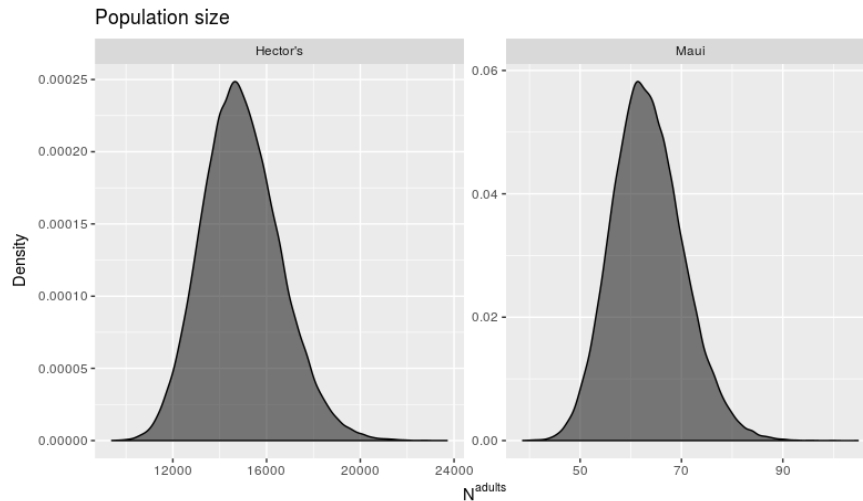
Figure 3: Population size (N_s) priors for Hector's and Māui dolphins.

Uninformative but non-uniform vulnerability priors were specified in log-space to help with Markov chain Monte Carlo (MCMC) mixing

$$\log(v_g) \sim \text{normal}(0, 10^2)$$

The prior for the probability that an event is observable was obtained from a review of the information relating to dolphin and porpoise species interactions with fishing gear (Appendix 10). Informed priors were assumed for set net captures

$$p_{g=\text{Set net}}^{\text{obs}} \sim \text{beta}(6.916, 6.916)$$

consistent with a 95% CI of 0.25 and 0.75; and for inshore trawl captures

$$p_{g=\text{Trawl}}^{\text{obs}} \sim \text{uniform}(0.5, 1.0)$$

A vaguely informative prior is used for the probability of an individual being alive given that it is caught in commercial fishery group (g)

$$\psi_g \sim \text{beta}(1, 3)$$

The live-release survival rate random variable was also obtained from a review of information across dolphin and porpoise species (Appendix 10) and was simulated from

$$\omega_g \sim \text{uniform}(0.5, 0.9)$$

Priors for the intrinsic population growth rate ($r_s^{\max}$) random variable were developed by fitting normal distributions to posterior samples produced by the analysis of Edwards et al. (2018), updated in Appendix 2 (for Hector's dolphin) and from an analysis adjusting for small population size in Appendix 3 (for Māui dolphin). The prior for Hector's dolphin is simulated from

$$r_{s=\text{HDO}}^{\max} \sim \text{normal}(0.050, 0.011^2)$$

and for Māui dolphin

$$r_{s=\text{HDM}}^{\max} \sim \text{normal}(0.045, 0.011^2)$$

Both of these priors are illustrated in Figure 4.
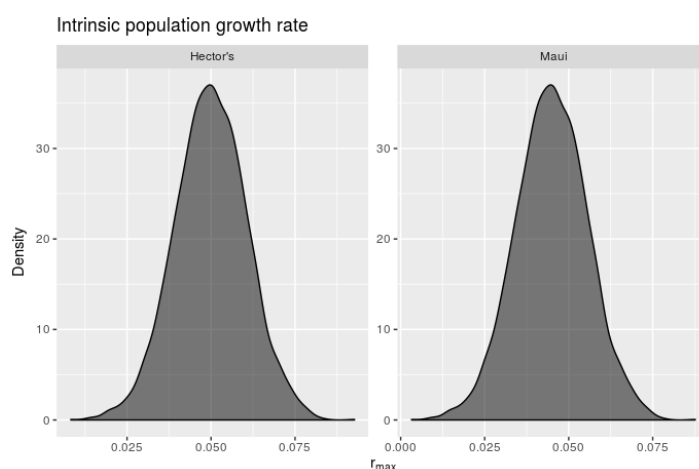
Figure 4: Intrinsic population growth rate ($r_s^{\max}$) priors for Hector's and Māui dolphins.

Beta priors were derived for adult survival (survival of individuals equal to or greater than one year old represented by 1+). For Hector's dolphins we specify a beta prior with an expectation

$$\mathbb{E}[S_s^{1+}] = \frac{\alpha}{\alpha + \beta} = 0.92$$

based on Gormley et al. (2012) with an upper 99% of 0.96 based on estimates of non-calf survival consistent with $r_s^{\max}$ (Edwards et al. 2018, updated in Appendix 2). Therefore, using the CDF of a beta distribution we write the regularised incomplete beta function as

$$I_{x=0.96}(\alpha, \beta) = 0.99$$

Solving this system of nonlinear equations for alpha and beta results in

$$S_{s=\text{HDO}}^{1+} \sim \text{beta}(164.0, 14.3)$$

This prior is illustrated in Figure 5.
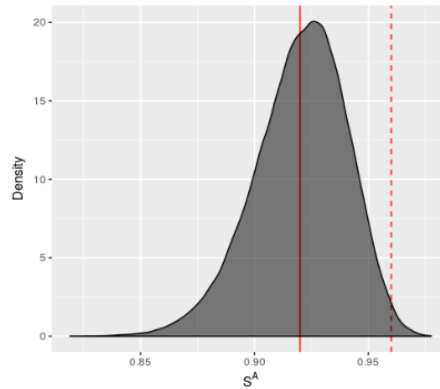
Figure 5: Non-calf annual adult survival (S_s^{1+}) prior for Hector's dolphin. The solid vertical line is 0.92 and dashed line is 0.96 where 1% of the distribution is > 0.96.

For Māui dolphin, we fit a beta distribution to the posterior samples based on demographic assessment fitted to genetic mark-recapture observations (Roberts et al. 2019):

$$S_{s=\text{HDM}}^{1+} \sim \text{beta}(720.2, 86.4)$$

This prior is illustrated in Figure 6. A summary of all priors and random variables is provided in Table 5.
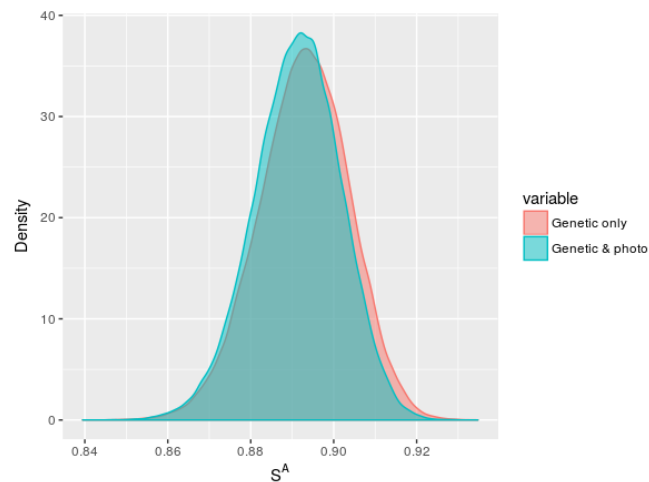
Figure 6: Non-calf annual survival (S_s^{1+}) prior for Māui dolphins. The estimate using genetic mark-recapture observations only "Genetic only" (i.e. not photo-based mark-ID also) was used for all model runs.

Table 5: Table of priors for each of the model parameters and simulated random variables.

Parameter	Symbol	Subscript	Prior type	Prior parameters	
Vulnerability	$\log(v_g)$	$\forall g$	normal	$\mu = 0$	$\sigma = 100$
Probability capture event is observable	p_g^{obs}	$g = \text{Set net}$	beta	$\alpha = 6.916$	$\beta = 6.916$
		$g = \text{Trawl}$	uniform	$a = 0.5$	$b = 1$
Probability an individual is alive when captured	ψ_g	$\forall g$	beta	$\alpha = 1$	$\beta = 3$
Total population size	N_s	$s = \text{HDO}$	lognormal	$\mu = 8968$	$\sigma = 0.149$
		$s = \text{HDM}$	lognormal	$\mu = 63$	$\sigma = 0.110$
Cause of death as a proportion of necropsy sample	ρ_k	$\forall k$	Dirichlet	$\boldsymbol{\alpha} = \{1,1,1\}$	
Live-release survival probability	ω_g	$\forall g$	uniform	$a = 0.5$	$b = 0.9$
Intrinsic population growth rate	$r_s^{\max}$	$s = \text{HDO}$	lognormal	$\mu = 0.050$	$\sigma = 0.011$
		$s = \text{HDM}$	lognormal	$\mu = 0.045$	$\sigma = 0.011$
Non-calf annual survival	S_s^{1+}	$s = \text{HDO}$	beta	$\alpha = 164.0$	$\beta = 14.3$
		$s = \text{HDM}$	beta	$\alpha = 720.2$	$\beta = 86.4$

Likelihood

A Poisson distribution is assumed for the observable alive and dead captures

$$\left(C_{sg}^{\text{live}}\right)' \sim \text{Poisson}\left(\lambda_{sg}^{\text{live}}\right)$$
$$\left(C_{sg}^{\text{dead}}\right)' \sim \text{Poisson}\left(\lambda_{sg}^{\text{dead}}\right)$$

noting that the Poisson distribution assumes the same mean and variance.

Bayesian inference was done using *Stan* making use of its Hamiltonian Monte Carlo (HMC) algorithm (Stan Development Team, 2016). Four separate MCMC simulations were undertaken. Each chain was run for 14 000 iterations, the first 10 000 iterations were used to warm-up the HMC chain and were discarded, as was every fourth iteration after warm-up. This resulted in a total of 4000 samples from the posterior distribution of the model.

Model predictions

Model predictions are done using both observed and unobserved fishing events (a_{gi}). Mean annual overlap (observed and unobserved fishing events) is calculated by commercial fishery group (g) for both sub-species (s). To approximate 'current' patterns and intensity of fishing effort, we used the most recent three years of data (2014/15 to 2016/17), and estimate of average annual overlap across these three years

$$O_{sg} = \begin{cases} \dfrac{1}{n}\sum_i a_{gi} p_{si}^{S} & i \in \text{summer} \\ \dfrac{1}{n}\sum_i a_{gi} p_{si}^{W} & i \in \text{winter} \end{cases}$$

where n is the number of years that we are averaging across ($n = 3$).

A live-release survival rate parameter (ω_g) is used to calculate the number of deaths

$$D_{sg} = O_{sg} N_s v_g \left(1 - \psi_g \omega_g\right)$$

A mortality constraint (whereby total deaths are not allowed to exceed 1 minus the annual non-calf survival rate), as described in Sharp (2018) was not required because the number of deaths never approached $(1 - S_s^{1+})N_s$.

The population sustainability threshold (PST) was calculated for each sub-species (or subpopulation unit) as

$$PST_s = \frac{1}{2} \phi r_s^{\max} N_s$$

where ϕ is a calibration coefficient set to the value of $\phi = 0.2$ specified by Fisheries New Zealand. This value of ϕ is consistent with population recovery to at least 90 % of carrying capacity when assuming logistic population growth (Darryl Mackenzie unpublished data). A sensitivity run was also undertaken using $\phi = 0.5$, consistent with population recovery to at least 75 % of carrying capacity. The risk ratio (R_{sg}) is

$$R_{sg} = \frac{D_{sg}}{PST_s}$$

where a risk ratio > 1 is consistent with annual deaths exceeding the PST for a sub-species or subpopulation unit.

Extension of spatial risk model to assess non-fishery deaths

Total deaths, including commercial fishery related deaths (set net and inshore trawl) and non-fishery deaths (disease, predation and other), are calculated as $(1 - S_s^{1+})N_s$. Thus, total non-fishery deaths can be calculated as

$$(1 - S_s^{1+})N_s - \sum_g D_{sg}$$

Non-fishery deaths due to threat k are then calculated using a simplex of estimated proportions $p_k = \{p_1, p_2, p_3\}$ where $\sum_k p_k = 1$ and $\{p_1, p_2, p_3\}$ respectively refer to the proportion of non-fishery deaths due to toxoplasmosis, predation by sharks, and other sources of non-fishery mortality. These proportions are then applied to the total non-fishery (NF) deaths to get the number of deaths for each sub-species or sub-population and category

$$D_{sk}^{NF} = \left((1 - S_s^{1+})N_s - \sum_g D_{sg} \right) p_k$$

The proportions are estimated, with uncertainty, using a categorical distribution and an uninformative Dirichlet prior is placed on the estimated proportions

$$\eta_l \sim \text{categorical}(p_k)$$
$$p_k \sim \text{Dirichlet}(\{1,1,1\})$$

This assumes that the detection probability of deaths arising from each lethal non-fishery threat is the same. But if the carcasses of dolphins dying from particular threats have lower/higher probabilities of detection (e.g. predation events may not be detected if sharks consume their prey) then we can include a detection probability multiplier

$$p_k = \{\partial_1 p_1, \partial_2 p_2, \partial_3 p_3\}$$

ensuring that $\sum_k p_k = 1$. Relative detection probability multipliers of 1 and 0.1 were applied for predation events ("equal detection" run and "predation sensitivity" run, respectively) on the assumption that even partial consumption of a carcass by sharks may reduce its buoyancy and, hence, its likelihood of being beachcast and detected. The relative spatial intensity of predation was approximated using the estimated spatial distribution of broadnose sevengill sharks (*Notorynchus cepedianus*) only (see Appendix 8). Necropsy cause of death information was only used for cases attributed with "Full" or "Partial" confidence rating of the diagnosis, and only for non-calf individuals (i.e., deemed to be age 1 and older).

If we have a spatial distribution layer for a non-fishery threat, then we can explore spatially explicit deaths (the same as we can for fishery threats) and we do so for toxoplasmosis and predation. For those non-fishery threats for which a spatial distribution is not available we can produce an estimate of the total number of deaths. Sub-population non-fishery deaths are generated by multiplying the total deaths for each of toxoplasmosis and predation by their respective seasonal non-commercial fishery threat rasters (T_t^S and T_t^W)

$$D_{sk}^{\text{NF}} T_t^S + D_{sk}^{\text{NF}} T_t^W$$

where $T_t^S + T_t^W = 1$. These spatial layers are then integrated within each sub-population to produce non-fishery deaths by sub-population.

5.   RESULTS

5.1   Risk model inputs

Spatial abundance of Hector's and Māui dolphin

Hector's dolphin aerial survey observations

The habitat preference modelling only used aerial survey line transect segments in 1 km grid cells for which all habitat variables listed in Table 3 were collated. For ECSI and WCSI surveys, excluding incomplete rows meant that a relatively small proportion of segments with a sighting were omitted (ranging from 4.0 to 17.3% across surveys) (Table 6). For SCSI surveys, this resulted in the majority of positive survey line segments being omitted (70.5 to 73.0%) due to unavailability of prey species presence. However, since habitat models were fitted using observations from all areas simultaneously (and area was not offered as a predictor variable), the combined percentage of line segments omitted from habitat model fitting was relatively low (15.1%), and comprised 15.8% of the estimated population size for positive segments (Table 6).

The spatial distribution of summer and winter survey line segments and associated abundance estimates are shown in Figure 7. The raw observations are consistent with a similar alongshore distribution throughout the year, although with a slightly more offshore distribution in winter, as previously noted by the survey report (Mackenzie & Clement 2016).

Table 6: Summary of Hector's dolphin aerial survey data by location and season. Numbers in parentheses indicate observations for which habitat data were collated and used to fit habitat preference models.

Survey area	Season	Dates of survey	Count of line transect segments with positive sightings	Estimate of total individuals estimated for positive events
West Coast	Summer	26 Jan – 1 Mar 2015	196 (162)	1 418 (1 184)
South Island	Winter	4 Jul – 1 Aug 2015	219 (194)	1 500 (1 334)
East Coast	Summer	28 Jan – 13 Mar 2013	282 (246)	1 975 (1 722)
South Island	Winter	1 Jul – 18 Aug 2013	274 (263)	1 312 (1 265)
South Coast	Summer	1 Mar – 31 Mar 2010	37 (10)	279 (68)
South Island	Winter	1 Aug – 31 Aug 2010	34 (10)	207 (59)
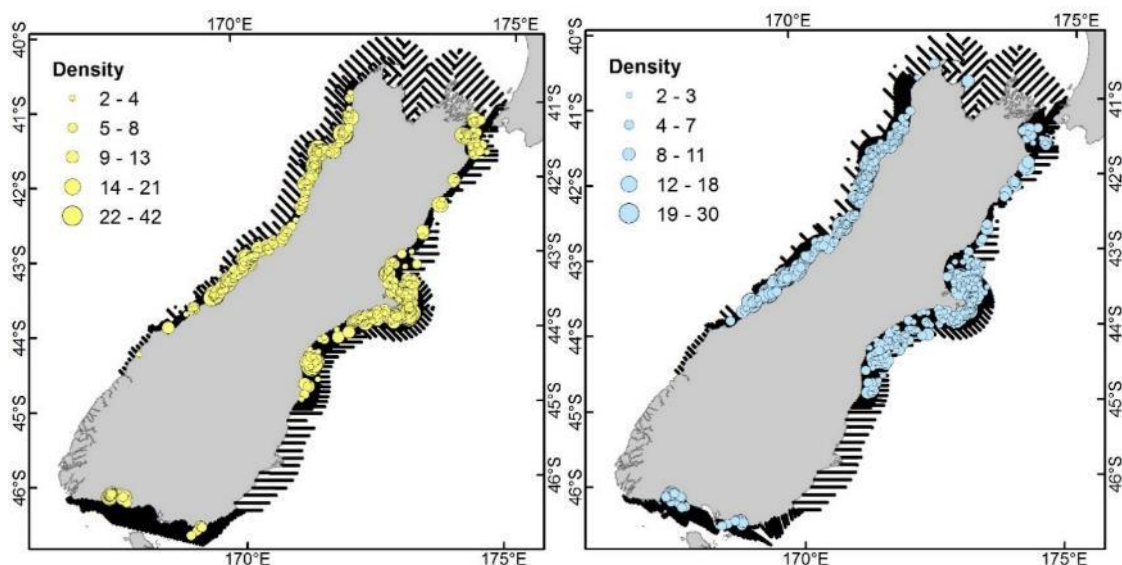
Figure 7: Aerial survey effort (black lines) and Hector's dolphin density estimates for summer (yellow, left panel) and winter (blue, right panel) aerial surveys. Size of circles represents estimated number of Hector's dolphins per 1-km survey transect segment.

Habitat variables

Satellite-derived habitat variables (surface chlorophyll a, turbidity and downwelling light attenuation (K_{PAR})) were all strongly positively correlated with each other, and so could not be included in the same model. Bathymetric depth was correlated with three of the prey species and some of the prey species were also strongly correlated with each other, including sprat, red cod, *Pelthoramphus* sp. (sole) and ahuru. These species layers were all positively correlated in space, limiting the inclusion of multiple prey species in the same model (Figure 8).
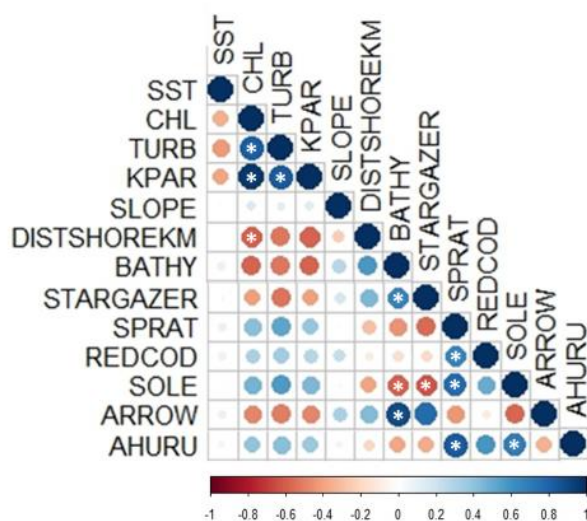
Figure 8: Correlation matrix of all variables considered in the model. Correlations are depicted as circles (left) and as numbers (right). Dark red indicates a strong negative correlation and dark blue indicates a strong positive correlation. Pairings with correlation greater than 0.6 marked with white stars. Predictor variables are decribed in Table 3 (SST = sea surface temperature, CHL = chorophyll a, TURB = tubidity, KPAR = light attenuation (K_{PAR}), SLOPE = bathymetric slope, DISTSHOREKM = distance to shore, BATHY = bathymetric depth, STARGAZER = presence of giant stargazer, SPRAT = presence of sprat spp., REDCOD = presence of red cod, SOLE = presence of sole spp., ARROW = presence of arrow squid sp., AHURU = presence of ahuru).

Model development

Of models with a single term only, the seasonal turbidity model had the lowest AIC and explained the greatest percentage of model deviance (11%). The best single term models selected by AIC used the other two satellite-derived variables—chlorophyll a and vertical light attenuation (K_{PAR}). Prey species models were the next best in terms of AIC, particularly sprat, *Pelthoramphus* (sole) sp. and ahuru. As such seasonal turbidity was retained as the first model term.

Adding the prey species sprat, *Pelthoramphus* (sole) sp., ahuru or red cod produced the best two-term models, in ascending order of model AIC (Table 7). Retaining sprat as the second model term, only the addition of sea surface temperature explained more than an addition percentage of model AIC, though it was decided to reject this model, since using this model to predict spatial abundance on the WCNI would have required extrapolation into warmer temperatures than covered by aerial survey data (comparing the WCNI region with waters surrounding the South Island, Figure A6-6.

Via the Fisheries New Zealand Aquatic Environment Working Group it was decided to retain only two model terms (with seasonal turbidity as the first term) and to retain ahuru presence as the second model term. The 'Ahuru model' was assumed to be the base case model for predicting the spatial abundance of Hector's and Māui dolphins (based on visual inspection of model predictions relative to commercial fishery observer sightings in lower abundance areas). The quantile-quantile plots for this model indicated that negative binomial model was appropriate for these data (Figure 9).

Table 7: Comparison of models considered for predicting coastal spatial abundance of Hector's/Māui dolphins from aerial survey line transects.

Model terms	% deviance	d-AIC	Model label for spatial prediction of Hector's and Māui abundance
s(turbidity|season) + s(sprat)	26.1	0	–
s(turbidity|season) + s(pelthoramphus)	24.2	56	–
s(turbidity|season) + s(ahuru)	24.1	60	Ahuru model
s(turbidity|season) + s(redcod)	23.3	85	–
s(turbidity|season) + s(arrowsquid)	21.3	144	–
s(turbidity|season) + s(stargazer)	21	151	–
s(turbidity|season) + s(chlorophyll|season)	20.5	522	–
s(turbidity|season) + s(distance shore)	21.9	566	–
s(turbidity|season) + s(depth)	21.4	582	–
s(turbidity|season) + s(kpar|season)	20.5	583	–
s(turbidity|season) + s(slope)	20.5	607	–
s(turbidity|season)	11	854	–
s(chlorophyll|season)	6.8	876	–
s(K_{PAR}|season)	7.2	950	–
s(sprat)	10.6	1 773	–
s(ahuru)	9.6	1 799	–
s(pelthoramphus)	9.5	1 803	–
s(redcod)	4.5	1 936	–
s(arrowsquid)	3.5	1 962	–
s(stargazer)	3.3	1 969	–
s(depth)	5.9	2 698	–
s(distance shore)	5.8	2 698	–
s(slope)	0	2 852	–
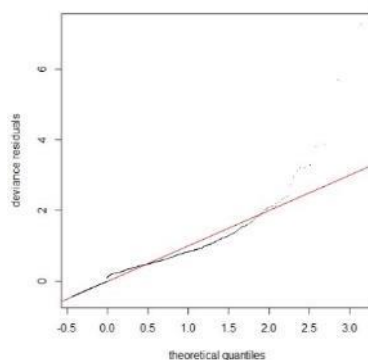
Figure 9: Quantile-quantile plot for models estimating the spatial abundance of Hector's dolphin, using the Ahuru model.

Model predictions

Plots of model splines for the Ahuru model indicated very low abundance in low turbidity areas (in both summer and winter) and low abundance in low ahuru presence areas and a slight reduction approaching the maximum prey presence (Figure 10). The shape of the relationship with turbidity was slightly different in summer and winter, with a plateau in abundance at turbidity levels above approximately 0.5 NTU in summer and a slightly declining trend in abundance at turbidity values greater than 1 NTU in winter (Figure 10).
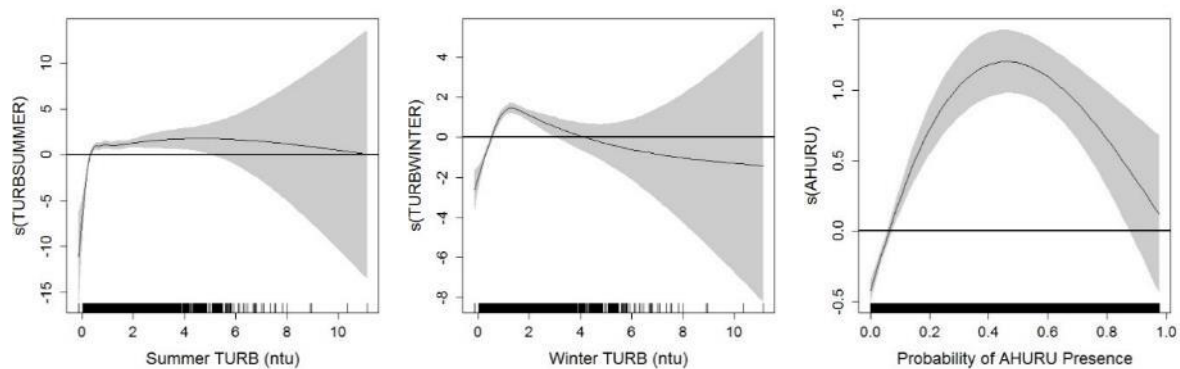
Figure 10: GAM splines of Hector's dolphin abundance in response to habitat variables for the "Ahuru model" (the final model for estimating spatial abundance of Hector's/Māui dolphins in coastal areas).

With respect to model predictions of spatial abundance, the coefficient of variation was relatively low (CV less than 0.3) across all coastal regions of both the North and South Island, indicating that the habitat used to make predictions was consistently within the modelled habitat envelope. The main exception to this was the harbours in the west coast of the North Island, where a CV of greater than 1 was obtained for a number of grid cells. This was caused by very high turbidity values beyond the range used to fit the habitat model (Figure 11). This indicates that the habitat models developed are suitable for predicting abundance in coastal and offshore waters, though not into high turbidity harbour areas.

From visual inspection, the predicted spatial abundance from the Ahuru model agreed with the raw abundance estimates from the South Island aerial surveys, especially in lower dolphin density areas, and represented the apparent off-shore movement in winter (comparing Figure 7 with Figure 11). An additional model run (using the Ahuru model) predicted dolphin density based on the habitat state in the particular year and month of the survey period and obtained an even better fit from visual inspection (not displayed in this report).

Along the West Coast of the North Island the habitat model predicted greatest density between Kaipara Harbour (in the north) and the North Taranaki bight (in the south) (Figure 11). This is broadly consistent with the spatial distribution of public sightings along this stretch of coast (Figure 13) and the associated model prediction using the public sightings data (Figure 16). A location of apparent high habitat suitability was also predicted on the east coast of the North Island, around Hawke's Bay, where public sightings of Hector's or Māui dolphins have also been reported despite no evidence of a permanent population. Predicted highly suitable habitats were in all cases characterised by high turbidity and high ahuru presence (comparing Figure 11 with Figure A5-5 and Figure A6-2).

The seasonal Ahuru model predictions are consistent with the movement of dolphins to locations further offshore in winter (Figure 11, although easier to discern from Figure 17 and Figure 18). These predictions are also consistent with the raw data and conclusions of the South Island aerial survey (MacKenzie & Clement 2016).
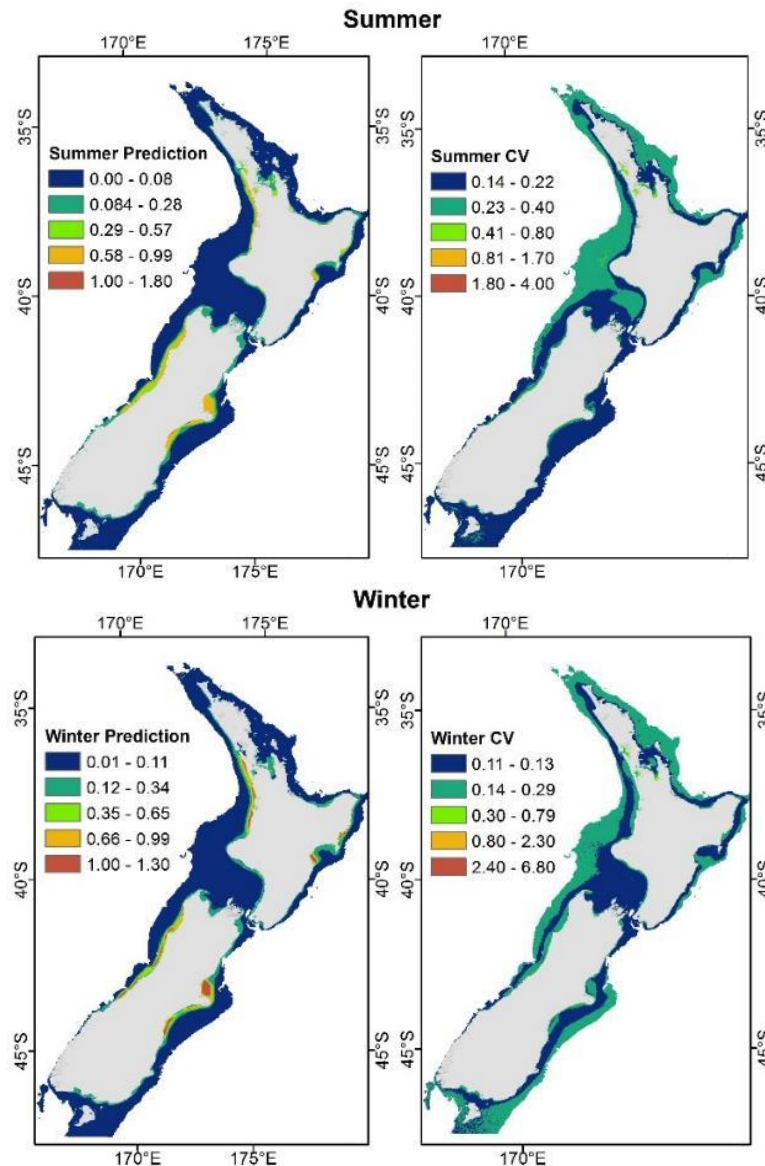
Figure 11: Predicted spatial abundance (left) and spatial CV associated with the prediction (right) of Hector's/Māui dolphins in summer (top) and winter (bottom) from the Ahuru model.

Population size predictions from habitat preference models

The ahuru model (the base model for predicting coastal Hector's/Māui dolphin spatial abundance) was used to estimate the total abundance across areas consistent with the South Island aerial surveys as well as the west coast of the North Island (Figure 12). Note that the spatial extent of the population groups is inconsistent with that of the sub-population areas used to estimate risk, and survey strata used to rescale spatial densities (comparing Figure 2 with Figure 12).

This was achieved by summing the population size estimates for each cell and dividing by 0.6, to account for the truncation of aerial survey sightings at 0.3 km either side of the survey line transect (MacKenzie & Clement 2016). This produced total population size estimates for the ECSI and WCSI that were within the 95% CI of the respective aerial survey estimates for those areas, and towards or slightly above the upper 95% CI of the aerial survey estimate for the SCSI (Table 8).

For the WCNI (marked as "MAUI" in Figure 12, although it could in theory comprise either Hector's or Māui dolphins across this area), the total population size estimates (3690 individuals in summer and 5223 in winter) was far in excess of the latest genetic mark-recapture based population size estimate of 63 Māui dolphins (95% CI = 57–75) (Baker et al. 2016a).
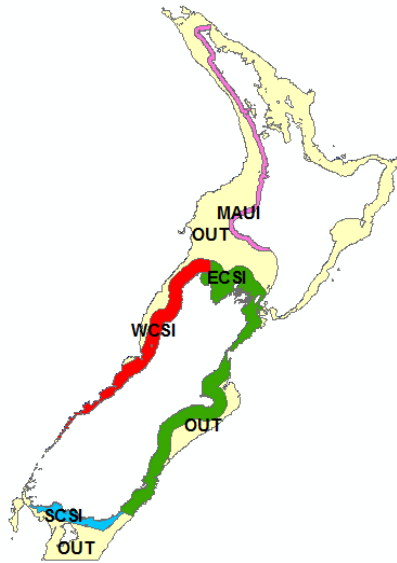
Figure 12: Spatial extent of areas used by the Hector's dolphin habitat model to estimate potential habitat capacity given the available habitat in each area (see Table 8). Area label notation was as follows: "WCSI" = West Coast South Island; "ECSI" = East Coast South Island; "SCSI" = South Coast South Island; "MĀUI" = West Coast North Island (could comprise Hector's or Māui dolphins across this area); "OUT" = all other grid cells out to a depth of 250 m. Note that these areas do not correspond with those used to define sub-populations used by the SEFRA model (Figure 2).

**Table 8: Estimated potential habitat capacity from the 'Ahuru' habitat model fitted to Hector's aerial survey observations (MacKenzie & Clement 2016; MacKenzie & Clement unpublished data for the summer survey of the south coast South Island) and used to predict the spatial abundance of Hector's dolphin. Note that the extent of the area over which the habitat model estimate was produced extends further offshore than the respective aerial surveys in many areas.**

Season	Source of estimate	Area (labels consistent with Figure 12)				
		East Coast South Island (ECSI)	South Coast South Island (SCSI)	West Coast South Island (WCSI)	West coast North Island (MĀUI)	Outside of current core distribution (OUT)
Summer	Ahuru model	8 607	675	7 038	3 690	7 215
	Aerial survey estimate	9 728 (7 001–13 517)	332 (217–508)	5 482 (3 319–9 079)	–	–
Winter	Ahuru model	10 625	800	7 643	5 223	11 238
	Aerial survey estimate	8 208 (4 888–13 785)	332 (217–508)	5 802 (3 879–8 679)	–	–

Relative abundance in harbours from public sightings

Public sightings, effort proxy and habitat variables

The habitat preference modelling used public sightings in 1 km grid cells for which habitat variables listed in Table 3 were collated. The final model used a turbidity layer that extended further into harbours than habitat variables used to identify the habitat model structure. The final model used 153 out of 173 boat-based public sighting events (88.4%) within the area extent and depth subset (see above) (Table 9). These events included 559 out of 679 sighted individuals (82.3%). The remainder of sightings events occurred in 1 km grid cells centred on land, where habitat variables were missing. A solitary offshore validated sighting was omitted from the analysis because it was located in water deeper than 250 m, for which habitat data were not collated.

The spatial distributions of boat-based public sightings and of all recreational boats recorded by aerial surveys (as a proxy for total sighting 'effort') are shown in Figure 13. The raw data are consistent with high densities of sighting effort in harbours of the west coast of the North Island and very few validated boat-based public sightings in harbours (a solitary sighting in Kaipara Harbour is the only exception to this) (Figure 13).

Table 9: Summary of annual Hector's/Māui dolphin boat-based public sightings in summer and validation categories 1-3).

Year	Sighting events		Sum of dolphins observed	
	Sightings in area and depth subset	Sightings fitted to by final habitat preference model	Sightings in area and depth subset	Sightings fitted to by final habitat preference model
1997	1	1	2	2
2004	1	1	10	10
2005	1	1	6	6
2006	2	2	13	13
2007	5	4	15	14
2008	17	13	70	56
2009	26	24	111	87
2010	12	10	61	54
2011	11	10	19	17
2012	22	18	78	65
2013	14	14	87	87
2014	16	10	59	21
2015	16	16	69	59
2016	22	22	53	44
2017	7	7	26	24
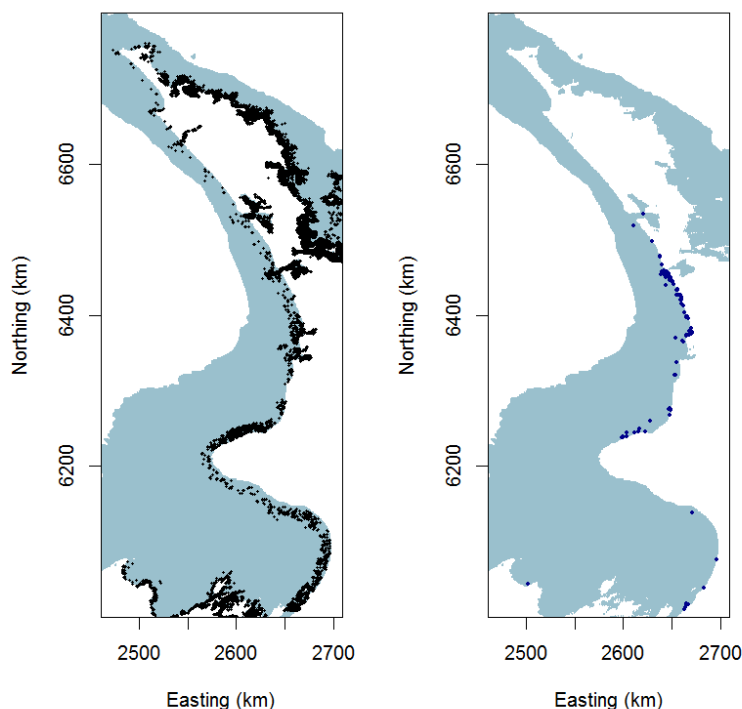
Figure 13: Spatial distribution of recreational fishing boats from aerial surveys in summer months (left panel); and spatial distribution of boat-based public sightings of Hector's and Māui dolphins attributed with validation categories 1-3 (right panel); note that the right-hand plot excludes a single sighting event in water deeper than 250 m depth (which was not included in habitat predictions because habitat variables were not collated at this depth).

Habitat variables

The habitat variables to which habitat preference models were fitted using validated public sightings are shown in Appendix 6. Note that two versions of the summer turbidity layer were used: one used to identify the optimal model structure, but that did not include measurements for the upper reaches of west coast North Island harbours (also fitted to by coastal models using aerial sightings) (Figure A6-2); and another that was used for the final prediction that included measurements in upper reaches of harbours, obtained by flooding from adjacent cells (Figure A6-3).

Model development

The initial model structure with a bivariate spline for longitude and latitude explained 81.5% of the model deviance. Of the models with an additional habitat term, only satellite-derived habitat variables (surface chlorophyll a, turbidity and downwelling light attenuation (K_{PAR})) resulted in a reduction in model AIC (Table 10). Of these, the model including turbidity had the lowest AIC (Table 10), consistent with coastal habitat models fitted to aerial survey observations, which also selected turbidity as the first model term based on AIC (Table 7). Exploration with the addition of a second habitat term routinely obtained implausible relationships, indicating overfitting to the relatively small number of positive sightings in the data subset used. As such, the turbidity model (with latitude and longitude) was retained as the optimal model structure.

Table 10: Summary of models predicting sightings of Hector's/Māui dolphins from public sightings data.

Model terms	% deviance explained	Delta-AIC
s(longitude, latitude) + s(turbidity)	81.9	0.0
s(longitude, latitude) + s(kpar)	82.2	3.7
s(longitude, latitude) + s(chlorophyll)	81.2	7.6
s(longitude, latitude)	81.5	13.4
s(longitude, latitude) + s(slope)	81.7	13.9
s(longitude, latitude) + s(redcod)	81.5	16.7
s(longitude, latitude) + s(sole)	81.4	17.6
s(longitude, latitude) + s(ahuru)	81.4	18.6
s(longitude, latitude) + s(arrowsquid)	81.4	19.2
s(longitude, latitude) + s(depth)	81.4	20.3
s(longitude, latitude) + s(stargazer)	80.9	25.4
s(longitude, latitude) + s(distance shore)	80.8	30.0
s(longitude, latitude) + s(sprat)	81.4	40.2

The optimal model structure was refitted using the turbidity layer with values estimated for upper reaches of harbours (Figure A6-3). Quantile-Quantile plots were produced for model residuals and indicated a passable model fit, i.e., residuals were at the edge of the range simulated from the fitted model (Figure 14).
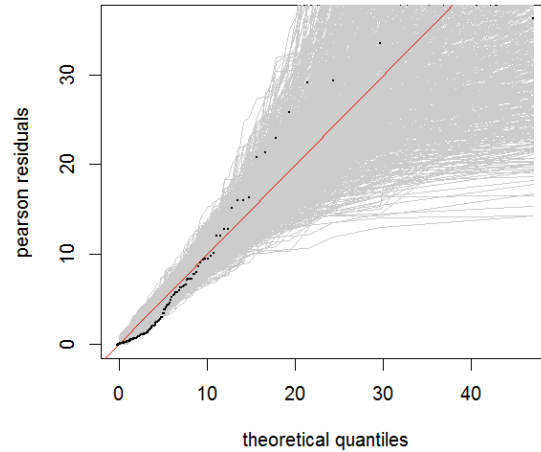
Figure 14: Simulation-based quantile-quantile plots GAMs fitting to public sightings with Pearson residuals and 200 simulation replicates.

Model predictions

Plots of model splines for the final model indicated very low abundance in low turbidity areas (in summer) (right-hand panel of Figure 15). The shape of this relationship is slightly different from that predicted from aerial survey sightings in which predicted dolphin abundance reached a plateau at high turbidity levels (Figure 10). This may be explained by the incorporation of the bivariate spline for latitude and longitude in the sightings model, which has the potential to alias for turbidity using this model structure.
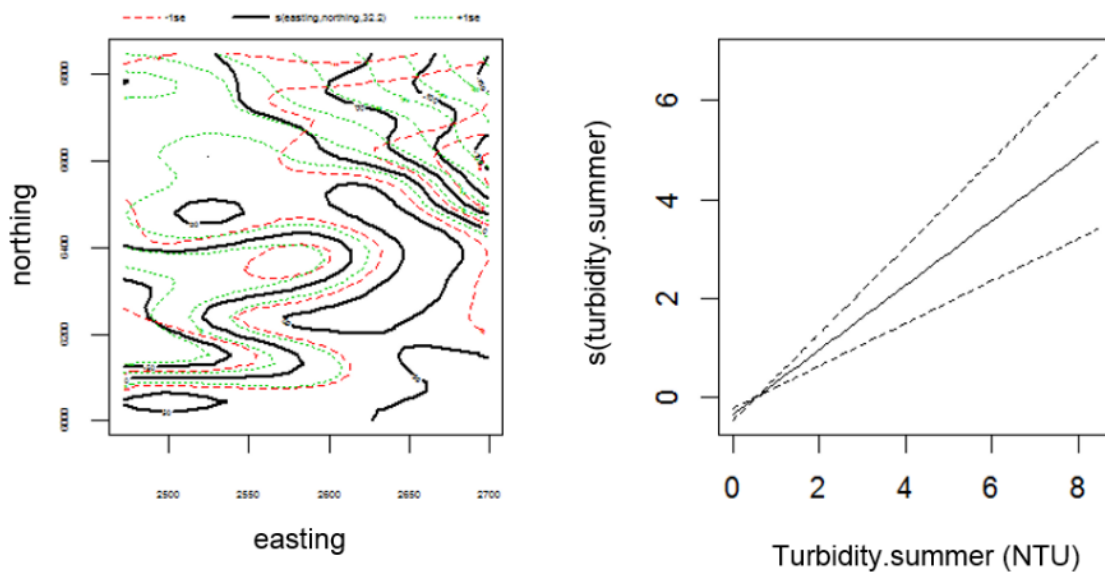
Figure 15: GAM splines of Hector's/Māui dolphin abundance in response to habitat variables for the optimal model fitting to public sightings.

With respect to model predictions of spatial abundance, the coefficient of variation (expressed as a proportion of the prediction) was lower than 0.5 across all coastal regions and harbours of the west coast North Island, and lower than 5 in the upper reaches of Manakau and Kaipara Harbours (Figure 16). The predicted abundance along the coast (relatively high abundance immediately to the south of Manakau Harbour and intermediate abundance between Kaipara Harbour in the North and New Plymouth in the South) (Figure 16) agreed strongly with estimated densities from the habitat model fitted to summer

---

aerial survey observations (i.e. constituting independent validation using a totally independent dataset) (e.g., comparing with Figure 11).
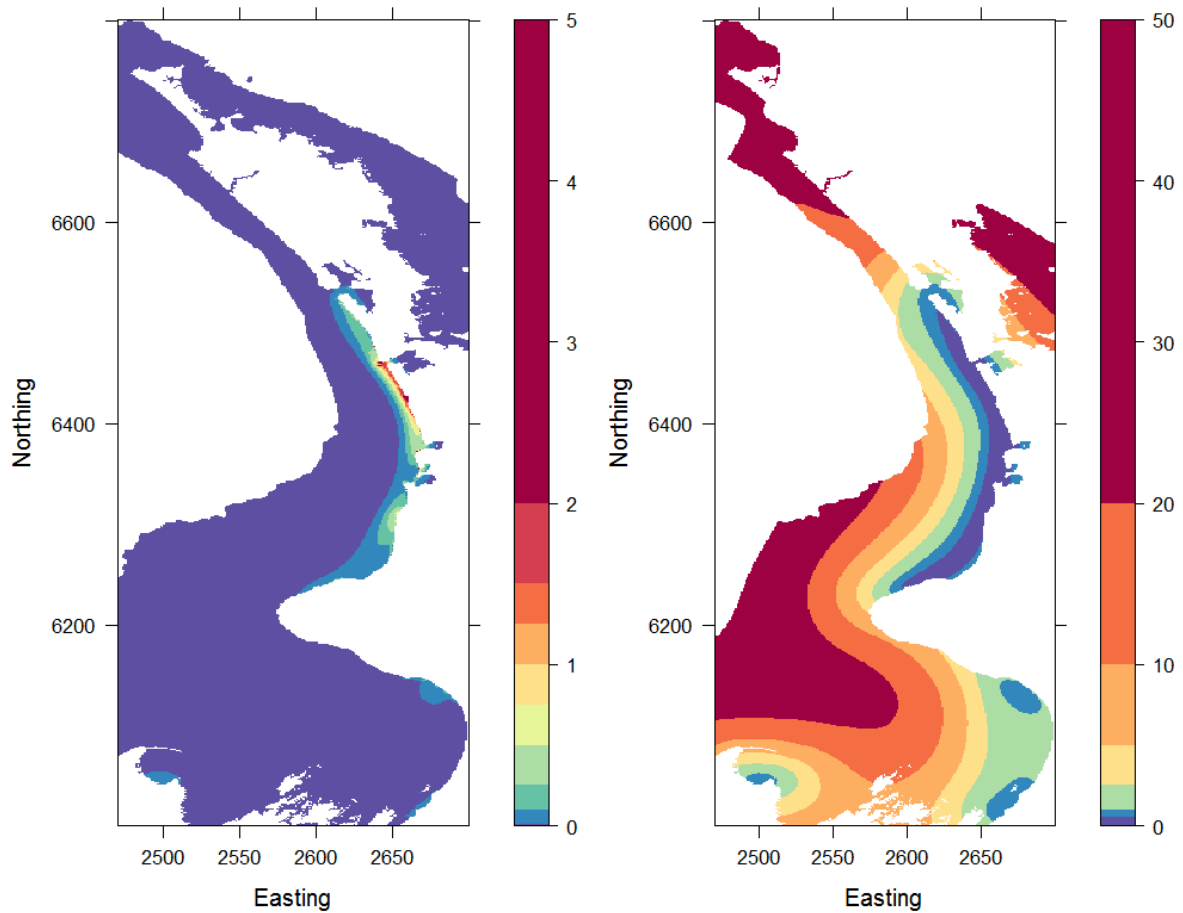
Figure 16: Estimated spatial density (left) and spatial CV associated with this model prediction (right) of Hector's/Māui dolphins off the coast of the North Island using model fitting to public sightings

Final Hector's and Māui dolphin spatial density prediction

The final seasonal spatial abundance predictions for Hector's and Māui dolphins are shown in Figure 17 and Figure 18. These are the spatial abundance predictions, post-rescaling by sub-population size (Figure 2 and Table 2). The estimated summer densities are (from visual inspection) highly correlated with the spatial distribution of public sightings of live (mostly at-sea) and dead (mostly stranded) individuals as well as commercial fisheries observer sightings and commercial fishery-reported captures (Appendix 7).
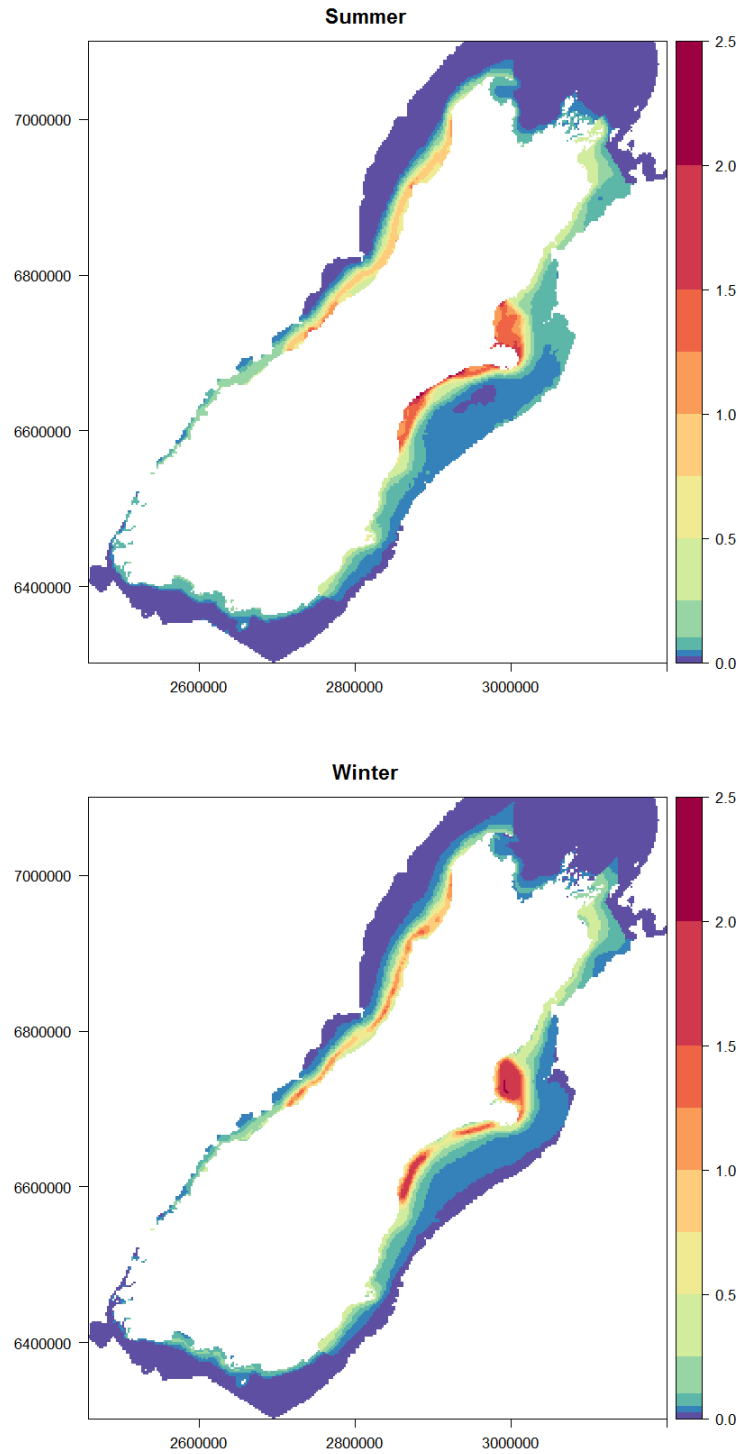
Figure 17: Final seasonal estimated spatial density of Hector's and Māui dolphins used for spatial risk assessment—South Island.
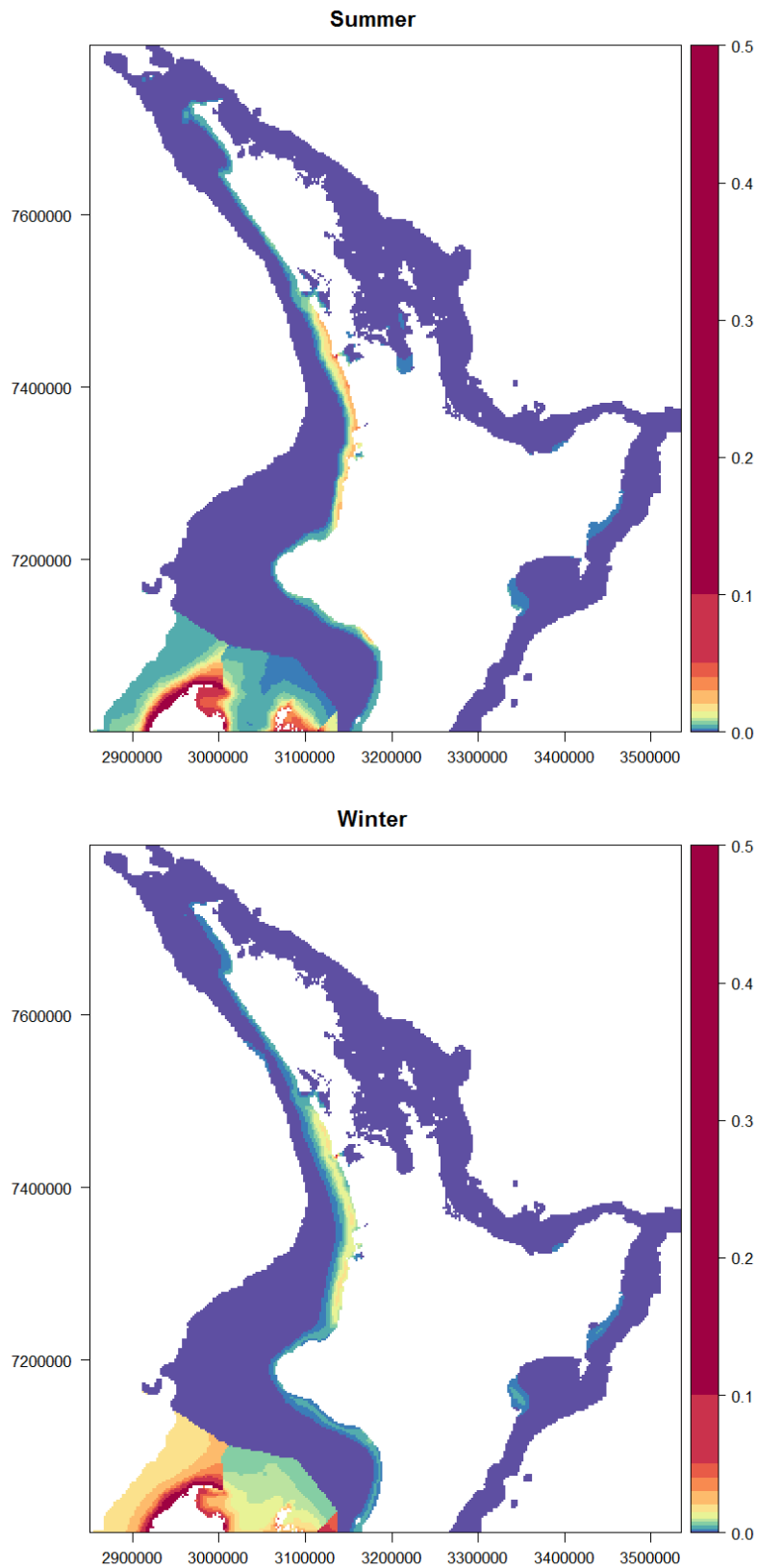
Figure 18: Final seasonal estimated spatial density of Hector's and Māui dolphins in winter used for spatial risk assessment—North Island.

Commercial fishery captures of Hector's and Māui dolphins

Commercial fisheries protected species captures data were received 3 July 2018 from Dragonfly Data Science via Fisheries New Zealand. The number of observed dolphin captures by fisheries group and fishing year from 1995/96 to 2016/17 is shown in Table 11. There have been no observed captures of Māui dolphins during this time. All 16 Hector's dolphin captures were from the East Coast of the South Island. The majority of the captures were in set nets, with just one of the captures in an inshore trawl. Only three of the 16 captures were alive.

Table 11: Observed commercial fishery captures of Hector's dolphin by fishing year between 1995/96 and 2016/17. All observed captures were from the East Coast of the South Island.

| Fishing year	Set net			Inshore trawl		
	Alive	Dead	Total	Alive	Dead	Total
1995/96	0	0	0	0	0	0
1996/97	0	0	0	0	0	0
1997/98	2	6	8	0	1	1
1998/99	0	0	0	0	0	0
1999/00	0	0	0	0	0	0
2000/01	0	0	0	0	0	0
2001/02	0	0	0	0	0	0
2002/03	0	0	0	0	0	0
2003/04	0	0	0	0	0	0
2004/05	0	0	0	0	0	0
2005/06	0	0	0	0	0	0
2006/07	0	1	1	0	0	0
2007/08	0	1	1	0	0	0
2009/10	0	2	2	0	0	0
2010/11	0	0	0	0	0	0
2011/12	0	0	0	0	0	0
2012/13	1	0	1	0	0	0
2013/14	0	1	1	0	0	0
2014/15	0	0	0	0	0	0
2015/16	0	0	0	0	0	0
2016/17	0	1	1	0	0	0
Total	3	12	15	0	1	1

Cause of death from necropsy of recovered Hector's and Māui dolphins

The necropsy diagnosis of cause of death for non-calf carcasses (n = 55) is shown in Table 12, disaggregated by sub-population. Disease (including toxoplasmosis, brucellosis, tuberculosis, pneumonia, or others) was the diagnosed cause of death for 23 out of 55 individuals. Known or probable bycatch was the diagnosed cause of death for 11 out of 55 individuals. Less frequent diagnoses were congenital deformity, predation and possible bycatch. The 'miscellaneous' category included unusual conditions such as severe parasitism with impacted stomach contents, kidney dysfunction, aortic and heart disease, and internal haemorrhage of unknown cause. An open/unknown diagnosis was made in 12 out of 55 cases.

The same data are also summarised by year (Table A4-3), sex (Table A4-5) and by maturity stage for females (Table A4-6). Notably, seven out of nine confirmed toxoplasmosis deaths were females, of which six were deemed to be mature (Table A4-5 and Table A4-6). Also, 2012 was the year with the greatest number of necropsied calves (10 individuals) and non-calves (five individuals) (Table A4-3).

For necropsied calves (Table A4-2), the most common diagnosis was maternal separation (14 out of 21 cases), followed by disease (three cases, including two cases of inflammatory heart disease and one of lung and liver disease of unknown cause), with one case each of deformity, pneumonia and known bycatch, and a single open diagnosis.

The final data fitted to by the spatial risk model are shown in Table 13. For the two populations with the greatest sample of necropsied individuals (ECSI and WCSI; also the largest populations, see Table 2) the relative proportion of toxoplasmosis, predation and other deaths were similar (Table 13). Note that bycatch diagnoses ("known", "probable" or "possible") were not fitted to by the spatial risk model since commercial fishery-related deaths were independently estimated from commercial fisheries observer data, using the standard SEFRA approach (see methods section).

Table 12: Diagnosed cause of death at necropsy – non-calves, both sexes by population (intermediate and full confidence only).

| Cause of death | Hector's dolphin | | | | Māui dolphin | Total |
	ECSI	WCSI	SCSI	WCNI	WCNI	
Brucellosis	0	1	0	0	1	2
Deformity	0	0	1	0	0	1
Disease (other)	4	2	0	1	0	7
Miscellaneous	2	2	0	0	1	5
Pneumonia	3	1	0	0	0	4
Predation	0	0	1	0	1	2
Toxoplasmosis	5	2	0	0	2	9
Tuberculosis	1	0	0	0	0	1
Known bycatch	5	0	0	0	0	5
Probable bycatch	4	2	0	0	0	6
Possible bycatch	0	1	0	0	0	1
Unknown/Open	9	3	0	0	0	12
Total	33	14	2	1	5	55

Table 13: Necropsy data used in the spatial risk model.

| Cause of death | Hector's dolphin | | | | Māui dolphin | Total |
	ECSI	WCSI	SCSI	WCNI	WCNI	
Toxoplasmosis	5	2	0	0	2	9
Predation	0	0	1	0	1	2
Other	10	6	1	1	2	20
Total	15	8	2	1	5	31

Spatial threat intensity

Threats in the spatial risk model

The spatial threat intensity layers for commercial fisheries (set net and inshore trawl) are shown in Appendix 15, along with spatial quantities (e.g. overlap) estimated by the spatial risk model. With respect to set net effort, high intensity areas include the Hauraki Gulf (but note that overlap is near zero here due to negligible dolphin densities), harbours of the west coast North Island and the Kaikoura Coast on the South Island (Figure A15-4).

The seasonal spatial threat intensities of other threats included in the spatial risk model are displayed in the other Appendices: predation by broadnose sevengill sharks (Appendix 8 with methods); and toxoplasmosis (Appendix 9 with methods). Spatial threat intensity plots for predation and toxoplasmosis are also shown in Appendix 11 alongside other spatially-resolved threats.

The spatial threat intensity for toxoplasmosis was estimated using human population density as a proxy for cat population density combined with seasonally-resolved runoff from a high spatial and temporal resolution hydrological model to estimate relative *T. gondii* oocyst densities in rivers and coastal waters. A similar approach adopted to estimate toxoplasmosis loading affecting California sea otters has been shown to produce useful predictions (VanWormer et al. 2016). The exposure of Hector's and Māui dolphins to toxoplasmosis was estimated to be highest in the following locations

- South Island—the ECSI around the estuary of the Waitaki River and the WCSI around the estuaries of the Buller and Grey Rivers; and
- North Island—the WCNI around the Waikato River in winter has the highest estimated *T. gondii* exposure of any location around New Zealand, located close to the core of Māui dolphin habitat.

Because seven-gilled sharks exhibit a habitat preference for turbid water, the predation and toxoplasmosis threat intensity layers had similar spatial patterns, with relatively high predation threat intensities estimated around the estuaries of these same major rivers. In addition to these, a relatively high predation intensity was estimated for the region around Te Waewae (Waiau River) on the SCSI (Figure A11-2).

A distinct seasonal pattern was obtained in the relative threat intensity for toxoplasmosis, with generally higher estimated oocyst densities in winter (Figure A11-1) associated with greater rainfall and river flow during the winter period (see Appendix 9). Exceptions to this include the Waitaki River on the ECSI, which has elevated flow in the summer period (Leong & Chesterton 2005) associated with increased glacial meltwater.

Other spatially-resolved threats

Regions with relatively high levels of recreational netting effort (including drag, throw and set netting) around the North Island include: the Hauraki Gulf and the Kapiti Coast and areas around the South Island include Golden Bay/Tasman Bay, Banks Peninsula and coastline adjacent to Invercargill (Figure A11-3). Of these, only set netting is thought to produce a risk to dolphins, however the recreational netting types were not adequately distinguished in the survey data from which the estimates are derived, so it was not possible in this assessment to consider set netting in isolation. The spatial pattern described above was consistent comparing two separate survey periods (2011/12 and 2017/18); these surveys were combined to produce the composite spatial layer used to estimate relative risk to the dolphins from recreational netting (Andy McKay, Fisheries New Zealand unpublished data). Note that the location of recreational netting in these data was reported only with reference to coastal features; the off-shore extent of this recreational netting effort was therefore subjectively constrained within 2 nautical miles (Andy McKay, Fisheries New Zealand unpublished data).

Current aquaculture operations are limited to small discrete areas along the coast of New Zealand, including Firth of Thames on the North Island and Golden Bay/Tasman Bay, the Marlborough Sounds, Akaroa Harbour on the Banks Peninsula and Paterson Inlet on the South Island (Figure A11-4).

Oil spill risk is relatively high in the following areas: around the NCNI between Whangarei and Tauranga; around New Plymouth; the Cook Strait region between Wellington and Picton; and around Christchurch. The ECSI north of Banks Peninsula was a region of intermediate oil spill risk, though this tended to be lower close to the shore (Figure A11-5) (Navigatus 2015).

The general spatial pattern of cumulative noise from vessel traffic (with AIS) and oil and gas seismic surveys was consistent comparing the two sample months (July of 2014 and March of 2015, related to winter and summer Hector's and Māui dolphin spatial abundance, respectively) (Figure A11-6). Vessel traffic noise was most intense on the NCNI and between New Plymouth on the WCNI and the NCSI (although with relatively low activity in the North Taranaki Bight region). The most prominent sources

of underwater noise in the modelled region (both broadband and high frequency) were two Floating Production Storage and Offloading (FPSO) facilities (UMUROA and RAROA) located to the west of Cape Egmont, but spatial overlap between noise sources and Māui dolphin densities was highest in high vessel-traffic areas around New Plymouth (see below).

5.2   Spatial overlap of threats with Hector's and Māui dolphins

Alternative presentations of spatial overlap

Spatial overlap plots relating the spatial abundance of Hector's and Māui dolphins and various threats are all displayed in Appendix 12. For lethal threats, the spatial overlap plots indicate the spatial relative density of deaths (across all sub-populations) from each respective threat. For other threats, the spatial plots give an indication of the potential spatial impact (including sublethal effects, and potentially deaths if a threat is lethal though has not yet been determined as a cause of death by necropsies) of a threat scaled by the density of Hector's and Māui dolphins.

Additionally, a relative overlap statistic was produced for each threat and sub-population (seasonally disaggregated where a respective threat was seasonal) that scaled overlap for population size in each area (Figure 2 and Table 2). The statistic was rescaled to facilitate reader comparison across sub-populations and threats, by presenting them as a proportion of the maximum value for a respective threat across all sub-populations and seasons (Table 14 and Figure 19). The overlap statistic can be interpreted as the relative threat intensity experienced by individual dolphins within a respective sub-population or summary area (Figure 2) and was calculated for all threats except underwater noise (limited spatial coverage) and commercial fisheries. For commercial fisheries and toxoplasmosis, comparable information was provided in the form of sub- population risk ratio estimates (Table 16), confirmed by similar between-sub-population patterns of risk ratio and overlap statistic values obtained for toxoplasmosis (comparing Table 14 and Table 16).

Risk model threats

Commercial fisheries

From total effort between 2014/15 to 2016/17 (observed and unobserved), the regions of greatest estimated spatial overlap with Hector's and Māui dolphins are slightly different for commercial set net and inshore trawl fisheries (Figure A15-5). For set net fisheries, there are three regions of high spatial overlap corresponding to locations with high dolphin densities in areas further offshore than the existing commercial setnet closures (from north to south):

1. Along the Kaikoura Coast;
2. In Pegasus Bay to the north of Banks Peninsula; and
3. In the Southern Canterbury Bight.

In contrast, on the WCNI, the areas of highest spatial overlap between commercial setnets and dolphins are in locations with relatively low dolphin densities, e.g., the north coast of Cape Egmont and in Kaipara Harbour (Figure A15-5). This residual overlap (hence risk) occurs primarily in low dolphin density areas reflecting the effects of past spatial management measures which have excluded commercial setnet fisheries from areas of higher Māui dolphin density.

For inshore trawl fisheries, the highest overlap with Hector's dolphins was estimated in the southern Canterbury Bight, around Timaru (Figure A15-5). On the WCNI, the location of highest estimated overlap was between Port Waikato and to the south of Kawhia, and just outside the boundary of the existing trawl fishery closure (Figure A15-5).

Toxoplasmosis

For all sub-populations, spatial overlap was increased in winter on account of relatively greater *T. gondii* oocyst loads estimated in coastal water through the winter period (Table 14, Figure 19, Figure A12-1).

With respect to overlap scaled by population size (the overlap statistic), the estimated *T. gondii* overlap was highest for the WCNI (Māui dolphin) sub-population and relatively high also in the TAKA (Taranaki to Kapiti Coast) area. This indicates that Māui dolphins (and potentially dispersing or transient Hector's dolphins elsewhere around the North Island) are likely to experience the highest mortality rates from Toxoplasmosis, relative to Hector's dolphins in the South Island, consistent with generally high *T. gondii* oocyst load estimates all around the North Island (Figure A11-1).

On the South Island, WCSI was the only sub-population for which a relatively high overlap was estimated between dolphins and *T. gondii* exposure. However, all sub-populations had an estimated overlap greater than 10% of the maximum for any sub-population (WCNI), indicating that all sub-populations will potentially be exposed to some degree of toxoplasmosis risk (Table 14, Figure 19).

Predation

Locations with relatively high estimated predator density included the WCSI, SCSI and regions of the WCNI and ECSI (Figure A11-2). In terms of spatial overlap (not scaled for population size), the greatest overlap was on the WCSI and ECSI, indicating the greatest overall *number* of predation events would occur in these regions (where Hector's dolphin are most abundant) (Figure A12-2).

When scaled for population size, dolphins on the WCSI had the highest estimated overlap with predation, followed by the SCSI (Table 14, Figure 19), indicating that the highest proportional mortality from predation would occur in these areas. A low and similar degree of overlap was estimated for all other sub-populations and summary areas except NI (North Island excluding WCNI and TAKA), where predator densities were estimated to be uniformly low (Figure A11-2).

Other threats

Recreational netting

For all sub-populations, overlap with recreational netting was estimated to be much higher in the summer period (Table 14, Figure 19). When scaled for population size, the highest overlap (and hence the highest estimated encounter rate per dolphin with recreational netting events) was estimated for the TAKA (Taranaki to Kapiti) sub-area, which was more than double any other sub-population. Relatively moderate levels of overlap (again, scaled for population size) were estimated for NI and NCSI and the lowest levels were estimated for the large Hector's dolphin populations of the ECSI and WCSI (Table 14, Figure 19).

Aquaculture

High spatial overlap with aquaculture facilities was limited to the locations of a small number of farms on the ECSI (Pegasus Bay and Cloudy Bay) and NCSI (Golden Bay and Tasman Bay). Other farms were generally in areas of low estimated Hector's or Māui dolphin density, such as Hauraki Gulf, Bay of Plenty and Hawke's Bay (all within the NI sub-population area) and so were estimated to have minimal overlap in terms of the total numbers of dolphins affected (Figure A11-4).

The greatest degree of overlap when scaling for population size, was estimated for the NCSI, indicating that the highest encounter rate per dolphin between Hector's dolphins and aquaculture facilities would occur in this area relative to other sub-populations (although note that the spatial extent of this overlap is still small) (Table 14, Figure 19).

Oil spill risk

Spatial oil spill risk is relatively high on the north coast of the North Island, Cook Strait and northern Banks Peninsula (Figure A11-5). Of these locations, only northern Banks Peninsula has a high estimated density of Hector's dolphins (Figure 17) and, so, this location has the greatest threat to dolphins in terms of number of dolphins that might be affected if oil spill events are consistent with the estimated spatial threat intensity (Figure A12-4).

When scaling for population size, the ECSI had the greatest overlap with oil spill risk (i.e., on a per individual basis, dolphins in this subpopulation are most likely to be affected) (Table 14, Figure 19).

Table 14: Relative overlap between threats and Hector's/Māui dolphins by threat, subpopulation and season. Rescaled as a proportion of the maximum value for a respective threat across all sub-populations and both seasons. Colours range from dark green (lowest overlap) to red (greatest overlap).

| Sub-population	Toxoplasmosis	Predation	Recreational netting	Oil spill risk	Aquaculture
					Summer
ECSI	0.15	0.16	0.04	0.95	0.12
SCSI	0.19	0.69	0.21	0.36	0.02
WCNI	0.20	0.23	0.16	0.08	0.00
TAKA	0.24	0.20	1.00	0.30	0.00
WCSI	0.48	1.00	0.02	0.01	0.00
NI	0.14	0.01	0.41	0.77	0.20
NCSI	0.06	0.29	0.29	0.19	1.00
					Winter
ECSI	0.26	0.15	0.01	1.00	0.17
SCSI	0.34	0.68	0.02	0.38	0.01
WCNI	1.00	0.20	0.02	0.10	0.00
TAKA	0.82	0.22	0.09	0.34	0.00
WCSI	0.71	0.98	0.01	0.01	0.00
NI	0.73	0.01	0.05	0.67	0.20
NCSI	0.12	0.33	0.05	0.18	0.80
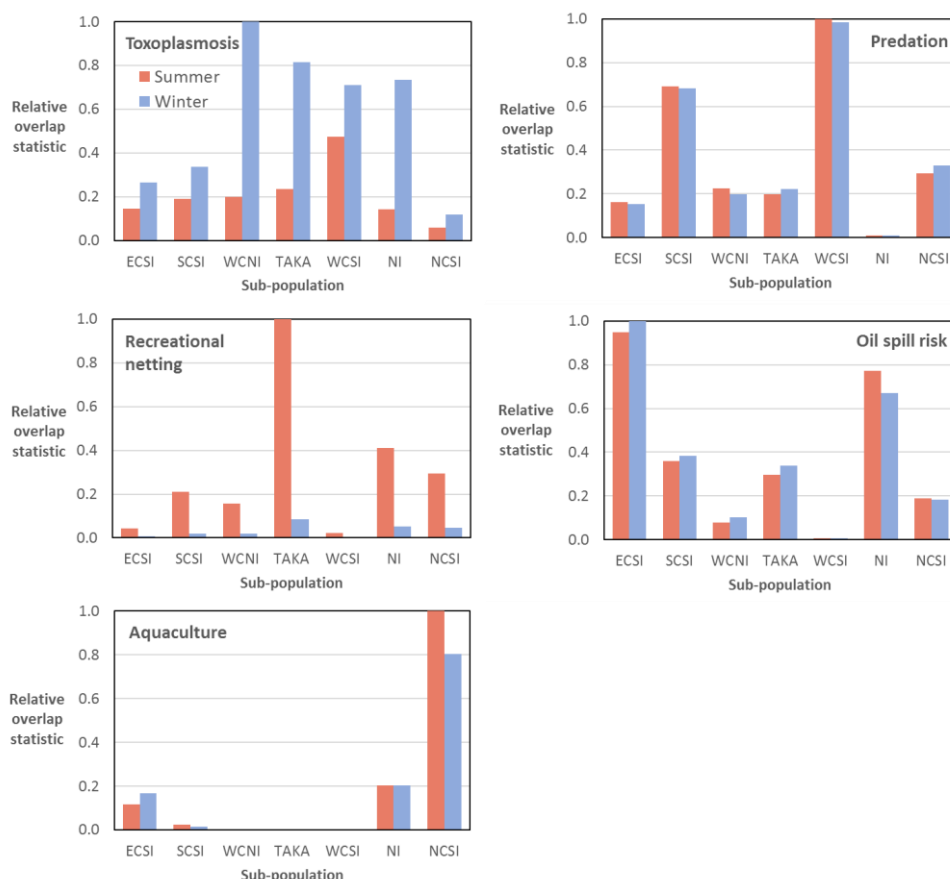
Figure 19: Relative overlap statistic between threats and Hector's/Māui dolphins by threat, subpopulation and season. Rescaled as a proportion of the maximum value for a respective threat across all sub-populations and season. A graphical representation of the same estimates in Table 14.

5.3   Model estimates of annual deaths and risk

Risk model diagnostics

MCMC diagnostics

SEFRA model diagnostics can be found in Appendix 13. MCMC mixing for all model parameters were acceptable across all four MCMC chains (Figure A13-1). The prior and the posterior distributions were equivalent for the population size (N_s) and probability observable parameters (p_g^{obs}) (Figure A13-2). The posterior updates the prior for the vulnerability parameters (v_g) and probability of live capture parameters (ψ_g) (Figure A13-2). The model fit is excellent with respect to the observed and predicted number of captures (Figure A13-3).

Spatial fit to observed captures

The spatial agreement between actual observed captures in commercial set nets and captures predicted by the risk model was very good (Figure A15-3, top), i.e., relatively high observed captures in the region of Kaikoura and the Canterbury Bight correspond well with predicted patterns. This result suggests that the estimated spatial density of the dolphins is a good approximation to their true spatial density and that vulnerability (probability of capture or death per encounter) is relatively constant in space and time. Too few captures were observed in the inshore trawl fishery to allow for a meaningful comparison with model estimated captures, though the single observed capture event was in an area of relatively high estimated captures in southern Canterbury Bight (Figure A15-3). No captures were recorded on observed trawls in a region immediately to the north of Banks Peninsula, where the estimated observed captures were relatively high (Figure A15-3). However, vessel-reported trawl capture events have been recorded there since 2014/15, and all other vessel-reported trawl captures since then were located on the east coast of the South Island and in areas of relatively high model-predicted observed captures (DOC 2019). There were no observed captures in observed WCNI commercial set net fisheries; this is consistent with model predictions, for which estimated numbers of observed captures are close to zero, reflecting very low estimated captures in the present, and low observer coverage in the past when estimated capture rates were higher.

Risk model outputs

Annual deaths

Because species vulnerability reflects inherent biological and physiological properties of the species (i.e., it does not vary in space and time) and there is only a single fishery group for setnet fishing and a single fishery group for inshore trawls the estimated spatial distribution of captures and deaths for setnets and for trawls will have exactly the same spatial pattern as the corresponding spatial overlap (comparing A15-6 with A15-5).

With respect to annual deaths, commercial set net fisheries are estimated to kill considerably more Hector's and Māui dolphins than inshore trawl fisheries (Table 15 and Figure 20), despite higher levels of effort (reflecting much lower dolphin catchability in trawls relative to setnets, and higher cryptic mortality in setnets relative to trawls). The ECSI was the sub-population with the greatest estimated number of annual deaths from both commercial set nets (38.9 individuals per annum, 95% CI = 18.6–88.3) and inshore trawls (3.0 individuals per annum, 95% CI = 0.1–15.6) across the period 2014/15 to 2016/17. For the WCSI, the estimated annual deaths are low from both commercial set nets (0.3 individuals per annum, 95% CI = 0.2–0.7) and inshore trawls (1.8 individuals per annum, 95% CI = 0.1–9.4) (Table 15, Figure 20 and Figure 21).

Fisheries observers have recorded a single Hector's dolphin capture in the inshore trawl fisheries. Of the 13 inshore trawl events since 1977 on which Hector's dolphins were reported as captured by the fishing industry, six captured more than one individual, with a maximum of four individuals captured

by a single trawl. A mean of 1.92 individuals per positive capture event was obtained for inshore trawls using fishing industry reported capture records (this includes three individuals reported captured on a single trawl in 2019). Assuming that two individuals were captured per inshore trawl event with a capture, this would lead to a doubling of the estimated annual deaths from the risk model (Table A17-1 compared with Table 15).

Estimated annual deaths from toxoplasmosis were greater than those from commercial fisheries for all sub-populations. This was the case for the model run assuming an equal detection probability of non-fishery causes of death and for the predation sensitivity model run, assuming a 10-fold reduction in the detection of predation events. The highest number of annual toxoplasmosis deaths was estimated for the WCSI population (187.0 individuals per annum, 95% CI = 67.9–432.1); this estimate was lower for the predation sensitivity (106.8 individuals per annum, 95% CI = 32.7–284.4) under which predation was responsible for a corresponding increased proportion of non-fishery deaths (Table 15, Figure 20 and Figure 21).

For the WCNI where Māui dolphins occur (labelled "MĀUI" in Table 15), the estimated annual deaths from toxoplasmosis (1.9 individuals per annum, 95% CI = 1.0–3.3) were much higher than from either commercial set nets (0.1 individuals per annum, 95% CI = 0.0–0.3) or the inshore trawl fishery (0.0 individuals per annum, 95% CI = 0.0–0.1) (Table 15, Figure 20 and Figure 21). This was also the case for the predation sensitivity model run, which estimated a slightly lower number of annual deaths from toxoplasmosis (1.1 individuals per annum, 95% CI = 0.4–2.3), but under which toxoplasmosis remained a substantially greater threat than commercial fishing (Table 15, Figure 20 and Figure 21).

Table 15: Risk model estimates of annual deaths for commercial fisheries, toxoplasmosis, predation and other non-fishery causes by sub-population (defined in Table 2), showing the median and 95% credible intervals.

Cause of death	Sub-population	Deaths equal detection			Deaths predation sensitivity		
		50.0%	2.5%	97.5%	50.0%	2.5%	97.5%
Set net	MĀUI	0.10	0.00	0.30	0.10	0.00	0.30
Set net	NI*	0.07	0.04	0.17	0.08	0.04	0.17
Set net	TAKA	0.06	0.03	0.13	0.06	0.03	0.13
Set net	NCSI	0.65	0.31	1.47	0.65	0.32	1.49
Set net	WCSI	0.32	0.15	0.74	0.33	0.16	0.75
Set net	ECSI	38.86	18.57	88.25	39.14	19.41	89.42
Set net	SCSI	0.80	0.38	1.81	0.80	0.40	1.84
Inshore trawl	MĀUI	0.00	0.00	0.05	0.00	0.00	0.05
Inshore trawl	NI*	0.00	0.00	0.02	0.00	0.00	0.02
Inshore trawl	TAKA	0.00	0.00	0.00	0.00	0.00	0.00
Inshore trawl	NCSI	0.10	0.00	0.54	0.10	0.00	0.59
Inshore trawl	WCSI	1.84	0.08	9.40	1.77	0.07	10.29
Inshore trawl	ECSI	3.04	0.14	15.56	2.93	0.12	17.04
Inshore trawl	SCSI	0.11	0.00	0.56	0.11	0.00	0.62
Toxoplasmosis	MĀUI	1.90	0.96	3.27	1.11	0.44	2.31
Toxoplasmosis	NI*	0.25	0.09	0.58	0.14	0.04	0.38
Toxoplasmosis	TAKA	0.40	0.15	0.93	0.23	0.07	0.61
Toxoplasmosis	NCSI	1.10	0.40	2.54	0.63	0.19	1.67
Toxoplasmosis	WCSI	187.03	67.86	432.09	106.80	32.69	284.43
Toxoplasmosis	ECSI	115.06	41.75	265.81	65.70	20.11	174.97
Toxoplasmosis	SCSI	5.05	1.83	11.67	2.88	0.88	7.68
Predation	MĀUI	0.53	0.11	1.42	3.04	1.05	5.27
Predation	NI*	0.00	0.00	0.00	0.01	0.00	0.02
Predation	TAKA	0.03	0.01	0.11	0.19	0.05	0.44
Predation	NCSI	0.77	0.16	2.63	4.47	1.19	10.56
Predation	WCSI	62.64	12.72	214.41	363.62	97.13	859.84
Predation	ECSI	17.64	3.58	60.37	102.38	27.35	242.09
Predation	SCSI	2.63	0.53	9.00	15.26	4.08	36.08
Other	MĀUI	4.06	2.65	5.99	2.35	1.15	4.27
Other	NI*	0.42	0.17	0.88	0.24	0.08	0.57
Other	TAKA	0.56	0.23	1.16	0.32	0.11	0.75
Other	NCSI	9.06	3.69	18.78	5.22	1.77	12.15
Other	WCSI	232.05	94.49	480.99	133.72	45.30	311.15
Other	ECSI	411.79	167.67	853.54	237.29	80.39	552.14
Other	SCSI	14.05	5.72	29.13	8.10	2.74	18.84

*The "NI" area is a hyopthetical distribution and much of the overlap is in the Huaraki Gulf where there have been no sightings, thus these numbers are not meaningful
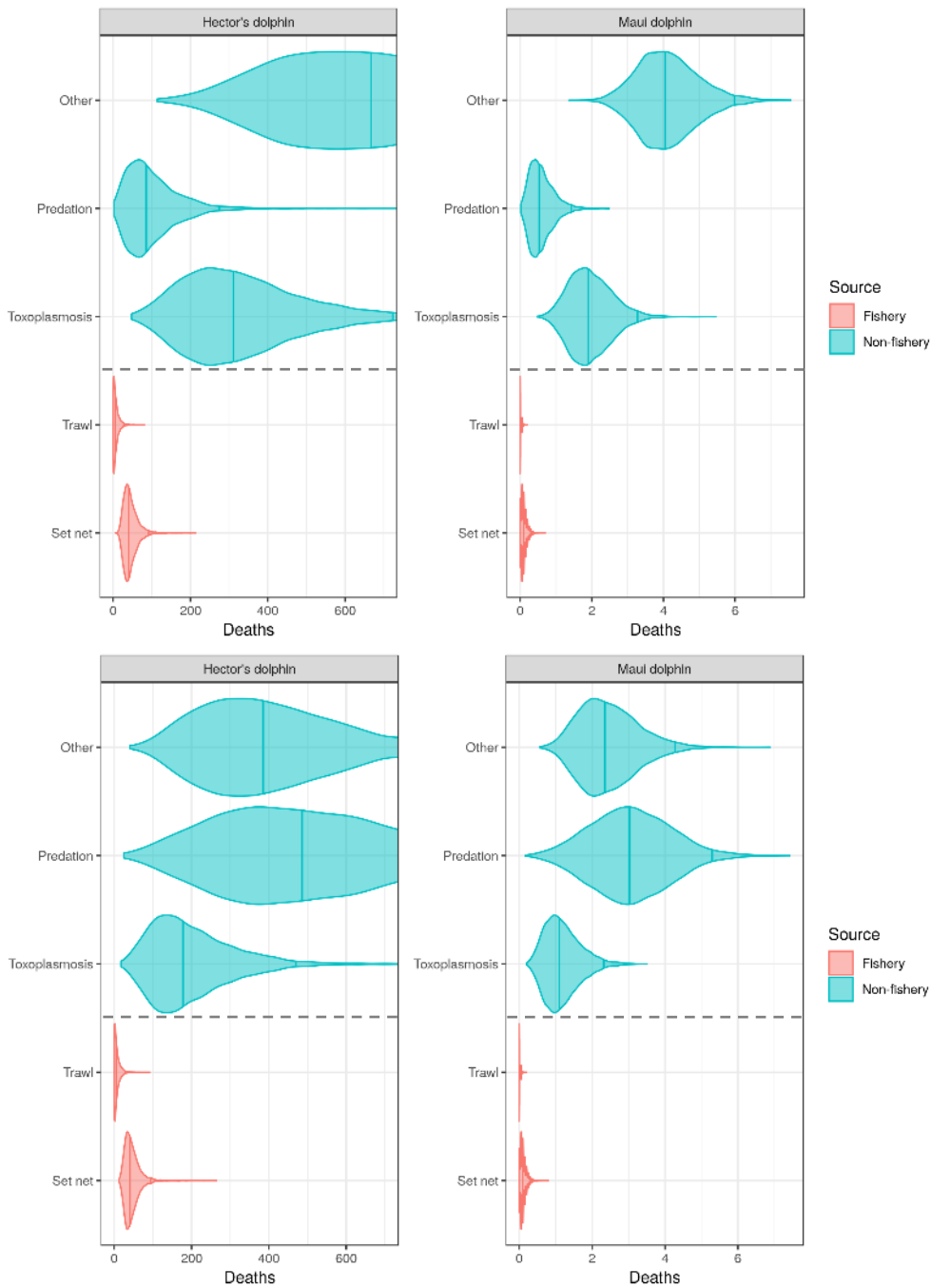
Figure 20: Annual estimated commercial fishery (set net and inshore trawl) and non-fishery (toxoplasmosis, predation and other) deaths for Hector's (left) and Māui dolphins (right), assuming equal detection probability of non-fishery causes of death (top), or a ten-fold reduction in the relative detection probability of predation mortality (bottom). The median and 97.5% quantile are indicated as vertical lines within each density. Dashed lines delineate threats for which differing methods were used to estimate annual deaths (above the line = based on proportions in the necropsied sample; below the line = using observer and vessel-reported commercial fishery data).
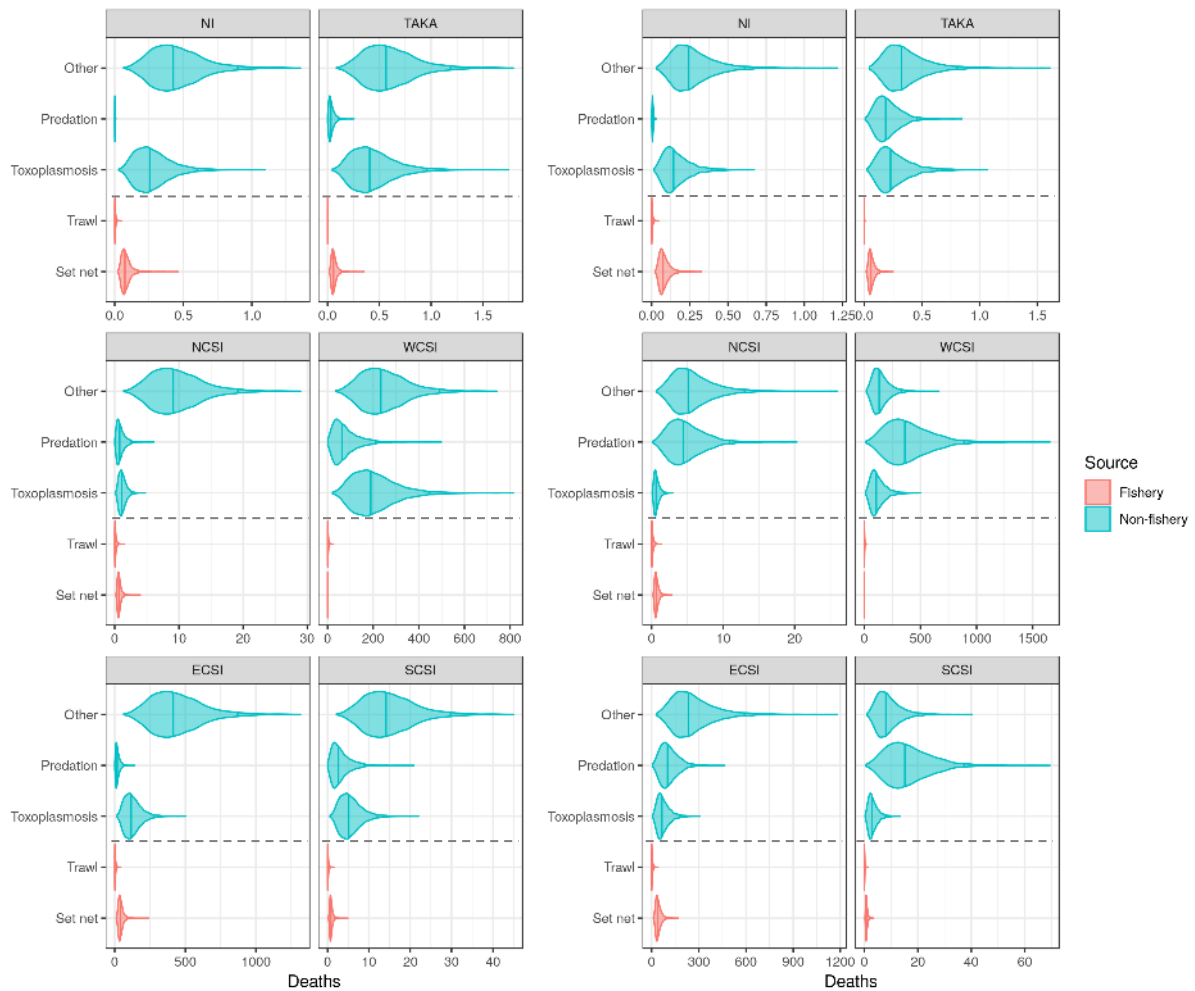
Figure 21: Annual estimated commercial fishery (set net and inshore trawl) and non-fishery (toxoplasmosis, predation and other) deaths for Hector's dolphins by sub-population or summary area (defined in Table 2), assuming equal detection probability of non-fishery causes of death (left-hand panel of plots), or a ten-fold reduction in the relative detection probability of predation mortality right-hand panel of plots). The median and 97.5% quantile are indicated as vertical lines within each density. Dashed lines delineate threats for which differing methods were used to estimate annual deaths (above the line = based on proportions in the necropsied sample; below the line = using observer and vessel-reported commercial fishery data).

Annual risk

Spatial plots of annual risk ratio were produced highlighting locations where estimated annual deaths from commercial fisheries were highest relative to the estimated PST (Figure A15-7). These had a similar spatial pattern to the spatial overlap and death plots, with the highest contribution to sub-population-scale risk arising from the commercial set net fishery along the Kaikoura Coast, in Pegasus Bay north of Banks Peninsula and in the southern Canterbury Bight. From inshore trawls, the locations contributing most to the sub-population-scale risk ratio were in the southern Canterbury Bight, close to Timaru (Figure A15-7), but collectively trawl risk remains substantially lower than commercial set net risk.

For commercial set net fisheries, the upper 95% credible interval of the risk ratio (calculated as estimated deaths as a proportion of the estimated population sustainability threshold (PST)) was above 1 for all sub-populations, except the West Coast South Island. However, the median value of risk ratio was below 1 for all sub- populations except for the east and north coasts of the North Island (risk ratio of 1.61) (Table 16, Figure 22 and Figure 23). That is, for all other sub-populations, the best estimate of annual mortalities for either of the assessed commercial fisheries did not exceed the annual PST between

2014/15 and 2016/17, indicating that the recent mortality levels for these fisheries would not individually depress the equilibrium population below 90% of carrying capacity (i.e., assuming a calibration coefficient (ϕ) value of 0.2). Despite the credible intervals for inshore trawl fisheries being broad, the upper 95% CI of the risk ratio did not exceed 0.63 for any sub-population) (Table 16, Figure 22 and Figure 23). When doubling estimated deaths and risk ratios for inshore trawls (consistent with the mean of 1.9 individuals per capture event reported by the fishing industry since 1973) the upper 95% CI of the risk ratio exceeded 1 for the NCSI only (1.26), and the median risk ratio was 0.20 or lower for all sub-populations (Table A17-2).

With respect to toxoplasmosis, the median estimated annual risk ratio exceeded 1 for all sub-populations when assuming equal detection probability of non-fishery causes of death. For the predation sensitivity model run, all sub-populations except the north coast of the South Island were estimated to have a median risk ratio above 1 (Table 16, Figure 22 and Figure 23), such that the estimated number of annual deaths would be sufficient to depress the equilibrium population below 90% of carrying capacity, given the calibration coefficient (ϕ) value of 0.2 used in the PST calculation. Uncertainty with respect to the annual risk ratio for toxoplasmosis was generally high (e.g., 95% CI = 3.2–14.8 for the WCNI, where Māui dolphin occurr).

A sensitivy model run assuming a calibration coefficient (ϕ) value of 0.5 (consistent with population recovery to at least 75% of carrying capacity) obtained risk ratio estimates approximately 2.5-times lower than the run assuming a calibration coefficient (ϕ) value of 0.2 (comparing Table A14-3 and Table A14-4) (also compare Table A17-2 and Table A17-3). For this model run, the median risk for toxoplasmosis still exceeded one for nearly all populations (the north coast of the North Island was the single exception) and was higher than the median risk ratio of commercial set netting for most populations regardless of the assumption of relative detection probability (Table 16).

Note that under the default assumption of linear density dependence, the equilibrium population outcome scales directly with the combined risk ratio for all anthropogenic threats (corresponding to the proportion of r^{max} that is killed). This allows the translation of risk scores other than 1 to a corresponding population outcome, i.e., using the risk ratio definition in Table 16 ($\phi = 0.2$) a combined anthropogenic risk score of 1 corresponds to a population outcome at 90% of unimpacted status; a risk ratio of 2 corresponds to a population outcome at 80% of unimpacted status; and a risk ratio of 5 corresponds to a population outcome at 50% of unimpacted status. Note also that risk scores arising from different anthropogenic threats are additive.

Table 16: Risk model estimates of annual risk ratio for commercial fisheries and toxoplasmosis by sub-population (defined in Table 2), assuming a calibration coefficient (ϕ) of 0.2. Colours range from dark green (lowest risk ratio) to red (greatest risk ratio).

Cause of death	Sub-population	Risk ratio equal detection			Risk ratio predation sensitivity		
		50.0%	2.5%	97.5%	50.0%	2.5%	97.5%
Set net	MAUI	0.28	0.00	1.23	0.30	0.00	1.30
Set net	NI*	1.61	0.68	4.23	1.63	0.72	4.57
Set net	TAKA	0.94	0.39	2.46	0.95	0.42	2.66
Set net	NCSI	0.65	0.27	1.72	0.66	0.29	1.85
Set net	WCSI	0.01	0.01	0.03	0.01	0.01	0.04
Set net	ECSI	0.86	0.36	2.27	0.87	0.39	2.45
Set net	SCSI	0.52	0.22	1.36	0.52	0.23	1.47
Inshore trawl	MAUI	0.00	0.00	0.30	0.00	0.00	0.29
Inshore trawl	NI*	0.07	0.00	0.42	0.07	0.00	0.44
Inshore trawl	TAKA	0.01	0.00	0.05	0.01	0.00	0.05
Inshore trawl	NCSI	0.10	0.00	0.63	0.10	0.00	0.66
Inshore trawl	WCSI	0.07	0.00	0.43	0.07	0.00	0.45
Inshore trawl	ECSI	0.07	0.00	0.40	0.07	0.00	0.42
Inshore trawl	SCSI	0.07	0.00	0.43	0.07	0.00	0.45
Toxoplasmosis	MAUI	6.81	3.17	14.73	4.01	1.47	10.47
Toxoplasmosis	NI*	5.38	1.87	14.21	3.14	0.91	9.41
Toxoplasmosis	TAKA	6.47	2.25	17.07	3.77	1.10	11.31
Toxoplasmosis	NCSI	1.10	0.38	2.90	0.64	0.19	1.92
Toxoplasmosis	WCSI	7.30	2.54	19.27	4.26	1.24	12.77
Toxoplasmosis	ECSI	2.53	0.88	6.68	1.48	0.43	4.43
Toxoplasmosis	SCSI	3.26	1.13	8.59	1.90	0.55	5.69

*The "NI" area is a hyopthetical distribution and much of the overlap is in the Huaraki Gulf where there have been no sightings, thus these numbers are not meaningful
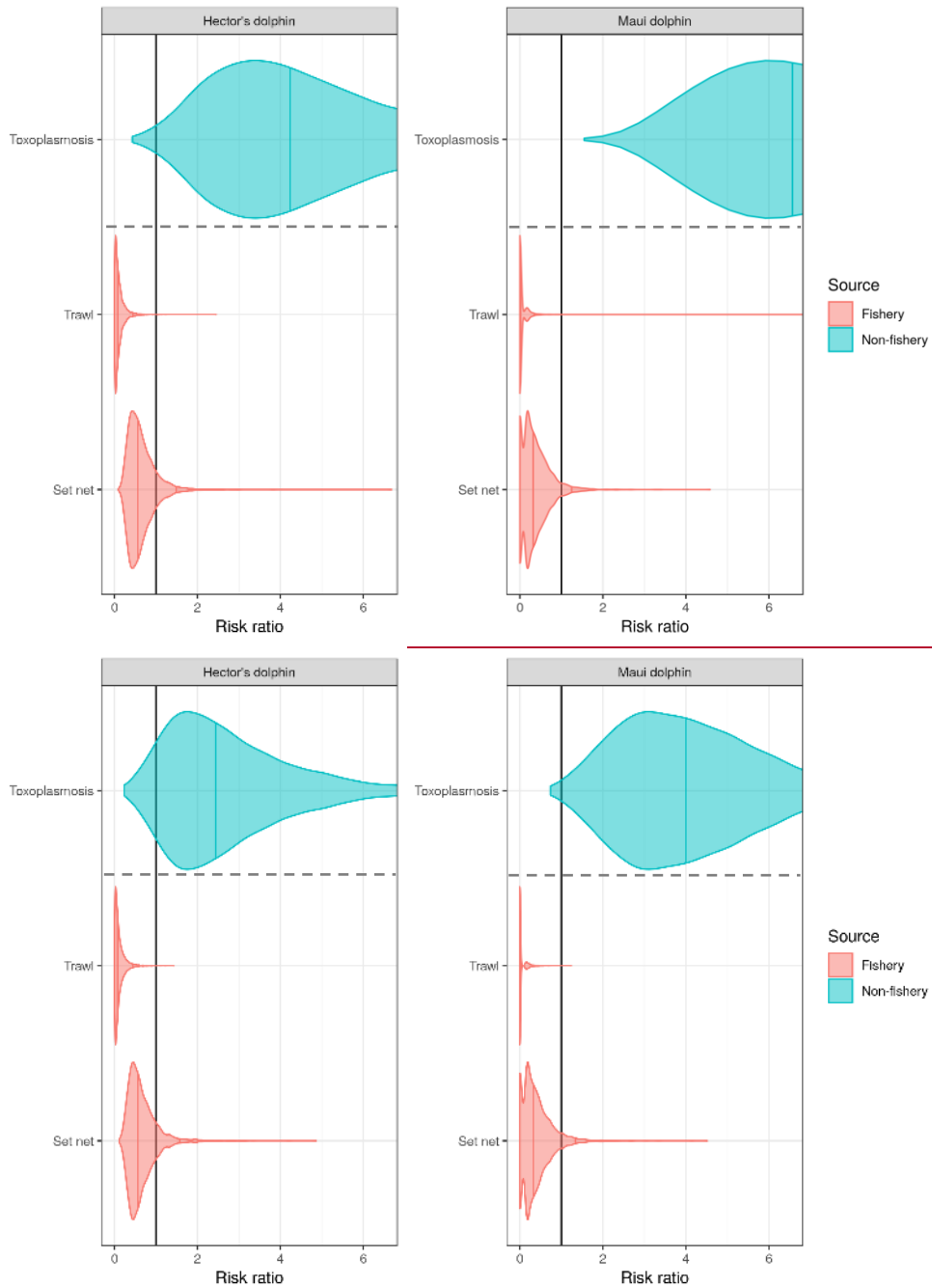
Figure 22: Annual commercial fishery (set net and inshore trawl) and toxoplasmosis risk ratios for Hector's dolphins (left) and Māui dolphins (right), assuming equal detection probability of non-fishery causes of death (top), or a ten-fold reduction in the relative detection probability of predation mortality (bottom). The median and 97.5% quantile are indicated as vertical lines within each density. Dashed lines delineate threats for which differing methods were used to estimate annual risk ratio (above the line = based on proportions in the necropsied sample; below the line = using observer and vessel-reported commercial fishery data).
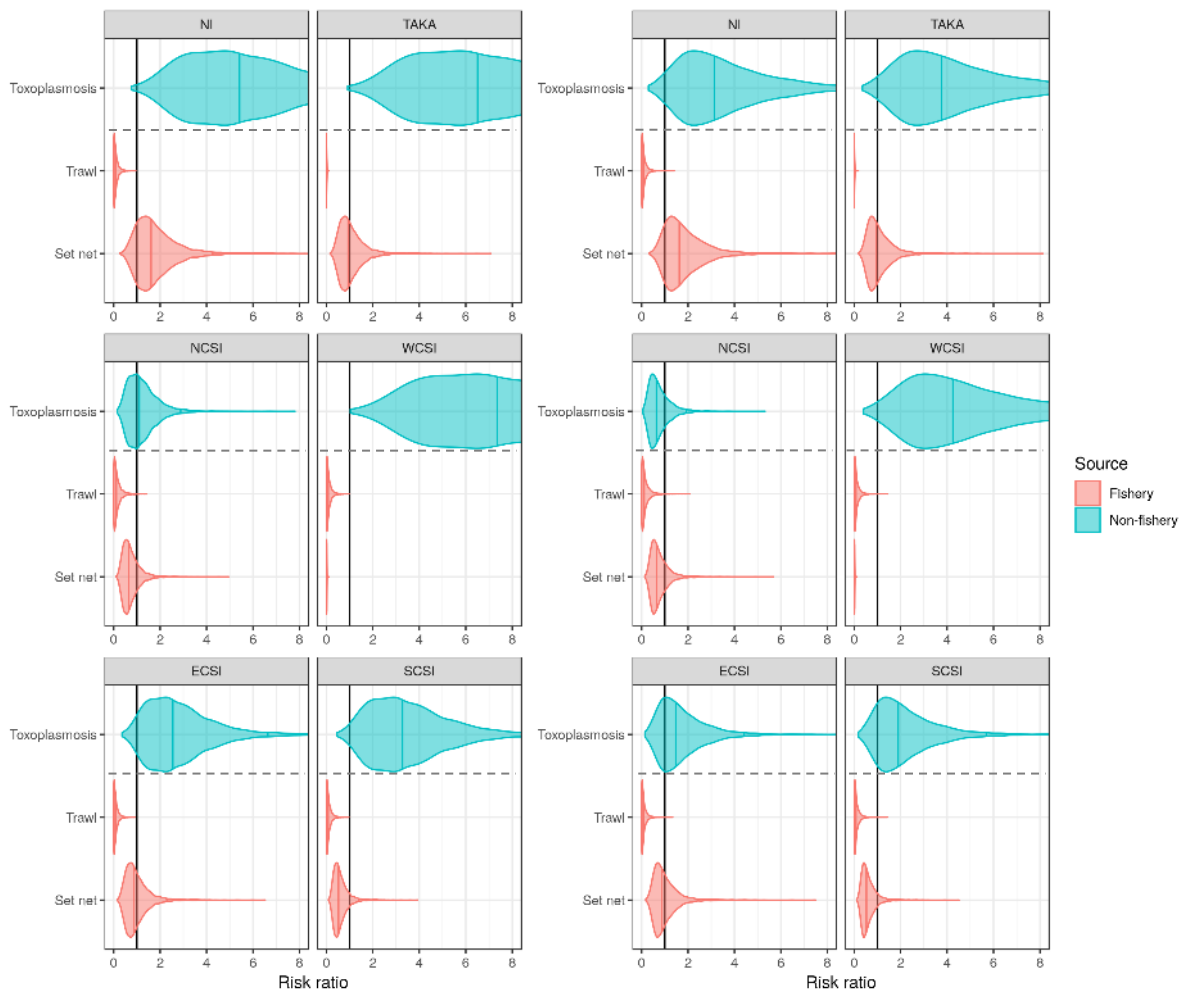
Figure 23: Annual commercial fishery (set net and inshore trawl) and toxoplasmosis risk ratios for Hector's dolphins by summary area (defined in Table 2), equal detection probability of non-fishery causes of death (left-hand panel of plots), or a ten-fold reduction in the relative detection probability of predation mortality right-hand panel of plots). The median and 97.5% quantile are indicated as vertical lines within each density. Dashed lines delineate threats for which differing methods were used to estimate annual risk ratio (above the line = based on proportions in the necropsied sample; below the line = using observer and vessel-reported commercial fishery data).

Changes in risk through time

For the commercial set net and inshore trawl fisheries, the total number of fishing events, spatial overlap, annual deaths, and annual risk ratio were estimated for individual years from 1992/93 to 2016/17 for Māui dolphins (WCNI) and Hector's dolphins (all other areas aggregated) (Figure A16-1, Figure A16-2, Figure A16-3 and Figure A16-4).

With respect to the commercial set net fishery, a decline in total effort has occurred in the areas occupied by both Hector's (Figure A16-1) and Māui dolphins (Figure A16-2). For Hector's dolphin sub-populations, the spatial overlap per unit effort has fluctuated throughout the time period, causing fluctuations in estimated annual deaths and risk ratio, although the median risk ratio did not exceed 1 for any single year (across the sub-species) (Figure A16-1). For Māui dolphin, the trend in estimated overlap per unit effort increased slightly between 1992/93 and 2006/07, then decreased until the latest year. In tandem with the reduction in overall effort, this led to a decrease in estimated annual deaths and risk ratio since the early 2000s (Figure A16-2). The median risk ratio was close to 1 for Māui dolphin in all years between 1996/97 and 2002/03 and has gradually declined in subsequent years. Assuming that commercial set net vulnerability has not changed over time, this indicates that, in the absence of other anthropogenic threats, annual commercial set net deaths are unlikely to have been sufficient to suppress the population of Hector's or Māui dolphins below 90% of carrying capacity

across the period 1992/93 to 2016/17 (or to prevent their recovery to levels above 90%, assuming the population started from a level lower than this).

For the inshore trawl fishery, a declining trend in annual deaths and risk ratio was estimated for both Hector's and Māui dolphins. This was driven by declining trends in effort and spatial overlap per unit effort with Hector's and Māui dolphins (Figure A16-3 and Figure A16-4). The estimated annual commercial set net deaths since 1992/93 were highly unlikely to depress either Hector's or Māui dolphin populations to below 90% of carrying capacity (or to prevent their recovery to these levels). The median estimate of risk ratio for inshore trawl fisheries did not exceed 0.25 for Hector's or Māui dolphins in any year since 1992/93.

6.   DISCUSSION
6.1   Demographic inputs

Intrinsic population growth rate (r^{max})

This assessment updated the base case estimate of intrinsic rate of population growth ($r^{\max}$) for Hector's dolphins (Edwards et al. 2018, updated by Appendix 3), based on a life history invariant with optimal generation time (the mean age of breeders during optimal population growth) observed across vertebrate species including other cetaceans (Dillingham et al. 2016; Moore 2015). The revised estimate for Hector's dolphins ($r^{\max} = 0.050$; 95% CI = 0.029–0.071) is almost triple the base case value applied for the TMP risk assessment for Māui dolphins of 0.018 (Currey et al. 2012). The SEFRA derivation of the annual PST follows the PBR calculation in that there is a direct linear relationship between the input value of $r^{\max}$ and the threshold of annual deaths obtained (i.e. a doubling of $r^{\max}$ will lead to a doubling of the annual PST or PBR). As such, with all other inputs to the PST calculation being equal, assuming the updated value of $r^{\max}$ effects an almost 3-fold increase in the estimated annual anthropogenic mortality that may be borne by Hector's and Māui dolphins whilst meeting the same respective population recovery reference point.

Slooten & Lad (1991) developed the previous base case value of $r^{\max} = 0.018$ using Leslie matrix population models incorporating the sparse information on Hector's dolphin fecundity and survival-at-age available at the time. The estimation procedure used by Slooten & Lad (1991) assumed a survivorship curve modified from a seal population by arbitrarily halving annual mortality at all ages (i.e. it did not use demographic rate estimates for Hector's dolphins). Also, their models assumed a maximum longevity of twenty years. The most recent published age distribution from the Banks Peninsula mark-recapture data set indicates that approximately 10% of individuals first observed in the mid-1980s have been observed over twenty subsequent years up to the 2005/06 field season (Gormley 2009, i.e. with a minimum age of twenty). As such, the demographic assumptions used to generate $r^{\max}$ = 0.018 needed revision.

The revised estimate of $r^{\max}$ used updated demographic information for Hector's dolphins and followed the method proposed by Dillingham et al. (2016), as implemented by Moore (2015). The revised estimate for Hector's dolphins ($r^{\max} = 0.050$; 95% CI = 0.029–0.071) is now consistent with the life history characteristics for this species, including estimated age at first reproduction (Duncan et al. 2007, Figure 24).
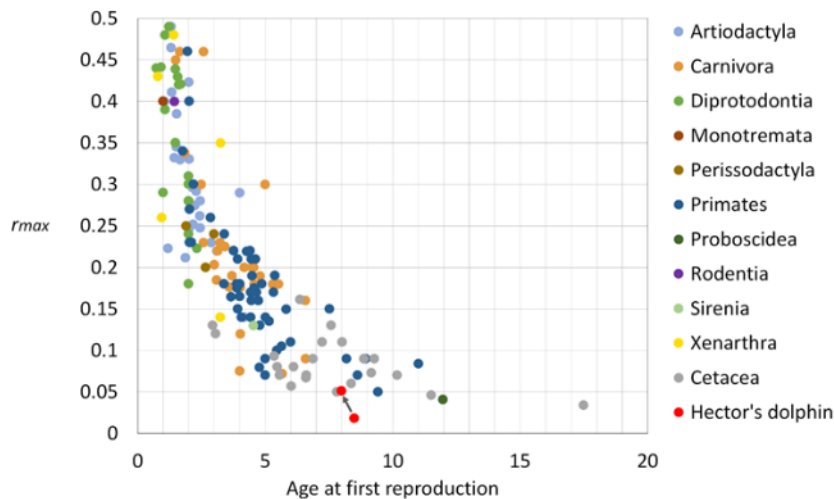
Figure 24: Comparative plot of $r^{\max}$ against age at first reproduction (AFR) for a variety of mammalian orders (Duncan et al. 2007). For Hector's dolphin, both the previous and updated values are shown (red points with an arrow between). The updated value of $r^{\max}$ derived here for Hector's dolphin is now consistent with that expected from other mammals, given estimated age at first reproduction.

For the Māui dolphin population, population simulations using an individual-based model in VORTEX assessed small population size effects on the achieved maximal growth rate given that demographic rates were consistent with $r^{\max} = 0.050$ (Appendix 3). This simulation accounted for demographic stochasticity and limited information on lethal alleles to inform a minor adjustment to the median of the $r^{\max}$ prior to 0.045, which was then used by the spatial risk model for Māui dolphins. The simulation study (Appendix 3) estimated a lower estimate of $r^{\max} = 0.040$ when assuming greater variability in demographic rates (e.g. that might arise from increased environmental variability at the range edge of the species) and increased rates of lethal alleles that might result from a lack of genetic diversity.

Other potential Allee effects that were not addressed include a breakdown of social mating systems and social defence from predators that might potentially arise at small population size. There is strong evidence that the size and demographic composition of Māui dolphin pods (small pods were typically mixed-sex) is different from that of Hector's dolphin (small pods were normally sex-segregated), indicating that social structures are different for Māui dolphins (Oremus et al. 2012; Webster et al. 2009). However, as with Hector's dolphins, Māui dolphin nursery groups were dominated by females (Oremus et al. 2012; Webster et al. 2009) and it is not clear if the apparent difference in small pod dynamics of Māui dolphins is driven by small population size.

A metanalysis by Hutchings (2015) concluded that the threshold for Allee effects in marine mammal populations (i.e. realised population growth is below $r^{\max}$, though not necessarily negative) occurs at approximately 20% of K. Meta-analyses such as this could also potentially be used to inform an appropriate Allee driven adjustment for Māui dolphin $r^{\max}$ based on a robust estimate of population status.

Non-calf survival

Priors for non-calf survival for Hector's and Māui dolphins were used by the spatial risk model to estimate the total number of non-fishery deaths attributable to toxoplasmosis, predation and other non-fishery causes of death. Ideally, recent population-specific estimates would have been available to inform the estimation of priors for all assessment sub-populations, but this was the case for Māui dolphins only (Roberts et al. 2019). For all Hector's dolphin sub-populations, a beta prior was specified (Figure 5) that encompassed the range of non-calf survival estimates that might be expected for this species (between 0.87 and 0.96) based on demographic assessments of Banks Peninsula Hector's dolphin (Gormley et al. 2012) and estimates of optimal non-calf survival by Edwards et al. (2018). Since the prior for Māui dolphins was more tightly constrained, this led to slightly more precise

estimates of toxoplasmosis annual deaths and risk ratio relative to estimates for Hector's dolphins (Table 15 and Table 16). As such, recent and precise non-calf survival estimates for Hector's dolphin sub-populations would increase the precision of model estimates of non-fishery deaths and risk for this sub-species.

Population size

The latest population size estimates for Māui and various Hector's dolphin sub-populations were used by the risk model to:

- Derive non-fishery deaths (from which toxoplasmosis, predation and other causes were estimated);
- Rescale Hector's and Māui dolphins spatial densities; and
- Derive sub-population PSTs.

The risk model used the same, consistent sub-species' population size MCMC samples for these multiple purposes. Since the data were not informative with respect to these parameters, the model posteriors were unchanged from the priors (comparing Table 5 and Table A14-1). Subsequent improvements to the precision of population size estimates would result in proportional increases in the precision of death and risk ratio estimates.

A nominal population size of 10 animals was assigned to the NI area, which includes the east and north coasts of the North Island, where there is currently no evidence of a permanent resident population, but where occasional sightings, including verified sightings, have been reported. Similarly, 15–17 dolphins were assigned to the TAKA (Taranaki to Kapiti) area based on habitat suitability, despite no indications of a permanent population. Assigning non-zero dolphin densities to areas without permanent populations allows fisheries risk to be estimated even for transient animals or hypothetical populations, e.g., to assess the extent to which fisheries risk may be sufficient to constitute a barrier to dispersal or prevent recolonization of favourable habitat. Because vulnerability is estimated at the species level and fisheries risk accrues per individual animal, the estimation of fisheries risk for hypothetical or transient dolphin populationswill be insensitive to the arbitrary choice of of population size.

Estimating risk to hypothetical populations in this way relies on the assumption that transient or hypothetical animals will inhabit the area proportional to habitat suitability as predicted by the habitat model. Regions of suitable habitat were identified on the east coast of the NI area, e.g., at the southern end of Hawke's Bay and along the Gisborne coast, which corresponded closely to the locations of public sightings (Figure A7-3), but commercial fisheries risk in these locations is low. This assessment also identified locations at which commercial set netting and recreational fishing may constitute a risk to dispersing or transient dolphins in the TAKA area, to inform threat management (Figure A15-7 and Figure A12-3).

6.2   Non-fishery causes of death

Importance of infectious disease

Disease was responsible for a significant proportion of the deaths for which cause of death could be identified by necropsy. Three particular infectious agents were identified as the underlying causes for 12 deaths: *Toxoplasma gondii* (nine cases), *Brucella pinnipedialis* (two cases) and *Mycobacterium tuberculosis* (one case). Both *T. gondii* and *Brucella pinnipedialis* have previously been found in Hector's dolphins (Buckle et al. 2017; Roe et al. 2013), while tuberculosis is a new finding for this species and has not previously been reported in any other cetacean species. The importance of full necropsy investigations on moderate to well-preserved carcasses is emphasised by these findings, as none of these diagnoses could have been made without histological and molecular analyses, which typically require well-preserved carcasses. Both toxoplasmosis and brucellosis can affect reproductive success, as well as causing direct mortality. *T gondii* infection has also been shown to cause behavioural

changes in mammals, leading to an increased risk of predation and trauma (Bowater et al. 2003, Kreuder et al. 2003).

Toxoplasmosis was a comparatively frequent diagnosis and has multiple adverse effects on individuals (reproductive, mortality and behavioural). New Zealand historically lacks any wild cat species and, so, *T. gondii* oocysts can only spread by the domestic cats (*Felis catus*) (background information is provided in Appendix 9). As such, toxoplasmosis is considered an exclusively anthropogenic threat in New Zealand.

Additional non-fishery anthropogenic threats

Other major non-fishery causes of death from the comprehensive and consistent necropsy records included maternal separation (affecting dependent calves only), other bacterial diseases (including tuberculosis, meningitis and pneumonia) and fungal disease, predation, renal disease, myocarditis, parasitism and deformity—none of which are considered to be directly anthropogenic in origin. A larger necropsied sample may have detected anthropogenic causes of death other than fishery-related and toxoplasmosis although, unless there is a very large bias in the relative detection probabilities of different threats, toxoplasmosis is likely to pose a greater population risk than other potential anthropogenic causes of death.

Spatial and temporal trends of mortality

There are no apparent trends for individual causes of mortality across years, although the power to detect this is low due to small sample size (Table A4-2 and Table A4-3). The number of necropsies conducted in 2012 stands out as particularly high (5 calves and 10 non-calves, compared with an annual average of 1.0 calves and 4.1 non-calves across all other years). In addition to a temporally variable mortality rate, this could be caused by an increased reporting rate of stranded individuals (potentially driven by increased public awareness during the 2012 TMP of Māui dolphin), increased stranding rates due to weather and coastal currents, or a random artefact due to the small sample size. Even so, a demographic assessment estimating a time series of demographic rates could give consideration of the elevated necropsy sample for calves and non-calves in 2012.

The necropsy data set includes approximately twice as many animals from the ECSI compared with the WCSI and included nine known or probable bycatch cases from the ECSI, compared with only two from the WCSI. Factors that could contribute to this difference include spatial variation in the relative density of the dolphin populations, mortality rate by threat, stranding rate, detection probability and reporting rate, or small sample size effects. With the exception of bycatch, the proportional causes of death were similar in the ECSI and WCSI areas. The spatial risk model was fitted to area aggregated estimates (i.e. relative spatial overlap with toxoplasmosis and predation was not used to generate population level fits to necropsy observations). However, it is unlikely that this would have altered model predictions given the comparable patterns in proportional cause of death and the low sample size.

6.3   Spatial density of Hector's and Māui dolphins

The optimal habitat model used to estimate the spatial density of Hector's and Māui dolphins included satellite-derived seasonal turbidity and trawl survey derived presence of ahuru as predictors. A predictive habitat-based approach was deemed preferable to a smoothed density derived from the aerial survey observations, because spatial turbidity is temporally-dynamic and the aerial survey provided only a snapshot of Hector's dolphin distribution during the survey months. Therefore the habitat model was fitted using spatial turbidity in the specific year and months of each respective survey and then used to predict the spatial density of dolphins across a 10-year average of turbidity for summer or winter.

The resulting spatial density prediction agreed well with the spatial abundance of public sightings and commercial fishery observer sightings of both Hector's and Māui dolphins (Figure 25), indicating that the habitat model accurately represented the true habitat requirements of both sub-species, despite being fitted to Hector's dolphin observations only. In addition, the inclusion of turbidity as the primary model

term was consistent with independent Boosted Regression Tree (BRT) assessments by Torres et al. (2013) and Stephenson et al. (in prep.) who found suspected particulate matter and turbidity to be major predictors of Hector's and Māui dolphin abundance. It is also consistent with the findings of Bräger (1998), who demonstrated that the occurrence of Hector's dolphins declined in water visibility greater than 4 metres (from *in situ* measurements using a Secchi disk) at all study sites around the South Island of New Zealand and in both summer and winter periods.
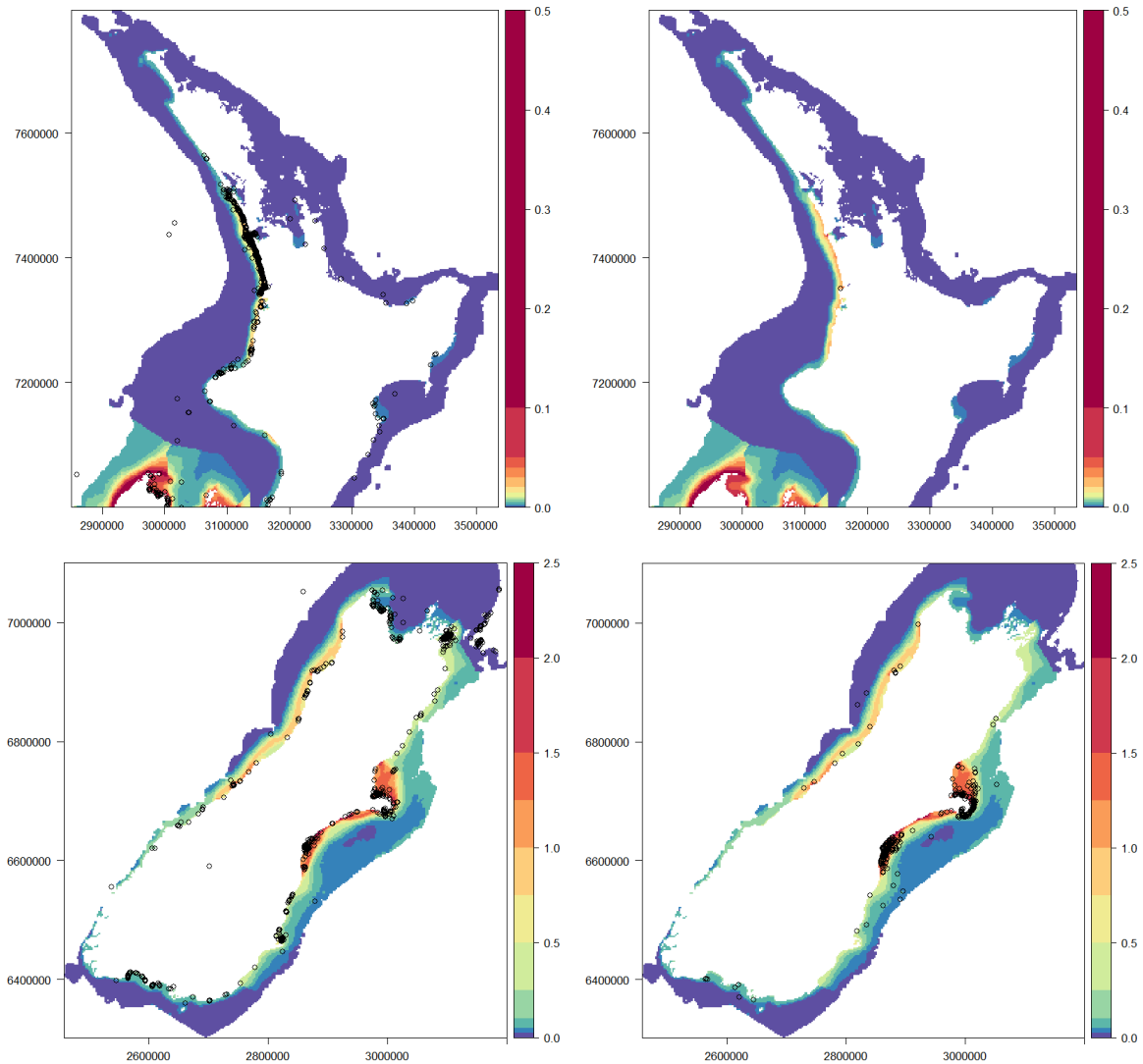

Figure 25: Final predicted spatial density of Hector's and Māui dolphins in summer used for spatial risk assessment compared with the spatial distribution of public (left) and commercial fishery observer sightings, also in summer months (right).

The spatial distribution of prey was not resolved to this temporal scale (or even seasonally) and future improvements to the habitat model could give consideration of probable temporal variation in prey distribution. For example, Miller (2015) demonstrated that the offshore movement of Hector's dolphins in winter months at the Banks Peninsula was correlated with the seasonal movements of red cod, the primary prey species of east and west coast Hector's dolphins, in terms of mass (Miller et al. 2013).

Other potential improvements to the habitat model include offering prey *biomass* predictors (rather than *presence*) as a candidate model term. In addition, multi-species indices could be considered, e.g., based on counts or the total biomass of key prey species. Initial exploration using trawl survey information from RVs *Kaharoa* and *Tangaroa* (Figure 26) indicated that Hector's dolphins are most abundant in

areas of high diversity of preferred prey species (comparing with Figure 25). Also, both the biomass and diversity of key prey species was almost uniformly low on the west and north coasts of the North Island, which may partly explain the much lower density of Māui dolphin relative to that observed for Hector's dolphin. Hence, using prey biomass or multi-species predictors may reduce the discrepancy between the estimate of habitat 'carrying capacity' (3690 individuals in summer and 5223 in winter) and the latest census estimate for Māui dolphin of 63 (95% c.i. = 57–75) (Baker et al. 2016a).
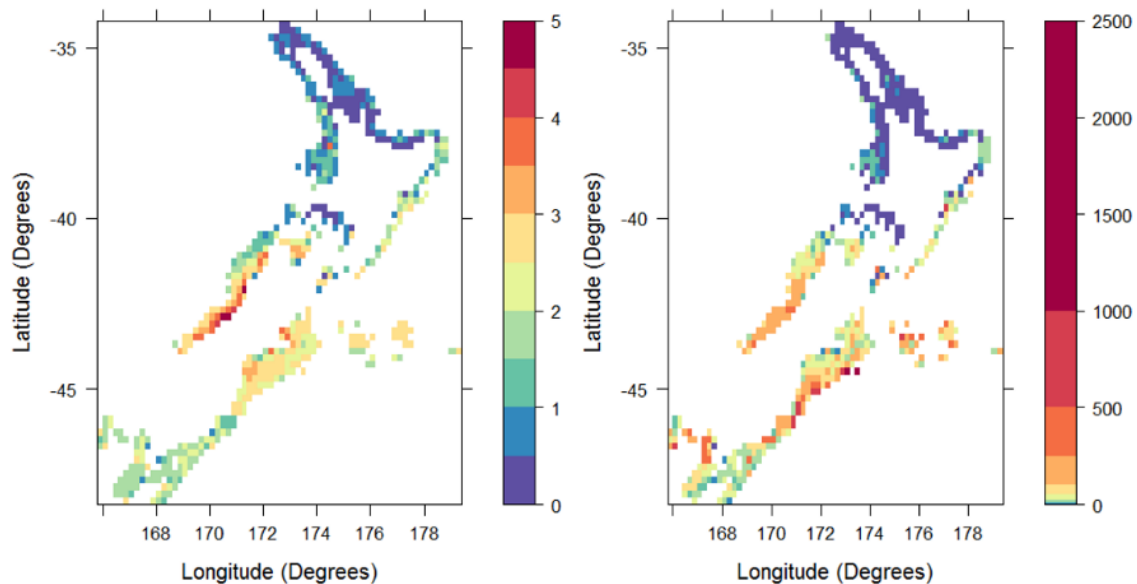

Figure 26: **Unstandardised mean count of species (left) and combined biomass in kg (right) of the six key prey taxa by diet mass (Miller et al. 2013 and Table A5-2) for combined *Kaharoa* and *Tangaroa* survey stations aggregated by 0.2-degree grid.**

Spatial prey information was lacking for the nearshore region of the south coast of the South Island, such that spatial predictions for this area would have been driven almost entirely by turbidity (Figure A5-1). Possibly as a consequence of this, the habitat model for SCSI Hector's dolphins predicts that the dolphins are dispersed much more widely than was observed in a recent aerial survey unavailable at the time that the habitat model was being fit (MacKenzie & Clement 2019). Hence, future research to estimate the relative presence or density of key prey here could be used to produce improved predictions in this area. Other sources of information for estimating prey density in the south coast (and seasonality elsewhere) could include commercial fishery observer catch records.

The habitat model fit to Hector's dolphin aerial survey observations was used to predict the spatial density of Māui (and Hector's) dolphins off the west coast of the North Island. Previous aerial line transect surveys targeting Māui dolphin obtained too few positive sightings to generate robust estimates of spatial density (e.g., eight sighting events by Slooten et al. (2006) in January 2004). Historical boat-based surveys (e.g., Baker et al. 2016a) have obtained a much larger number of positive sightings, although these were primarily designed for conducting a genetic biopsy mark-recapture study, rather than for understanding spatial distribuiton. Boat-based surveys were mostly centred in areas of relatively high abundance during the summer calving period when dolphins aggregate socially in locations close to shore for reasons related to calving. For these reasons the boat-based survey search effort was less intense in off-shore areas and at the tails of the dolphins' probable along-shore distribution (Baker et al. 2016a) and probably under-estimates their range due to seasonal bias.

Public sightings were also used to predict the relative density of dolphins in harbours of the west coast of the South Island. Ultimately, only a subset of boat-based public sightings were used, because this was the only grouping for which a corresponding effort layer could be produced, based on an aerial survey of recreational fishing craft. This meant that a large number of validated sightings were discarded for this analysis (e.g., made by surfers or from land), including some rare sightings within harbours.

Future research to develop respective effort density layers for these other sighting platforms will mean that they can be used in future habitat modelling for the west coast of the North Island.

Passive acoustic monitoring devices have previously been deployed on moorings to monitor the habitat use of Hector's and Māui dolphins (e.g. Hupman & Goetz 2018; Nelson et al. in prep.; Rayment et al. 2009; Rayment et al. 2011; Wright & Tregenza, in press). C-POD and T-POD click detectors obtained a large number of detection positive minutes per day (DPM day^{-1}) at nearshore locations (within 1 km of shore) of known relatively high abundance for Hector's dolphins around Banks Peninsula (mean of 74 DPM day^{-1}) (Rayment et al. 2009) and for Māui dolphins off Hamilton's Gap, immediately to the south of Manakau Harbour (39 DPM day^{-1}) (Nelson et al. in prep.). T-POD click detectors were also deployed in harbours of the west coast North Island (a total of 3211 days of acoustic monitoring) and obtained a small number of positive detections in the mouth of Manakau Harbour (38 click trains) and inside Kaipara Harbour (single click train) (Rayment et al. 2011). There were no positive detections from six other T-POD detectors around Manakau Harbour, or from six other T-PODs deployed in Kaipara, Raglan and Kawhia Harbours (Rayment et al. 2011). Wright & Treganza (in press) also obtained positive C-POD detections in the mouth of Manakau Harbour, where they obtained twelve positive detections, though all of these were subsequently reclassified, and mostly attributed to sonar. The same study obtained more than 2000 confirmed high-quality NBHF (narrow band high frequency) click trains in the coastal region immediately to the south of Manakau Harbour (Wright & Tregenza 2011). Positive C-POD detections were also obtained up to 14 km offshore of this location (a total of 28 detections) along a transect of C-POD deployments up to 18 km from shore (Nelson et al. in prep.). The relatively low number of positive clicks in the mouth of Manakau Harbour (38 clicks from the most comprehensve study) (Rayment et al. 2011) compared with the coast to the south (e.g. 10 thousand clicks 8 km from shore) (Nelson et al. in prep.) are consistent with Māui dolphins rarely using harbours of the west coast of the North Island.

6.4   Spatial threats & overlap

Risk model threats

Commercial fisheries

Spatial overlap plots with commercial set net (Figure 27) and inshore trawl effort (Figure A15-5) were produced from the spatial risk model outputs. The spatial pattern for captures, deaths, and risk are the same (Figure A15-7). These plots highlight some areas of the east coast South Island with relatively high spatial overlap, outside of areas currently closed to fishing. Notably the agreement between the spatial distribution of predicted and actual observed commercial fishery captures was good (Figure A15-3), indicating that the estimated spatial density of dolphins was a good approximation to the true density and that vulnerability is relatively constant in space.
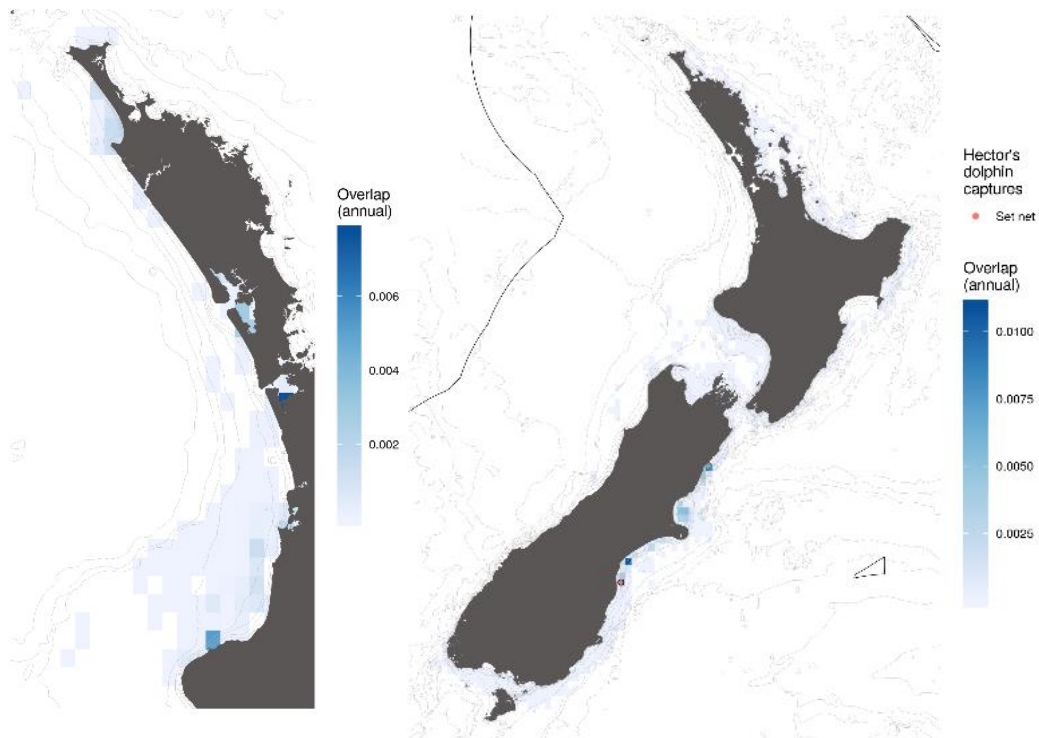
Figure 27: Total annual overlap (observed and unobserved) with the commercial set net fishery from 2014/15 to 2016/17. A single observed Hector's dolphin capture on the east coast of the South Island during this period is also displayed as a red point.

Toxoplasmosis

Following the approach of VanWormer et al. (2016), this risk assessment estimated the spatial density of *T. gondii* oocysts in the coastal water of New Zealand using a hydrological model and a human-based proxy for cat density (Appendix 9, discussed below with other spatial threats). This obtained very high estimated *T. gondii* densities around the North Island and particularly where Māui dolphin are most abundant (Figure 28), leading to the relatively high toxoplasmosis risk ratio for this sub-species and for other North Island areas (Table 16). Additional factors have been identified by other studies that might increase the spread of *T. gondii* oocysts including: loss of wetland vegetation and associated filtration capacity; a predominance of impervious surfaces in urbanised areas driving increased rates of runoff; and the size and composition of local cat populations (Burgess et al. 2018; Shapiro et al. 2010). Notably, Burgess et al. (2018) obtained a strong positive correlation between *T. gondii* prevalence in sea otters and coastal human density or human-dominated land-uses along the Pacific Rim, from Alaska to Southern California. This supports the use of human density as a proxy for estimating spatial toxoplasmosis in coastal water (Appendix 9; Aguilar et al. 2015).
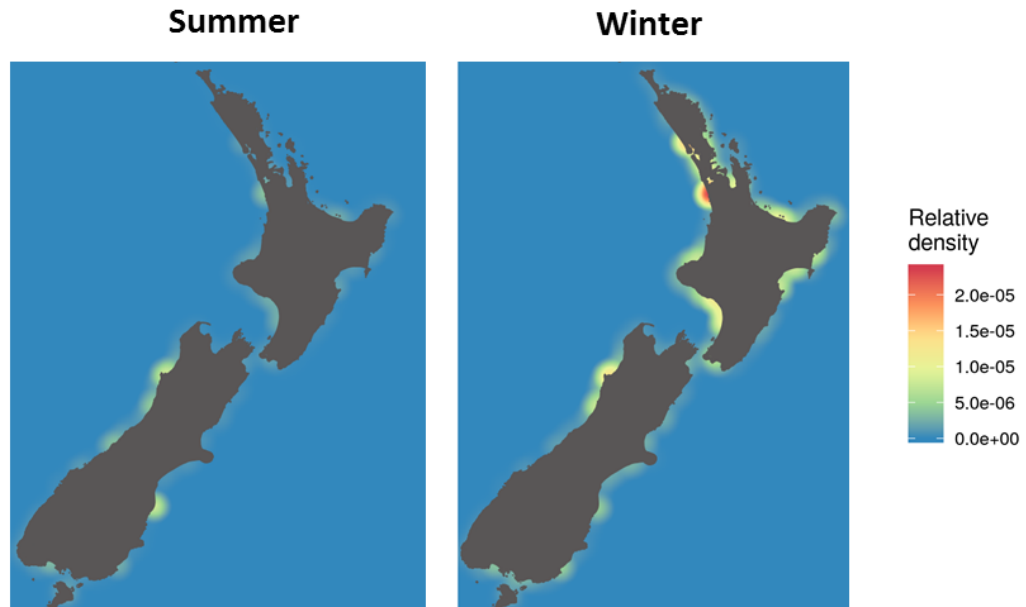
Figure 28: Estimated relative coastal water densities of *Toxoplasma gondii* oocysts in summer (left) and winter (right).

Further research is likely to improve our ability to identify geographic and seasonal variables associated with increased risk of toxoplasma infection, including pathogen-related factors. The strong seasonality in observed toxoplasmosis mortalities to date may also provide some clues as to risk factors of infection and subsequent progression to toxoplasmosis. All nine toxoplasmosis mortalities to date occurred in the period from September to November (Figure A9-1, and two additional mortalities since Roe et al. 2013 not included in this figure). This compares with an apparent peak in *T. gondii* infection of New Zealand green-lipped mussels in summer months (December to February) (Coupe et al. 2018) and the hydrological model based prediction of higher coastal *T. gondii* oocysts in winter months, during periods of elevated runoff (Figure A9-6). In addition, the rate at which domestic cats shed *T. gondii* oocysts is also seasonal with peak shedding rates in summer and autumn (Schares et al. 2016). Explaining these apparent discrepancies may elucidate the mechanisms of Hector's and Māui dolphin infection and subsequent progression to toxoplasmosis.

In addition, a better understanding of host-pathogen interactions would enhance our understanding of the likely effects of this disease at a population or subpopulation level. For example, of the nine animals in this current data set that died of toxoplasmosis, seven were female (six classified as mature) (Table A4-5 and Table A4-6), and all were found between September and November (Figure A9-1, note does not include two individuals recovered in September and October and were subsequently diagnosed with toxoplasmosis mortality). The causes and significance of this seasonality are not yet understood. In addition, Roe et al. (2013) found that one particular strain of *T. gondii* was responsible for the majority of mortalities, though the geographic distribution of this strain around New Zealand is not known.

Predation

The remains of Hector's/Māui dolphins have previously been found in the stomachs of the broadnose sevengill shark (*Notorynchus cepedianus*), great white shark (*Carcharodon carcharias*) and blue shark (*Prionace glauca*) (Cawthorn 1988; DOC 1992; Malcolm Francis, unpublished data). Of these, the broadnose sevengill shark was deemed by the Aquatic Environment Working Group to be the most plausible main predator of Hector's/Māui dolphins. They are well-known to be frequent predators of coastal dolphins and porpoises globally (Heithaus 2001) and their preference for turbid water (Ebert 1991) is likely to increase their spatial overlap with Hector's and Māui dolphins.

The modelling in Appendix 8 indicated that sevengill sharks are relatively abundant and widespread in New Zealand's coastal waters. Given anecdotal evidence of seasonality of sevengill shark movements and seasonal distribution around New Zealand (Clinton Duffy pers. comm.), it may be appropriate to estimate seasonal densities for this predator to include in future spatial risk modelling.

Selected other threats

When scaled for population size, the greatest overlap with recreational fishing was calculated for the TAKA assessment area (South Taranaki Bight and Kapiti Coast), which was estimated to be more than double that of any other sub-population or summary area. This area is not thought to have a resident Hector's or Māui dolphin population, though has had occasional sightings in the past (DOC 2018) and may provide opportunities for population connectivity between South Island Hector's dolphins and the Māui dolphin subpopulation on WCNI. Relatively moderate levels of overlap with recreational netting were also estimated for the north coast of the South Island (Table 14, Figure 19), a subpopulation for which the population estimate is highly uncertain and about which very little is known. In contrast, recreational setnet exposure in the more abundant Hector's dolphin populations is low, reflecting the effects of past spatial closures.

Summary plots of cumulative underwater noise from vessel traffic (using AIS data) and selected oil and gas seismic surveys are shown in Figure A11-6 and were produced by noise modelling by McPherson et al. (2019). This modelling was supplemented by a review of the potential impacts of petroleum and mineral exploration and production on Hector's and Māui dolphins by Lucke et al. (2019). The review by Lucke et al. (2019) illustrated the spatial distribution around New Zealand of 2-D seismic surveys since 1960 and 3-D surveys since 1987. This indicated most intensive historical activity to the west of the North Island, including survey activity prior to 2010 (although not since) in regions that would overlap with regions of moderately high Hector's and Māui dolphin density based on their predicted densities (based on visual comparison with Figure 17 and Figure 18). The review by Lucke et al. (2019) concluded that underwater noise from seismic surveys and offshore pile driving pose the greatest risk for causing auditory impairment, but this risk is low if the probable frequency-specific sensitivity of Hector's dolphin is considered. Behavioural reactions were considered the most probable response to the assessed noise sources and expected sound exposure levels, though the lack of scientifically-robust data for assessing the behavioural responses of Hector's and Māui dolphins was highlighted (Lucke et al. 2019).

6.5   Population risk

Commercial fisheries

The risk model outputs include parameters that relate observed captures of Hector's dolphin to sub-species spatial density and fishing effort. Other outputs include total (observed and unobserved) captures, deaths, and risk ratios.

The median of the risk ratio posteriors ($\phi = 0.2$) was below 1 for commercial set and inshore trawl fisheries at the sub-species level (Figure 22). However, the upper 95% CI of the commercial set net risk ratio estimate exceeded 1 for all assessment sub-populations except the WCSI (Table 16, Figure 22 and Figure 23). Areas of elevated risk were identified, particularly on the east coast of the South Island: along the Kaikoura coast, immediately to the north of Banks Peninsula and in the Southern Canterbury Bight (Figure A15-7).

The degree of uncertainty associated with the commercial fishery risk ratio estimates (Figure 22 and Figure 23) primarily stems from vague priors with respect to the cryptic mortality multiplier and live-release survival. By comparison, increased observer coverage would lead to a relatively minor increase in the precision of risk ratio estimates.

For Māui dolphins, the estimated annual deaths and risk ratios have declined through time since 1992/93 for both commercial set net and inshore trawl fisheries, driven by declining annual effort and overlap

per unit effort (Figure A16-2 and Figure A16-4). This is also the case for Hector's dolphin risk from inshore trawl (Figure A16-3). For Hector's dolphins risk from the commercial set net fishery, an overall reduction in effort has been offset by a general increase in overlap per unit effort resulting in little change in risk through time (Figure A16-1). The median estimate of risk ratio was below 1 in all years since 1992/93 (Figure A16-1), indicating that (in the absence of other anthropogenic mortality), the estimated annual mortalities across the last 25 years are unlikely to have been sufficient to prevent population recovery to or stabilisation at levels above at least 90% of carrying capacity.

Māui dolphin population trends were estimated using a demographic assessment model fitted to census and genetic mark-recapture observations (Roberts et al. 2019). When alleviating the median estimates of annual deaths from trawl and set net, the assessment by Roberts et al. (2019) estimated a small increase in growth rate from $\lambda = 0.980$ (95% CI = 0.962–0.998) to $\lambda = 0.982$ (95% CI = 0.963–1.002), with a further increase to $\lambda = 0.987$ (95% CI = 0.967–1.004) when alleviating the upper 95% CI of annual death estimates for commercial set net and trawl. These are the differences in population growth rate that correspond with the respective median risk ratios shown in Table 16.

The SEFRA model developed for this risk assessment produced much more optimistic risk ratios for Māui dolphin (a median risk ratio of 0.28 for commercial set nets and 0.00 for inshore trawl) than the previous PBR-based estimate from the 2012 TMP risk assessment (median risk ratio of 36.2 for set nets and 18.3 for trawls) (Currey et al. 2012). The primary causes of the greater than 2 orders of magnitude reduction in risk estimates are:

- Annual captures estimated empirically by the SEFRA model (median of 0.10 annual deaths from set net and 0.00 from inshore trawl) were much lower than those estimated using the Delphi method, which were based on collating subjective estimates from an expert panel (median of 2.48 annual deaths from set net and 1.21 from commercial trawl);

- A calibration coefficient (ϕ) of 0.2 was used by this implementation of the SEFRA model, consistent with a population recovery to 90% of K (Darryl MacKenzie unpublished data). This is smaller than the recovery factor (F_R) used by the PBR calculation (0.1), which was selected based on the Nationally Critical New Zealand Threat Classification System of this sub-species (Baker et al, 2016b); and

- This SEFRA risk assessment used an r^{max} prior with a median of 0.050, instead of the base case r^{max} of 0.018 assumed in the PBR calculation by Currey et al. (2012).

For both fisheries, a greater than 20-fold reduction in estimated annual deaths was affected by estimating this quantity empirically using the spatial risk model informed by commercial fisheries observer data, rather than basing it on subjective expert estimates. Along with changes associated with using the calibration factor and updated r^{max}, these changes contributed to a greater than 100-fold reduction in the estimated risk ratios for the commercial set net and trawl fisheries for Māui dolphin.

Note that the choice of (ϕ) for this risk assessment was a policy decision and need not be the same for all sub-populations; for example, decision-makers could choose to implement a lower (ϕ) for Māui dolphins than for Hector's dolphins, reflecting increased conservation urgency for this sub-species.

Toxoplasmosis

With respect to toxoplasmosis, the median estimated annual risk ratio ($\phi = 0.2$) exceeded 1 for all sub-populations (Table 16). When predation events were assumed to have a 10-fold reduction in detectability and, so, reduced the proportion of non-fishery deaths attributed to toxoplasmosis (Table 16, Figure 22 and Figure 23), only the north coast of the South Island had a median risk ratio below 1. A relatively low density with *T. gondii* oocysts was estimated for this area (Figure 28).

Māui dolphin demographic assessment runs alleviating the median annual toxoplasmosis deaths from the spatial risk model and the median estimates of commercial set net and trawl deaths estimated an

increase in population growth rate from $\lambda = 0.980$ (95% CI = 0.962–0.998) to $\lambda = 1.014$ (95% CI = 0.993–1.035), when assuming an equal detection probability of non-fishery causes of death (Roberts et al. 2019). This population growth rate was reduced to $\lambda = 0.998$ (95% CI = 0.982–1.017) for the predation sensitivity analysis (Roberts et al. 2019).

Estimates of non-fisheries death rely critically on assumptions about relative carcass detection probabilities arising from different causes of death. However, information to inform these assumptions is sparse. Heinemann (2017) and Moore & Read (2008) concluded that carcasses may be less likely to become beachcast if the animals are emaciated (hence less buoyant) or if carcasses are heavily scavenged or subjected to other sources of trauma, particularly where the body cavity is breached. The predation sensitivity trialled by the risk modelling here is plausible, since fully and partly-predated individuals would surely be less likely to become beachcast and be recovered for necropsy. However, assuming a large 10-fold reduction in the detection of predation events had only a minor effect on toxoplasmosis risk ratios (Table 16).

Although not trialled by this assessment, a scenario in which toxoplasmosis deaths have a greater relative detection probability would cause a much greater reduction in toxoplasmosis risk than does the predation sensitivity. The most likely reasons for a higher detection probability for toxoplasmosis deaths may include spatial and seasonal bias, e.g., if carcass detection rates were relatively high at locations and during months when deaths from toxoplasmosis were also disproportionately high. However, carcass recovery rates for Hector's and Māui dolphins are currently low for assessing potential spatial/seasonal bias and toxoplasmosis deaths have been recorded from a variety of locations around New Zealand, with no clear spatial pattern from the small sample available. An increased sample of recovered and necropsied Hector's and Māui dolphins may provide more information with respect to potential sources of bias and would improve the precision of model parameters estimating proportional causes of death.

Seven out of nine confirmed toxoplasmosis deaths were females, of which six were mature (Table A4-5 and Table A4-6). A similar sex-bias has been observed for Hawaiian monk seals, for which toxoplasmosis has been identified as a threat to their recovery (Barbieri et al. 2016). However, as with Hector's/Māui dolphins, firm conclusions are hampered by low sample size. If the positive female bias in the necropsied sample is representative of toxoplasmosis deaths in the wider population, then the population risk of toxoplasmosis may be greater than the risk ratio estimates indicate. A more exhaustive review of the literature and data may inform the estimation of the relative detection rates of toxplasmosis and other causes of death.

6.6   Discussion of other potential threats

Changes to prey availability

The diet and potential mechanisms of nutrional stress of Hector's and Māui dolphins were reviewed by Weir (2018). As with other members of the *Cephalorhynchus* genus, Hector's dolphins reach a small maximum size relative to other dolphin species, and females produce a large calf relative to their body size (Kastelein et al. 1993; Slooten 1991). For mothers, the energetic costs of reproduction will be greatest during lactation, which lasts for at least one year in Hector's dolphins, as was found to be the case for Commerson's dolphins (*Cephalorhynchus commersonii*) which increase their food intake with the onset of lactation (Kastelein et al. 1993). The review of the diet and energetics of Commerson's dolphin by Kastelein et al. (1993) concluded that "Prey availability in the distribution area of this species should therefore be a key parameter in the design of a rational management plan".

Hector's and Māui dolphins tend to predate on small size fractions of their preferred prey species (Miller et al. 2013) and this dependence on a limited range of prey species' age classes may cause increased vulnerability to factors that affect recruitment variability in their preferred prey species. A potential sea temperature-based predictor for red cod recruitment was identified by Beentjes & Renwick (2000), with increased recruitment in colder years. Inshore trawl surveys of the east and west coasts of the South Island have obtained temporal trends in a number of species through time, including red cod (Beentjes

et al. 2016; Stevenson & MacGibbon 2018). The relative abundance estimate for red cod tends to have low precision associated with occasional very large catches. Even so, periods of high and low abundance of red cod are apparent from the West Coast series (Stevenson & MacGibbon 2018), which could be related to time-varying demographic/reproductive rates of Hector's dolphin, as reported from the Banks Peninsula population (Gormley et al. 2012).

As noted above, the richness and biomass of preferred prey species are substantially lower off the west coast of the North Island relative to South Island locations where Hector's dolphins are abundant (at least an order of magnitude lower with respect to key prey biomass, without accounting for species differences in catchability) (Figure 26). As such, Māui dolphin may be especially susceptible to oceanic warming, particularly if prey species were also affected. This sub-species inhabits the warm end of the species' range (Figure A6-6), during the relatively warm Holocene interglacial period and, so, appears particularly vulnerable to further warming.

Many of the key prey of Hector's and Māui dolphins are also targeted by commercial fisheries around New Zealand, e.g. red cod, giant stargazer and southern arrow squid (Miller et al. 2013). However, Hector's and Māui dolphins tend to predate on small size fractions (Miller et al. 2013) and, so, appear to have limited potential for resource competition with commercial fisheries. Ongoing research will estimate the spatial density and fishing intensity for selected low information stocks including red cod (Fisheries New Zealand project code LSP2017-02) that could be related to the spatial density of marine megafauna predators.

As for Hector's dolphins, indices of Māui dolphin prey availability could be developed using fishery survey/commercial fishery catch rate information. These prey indices could then be related to potential climate/fishery stressors of their availability. Recent and future catch rate information from commercial fisheries will be constrained by fishing area restrictions, although trawl surveys could continue to collect the required information from the nearshore habitat used by Māui dolphins.

Changes to physical habitat

In addition to potential changes in prey recruitment patterns and spatial distribution, climate change may potentially affect the turbidity of coastal waters through increased rates of glacial melting in summer months, and by affecting wind-driven re-suspension of sediments from the seafloor in winter months. Factors that affect the intensity and spatial extent of coastal turbidity are likely to affect the spatial distribution of Hector's and Māui dolphins, based on their habitat preference (Figure 10). It is also likely that many of their preferred prey species (e.g. red cod, sprat, ahuru and NZ plaice) have an affinity for turbid water, given the moderate positive spatial correlation between these species and coastal turbidity patterns (Figure 8). As such, their prey may also be affected by potential climate warming effects on coastal turbidity.

Land management has also impacted on coastal and estuarine habitat via changes to sedimentation rates. For instance, coastal sedimentation rates were estimated to have increased in the Bay of Islands region by an order of magnitude following catchment deforestation (Swales et al. 2012).

Pollution

Marine pollutants that may be of greatest concern to the health of Hector's and Māui dolphins include organochlorine pesticides and heavy metal contamination. The usage of organochlorine pesticides and PCBs has been relatively low around New Zealand. The use of DDT had been restricted in New Zealand since the 1970s, although DDT has a long half-life and can persist in the environment for long periods. Notably, DDT concentrations were estimated to be an order of magnitude higher in both male and female Hector's dolphins on the East Coast of the South Island, relative to all other areas (Stockin et al. 2010). Regional sampling of soil concentrations of DDT around New Zealand confirmed a low usage of DDT pesticides compared with other countries, although it did find elevated concentrations in the Christchurch area (Buckland et al. 1998), which we speculate may be the cause of elevated tissue concentrations in east coast Hector's dolphin.

Heavy metal concentration has been monitored in oysters collected at various locations around Manakau harbour since 1987 (Kelly 2008). This study obtained elevated concentrations of zinc, copper and lead in sediments close to point sources, e.g. at the upper reaches of Manakau Harbour (also near to the Christchurch City outfall; Bolton-Ritchie & Lees 2012). These heavy metal concentrations were found to increase in trend through time, though concentrations were still low relative to international standards (Kelly 2008).

Vessel activity

As the aerial survey of recreational boats indicated (Figure 13), vessel activity tends to be most intense in harbour areas, near ports and large settlements. Vessel activity may cause injury and death in cetaceans through vessel strike and noise/visual disturbance may cause behavioural responses in Hector's dolphins (Martinez 2010). The DOC Hector's and Māui dolphin incidents database (https://www.doc.govt.nz/our-work/hectors-and-maui-dolphin-incident-database/1921-2008/) includes a record of a confirmed ship strike mortality on the east coast of the South Island.

The noise modelling assessment by McPherson et al. (2019) identified some locations of heavier vessel traffic and associated cumulative noise from vessels (Figure A11-6). However, the assessment by McPherson used vessel AIS data to locate vessels and so will have excluded most of the smaller boats close to shore that may produce high frequency noises closer to the hearing range of Hector's and Māui dolphins. Future assessments may identify new methods for estimating the spatial distribution of small vessels around New Zealand so that noise disturbance/potential ship strike effects can be better assessed.

Small population size effects

Very small populations may be subject to Allee effects that can lead to increased population extinction risk as result of demographic stochasticity, inbreeding depression, or social Allee mechanisms (Courchamp et al. 2008). Population simulations using individual based models that account for demographic stochasticity and lethal alelles estimated an extinction probability of less than 1% over 200 years for Hector's/Māui dolphin populations of at least 30 individuals (Ian Doonan, unpublished data), and estimated a stochastic r^{max} greater than 0.04 (Appendix 3). The Māui dolphin population is currently estimated to be 63 individuals (Baker et al. 2016b), though recent population assessments indicate that the Māui dolphin population may be declining and is highly unlikely to be achieving optimal growth (Cooke 2019; Roberts et al. 2019). SEFRA model estimated commercial setnet and trawl fishery deaths do not appear to be sufficient to prevent Māui dolphin population growth near to optimal values, though estimated toxoplasmosis deaths were more substantial (Cooke 2019; Roberts et al. 2019), and annual deaths were not estimated for some other potentially key anthropogenic threats, including recreational netting and stressors of prey availability. Future assessments could build on the individual-based modelling approach of Cooke (2019) and estimate the population effects of all key anthropogenic threats to Māui dolphins, while also accounting for Allee mechanisms.

6.7   Limitations of this assessment

Representativeness of necropsy observations

Representative determination of mortality rates and identification of all causes of death in a cetacean population is problematic, since the majority of deaths will occur at sea, and detection of a death is dependent on a carcass washing up on shore, being reported and subsequently observed, and being in an adequate state of preservation for reliable analysis. Necropsy data can, however, identify the presence of certain threats, and can provide clues as to the relative importance of detectable threats. An assumption can be made that in the absence of variables that affect the likelihood of a carcass washing up on shore, the chances of detection and investigation are similar for individual causes of death. Circumstances that could affect the chance of a body washing up include predation (where all or most of the body might be consumed by the predator), relative body condition affecting carcass buoyancy, and deliberate human interventions aimed at obscuring anthropogenic mortalities (e.g., the possibility

that bycaught animals could be retained or dumped further out at sea). Note that for commercial fishery bycatch deaths, we used the SEFRA method.

Use of spatial information

The statistical model underlying this implementation of the SEFRA does not fit to spatially explicit observations (i.e., observed captures and overlap are aggregated and then fitted), nor does it utilise covariance functions to determine the rate at which processes can change spatially. In addition, the spatial risk model does not propagate any uncertainty associated with the estimation of Hector's and Māui dolphin spatial densities, or the estimation threat intensities for non-fishery threats; instead the effects of uncertain spatial inputs were only evaluated using sensitivity analyses. The SEFRA method does not propagate any uncertainty related to the commercial effort data either (e.g. uncertainty in reported effort and positions of effort). Future implementations could consider a fully integrated model that predicts the spatial dolphin density and relates this to overlap using spatio-temporal methods. Such a model would have greater power to estimate spatial patterns, although it would be subject to overfitting unless tested by iteratively withholding spatial data for the purposes of cross-validating model predictions.

Estimation of fishery deaths

The SEFRA method also relies on good prior knowledge about some of the key model parameters, especially the probability that an event is observable (p_s^{obs}), a parameter to which the model results are very sensitive. The first part of the SEFRA method, in which numbers of observed captures are estimated, is the most certain component of the model because the estimated vulnerability parameters can soak up any mistakes made in the specification of the probability that an event is observable prior. The probability that an individual is alive given that it is caught parameter (ψ_g) is well defined if there are some observed captures that are dead and alive. However, moving from estimating observed captures to predicting deaths (i.e., including 'cryptic mortality') (see Appendix 10) requires a further assumption about the live-release survival rate (ω_g) and relies heavily on the probability that an event is observable prior being specified correctly. In this model, cryptic mortality accounts for roughly half of all estimated setnet deaths. A better understanding of the true rate at which dolphin carcasses drop out of commercial setnets without being visible to observers could greatly improve the accuracy and precision of model estimates.

It is plausible that different sectors of the commercial set net fleet (e.g., targeting different species or employing different mesh sizes) would have different vulnerabilities with respect to Hector's dolphin capture, warranting their assignment to separate fishery groups for which vulnerability would be estimated separately inside the model. These options were explored in working group discussions, but there are no clear gear distinctions in fisheries databases by which different groups could be distinguished, and it is likely that historical observed captures have been too low to detect a meaningful distinction. One possibility would be to use the SEFRA model to assess the sensitivities of set net risk ratio estimates to varying the vulnerability of different components of the fishing fleet (e.g., distinguished by target species, gear depth, or vessel characteristics). This could be used to identify commercial fishery characteristics for which additional observer coverage would be most beneficial to help better estimate risk ratios, and subsequently minimise risk.

A lack of information for estimating vulnerability to recreational fishing nets precluded the estimation of annual deaths and risk ratio by the SEFRA model. Previous studies have attempted basic characterisations of recreational netting operations (Aranovus 2007) and minimum estimates of recreational netting-related deaths of Hector's dolphins (Dawson 1991) that could be of use for informing the estimation of recreational netting vulnerability.

Indirect anthropogenic effects

Due to very high metabolic rate and energy requirements, Hector's and Māui dolphins are likely to be particularly susceptible to nutritional stress (Weir 2018). For income breeders, nutritional stress will typically impact on population growth through impaired reproduction rates (reduced breeding rates or

offspring survival) (Gaillard et al. 2000; Manlik et al. 2016). However, the required information was lacking for assessing potential prey availability effects on Hector's/Māui dolphins, or the potential stressors of prey availability, including climate variability or the indirect effects of fishing. The mechanical disturbance of benthic habitat by fishing and other marine industries was also not considered. As such, these and other indirect stressors of Hector's/Māui dolphins were not addressed quantitatively by this risk assessment.

Population status and trajectory

The SEFRA and PBR approaches do not necessarily require information with respect to population status and trajectory (although population size is required). SEFRA model outputs, especially annual time series of estimated threat-specific deaths that can be disaggregatged at different spatial scales, are inherently valuable to inform the estimation of status and trend, but still require additional assumptions, namely 'initial status' and the shape of the density dependence, in order to produce an estimate of population trend and final status. As noted by the project workshop expert panel (Taylor et al. 2018), this would have been valuable information for contextualising the outputs of the spatial risk assessment of Hector's and Māui dolphins. In addition, population status/trajectory information has intrinsic value for informing threat classification, risk assessment, and risk management.

Population trajectory has been inferred for some populations using Bayesian demographic assessments estimating key demographic rates. For example, a model fit to photo-ID based mark-recapture observations estimated a stable population trend ($\lambda = 0.995$; 95% CI = 0.927, 1.048) for Banks Peninsula Hector's dolphins between 1990 and 2005 (Gormley et al. 2012). A model fit to genetic capture-recapture observations produced median estimates consistent with a declining ($\lambda = 0.980$; 95% CI = 0.962–0.998) or increasing population trend ($\lambda = 1.025$ (0.968–1.086)) for Māui dolphins depending on how survival was parameterised, although with broad credible intervals spanning growth and decline (Baker et al. 2016a; Roberts et al. 2019). Given these outputs and uncertainty with respect to key reproductive parameters, none of the most recent demographic assessments provide clear information with respect to population trajectory (Gormley et al. 2012; Roberts et al. 2019).

Population status has also been estimated for Hector's and Māui dolphins by other studies (e.g. Martien et al. 1999; Burkhart & Slooten 2003; Slooten 2007; Slooten & Dawson 2010) using logistic population models assuming r^{max} and historical fishing mortality to derive area-disaggregated population size through time and current population status relative to historical estimates. These studies estimated very low population status in 2007 relative to 1970 for most populations, ranging from 7% (North Island, including Māui dolphins) to 51% (South Coast South Island Hector's dolphins), informing national and international threat classification systems.

However, the the latest of these assessments (Slooten 2007; Slooten & Dawson 2010) used boat-based survey estimates of population size on the east, north and south coasts of the South Island out to a distance of 4 nautical miles (1,880; 95% c.i. = 1384–2554) (Dawson et al. 2004) that has been superseded by an aerial survey with greater spatial coverage which estimated a much larger population size estimates for the east coast of the South Island in both summer (9728; 95% c.i. = 7001–13 517) and winter (8208; 95% c.i. = 4888–13 785) (MacKenzie & Clement 2016). Using the older boat-based survey estimates will have biased the estimate of vulnerability ("entanglement rate" in Slooten (2007)) upward by roughly a factor of five, which was estimated outside of the model using a more limited time series of observer records than is currently available. In addition, the latest assessments (Slooten 2007; Slooten & Dawson 2010) made some simplifying assumptions with respect to historical fishing effort and did not include other key anthropogenic threats, e.g., toxoplasmosis, that are likely to have impacted on the population status of Hector's and Māui dolphins (Table 16 and Figure 22).

Updated estimates of population status could be obtained by developing the assessment framework of Martien et al. (1999), Burkhart & Slooten (2003), Slooten (2007), and Slooten & Dawson (2010) by:

- Using updated information with respect to r^{max} and population size;

- Using fine-scale resolution information with respect to Hector's and Māui dolphin density and historical commercial fishery data;

- Using an updated time series of commercial fishing effort and fishery observer records of captures;

- Estimating dolphin vulnerability to commercial fisheries within a model that accounts for high-resolution estimates of spatial overlap;

- Considering anthropogenic threats in addition to commercial fisheries.

These updates to model structure and inputs would produce more comprehensive estimates of population status that could be complemented with demographic assessment-based estimates of current population trajectory to inform and prioritise conservation management.

7. CONCLUSIONS & FUTURE RESEARCH

The main conclusions from the spatial risk assessment of threats to Hector's and Māui dolphins are as follows:

- The intrinsic rate of population growth ($r^{\max}$) is an influential risk model input and was estimated for Hector's dolphins using a life history invariant with optimal generation time across vertebrates. The revised estimate ($r^{\max}$ = 0.050; 95% CI = 0.029–0.071) is now consistent with the life history characteristics of the species.

- The prior for $r^{\max}$ was adjusted for Māui dolphin (median = 0.045), based on a simulation accounting for some Allee effects associated with small population size. Other small population size issues, e.g., the breakdown of optimal social structures or sub-optimal habitat state were not addressed.

- A habitat model was fit to observations from the South Island Hector's dolphin aerial survey and included seasonal turbidity and prey species presence as predictors. The estimated spatial dolphin densities from this model corresponded very well with public and fisheries observer sightings of Hector's and Māui dolphins.

- Public sightings were also used to predict very low spatial density of Māui dolphins in harbours of the west coast North Island, where fishing effort is relatively high.

- A default calibration coefficient (ϕ) value of 0.2 was applied in the definition of the Population Sustainability Threshold (PST). The choice of ϕ is a policy decision. Applying this value, an anthropogenic mortality level resulting in a risk ratio of 1 would be expected to allow the population to recover to approximately 90% of their unimpacted status.

- For the inshore trawl fishery, the upper 95% credible interval of the risk ratio was below 1 for all sub-population areas. For the commercial set net fishery, the upper 95% credible interval of SEFRA model risk ratio estimates were above 1 for all sub-areas, except the West Coast South Island. However, the median value of risk ratio was below 1 for Māui dolphins and for all four sub-populations of Hector's dolphin. This indicates that recent commercial fisheries impacts are unlikely to be high enough to suppress the recovery of these dolphin populations to equilibrium levels lower than 90% of their unimpacted status.

- Local areas with particularly high setnet fishery risk were identified along the Kaikoura coast, immediately north of Banks Peninsula and in the southern Canterbury Bight. These results indicate that, unless dolphins in these locations mix with neighboring locations, these local populations would be expected to experience localised depletion to levels lower than the average.

- An update to the necropsy information identified toxoplasmosis (following infection with *T. gondii* oocysts originally shed by domestic cats) as the primary non-fishery cause of death for the necropsied sample of non-calf individuals. With the exception of fisheries bycatch, no other obvious anthropogenic causes of mortality were identified from the necropsy records.

- The SEFRA model was extended to include toxoplasmosis and predation deaths using spatially resolved threat intensities for both threats and fitting to necropsy observations. Toxoplasmosis risk ratios exceeded 1 for all sub-populations and this picture was mostly unchanged when assuming a 10-fold reduction in the detection of predation events. The representativeness of the small number of necropsy observations remains a primary uncertainty of this assessment. A relatively high spatial overlap was estimated between areas of favourable dolphin habitat and recreational netting along the South Taranaki and Kapiti Coasts, but annual deaths and risk ratio were not estimated for recreational netting. The estimated pattern of spatial overlap with other threats varied by threat.

- Some other probable key threats (e.g., climate change effects on prey and physical habitat) and the cumulative effects of multiple threats were not addressed spatially/quantitatively by this risk assessment, though may pose a substantial population risk to Hector's and Māui dolphins.

Future research and management that may be considered to improve various aspects of this risk assessment and to provide key additional information for the assessment of threats could include:

- Increasing the precision of risk ratio estimates for commercial fisheries by:
    - collecting information with the goal of more tightly constraining the priors for cryptic mortality and post-release survival; and
    - increasing commercial fisheries observer coverage on commercial set net vessels, focused in locations where fisheries overlap with high densities of dolphins.

- Increasing precision and assessing potential bias with respect to risk ratio estimates for non-fishery causes of death by:
    - reviewing information on factors affecting the relative carcass recovery rate and subsequent diagnosis at necropsy of different non-fishery causes of death;
    - increasing the recovered sample of dead Hector's and Māui dolphins for necropsy; and
    - also see recommendations in Appendix 9 with respect to the assessment of spatial risk of toxoplasmosis.

- Potential improvements to the Hector's/Māui dolphin habitat model, e.g., by:
    - reparameterising new habitat models at the scale of the NCSI and SCSI subpopulations, using alternate environmental data layers fitted to updated aerial and/or public sightings data at the subpopulation scale;
    - incorporating new predictors such as prey biomass and multi-species indices or the development of seasonal prey densities; and
    - the use of spatio-temporal modelling methods that consider spatial covariance to help improve predictions in area that have not been sampled well (e.g. Krainski et al. 2018).

- Collecting information on habitat use by individual dolphins in space (e.g., using satellite telemetry) and through the water column, including diel and seasonal patterns.

- Extending this SEFRA risk model for Hector's and Māui dolphins to generate estimates of historical population size and current population status, to inform threat classification and provide valuable context for risk assessment and management.

- Reconstructing historical fishing records to estimate effort in a spatially explicit manner as far back in time as historical evidence exists, to enable the SEFRA approach to be extended backwards including periods before the systematic collection of spatially resolved fisheries data.

- Collate information and undertake demographic assessments for estimating annual survival probability (note that this would improve the precision of non-fishery risk ratios) and population trajectory, also to inform risk assessment and management.

- Collect information that will facilitate the risk assessment of other potentially important anthropogenic threats to Hector's and Māui dolphins, e.g., the estimation of year-varying Hector's/Māui dolphin reproductive rates and the development of temporal indices of prey availaibility, that would inform the assessment of prey availability and stressors on Hector's/Māui dolphin productivity.

8. ACKNOWLEDGMENTS

9. REFERENCES

Abraham, E.R.; Neubauer, P.; Berkenbusch, K.; Richard, Y. (2017). Assessment of the risk to New Zealand marine mammals from commercial fisheries. *Aquatic Environment and Biodiversity Report 189*. 123 p.

Aguilar, G.D.; Farnworth, M.J.; Winder, L. (2015). Mapping the stray domestic cat (*Felis catus*) population in New Zealand: Species distribution modelling with a climate change scenario and implications for protected areas. *Applied Geography, 63*: 146–154.

Akaike, H. (1974). A new look at the statistical model identification. *IEEE Transactions on Automatic Control, 19 (6)*: 716–723.

[Aranovus] Aranovus Research (2007). A socio-economic impact assessment of fishers: Proposed options to mitigate fishing threats to Hector's and Maui's dolphins. Prepared by Aranovus Limited. 125 p.

Baker, C.S.; Chilvers, B.L.; Childerhouse, S.; Constantine, R.; Currey, R.; Mattlin, R.; Van Helden, A.; Hitchmough, R.; Rolfe, J. (2016b). Conservation status of New Zealand marine mammals, 2013. *New Zealand Threat Classification Series 14*. 18 p.

Baker, C.S.; Steel, D.; Hamner, R.M.; Hickman, G.; Boren, L.; Arlidge, W.; Constantine, R. (2016a). Estimating the abundance and effective population size of Māui dolphins using microsatellite genotypes in 2015–16, with retrospective matching to 2001–16. Department of Conservation, Auckland. 70 p.

Barbieri, M.M.; Kashinsky, L.; Rotstein, D.S.; Colegrove, K.M.; Haman, K.H.; Magargal, S.L.; Sweeny, A.R.; Kaufman, A.C.; Grigg, M.E.; Littnan C.L. (2016). Protozoal-related mortalities in endangered Hawaiian monk seals *Neomonachus schauinslandi*. *Diseases of Aquatic Organisms, 121*: 85–95.

Beentjes, M.P.; MacGibbon, D.J.; Parkinson, D. (2016). Inshore trawl survey of Canterbury Bight and Pegasus Bay April–June 2016, (KAH1605). *New Zealand Fisheries Assessment Report 2016/61*. 135 p.

Beentjes, M.P.; Renwick, J.A. (2000). The relationship between red cod recruitment and environmental variables. Final Research Report for Ministry of Fisheries Research Project RCO9801; Objective 3. 25 p. Unpublished report held by Fisheries New Zealand, Wellington.

Bräger, S. (1998). Behavioural Ecology and Population Structure of Hector's Dolphin (*Cephalorhynchus hectori*). (Thesis, Doctor of Philosophy). University of Otago. 167 p.

Bowater, R.O.; Norton, J.; Johnson, S.; Hill, B.; O'Donoghue, P.; Prior, H. (2003). Toxoplasmosis in IndoPacific humpbacked dolphins (*Sousa chinensis*), from Queensland. *Australian Veterinary Journal, 81*: 627–632.

Buckland S.J.; Ellis, H.K.; Salter R.T. (1998). Organochlorines in New Zealand: Ambient concentrations of selected organochlorines in soils. Ministry for the Environment, Wellington. 176 p.

Buckle, K.; Roe, W.D.; Howe, L.; Michael, S.; Duignan, P.J.; Burrows, E.; McDonald, W.L. (2017). Brucellosis in endangered Hector's dolphins (*Cephalorhynchus hectori*). *Veterinary Pathology, 54*: 838–845.

Burgess, T.L.; Tinker, M.T.; Miller, M.A.; Bodkin, J.L.; Murray, M.J.; Saarinen, J.A.; Nichol, L.M.; Larson, S.; Conrad, P.C.; Johnson, C.K. (2018). Defining the risk landscape in the context of pathogen pollution: *Toxoplasma gondii* in sea otters along the Pacific Rim. *Royal Society Open Science, 5*: 171178. http://dx.doi.org/10.1098/rsos.171178

Burkhart S.M.; Slooten, E. (2003). Population viability analysis for Hector's dolphin (*Cephalorhynchus hectori*): a stochastic population model for local populations. *New Zealand Journal of Marine and Freshwater Research 37*: 553–566.

Cawthorn, M.W. (1988). Recent observations of Hector's dolphin, *Cephalorhynchus hectori*, in New Zealand. Pp. 303–314 in Brownell, R.L. Jr; Donovan, G.P. (Eds): Biology of the genus *Cephalorhynchus*. *Report of the International Whaling Commission, Special Issue 9*.

Cooke, J.G.; Constantine, R.; Hamner, R.M.; Steel, D.; Baker, C. S. (2019). Population dynamic modelling of the Māui dolphin based on genotype capture-recapture with projections involving bycatch and disease risk. *New Zealand Aquatic Environment and Biodiversity Report No. 216*.

Coupe, A.; Howe, L.; Burrows, E.; Sine, A.; Pita, A.; Velathanthiri, N.; Vallée, E.; Hayman, D.l Shapiro, K.; Roe, W.D. (2018). First report of *Toxoplasma gondii* sporulated oocysts and *Giardia duodenalis* in commercial green-lipped mussels (*Perna canaliculus*) in New Zealand. *Parasitology Research, 117*:1453–1463.

Courchamp, F.; Berec, J.; Gascoigne, J. (2008). Allee effects in ecology and conservation. Oxford, New York, USA: Oxford University Press.

Currey, R.J.C.; Boren, L.J.; Sharp, B.R.; Peterson, D. (2012). A risk assessment of threats to Māui's dolphins. Ministry for Primary Industries and Department of Conservation, Wellington. 51 p.

Dawson, S.M. (1991). Incidental catch of Hector's dolphin in inshore gillnets. *Marine Mammal Science, 7*: 283–295.

Dawson, S.M.; Slooten, E.; DuFresne, S.; Wade, P., Clement, D. (2004). Small-boat surveys for coastal dolphins: Line-transect surveys for Hector's dolphins (*Cephalorhynchus hectori*). *Fisheries Bulletin 201*: 441–451.

Dillingham, P.W.; Moore, J.E.; Fletcher, D.; Cortes, E.; Curtis, K.A.; James, K.C.; Lewison, R.L. (2016). Improved estimation of intrinsic growth r max for long- lived species: integrating matrix models and allometry. *Ecological Applications 26 (1)*, 322–333.

[DOC] Department of Conservation (1992). Banks Peninsula Marine Mammal Sanctuary Technical Report, 1992. *Canterbury Conservancy Technical Report Series 4*. Department of Conservation, Christchurch. 111 p.

[DOC] Department of Conservation (2018). Māui and Hector's dolphin sightings database. URL https://www.doc.govt.nz/our-work/our-work-with-maui-dolphin/maui-dolphin-sightings/. Accessed 27th July 2018.

[DOC] Department of Conservation (2019). Hector's and Māui dolphin incident database. URL https://www.doc.govt.nz/our-work/hectors-and-maui-dolphin-incident-database/. Accessed 24th April 2019.

Duncan, R.P.; Forsyth, D.M.; Hone, J. (2007). Testing the metabolic theory of ecology: allometric scaling exponents in mammals. *Ecology, 88*: 324–333.

Ebert, D.A. (1991). Diet of the sevengill shark *Notorynchus cepedianus* in the temperate coastal waters of southern Africa. *South African Journal of Marine Science, 11*: 565–572.

Edwards, C.T.T.; Roberts, J.; Doonan, I. (2018). Estimation of the maximum rate of intrinsic growth for Hector's dolphin. Final Research Report available from Fisheries New Zealand. 22 p.

Gaillard, J.M.; Festa-Bianchet, M.; Yoccoz, N.G.; Loison, A.; Toïgo, C. (2000). Temporal variation in fitness components and population dynamics of large herbivores. *Annual Review of Ecology and Systematics 31*: 367–393.

Gormley, A.M. (2009). Population modelling of hector's dolphins. Phd. Thesis, University of Otago.

Gormley, A.M.; Slooten, E.; Dawson, S.; Barker, R.J.; Rayment, W.; du Fresne, S.; Bräger, S. (2012). First evidence that marine protected areas can work for marine mammals. *Journal of Applied Ecology, 49*: 474–480.

Hamner, R.M.; Pichler, F.B.; Heimeier, D.; Constantine, R.; Baker, C.S. (2012). Genetic differentiation and limited gene flow among fragmented populations of New Zealand endemic Hector's and Māui's dolphins. *Conservation Genetics 13*: 987–1002.

Hamner, R.M.; Wade, P.; Oremus, M.; Stanley, M.; Brown, P.; Constantine, R.; Baker, C.S. (2014). Critically low abundance and limits to human-related mortality for the Māui's dolphin. *Endangered Species Research, 26*: 87–92.

Hartill, B.; Vaughan, M.; Rush, N. (2011). Recreational harvest estimate for SNA 8 in 2006–07. *New Zealand Fisheries Assessment Report 2011/51*. 48 p.

Hayes, S.A.; Josephson, E.; Maze-Foley, K.; Rosel, P.E. et al. (2018). US Atlantic and Gulf of Mexico Marine Mammal Stock Assessments – 2017. NOAA Tech Memo NMFS NE-245; 371 p.

Heinemann, D. (2017). Cryptic mortality correction factors, In: National Marine Fisheries Service. (2017). Proceedings of the First National Protected Species Assessment Workshop. NOAA Technical Memorandum NMFS-F/SPO-172. pp. 60–63.

Heithaus, M.R. (2001). Predator-prey and competitive interactions between sharks (order Selachii) and dolphins (suborder Odontoceti): a review. *Journal of Zoological Society of London, 253*: 53–68.

Hupman, K.; Goetz, K. (2018). Māui Dolphin Acoustic Monitoring: Progress Report 1. Report produced for the Department of Conservation. 13 p.

Hutchings, J.A. (2015). Thresholds for impaired species recovery. *Proceedings of the Royal Society B 282*: 20150654.

[IWC] International Whaling Commission (2016). Report of the Scientific Committee. Bled, Slovenia, 7–19 June 2016. IWC/66/Rep01(2016).

Jepson, P.; Barbieri, M.; Barco, S.G.; de Quiros, Y.B.; Bogomolni, A.; Danil, K.; Rowles, T. (2013). Peracute underwater entrapment of pinnipeds and cetaceans. *Diseases of Aquatic Organisms, 103*: 235–239.

Kastelein, R.; McBain, J.; Neurohr, B.; Mohri, M.; Saijo, S.; Wakabayashi, I.; Wiepkema, P.R. (1993). The food consumption of Commerson's dolphins (*Cephalorhynchus commersonii*). *Aquatic Mammals, 19.2*: 99–121.

Kelly, S. (2008). Environmental condition and values of Manukau Harbour. Prepared by Coast and Catchment Ltd. for Auckland Regional Council. *Auckland Regional Council Technical Report 2009/112*. 154 p.

Krainski, E.T.; Gómez-Rubio, V.; Bakka, H.: Lenzi, A.; Castro-Camilo, D.; Simpson, D.; Lindgren, F.; Rue, H. (2018). Advanced Spatial Modeling with Stochastic Partial Differential Equations Using R and INLA. Chapman and Hall/CRC. 284 p.

Kreuder, C.; Miller, M.A.; Jessup, D.A.; Lowenstein, L.J.; Harris, M.D.; Ames, J.A.; Carpenter, T.E.; Conrad, P.A.; Mazet, J.A.K. (2003). Patterns of mortality in southern sea otters (*Enhydra lutris nereis*) from 1998 to 2001. *Journal of Wildlife Disease, 39*: 495–509.

Leong, D.; Chesterton, J. (2005). Waitaki Catchment Hydrological Information. Report commissioned by the Ministry for the Environment for consideration by the Waitaki Catchment Water Allocation Board. 135 p.

Linstone, H.A.; Turoff, M. (2002). The Delphi method. Techniques and applications. 618 p. Addison-Wesley, Reading, MA.

Lonergan, M.E.; Phillips, R.A.; Thomson, R.B.; Zhou, S. (2017). Independent review of New Zealand's Spatially Explicit Fisheries Risk Assessment approach – 2017. *New Zealand Fisheries Science Review 2017/2*. 36 p.

Lucke, K.; Clement, D.; Todd, V.; Williamson, L.; Johnston, O.; Floerl, L.; Cox, S.; Todd, I.; McPherson. C.R.; (2019). Potential Impacts of Petroleum and Mineral Exploration and Production on Hector's and Māui's Dolphins. Document 01725, Version 1.0 DRAFT. Technical report by JASCO Applied Sciences, Cawthron Institute, and Ocean Science Consulting Ltd. for the New Zealand for Department of Conservation and Fisheries.

MacKenzie, D.I.; Clement, D.M. (2014). Abundance and distribution of ECSI Hector's dolphin. *New Zealand Aquatic Environment and Biodiversity Report No. 123*. 79 p.

MacKenzie, D.I.; Clement, D.M. (2016). Abundance and distribution of WCSI Hector's dolphin. *New Zealand Aquatic Environment and Biodiversity Report No. 168*. 67 p + supplemental material.

MacKenzie, D.I.; Clement, D.M. (2019). Abundance and Distribution of Hector's dolphin on South Coast South Island. Draft New Zealand Aquatic Environment and Biodiversity Report held by Fisheries New Zealand. 32 p.

Manlik, O.; McDonald, J.A.; Mann, J.; Raudino, H.C.; Bejder, L.; Krützen, M.; Connor, R.C.; Heithaus, M.R.; Lacy, R; Sherwin, W.B. (2016). The relative importance of reproduction and survival for the conservation of two dolphin populations. *Ecology and Evolution 6*: 3496–3512.

Martien, K.K.; Taylor, B.L.; Slooten, E.; Dawson, S. (1999). A sensitivity analysis to guide research and management for Hector's dolphin. *Biological Conservation, 90*: 183–191.

Martinez, E. (2010). Responses of South Island Hector's dolphins (*Cephalorhynchus hectori hectori*) to vessel activity (including tourism operations) in Akaroa Harbour, Banks Peninsula, New Zealand. PhD Thesis, Massey University, Auckland, New Zealand.

McPherson, C.; Quijano, J.; Zizheng, L. (2019). Underwater acoustic modelling to examine potential noise exposure to Māui dolphins. Draft New Zealand Aquatic Environment and Biodiversity Report held by Fisheries New Zealand. 53 p.

McPherson, C.; Zizheng, L.; Quijano, J. (2019). Underwater sound propagation modelling to illustrate potential noise exposure to Maui dolphins from seismic surveys and vessel traffic on West Coast North Island, New Zealand. *New Zealand Aquatic Environment and Biodiversity Report No. 217.* 62 p.

Miller, E.J. (2015). Ecology of Hector's dolphin (*Cephalorhynchus hectori*): Quantifying diet and investigating habitat selection at Banks Peninsula (Thesis, Doctor of Philosophy). University of Otago. 168 p.

Miller, E.; Lalas, C.; Dawson, S.; Ratz, H.; Slooten, E. (2013). Hector's dolphin diet: The species, sizes and relative importance of prey eaten by *Cephalorhynchus hectori*, investigated using stomach content analysis. *Marine Mammal Science, 29*: 606–628.

Mitchell, J.S.; Mackay, K.A.; Neil, H.L.; Mackay, E.J.; Pallentin, A.; Notman P.; (2012). Undersea New Zealand, 1:5,000,000.

[MFISH/DOC] Ministry of Fisheries/Department of Conservation (2007). Hector's Dolphin Threat Management Discussion Document. Published by the Ministry of Fisheries and the Department of Conservation. 154 p.

Moore, J.E. (2015). Intrinsic growth (rmax) and generation time (t) estimates for the cetacean genera *Sousa*, *Orcaella*, and *Neophocaena*, in support of IUCN red list assessments. NOAA Technical Report NOAA-TM-NMFS-SWFSC-596.

Moore, J.E.; Read, A.J. (2008). A Bayesian uncertainty analysis of cetacean demography and bycatch mortality using age-at-death data. *Ecological Applications, 18*: 1914–1931.

[MPI/DOC] Ministry for Primary Industries/Department of Conservation (2012). Review of the Māui's Dolphin Threat Management Plan. MPI and DOC joint Discussion Paper No: 2012/18. 209 p.

[NASA] NASA Goddard Space Flight Center, Ocean Ecology Laboratory, Ocean Biology Processing Group; (2019): Sea-viewing Wide Field-of-view Sensor (SeaWiFS) Ocean Color Data, NASA OB.DAAC. doi: 10.5067/ORBVIEW-2/SEAWIFS_OC.2014.0. Accessed on 2019/05/01.

[Navigatus] Navigatus Consulting (2015). Marine Oil Spill Risk Assessment 2015 (MOSRA 15). Report prepared by Navigatus Consulting for Maritime New Zealand. 397 p. URL https://www.maritimenz.govt.nz/public/environment/documents/MOSRA-report-2015.pdf

Nelson, W. (in prep.) Occurrence of Māui Dolphin (Popoto) offshore from Hamilton's Gap, Manukau Coastline, Taranaki and Whanganui River. Summer Research Project Report: Nov. 2017 – Feb. 2018. University of Auckland. 14 p.

[NMFS] National Marine Fisheries Service. (2018). 2018 Revision to: Technical Guidance for Assessing the Effects of Anthropogenic Sound on Marine Mammal Hearing (Version 2.0): Underwater Thresholds for Onset of Permanent and Temporary Threshold Shifts. U.S. Department of Commerce, NOAA. NOAA Technical Memorandum NMFS-OPR-59. 167 pp. URL https://www.fisheries.noaa.gov/webdam/download/75962998.

Oremus, M.; Hamner, R.M.; Stanley, M.; Brown, P.; Baker, C.S.; Constantine, R. (2012). Distribution, group characteristics and movements of the Critically Endangered Māui's dolphin *Cephalorhynchus hectori Māui*. *Endangered Species Research, 19*: 1–10.

Pichler, F. (2001). Population structure and genetic variation in Hector's dolphin (*Cephalorhynchus hectori*). Phd. Thesis, University of Auckland. 169 p.

Pinkerton, M.H.; Gall, M.; Wood, S.; Zeldis, J. (2018). Measuring the effects of bivalve mariculture on water quality in northern New Zealand using MODIS-Aqua satellite observations. *Aquaculture Environment Interactions, 10*: 529–545.

Rayment, W.; Dawson, S.; Scali, S.; Slooten, E. (2011). Listening for a needle in a haystack: passive acoustic detection of dolphins at very low densities. *Endangered Species Research, 14*: 149–156.

Rayment, W.; Dawson, S.; Slooten, E. (2009). Use of T-PODs for acoustic monitoring of *Cephalorhynchus* dolphins: a case study with Hector's dolphins in a marine protected area. *Endangered Species Research, 10*: 333–339.

Reeves, R.R.; Dawson, S.M.; Jefferson, T.A.; Karczmarski, L.; Laidre, K.; O'Corry-Crowe, G.; Rojas-Bracho, L.; Secchi, E.R.; Slooten, E.; Smith, B.D.; Wang, J.Y.; Zhou, K. (2013a). *Cephalorhynchus hectori*. The IUCN Red List of Threatened Species 2013: e.T4162A44199757. http://dx.doi.org/10.2305/IUCN.UK.2013-1.RLTS.T4162A44199757.en.

Reeves, R.R.; Dawson, S.M.; Jefferson, T.A.; Karczmarski, L.; Laidre, K.; O'Corry-Crowe, G.; Rojas-Bracho, L.; Secchi, E.R.; Slooten, E.; Smith, B.D.; Wang, J.Y.; Zhou, K. (2013b). *Cephalorhynchus hectori ssp. Māui*. The IUCN Red List of Threatened Species 2013: e.T39427A44200192.http://dx.doi.org/10.2305/IUCN.UK.2013-1.RLTS.T39427A44200192.en.

Roberts, J.; Constantine, R.; Baker, C.S. (2019). Population Effects of Commercial Fishery and Non-Fishery Threats on Māui Dolphins (*Cephalorhynchus hectori maui*). *New Zealand Aquatic Environment and Biodiversity Report No. 215*. 18 p.

Roe, W.D.; Howe, L.; Baker, E.J.; Burrows, L.; Hunter, S.A. (2013). An atypical genotype of T*oxoplasma gondii* as a cause of mortality in Hector's dolphins (*Cephalorhynchus hectori*). *Veterinary Parasitology, 192*: 67–74.

R Core Team (2018). R: A language and environment for statistical computing. R Foundation for Statistical Computing, Vienna, Austria. URL http://www.R-project.org/.

Schares, G.; Ziller, M.; Herrmann, D.C.; Globokar, M.V.; Pantchev, N.; Conraths, F.J.(2016). Seasonality in the proportions of domestic cats shedding *Toxoplasma gondii* or *Hammondia hammondi* oocysts is associated with climatic factors. *International Journal for Parasitology*, 46: 263–273.

Shapiro, K.; Conrad, P.A.; Mazet, J.A.K.; Wallender, W.W.; Miller, W.A.; Largier, J.L. (2010). Effect of Estuarine Wetland Degradation on Transport of *Toxoplasma gondii* Surrogates from Land to Sea. *Applied and Environmental Microbiology, 76*: 6821–6828.

Sharp, B.R. (2018). Spatially-explicit fisheries risk assessment (SEFRA): a framework for quantifiying and managing incidental commercial fisheries impacts on non-target species. In: Aquatic Environment and Biodiversity Annual Review 2017. Ministry for Primary Industries. pp. 20–56. URL https://www.mpi.govt.nz/dmsdocument/34854-aquatic-environment-and-biodiversity-annual-review-aebar-2018-a-summary-of-environmental-interactions-between-the-seafood-sector-and-the-aquatic-environment

Slooten, E. (1991). Age, growth and reproduction in Hector's dolphins. *Canadian Journal of Zoology, 69*: 1689–1700.

Slooten, E. (2007). Conservation management in the face of uncertainty: effectiveness of four options for managing Hector's dolphin bycatch. *Endangered Species Research, 3*: 169–179.

Slooten, E.; Dawson, S.M. (2010). Assessing the effectiveness of conservation management decisions: likely effects of new protection measures for Hector's dolphin (*Cephalorhynchus hectori*). *Aquatic Conservation: Marine and Freshwater Ecosystems 20*: 334–347.

Slooten, E.; Dawson, S.M.; Rayment, W.J. (2004). Aerial surveys for coastal dolphins: abundance of Hector's dolphins off the South Island west coast, New Zealand. *Marine Mammal Science 20*: 117–130.

Slooten, E.; Dawson, S.M.; Rayment, W.J.; Childerhouse, S.J. (2006). A new abundance estimate for Māui's dolphin: What does it mean for managing this critically endangered species? *Biological Conservation 128*: 576–581.

Slooten, E.; Lad, F. (1991). Population biology and conservation of Hector's dolphin. *Canadian Journal of Zoology, 69*: 1701–1707.

Spearman, C. (1904). The Proof and Measurement of Association between Two Things. *American Journal of Psychology 15*, 72–101.

Stan Development Team (2016). Stan Modelling Language: User's Guide and Reference Manual. Version 2.14.0.

Stephenson, F.; Goetz, K.; Mouton, T.; Beats, F.; Hailes, S.; Roberts, J.; Pinkerton, M.; MacDiarmid, A. (in prep.). Spatial distribution modelling of New Zealand cetacean species.

Stevenson, M.L.; MacGibbon, D.J. (2018). Inshore trawl survey of the west coast South Island and Tasman and Golden Bays, March-April 2017 (KAH1703) *New Zealand Fisheries Assessment Report 2018/18*. 92 p.

Stockin, K.A.; Law, R.J.; Roe, W.D.; Meynier, L.; Martinez, E.; Duignan, P.J.; Bridgen, P.; Jones, B. (2010). PCBs and organochlorine pesticides in Hector's (*Cephalorhynchus hectori hectori*) and Maui's (*Cephalorhynchus hectori maui*) dolphins. *Marine Pollution Bulletin 60*: 834–842.

Swales, A.; Gibbs, M.; Hewitt, J.; Hailes, S.; Griffiths, R.; Olsen, G.; Ovenden, R.; Wadhwa, S. (2012). Sediment sources and accumulation rates in the Bay of Islands and implications for macro-benthic fauna, mangrove and saltmarsh habitats. NIWA Client Report prepared for Prepared for Northland Regional Council. 132 p.

Taylor, B.; Lonergan, M.; Reeves, R. (2018). Panel Comments and Recommendations–Workshop on spatial risk assessment of threats to Hector's and Māui dolphins. Unpublished report held by Fisheries New Zealand, Wellington. 15 p.

Torres, L.; Compton, T.; Fromant, A. (2013). Habitat models of southern right whales, Hector's dolphin, and killer whales in New Zealand. NIWA report prepared for Trans-Tasman Resources Limited. 59 p. URL https://www.epa.govt.nz/assets/FileAPI/proposal/EEZ000004/Applicants-proposal-documents/EEZ000004-Habitat-models-of-southern-right-whales-Hectors-dolphin-and-killer-whales-in-New-Zealand-NIWA-October-2013.pdf

VanWormer, E.; Carpenter, T.E.; Singh, P.; Shapiro, K.; Wallender, W.W.; Conrad, P.A.; Largier, J.L. Maneta, M.P.; Mazet, J.A.K. (2016). Coastal development and precipitation drive pathogen flow from land to sea: evidence from a *Toxoplasma gondii* and felid host system. *Scientific Reports, 6*: 29252.

Wade, P. (1998). Calculating limits to the allowable human-caused mortality of cetaceans and pinnipeds. *Marine Mammal Science, 14*: 1–37.

Webster, T.A.; Dawson, S.; Slooten, E. (2009). Evidence of sex segregation in Hector's dolphin (*Cephalorhynchus hectori*). *Aquatic Mammals, 35*: 212−219.

Weir, J. (2018). Review of Hector's and Māui dolphin diet, nutrition and potential mechanisms of nutritional stress. Unpublished report produced for the World Wildlife Fund and Department of Conservation. 20 p.

Wood, S.N. (2011) Fast stable restricted maximum likelihood and marginal likelihood estimation of semiparametric generalized linear models. *Journal of the Royal Statistical Society (B) 73*: 3-36.

Wright, A.J.; Tregenza, N. (in press). CPOD successful in trial for detecting Māui dolphin outside harbours. New Zealand Journal of Marine and Freshwater Research.

APPENDIX 1 – SUPPLEMENTARY AGEING TO INFORM ESTIMATION OF AGE AT FIRST REPRODUCTION AND INTRINSIC POPULATION GROWTH RATE

Introduction

The revised spatial risk assessment of threats to Hector's and Māui dolphins uses individual ageing information primarily for the estimation of female age at first maturity, required for the derivation of r^{max} for the species (Edwards et al. 2018). A secondary usage of individual age estimates was to explore the demographic composition with respect to causes of death from necropsy records (both sexes) (see Appendix 4). All ageing undertaken to date has been based on counts of growth layers across sections of teeth, primarily obtained from beachcast and bycaught individuals. Since the numbers of dead Hector's/Māui dolphins recovered each year is low (typically fewer than 10 individuals each year) and not all necropsied individuals have been aged, the historical aged sample is small.

Previously, ageing was undertaken of:

- 60 individuals recovered from 1984 to 1989 (Slooten 1991), including 32 females; and
- 67 individuals recovered from 1998 to 2003 (Duignan et al. 2003, Duignan et al. 2004, Duignan & Jones 2005), including 24 females.

The Department of Conservation requested supplementary ageing using teeth sampled from recovered Hector's/Māui dolphin. Additional validated age estimates were then combined with historical age estimates and used to inform the life history/demographic information requirements of the updated Hector's/Māui multi-threat risk assessment.

Methods

The supplementary sample for ageing was of a total sample of 73 individuals recovered from stranding or bycatch events. Methods for age determination, including the sectioning and preparation of teeth were consistent with methods described by Duignan et al. (2004), which was based on a modification of the protocol adopted by Slooten (1991).

This sample was split into two batches of samples:

- Batch 1 – 37 individuals recovered from 1997 to 2009, for which teeth were originally sectioned in 2009; and
- Batch 2 – 36 individuals recovered from 2009 to 2015.

In order to highlight growth rings, tooth sections were stained with toluene blue prior to mounting on glass slides. Mounted sections were then photographed and the resulting digital images were marked with a unique identifier allowing age estimates to be linked to necropsy information with respect to individual maturity stage and morphometric measurements. The two batches of imaged sections were then sent to three independent readers:

1. Liz Slooten (University of Otago);
2. Emma Betty (Massey University); and
3. Evan Leunissen (University of Otago/Yellow-eyed Penguin Trust).

Methods for age determination from the sectioned tooth were consistent with those described by Duignan et al. (2004) and Slooten (1991). The estimated age for each individual was then derived from the average of the three reader's estimates. Where a reader declined to give a point estimate (i.e. rather than a point age estimate, they provided an age range or no estimate at all), this was omitted from the cross-reader average for an individual.

Results

The agreement between reader age estimates was generally good, with the exception of a small positive bias (approximately 2 years) that was detected for age estimates by Reader 2 for Batch 1 samples, which was not apparent for Batch 2 (Figure A1-1). As such, Reader 2 age estimates were omitted from the combined age estimates for Batch 1 only.

One of the readers deemed that 20 of the tooth sections in Batch 2 missed the tooth centroid. Since this may have led to an underestimate of age for these individuals, these samples were omitted from the final data set used for subsequent life history assessment (Table A1-1). The final sample of validated age estimates was then successfully related to necropsy information with respect to maturity stage and morphometric measurements for all except five individuals (all in Batch 1). For these individuals, non-standard identifiers were provided that were not found on Massey University necropsy database (Table A1-1 and Table A1-2).
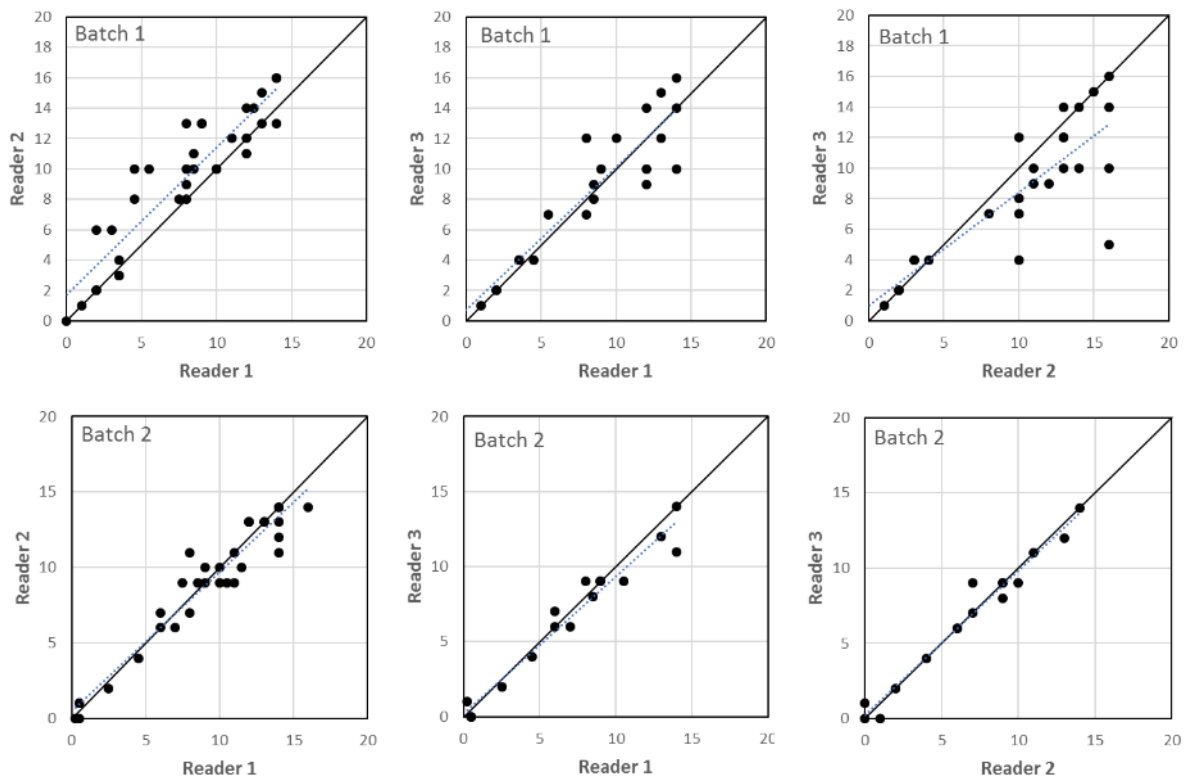
**Figure A1-1: Pairwise comparison of reader estimates comparing all three readers separately for sample Batch 1 (top) and Batch 2 (bottom). Note consistent positive bias with estimates for Reader 2 in Batch 1, which was not apparent in Batch 2. The solid line highlights the relationship that would occur with perfect agreement between reader estimates. The dotted blue line highlights the linear trendline between reader estimates.**

Table A1-1: Individual age estimates and linked necropsy information, Batch 1. Sex denoted as M (male), F (female), or U (unknown).

	Estimated age				Linked necropsy information			
MUCIC ID	Reader 1	Reader 2**	Reader 3	Combined estimate	Sex	Standard length (m)	Ovaries active	Prior pregnancy
W97-58bCh	8	10		8.0	M			
W04-14Chh	11	12		11.0	U			
W06-07Ch	12.5	14		12.5	U			
W07-26ch	8	9		8.0	F	1.41	Yes	
W07-28Ch	14	16	16	15.0	F	1.53	Yes	Yes
W07-29ch	1	1	1	1.0	M	1.35		
W08-01ch	14	16	10	12.0	F	1.49	Yes	Yes
W08-13ch	9	13	10	9.5	F	1.39	Yes	Yes
W08-19ch	3.5	3	4	3.8	M	1.20		
W08-20ch		14	10	10.0	F	1.36	Yes	Yes
W08-21ch		16	14	14.0	F	1.33	Yes	Yes
W08-28ch*	12	12	9	10.5	Cannot link to necropsy records for individual			
W09-01ch	12	14	14	13.0	F	1.37		
W00-09Ch	3	6		3.0	F	1.45		
W01-06ch	10	10	12	11.0	U			
W02-12Ch	5.5	10	7	6.3	M			
W02-16Ch	4.5	8		4.5	M			
W04-17Chh	13	15	15	14.0	F			
W04-20Chh	13	13	12	12.5	F			
W04-26Ch		16	5	5.0	F			
WB04-28chh*	4.5	10	4	4.3	Cannot link to necropsy records for individual			
W05-07Ch	14	13	14	14.0	U			
W05-09Ch	12	11	10	11.0	M			
W05-10Ch	2	2	2	2.0	F			
W05-11Ch	3.5	3	4	3.8	F			
W05-14Ch	10	10		10.0	M			
W05-15Ch	7.5	8		7.5	M			
WOL-2+chm*	2	6		2.0	Cannot link to necropsy records for individual			
WOR-15chm*	8	8	7	7.5	Cannot link to necropsy records for individual			
W05-30Chh	8	13	12	10.0	M	1.21		
W05-34Chh		22			F	1.43	Yes	Yes
W05-35Chh	3.5	4	4	3.8	M	1.16		
W05-36Chh	8.5	10	8	8.3	F	1.33	Yes	Yes
W06-03Chh	2	2	2	2.0	M	1.21		
W07-24Ch	9	13		9.0	F	1.39	Yes	Yes
WS97-59ch*	0	0		0.0	Cannot link to necropsy records for individual			
W98-32Ch	8.5	11	9	8.8	F			

*Non-standard ID format. Not possible to link to necropsy records for respective individuals.
**Estimates by Reader 2 were not used in the combined estimate for Batch 1.

Table A1-2: Individual age estimates and linked necropsy information, Batch 2.

DOC ID	Reader 1	Reader 2	Reader 3	Combined estimate	Sex	Standard length (m)	Ovaries active	Prior pregnancy
		Age estimate (year)				Linked necropsy information		
H189	7	6	6	6.3	M	1.22		
H207	12	13	MC		F	1.42	Yes	Yes
H208	0.5	1	0	0.5	M	0.94		
H210	9	9	9	9.0	F	1.34	Yes	Yes
H211	13	13	12	12.7	F	1.35	Yes	
H213	8	7	9	8.0	M	1.27		
H214	9	10	9	9.3	U	1.35		
H215	2.5	2	2	2.2	U	1.21		
H217	10	10	MC		F	1.34	Yes	Yes
H219	4.5	4	4	4.2	F	1.28	No	No
H221	14	14	14	14.0	M	1.27		
H225	11	9	MC		F	1.41	Yes	Yes
H226	≥ 8	13	MC		M	1.24		
H227	11	11	MC		U	1.41		
H228	8.5	9	8	8.5	F	1.42	No	No
H230	6	7	7	6.7	F	1.52	No	No
H233	12	13	MC		F	1.55	Yes	Yes
H234	10	9	MC		F	1.30		
H235	14	13	MC		F		Yes	Yes
H238	12	13	MC		M	1.22		
H241	14	14	MC		M	1.29		
H243	≥ 9	9	MC		F	1.51	Yes	Yes
H244	0.5	1	MC		F	0.86	No	No
H248	14	11	11	12.0	M	1.30		
H249	16	14	MC		M	1.26		
H250	0.5	0	0	0.2	M	1.05		
H251	10.5	9	9	9.5	M	1.23		
H253	0.25	0	1	0.4	M	0.84		
H254	13	13	MC		F	1.49	Yes	Yes
H255	6	6	6	6.0	M	1.21		
H256	7.5	9	MC		F	1.41	Yes	Yes
H257	≥ 10	13	MC		F	1.45	Yes	
H260	8	11	MC		F	1.40		
H261	11.5	10	MC		M	1.29		
H263	≥ 7.5	10	MC		U			
H264	14	12	MC		M			

"MC" indicates that the reader deemed the tooth section to have "missed centroid". No age estimate used for respective individuals.

From visual inspection, the length-at-age relationship of females from the supplementary aged sample was consistent with that obtained from females from previous ageing work (Duignan et al. 2003, Duignan et al. 2004, Duignan & Jones 2005, Slooten 1991).
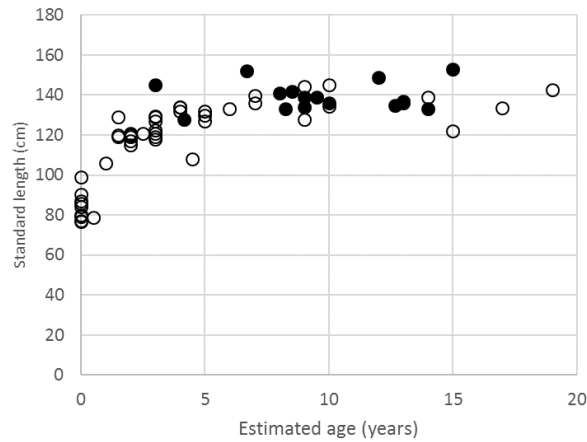

Figure A1-2: Standard length-at-age of all female Hector's/Māui dolphins; used for estimation of r^{max} by Edwards et al. (2018). Black circles are estimates from supplementary sampling, open circles are measurements and previous estimates (Duignan et al. 2003, Duignan et al. 2004, Duignan & Jones 2005, Slooten 1991).
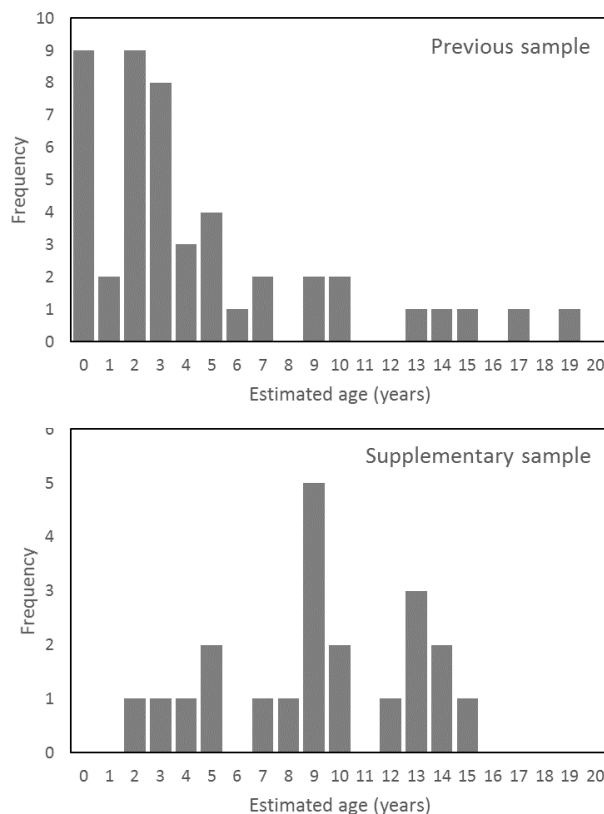

Figure A1-3: Age composition of females aged by previous assessments (Duignan et al. 2003, Duignan et al. 2004, Duignan & Jones 2005, Slooten 1991) (top) and by the supplementary sampling reported in this Appendix (bottom).

Conclusions and risk assessment inputs

Validated female age estimates (i.e. those in Tables A1-1 and A1-2 with a combined age estimate) were combined with previous estimates of females to inform the estimation of age at maturity and r^{max} (Edwards et al. 2018). The supplementary sample included a greater proportion of females at ages when maturation is likely to occur for this species (5–10 years) (Gormley et al. 2012) and older (Figure A1-2).

Future work could consider re-sectioning the 20 tooth samples for Batch 2 that were deemed to have missed the centroid of the tooth and were excluded from final outputs (Table A1-2). This sample includes 12 females that would better inform the estimation of key life history parameters if reliable age estimates could be obtained.

Acknowledgements

References

Duignan, P.J.; Gibbs, N.J.; Jones, G.W. (2003). Autopsy of cetaceans incidentally caught in fishing operations 1997/98, 1999/2000, and 2000/01. DOC Science Internal Series 119. 66 p.

Duignan, P.J.; Gibbs, N.J.; Jones, G.W. (2004). Autopsy of cetaceans incidentally caught in commercial fisheries, and all beachcast specimens of Hector's dolphins, 2001/02. DOC Science Internal Series 176. 28 p.

Duignan, P.J.; Jones, G.W. (2005). Autopsy of cetaceans including those incidentally caught in commercial fisheries, 2002/03. DOC Science Internal Series 195. 22 p.

Edwards, C.T.T.; Roberts, J.O.; Doonan, I.J. (2018). Estimation of the maximum rate of intrinsic growth for Hector's dolphin. Final Research Report available from Fisheries New Zealand. 22 p.

Gormley, A.M.; Slooten, E.; Dawson, S.; Barker, R.J.; Rayment, W.; du Fresne, S.; Brager, S. (2012). First evidence that marine protected areas can work for marine mammals. *Journal of Applied Ecology, 49*: 474–480.

Slooten, E. (1991). Age, growth, and reproduction in hector dolphins. *Canadian Journal of Zoology, 69*: 1689–1700.

APPENDIX 2 – ESTIMATION OF $r^{\max}$ FOR HECTOR'S DOLPHIN

Introduction

The revised spatial risk assessment of threats to Hector's/Māui dolphins used individual size at age and maturity stage information to derive an $r^{\max}$ for the species (Edwards et al. 2018). This assessment followed the method proposed by Dillingham et al. (2016) and implemented by Moore (2015), which uses an allometric invariant between optimal generation time (the average age of a breeder during optimal growth) and $r^{\max}$ observed across vertebrate species. See Edwards et al. (2018) for a detailed description of methods and sensitivity runs.

The assessment by Edwards et al. (2018) obtained base case Monte Carlo distributions of age at maturity of 6.91 (95% CI = 5.82 – 8.24) and $r^{\max}$ of 0.050 (95% CI = 0.029 – 0.071) for Hector's dolphin. This updated the previous base case $r^{\max}$ of 0.018 assumed by the most recent Māui dolphin multi-threat assessment (Currey et al. 2012), although this was based on a maximum longevity of 20 (Slooten & Lad 1991), which is now known to be an underestimate for this species (e.g. Gormley 2009).

Here, the assessment by Edwards et al. (2018) was updated with the supplementary ageing and maturity information detailed in Appendix 1 (new data are displayed in Tables A1-1 and A1-2).

In addition, a sensitivity model run was undertaken, in which the sensitivity of the $r^{\max}$ posterior to assuming a maximum breeding age of 30 was assessed (previously this was infinite).

Results

Update using supplementary age and maturity information

Updating the assessment by Edwards et al. (2018) with supplementary ageing produced an identical median and 95% CI for $r^{\max}$ to three decimal places, i.e. 0.050 (95% CI = 0.029 – 0.071). The updated posterior is displayed in Figure A2-1.
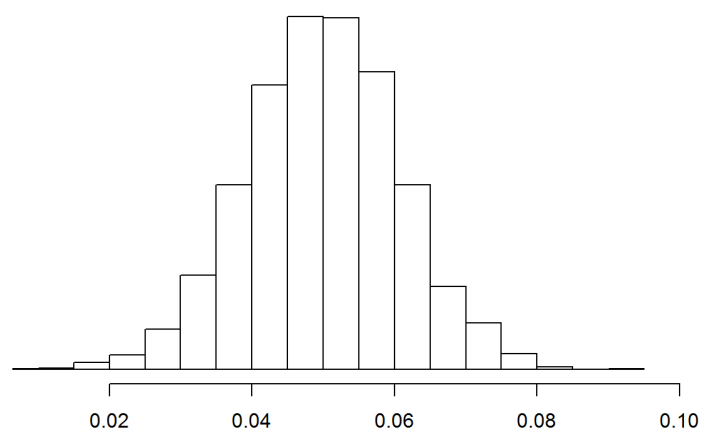

Figure A2-1: Posterior distribution of $r^{\max}$ using the model developed by Edwards et al. (2018), updated with supplementary ageing and maturity stage information shown in Appendix 1.

Sensitivity run assuming maximum breeding age of 30

The assessment described above (with updated age and maturity information) was replicated, except that a maximum breeding age of 30 years was imposed (instead of infinite). This run obtained a slightly increased median $r^{\max}$ of 0.052 (compared with 0.050) and slightly broader 95% CI of 0.029 – 0.072 (compared with 0.029 – 0.071).

Imposing a maximum breeding age (without altering other life history parameters) will have the effect of decreasing generation time (the average age of a breeder) and, according to the invariant between optimal generation time and $r^{\max}$, lead to increased $r^{\max}$ estimates. In order to achieve the required

increase in optimal population growth rate, a small, compensatory shift towards higher values of non-calf survival values was obtained (Figure A2-2).
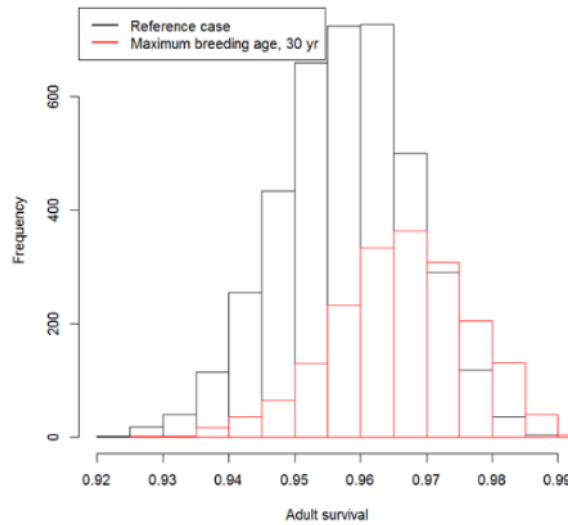

Figure A2-2: Histograms of accepted non-calf survival rates for the base case run (here labelled as "Reference case", black bars) and that using a maximum breeding age of 30 years (red bars).

Conclusions and risk assessment inputs

The updated base case assessment produced a Monte Carlo distribution of r^{max} of 0.050 (95% CI = 0.029–0.071). This estimate was insensitive to various alterative assumptions explored by Edwards et al. (2018) and with respect to maximum breeding age. The updated estimate of r^{max} for Hector's dolphin is now consistent with that expected from other mammals including other cetacean species, given estimated age at first reproduction (Duncan et al. 2007) (Figure A2-3).

The base case posterior for r^{max} was assumed for the spatial risk assessment of all Hector's dolphin populations, excluding the west coast of the North Island (i.e., not Māui dolphin). An individual based modelling assessment was undertaken to adjust this value of r^{max} for the Māui dolphin population, given small population size effects (Appendix 3).
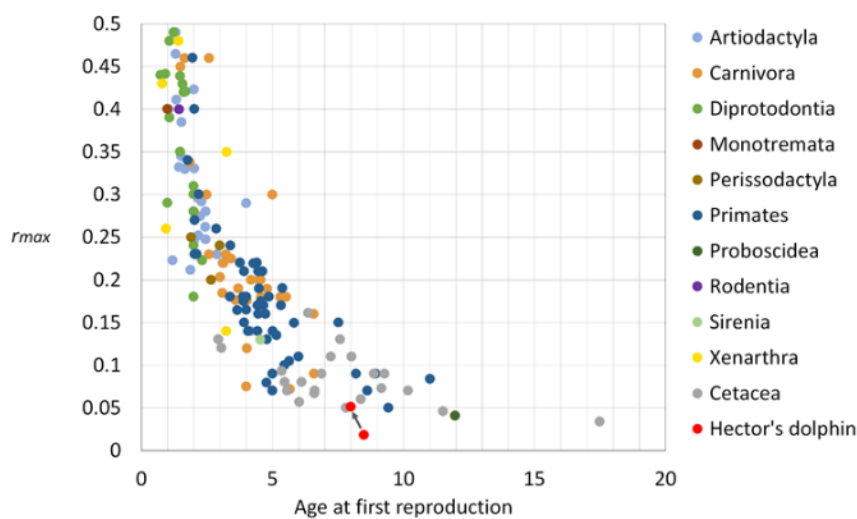
Figure A2-3: Comparative plot of r^{max} against age at first reproduction (AFR) for a variety of mammalian orders (Duncan et al. 2007). For Hector's dolphin, both the previous and updated values are shown (red points). The updated value of r^{max} derived here for Hector's dolphin is now consistent with that expected from other mammals, given estimated age at first reproduction.

References

Currey, R.J.C.; Boren, L.J.; Sharp, B.R.; Peterson, D. (2012). A risk assessment of threats to Māui's dolphins. Ministry for Primary Industries and Department of Conservation, Wellington. 51 p.

Dillingham, P.W.; Moore, J.E.; Fletcher, D.; Cortes, E.; Curtis, K.A.; James, K.C.; Lewison, R.L. (2016). Improved estimation of intrinsic growth r max for long- lived species: integrating matrix models and allometry. *Ecological Applications, 26*: 322–333.

Duncan, R.P.; Forsyth, D.M.; Hone, J. (2007). Testing the metabolic theory of ecology: allometric scaling exponents in mammals. *Ecology, 88*: 324–333.

Edwards, C.T.T.; Roberts, J.O.; Doonan, I.J. (2018). Estimation of the maximum rate of intrinsic growth for Hector's dolphin. Final Research Report available from Fisheries New Zealand. 22 p.

Gormley, A.M. (2009). Population modelling of hector's dolphins. PhD. thesis.

Moore, J.E., 2015. Intrinsic growth (rmax) and generation time (t) estimates for the cetacean genera *Sousa*, *Orcaella*, and *Neophocaena*, in support of IUCN Red list assessments.

Slooten, E.; Lad, F. (1991). Population biology and conservation of hector's dolphin. *Canadian Journal of Zoology, 69*: 1701–1707.

APPENDIX 3 – STOCHASTIC $r^{\max}$ ADJUSTMENTS FOR LOW POPULATION SIZE

Background

The spatial risk model developed for Hector's and Māui dolphins (see main body of the report) requires a prior distribution of $r^{\max}$ (intrinsic population growth rate)—the maximum growth rate that will occur at small population size when resources are replete. However, at *very* small population sizes (e.g., Māui dolphin) Allee effects may adversely affect realised population growth and increase the probability of extinction. The mechanisms from which Allee effects arise all impact on individual survival and reproduction, and include an array of demographic, genetic, social and potentially anthropogenic mechanisms that can suppress the realisation of maximal growth rate in small populations, despite replete resources:

- **Demographic stochasticity**, a sustained period of 'bad luck' (e.g. skewed sex ratio of offspring) can greatly increase the probability of extinction at small population size. Vulnerability to demographic variation increases if there are further decreases in population size. Demographic stochasticity may be exacerbated by environmental variability, where periods of adverse conditions are not compensated for by sustained periods of optimal conditions.

- **Inbreeding depression** (Clark & Seebeck 1990) is an example of a genetic Allee mechanism that can adversely affect productivity at small population size. Inbreeding depression is caused by the expression of lethal or deleterious genes, which becomes more likely in small populations with increased inbreeding. Lethal genes have a short-term impact since these will be purged if the population survives for a few generations. Deleterious genes (e.g., smaller litter sizes or higher mortality for new-borns) can become "fixed" into the genome, causing longer-term decreases in population growth rate.

- **Social Allee mechanisms** include the disruption of mating, feeding, or defense systems when the population size falls below threshold values.

All of these have the potential to prevent very small populations (e.g. Māui dolphin) from attaining maximal growth rates (i.e., consistent with $r^{\max}$) despite the absence of density dependent effects on population growth rate.

Objectives of this study

The deterministic maximum growth rate (D-$r^{\max}$) for a population (i.e. in the absence of demographic stochasticity) will be greater than the mean of the stochastic maximum growth rate (S-$r^{\max}$) for the same population (i.e. in the presence of demographic stochasticity). This effect will be amplified for smaller populations, such that the reduction in S-$r^{\max}$ will be greater given the same D-$r^{\max}$.

A median D-$r^{\max}$ of 0.05 was estimated for Hector's dolphin (Edwards et al. 2018, updated by Appendix 2). The aim of this analysis was to estimate the appropriate median value of S-$r^{\max}$ to use for the Māui dolphin population in the spatial risk model, given a starting population size consistent with the most recent population estimate of 63 individuals (95% c.i. = 57–75) (Baker et al. 2016). The effects of demographic stochasticity and inbreeding depression were accounted for by conducting population simulations using an individual-based model (IBM) assuming alternative starting sizes encompassing the latest population estimate for Māui dolphin.

Catastrophic events, such as disease and extreme environmental variation, were not considered here even though small population sizes may result from such events and they may have ongoing influence. Catastrophic events and potential social Allee mechanisms are difficult to understand and represent with realism. We interpret the results obtained from this assessment as the S-$r^{\max}$ to assume for the Māui dolphin population (and other small populations of Hector's dolphin), under "normal" (i.e., not catastrophic) conditions and in the absence of social Allee mechanisms.

Methods

Simulations

Population simulations were conducted using the using Vortex (Version 10), which was developed primarily to undertake Population Viability Analyses (PVAs) (Lacy & Pollak 2017). Vortex can simulate individual survival and breeding over time, and when applied randomly to individuals each year, the population size is stochastic over time, which can lead to small, isolated populations becoming locally extinct due to a run of adverse demographic rates. Vortex can allow demographic rates to vary over time in a specified pattern and to also vary stochastically to represent environmental variation. In addition, Vortex allows the application of inbreeding depression. Under the application of the above processes, the population growth rate for each simulation varies between runs and the average obtained over many population simulations is used to estimate S-$r^{\max}$.

Alternative starting population sizes (N, including calves) were assumed, ranging from 10 to 300 individuals. For each simulation, we projected populations over a 200-year period—an arbitrary time frame, although generally sufficient for marine mammal populations to reach carrying capacity regardless of starting population size. An arbitrary carrying capacity of 1000 individuals was specified, which was large enough not to affect population growth at low population sizes (i.e., under 100), so that density dependent effects would not interfere with the determination of S-$r^{\max}$.

The Edwards et al. (2018) assessment for D-$r^{\max}$ generated distributions of optimal age at first reproduction (AFR), non-calf survival (S^{1+}), calf survival (S^{0}), and annual breeding rate, which produced their distribution of D-$r^{\max}$. For all demographic parameters except annual breeding rate, we used the median value from the distribution obtained by Edwards et al. (2018) (Note that the parameters accepted for the distribution for D-$r^{\max}$ are correlated, so that using the medians for all parameters simultaneously will not necessarily give a D-$r^{\max}$ of 0.05). Annual breeding rate was then adjusted to make the D-$r^{\max}$obtained from the combined parameters used for population simulations equal to the median of the D-$r^{\max}$ distribution obtained by Edwards et al. (2018). The Vortex population model structure replicated that used by Edwards et al. (2018). Parameters used are shown in Table A3-1.

Table A3-1: Base parameter values used in the simulations. "–", not used.

Parameter	D-$r^{\max}$ = 0.0500	D-$r^{\max}$ = 0.0516	Environment variation SD (%)
Age at first reproduction (AFR)	8	8	–
Non-calf survival (S^{1+})	0.958	0.967	4.5
Calf survival (S^{0})	0.795	0.811	7.8
Breeding rate	0.450	0.448	10
Environment variation: correlation between survival and breeding rate (%)	50	50	–
Max breeding age	80	30	–
Carrying capacity	1,000	1,000	–
Inbreeding depression, LE	6.29	6.29	–
Inbreeding depression, percentage lethal	50	50	–

The analysis by Edwards et al. (2018) did not assume a maximum breeding age. To replicate this our base case model assumed a maximum breeding age of 80 (effectively infinite). The analysis by Edwards et al. (2018) was also updated with a sensitivity run assuming a maximum breeding age of 30 years (see Appendix 2). This run obtained a median D-$r^{\max}$ of 0.0516 (instead of 0.05 for infinite breeding age). We conducted a sensitivity set of model runs (for the same array of starting population sizes) with a maximum breeding age of 30 and with parameters consistent with a D-$r^{\max}$ of 0.0516.

Further sensitivity runs were conducted halving and doubling environmental and inbreeding parameters for D-$r^{\max}$ = 0.05 and N = 50.

The resulting mean values of S-$r^{\max}$ were regressed against $1/N$ to obtain an analytic equation for S-$r^{\max}$ given the starting population size (N).

Environmental variation

Gormley (2009) analysed mark-recapture data on Hector dolphin at Banks Peninsula and reported levels of uncertainty (standard deviation, SD) associated with estimates of survival to age 1 and non-calf survival (i.e., all older ages), which were assumed for this assessment (noting that the precision of these estimates will have been affected by sample size as well as environmental variation). The variability of annual breeding rate was set to the value in Gaillard et al. (2000), which was based on field data on large income breeder herbivores in temperate climates. The correlation of environmental variations of annual survival and breeding rate assumed the Vortex default values of 50%.

Inbreeding depression

Inbreeding was parameterised using lethal equivalents per haploid genome (LE, Lacy 1997). Although inbreeding depression applies to most demographic parameters, by default Vortex only imposes it on calf survival. Given the lack of required information on Hector's dolphin genetics, we adopted Vortex's default of 6.29 lethal equivalents per haploid genome, which was estimated by O'Grady et al. (2006) using data from field studies on wild populations. We also adopted Vortex's defaults for the percentage that are lethal (i.e., that can be purged from the population) at 50%.

Results

Stochastic $r^{\max}$ (S-$r^{\max}$)

The median S-$r^{\max}$ values obtained for alternative starting population sizes (N) are shown in Table A3-2. For both the base case assuming a D-$r^{\max}$ of 0.05 and the sensitivity run assuming a D-$r^{\max}$ of 0.0516 the regression R^2 values were very high (99.9%). For the base case runs assuming a D-$r^{\max}$ of 0.05 (maximum breeding age of 80) the regression equation was as follows

$$\text{S-}r^{\max} = 0.0481 - 0.154/N$$

The regression plot for this relationship is shown in Figure A3-1. For the sensitivity run assuming a D-$r^{\max}$ of 0.0516 (maximum breeding age of 30), the regression R^2 = 99.9% and the equation was

$$\text{S-}r^{\max} = 0.0497 - 0.180/N$$

Table A3-2: Mean stochastic $r^{\max}$ (S-$r^{\max}$) and associated standard error, given alternative starting population sizes (N). Demographic parameter values consistent with deterministic $r^{\max}$ (D-$r^{\max}$) of 0.05 (for maximum breeding age of 80 years) or 0.0516 (maximum breeding age of 30 years).

| Starting population size (N) | S-$r^{\max}$ | | | |
| | (D-$r^{\max}$ = 0.0500, breeding age = 80) | | (D-$r^{\max}$ = 0.0516, maximum breeding age = 30) | |
	Mean	SE (%)	Mean	SE (%)
10	0.0327	7.44	0.0318	7.42
20	0.0405	6.76	0.0404	6.67
30	0.0428	6.63	0.0437	6.49
50	0.0451	6.53	0.0463	6.41
75	0.0460	6.48	0.0474	6.37
100	0.0467	6.46	0.0477	6.36
150	0.0471	6.46	0.0485	6.35
300	0.0477	6.44	0.0493	6.31
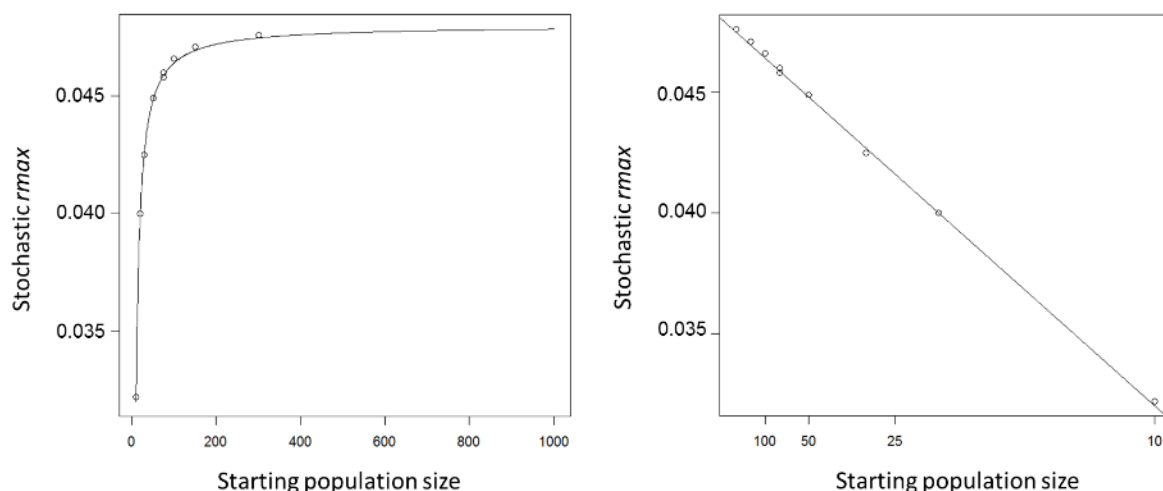
Figure A3-1: Mean stochastic $r^{\max}$ (S-$r^{\max}$) for alternative starting population size (*N*) and deterministic $r^{\max}$ (D-$r^{\max}$) of 0.05, with fitted regression line. Right panel, linear regression on 1/*N*; left panel, transposed regression on S-$r^{\max}$-*N* space.

S-$r^{\max}$ was insensitive to changes in environmental variation for breeding rate and calf survival (Table A3-3), although doubling environmental variation in non-calf survival caused a 10% reduction in S-$r^{\max}$. This result is expected since non-calf survival applies to a greater proportion of the population than calf survival. Doubling the frequency of lethal alleles reduced S-$r^{\max}$ by 7% (Table A3-3).

Table A3-3: Sensitivity of stochastic $r^{\max}$ (S-$r^{\max}$) to halving/doubling the SD of environmental variation and lethal alleles (LE). Deterministic $r^{\max}$= 0.05 and starting population size = 50 (corresponding median S-$r^{\max}$ for the base case = 0.0451).

Model run	S-$r^{\max}$	SD	Halve SD/LE Percent change in $r^{\max}$	S-$r^{\max}$	SD	Double SD/LE Percent change in $r^{\max}$
Inbreeding LE	0.0469	6.56	+4.0	0.0418	6.47	-7.30
Breeding rate SD	0.0449	5.94	-0.4	0.0451	7.93	0.00
Calf survival SD	0.0450	6.16	-0.2	0.0453	7.21	+0.40
Non-calf survival SD	0.0462	4.47	+2.4	0.0402	11.5	-10.9

Conclusions and risk assessment inputs

- For the Māui dolphin population, stochastic $r^{\max}$ (S-$r^{\max}$) can be calculated by substituting the Māui population size (*N*) into the regression: 0.0481 – 0.154/*N*, noting that *N* includes calves.

- Adjusting the median of Hector's dolphin $r^{\max}$ from 0.05 estimated by Edwards et al. (2018) to 0.045 would account for demographic stochasticity and the assumed frequency of lethal alleles, with a starting population size of 50 individuals (below the latest estimate for Māui dolphins of 63 individuals).

- Comparatively lower estimates of stochastic $r^{\max}$ were obtained when assuming greater environmental variability in non-calf survival and a doubling of lethal alleles (S-$r^{\max}$ = 0.04).

- Note that this assessment did not account for catastrophic events or disruption to social systems that might occur at small population size and that would further reduce S-$r^{\max}$.

References

Baker, C.S.; Steel, D.; Hamner, R.M.; Hickman, G.; Boren, L.; Arlidge, W.; Constantine, R. (2016). Estimating the abundance and effective population size of Māui dolphins using microsatellite genotypes in 2015–16, with retrospective matching to 2001–16. Department of Conservation, Auckland. 70 p.

Clark, T.W.; Seebeck, J.H. (1990). *Management and conservation of small populations: proceedings of a conference held in Melbourne, Australia, September 26-27, 1989.* Chicago Zoological Society: Brookfield, Illinois.

Edwards, C.T.T.; Roberts, J.O.; Doonan, I.J. (2018). Estimation of the maximum rate of intrinsic growth for Hector's dolphin. Final Research Report available from Fisheries New Zealand. 22 p.

Gaillard, J.M.; Festa-Bianchet, M.; Yoccoz, N.G.; Loison, A.; Toïgo, C. (2000). Temporal variation in fitness components and population dynamics of large herbivores. *Annual Review of Ecology and Systematics 31*:367–393.

Gormley, A.M. (2009). Population Modelling of Hector's Dolphins. A thesis submitted for the degree of Doctor of Philosophy at the University of Otago, Dunedin, New Zealand.

Lacy, R.C.; Pollak, J.P. (2017). Vortex: A Stochastic Simulation of the Extinction Process. Version 10.2.9. Chicago Zoological Society, Brookfield, Illinois, USA. www.vortex10.org/Vortex10.aspx. Downloaded on 14/7/2017.

Lacy, R.C. (1997). Importance of Genetic Variation to the Viability of Mammalian Populations, *Journal of Mammalogy*, *78*: 320–335. https://doi.org/10.2307/1382885

O'Grady, J.J.; Brook, B.W; Reed, D.H.; Ballou, J.D.; Tonkyn, D.W.; Frankham, R. (2006). Realistic levels of inbreeding depression strongly affect extinction risk in wild populations. *Biological Conservation 133.* p. 41.

Vortex Manual (not cited)

Lacy, R.C.; Miller, P.S.; Traylor-Holzer, K. (2017). Vortex 10 User's Manual. 6 September 2017 update. IUCN SSC Conservation Breeding Specialist Group, and Chicago Zoological Society, Apple Valley, Minnesota, USA.

APPENDIX 4 – NECROPSY CAUSE OF DEATH SUMMARY TABLES

Table A4-1: Diagnosed cause of death at necropsy by age stage (intermediate and full confidence only).

Cause of death	Calf	Sub-adult	Adult	Total
		Age stage		
Maternal separation	14	0	0	14
Brucellosis	0	0	2	2
Deformity	1	0	1	2
Disease (other)	3	0	7	10
Miscellaneous	0	1	4	5
Pneumonia	1	0	4	5
Predation	0	0	2	2
Toxoplasmosis	0	2	7	9
Tuberculosis	0	0	1	1
Known bycatch	1	4	1	6
Probable bycatch	0	2	4	6
Possible bycatch	0	0	1	1
Unknown/Open	1	1	11	13
Total	21	10	45	76

Table A4-2: Diagnosed cause of death at necropsy – calves, by year of stranding/capture (intermediate and full confidence only).

Cause of death	2007	2008	2009	2010	2011	2012	2013	2014	2015	2016	2017	2018	Total
												Year of stranding/capture	
Deformity	0	0	0	0	0	0	0	1	0	0	0	0	1
Disease (other)	0	0	0	0	0	0	1	1	0	1	0	0	3
Maternal seperation	0	2	2	1	2	5	1	0	0	0	1	0	14
Pneumonia	0	0	0	0	0	0	0	0	0	0	1	0	1
Known bycatch	0	0	0	0	0	0	0	0	1	0	0	0	1
Unknown/Open	0	0	0	1	0	0	0	0	0	0	0	0	1
Total	0	2	2	2	2	5	2	2	1	1	2	0	21

Table A4-3: Diagnosed cause of death at necropsy – non-calves, by year of stranding/capture (intermediate and full confidence only).

							Year of stranding/capture						
Cause of death	2007	2008	2009	2010	2011	2012	2013	2014	2015	2016	2017	2018	Total
Brucellosis	0	0	0	1	0	0	0	0	0	0	0	1	2
Deformity	0	0	0	0	0	0	0	0	1	0	0	0	1
Disease (other)	0	1	1	0	0	2	2	1	0	0	0	0	7
Miscellaneous	0	1	0	0	0	1	1	0	0	0	0	2	5
Pneumonia	0	0	0	0	0	1	2	0	0	0	1	0	4
Predation	0	1	0	0	0	0	0	0	0	0	0	1	2
Toxoplasmosis	1	2	1	2	1	0	0	0	1	0	1	0	9
Tuberculosis	0	0	0	0	0	0	0	0	0	1	0	0	1
Known bycatch	0	0	2	1	0	1	0	0	0	0	1	0	5
Probable bycatch	0	0	0	1	0	2	1	0	1	0	0	1	6
Possible bycatch	0	0	0	0	0	0	0	0	0	0	1	0	1
Unknown/Open	0	2	4	0	1	3	0	1	1	0	0	0	12
Total	1	7	8	5	2	10	6	2	4	1	4	5	55

Table A4-4: Diagnosed cause of death at necropsy – non-calves, by population (intermediate and full confidence only).

	Hector's dolphin				Māui dolphin	
Cause of death	ECSI	WCSI	SCSI	WCNI	WCNI	Total
Brucellosis	0	1	0	0	1	2
Deformity	0	0	1	0	0	1
Disease (other)	4	2	0	1	0	7
Miscellaneous	2	2	0	0	1	5
Pneumonia	3	1	0	0	0	4
Predation	0	0	1	0	1	2
Toxoplasmosis	5	2	0	0	2	9
Tuberculosis	1	0	0	0	0	1
Known bycatch	5	0	0	0	0	5
Probable bycatch	4	2	0	0	0	6
Possible bycatch	0	1	0	0	0	1
Unknown/Open	9	3	0	0	0	12
Total	33	14	2	1	5	55

Table A4-5: Diagnosed cause of death at necropsy – non-calves, by sex (intermediate and full confidence only).

	Sex			
Cause of death	Female	Male	Unknown	Total
Brucellosis	2	0	0	2
Deformity	1	0	0	1
Disease (other)	3	4	0	7
Miscellaneous	3	1	1	5
Pneumonia	1	3	0	4
Predation	1	1	0	2
Toxoplasmosis	7	2	0	9
Tuberculosis	1	0	0	1
Known bycatch	1	4	0	5
Probable bycatch	2	2	2	6
Possible bycatch	0	0	1	1
Unknown/Open	7	5	0	12
Total	29	22	4	55

Table A4-6: Diagnosed cause of death at necropsy – non-calves, females by maturity stage (intermediate and full confidence only).

	Female maturity stage			
Cause of death	Mature	Immature	Unknown	Total
Brucellosis	1	0	1	2
Deformity	1	0	0	1
Disease (other)	2	0	1	3
Miscellaneous	2	0	1	3
Pneumonia	1	0	0	1
Predation	1	0	0	1
Toxoplasmosis	6	1	0	7
Tuberculosis	0	0	1	1
Known bycatch	0	1	0	1
Probable bycatch	1	1	0	2
Possible bycatch	0	0	0	0
Unknown/Open	4	2	1	7
Total	19	5	5	29

APPENDIX 5 – HECTOR'S/MĀUI DOLPHIN PREY SPECIES DISTRIBUTIONS

Background

Dietary studies of Hector's/Māui dolphin are limited to a single published study based on the analysis of stomach contents of 63 beachcast and bycaught individuals, recovered betwwen 1984 and 2006 (Miller et al. 2013). This study found that the diet of this species was primarily composed of six prey taxa: red cod (*Pseudophycis bachus*), arrow squid spp. (*Nototodarus* sp.), New Zealand sole (*Peltorhamphus* sp.), ahuru (*Auchenoceros punctatus*), sprat sp. (*Sprattus* spp.), and stargazer sp. (*Crapatalus* sp.), which together contributed approximately 80% of the total diet composition by mass (Miller et al. 2013) (Table A5-1). Miller et al. (2013) noted some difference with respect to the dietary composition comparing samples from the East and West Coasts of the South Island, with an increased contribution of middle depth prey species such as hoki (*Macruronus novaezelandiae*), hake (*Merluccius australis*) and javelinfish (*Lepidorhynchus denticulatus*) in West Coast dolphins. However, the top six prey species listed in Table A5-1 had a similar dietary composition in the East and West Coast populations, indicating that these two large populations have highly overlapping trophic habitat preferences.

Table A5-1: Dietary composition of major prey species of Hector's amd Māui dolphins. Figures taken from Miller et al. (2013).

Prey species	Estimated percentage of reconstructed diet mass
Red cod (*Pseudophycis bachus*)	37
Arrow squid spp. (*Nototodarus* sp.)	13
Sole sp. (*Pelthoramphus* sp.)	7
Ahuru (*Auchenoceros punctatus*)	7
Sprat (*Sprattus* spp.)	7
Stargazer sp. (*Crapatalus* sp.)	6
All other species	23

Miller (2015) also found a strong spatial-seasonal correlation around Banks Peninsula between red cod catch rates in bottom-set fish traps and surface Hector's/Māui abundance from boat-based visual strip surveys. Generalised Additive Models (GAMs) predicting Hector's dolphin abundance in response to various habitat variables found that red cod mass (in fish traps) was the strongest predictor of both off-shore and alongshore Hector's dolphin abundance (Miller 2015). This indicated that habitat models for predicting Hector's and Māui dolphin distribution may be improved by incorporating estimated spatial distributions of their prey species.

All six of the key prey species identified in Table A5-1 are captured by inshore trawl surveys that have operated around New Zealand (e.g. Bagley & Hurst 1996; Beentjes & Stevenson 2000, 2001; Morrison et al. 2001a, 2001b; Stevenson & Hanchet 1999, 2000; Stevenson & MacGibbon 2018), using a standardised methodology since 1991 (Hurst et al. 1992). Surveys were conducted in years prior to 1991, though potentially using methods inconsistent with the later period.

This Appendix describes an analysis that uses inshore trawl survey catch rate information for the key prey taxa of Hector's and Māui dolphins.

Methods

GAMs were used for all predictive models, with a binomial error structure assumed for all presence/absence single prey species models.

Data - subsetting

The primary data source for this analysis was catch effort information from inshore surveys by *RVs Kaharoa* and *Tangaroa*. A number of survey data subsets were made:

- **Gear method** ("gear_meth") = "1 – Bottom trawl" or "3 – High-opening bottom trawl" (excluding "High-opening bottom trawl" would have greatly reduced the number of survey stations along the West Coast North Island);
- **Gear performance** ("gear_perf") = "1" or "2";
- **Gear depth** (mean of "gear_s" and "gear_f") < 250 m.

Data - explanatory variables

A bivariate spline for station northing and easting was selected as the first model term (the smooth basis dimension "*k*" was initially set to 100 to allow complex surface smoothers). In addition, candidate predictor variables offered to GAMs included:

- Gear depth (mean of "gear_s" and "gear_f") (univariate spline with "k" set to 3);
- Trawled area (km², calculated as "distance"×1.852×"dist_door"/1000) (univariate spline with "*k*" set to 3);
- Gear method (bottom trawl or high-opening bottom trawl) (categorical); and
- Cod end mesh size (obtained from respective survey reports) (categorical).

Vessel was not offered as a model term due to insufficient spatial overlap between station locations from the *Kaharoa* and *Tangaroa* surveys (Figure A5-1). As such, a vessel effect would very likely have been confounded with spatial effects, given the high resolution bivariate spline for northing and easting.

Prey species predictions may potentially have been improved with the inclusion of habitat variables in prey models. However, this was not donethe here as habitat variables were also offered to Hector's/Māui dolphin habitat preference models that used the predicted prey distributions and it was considered desirable to avoid including the habitat variables twice.

Data - response variable

The response variable was the binomial presence/absence of respective prey species listed in Table A5-1 in a survey trawl. As a time-saving measure, the derivation of species' presence/absence ignored information with respect to body size composition from survey biological sampling, despite a probable bias for Hector's and Māui dolphins to target smaller size fractions of key prey species (Miller et al. 2013).

Modelling approach

Model selection followed the standard Fisheries New Zealand approach used for predictive modelling in which terms were sequentially added until they explained less than 1% of the model deviance. Standard diagnostics were used to compare models (model AIC and the percentage of deviance explained) and to check that distributional assumptions were met (quantile-quantile plots).

Once the optimal model structure was identified, the smooth basis dimension (*k*) for the bivariate spline on northing and easting was increased in units of 10 until the maximum possible effective degrees of freedom (EDF) for this term was more than 110% of the optimised EDF.

Data – prediction

Model predictions were made for a grid of northing and easting values of a 1×1 km resolution. The resulting grid locations were used to derive bathymetric depth using the NIWA bathymetry layer. Prey species probability of presence (in a survey trawl) was then predicted for grid cell values of northing, easting, and the associated bathymetric depth.

Results

The temporal spatial coverage of trawl survey stations was generally very good for the specified survey of trawls (< 250 m and others listed above) (Table A5-2 and Figure A5-1). More than 1000 stations

were undertaken in each of the West Coast and East Coast South Island areas, including the areas of highest abundance for Hector's dolphin (comparing Figure A5-1 with figure 18 of MacKenzie & Clement 2016) and for Māui dolphin (comparing Figure A5-1 with figure 1 of Currey et al. 2012). Notable areas of historically low survey effort include Fiordland, Dunedin to Moeraki, Kaikoura to Queen Charlotte Sound (all South Island), Wellington to Paraparaumu, and western Cape Egmont (both North Island) (Figure A5-1).

Table A5-2: Count of survey stations by year and area (for *RV Kaharoa* only). Stations meeting subset criteria, specified above.

	RV *Kaharoa* survey stations					*RV Tangaroa* survey stations
Survey year	ECSI	WCSI	ECNI	NCNI	WCNI	
1991	54	0	0	0	108	0
1992	73	100	0	230	0	5
1993	62	0	71	148	0	92
1994	86	102	93	70	73	93
1995	19	131	111	0	0	113
1996	163	55	87	78	120	104
1997	161	78	0	47	0	0
1998	85	0	0	0	0	1
1999	101	0	0	78	100	4
2000	151	75	0	48	0	0
2001	25	0	0	0	0	5
2002	0	0	0	0	0	3
2003	0	73	0	0	0	3
2004	0	0	0	0	0	5
2005	0	67	0	0	0	2
2006	0	0	0	0	0	2
2007	97	82	0	0	0	3
2008	89	0	0	0	0	7
2009	82	65	0	40	0	3
2010	0	0	0	0	0	2
2011	0	76	0	0	0	4
2012	92	0	0	0	0	32
2013	0	72	0	0	0	4
2014	104	0	0	0	0	2
2015	0	52	0	0	0	2
2016	103	0	0	0	0	32
Total	1 547	1 028	362	739	401	523
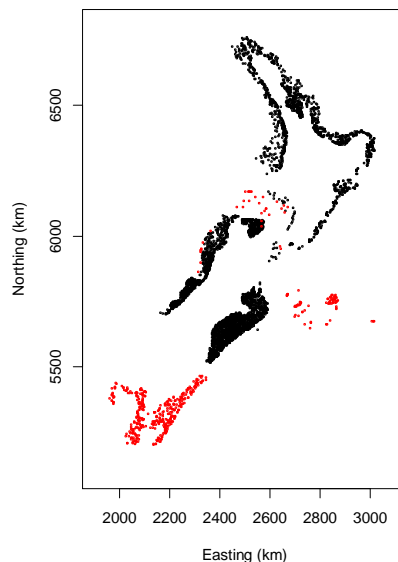
Figure A5-1: The spatial distribution of RV *Kaharoa* (black circles) and RV *Tangaroa* (red circles) survey trawls meeting subset criteria, specified above.

Candidate survey operational terms (trawled area, cod-end mesh size and gear method) were not retained in the final models for any of the six prey taxa (Table A5-3). In addition to the bivariate spline

for northing and easting, depth was retained for all prey taxa except red cod and sprat. For all prey taxa, the percentage of deviance explained was high (over 40%). Q-Q plots were produced for model residuals and indicated good model fit for all prey taxa (Figure A5-2). Prey taxa GAM splines are shown in Figure A5-3, which indicate increasing probability of presence with depth for arrow squid and giant stargazer and a decreasing relationship with depth for sole and ahuru. For red cod and sprat, the spatio-bathymetric distribution was entirely described by the bivariate spline on northing and easting (Figure A5-3).

Table A5-3: Final prey species GAM structures.

Prey taxon	Final GAM structure	R^2	% deviance explained
Red cod	Presence/absence ~ s(easting, northing, k = 110, bs = "ts")	0.495	44.6
Arrow squid spp.	Presence/absence ~ s(easting, northing, k = 100, bs = "ts") + s(depth, k = 3, bs = "cs")	0.534	48.1
Giant stargazer	Presence/absence ~ s(easting, northing, k = 180, bs = "ts") + s(depth, k = 3, bs = "cs")	0.659	61.2
Sprat spp.	Presence/absence ~ s(easting, northing, k = 80, bs = "ts")	0.452	52.6
Sole (*Pelthoramphus* spp.)	Presence/absence ~ s(easting, northing, k = 140, bs = "ts") + s(depth, k = 3, bs = "cs")	0.529	55.9
Ahuru	Presence/absence ~ s(easting, northing, k = 100, bs = "ts") + s(depth, k = 3, bs = "cs")	0.343	48.5
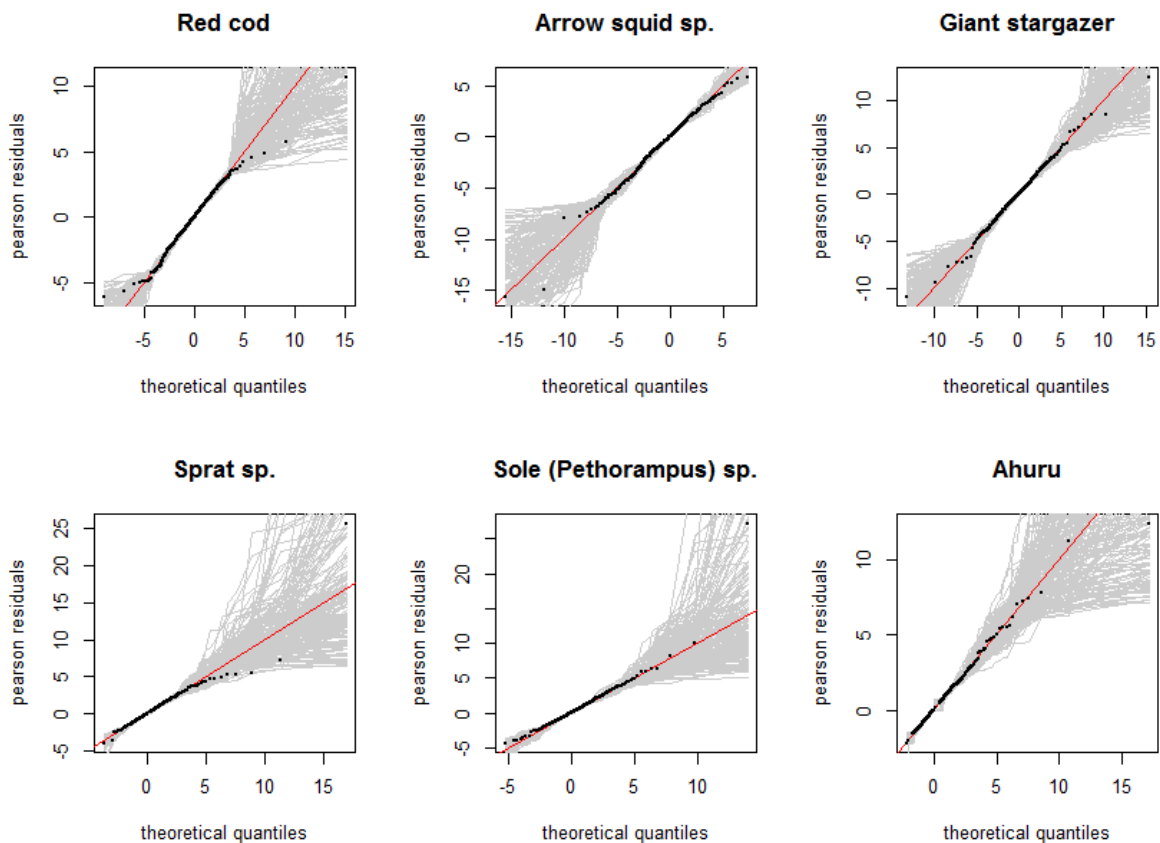
Figure A5-2: Simulation-based quantile-quantile plots for final prey species GAMs, with Pearson residuals and 200 simulation replicates.

Red cod
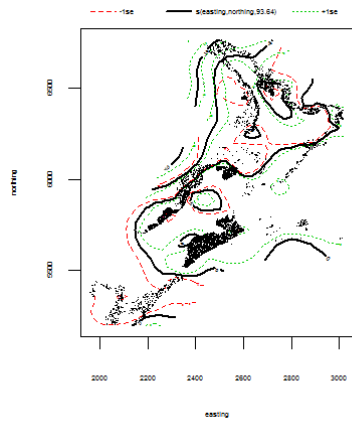
Arrow squid sp.
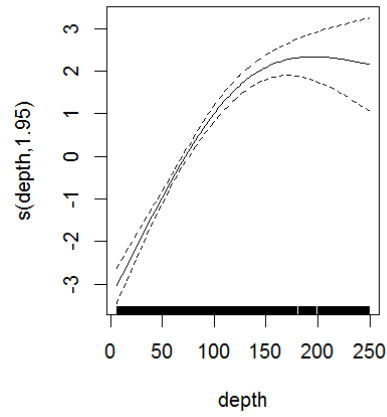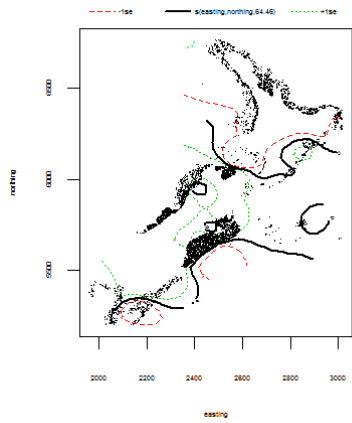
Giant stargazer
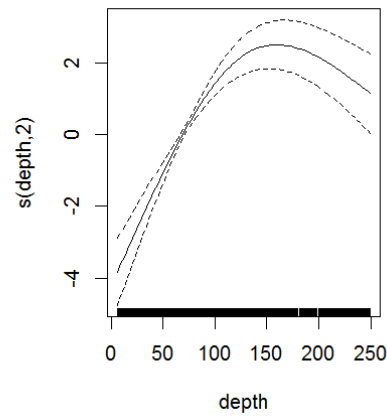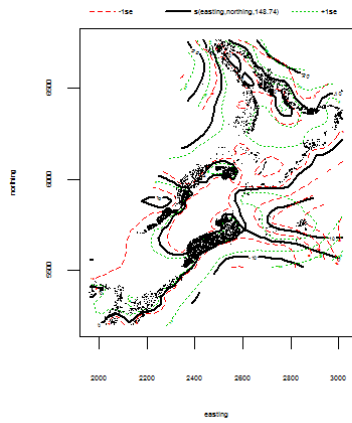
Figure A5-3: Prey taxon GAM splines for all splined terms in a prey's respective final model.

Sprat sp.
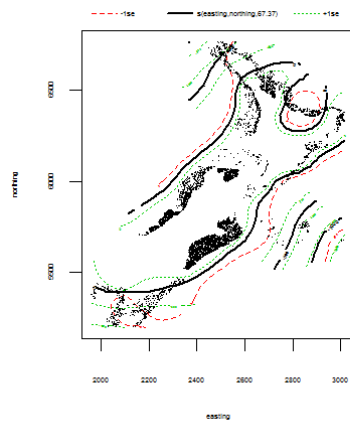
Sole (*Pelthoramphus*) sp.
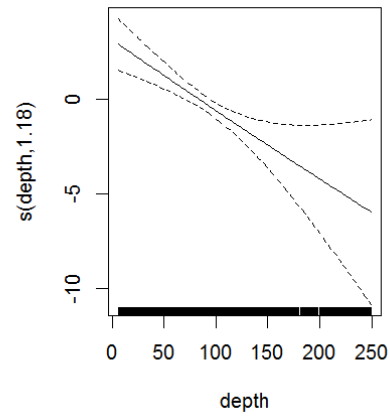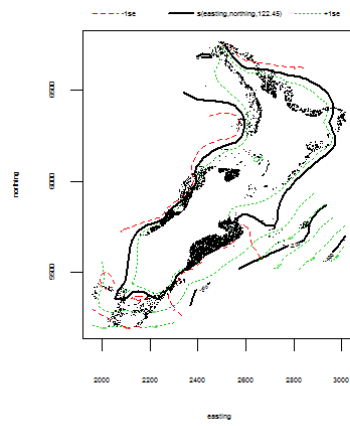
Ahuru
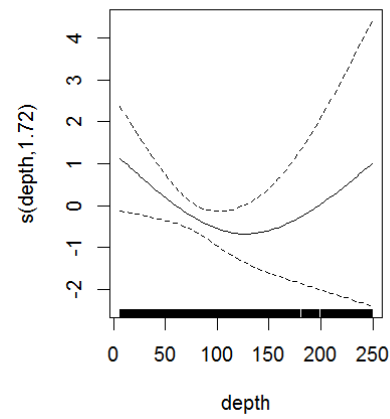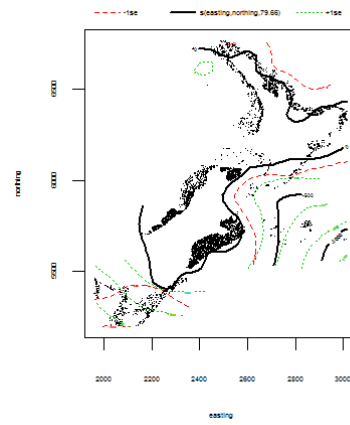
Figure A5-3 continued: Prey taxon GAM splines for all splined terms in a prey's respective final model.

Spatial model predictions generally agreed well with raw area grid-cell averaged values (comparing Figure A5-4 and Figure A5-5). Spurious predictions in regions of low survey effort were not produced for any prey taxa, with the exception of the Fiordland area prediction for sprat sp., for which almost 100% presence was predicted (bottom left-hand plot of Figure A5-5).

The estimated spatial distributions of sprat sp., sole sp. and ahuru were all very similar with peak presence in high turbidity areas of the east and west coast of the South Island and patchy areas of moderate presence on the east and west coast of the North Island (Figure A5-5). Red cod (the main prey of east and west coast South Island populations of Hector's dolphins) were present on most trawls on the South Island north of Otago and mostly absent from trawls at inshore southland and on the west and north coasts of the North Island (Figure A5-5).
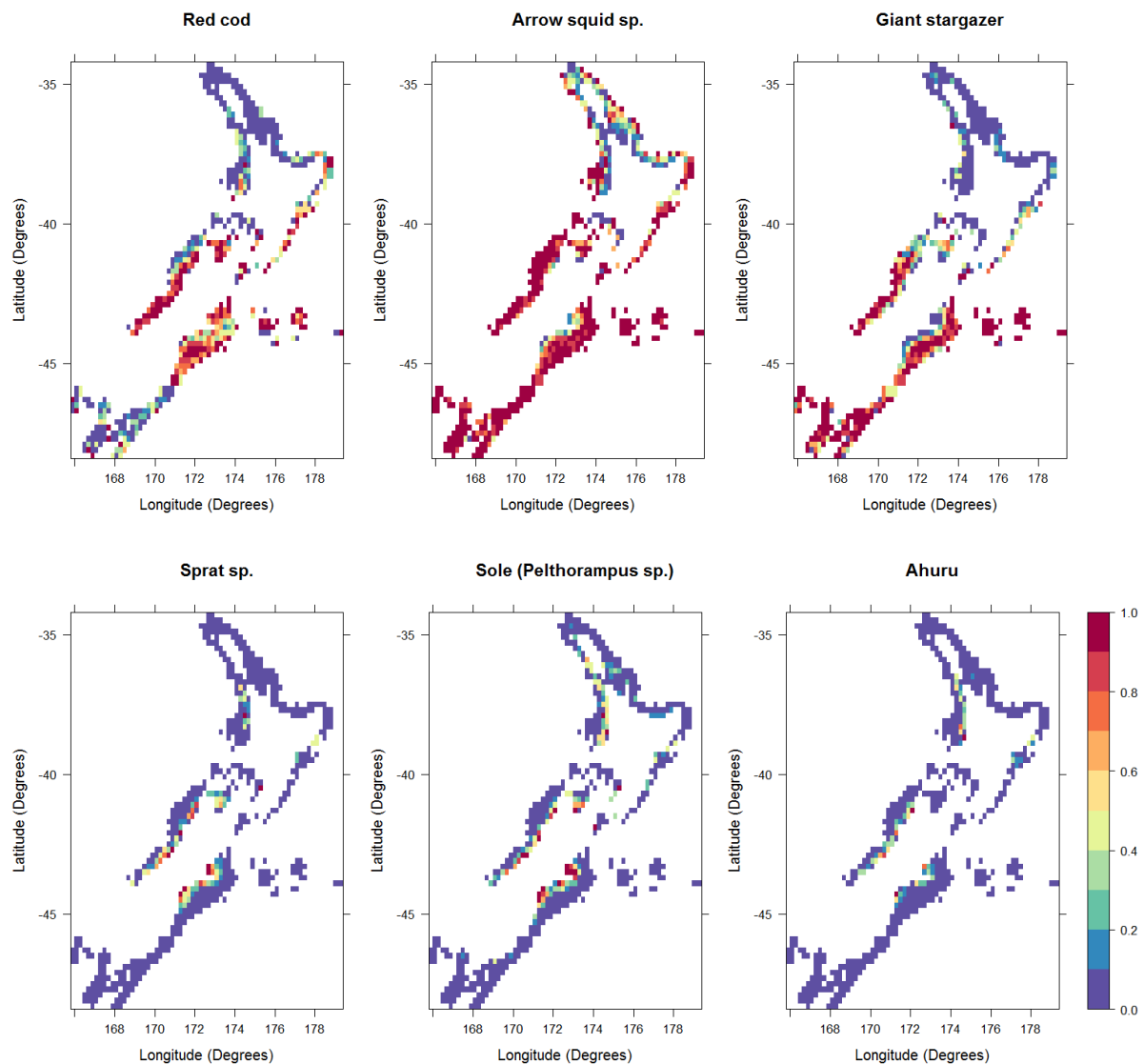
Figure A5-4: Unstandardised mean proportion of *Kaharoa* and *Tangaroa* survey stations in which key prey species (Table A5-2) were present, aggregated by 0.2-degree grid.
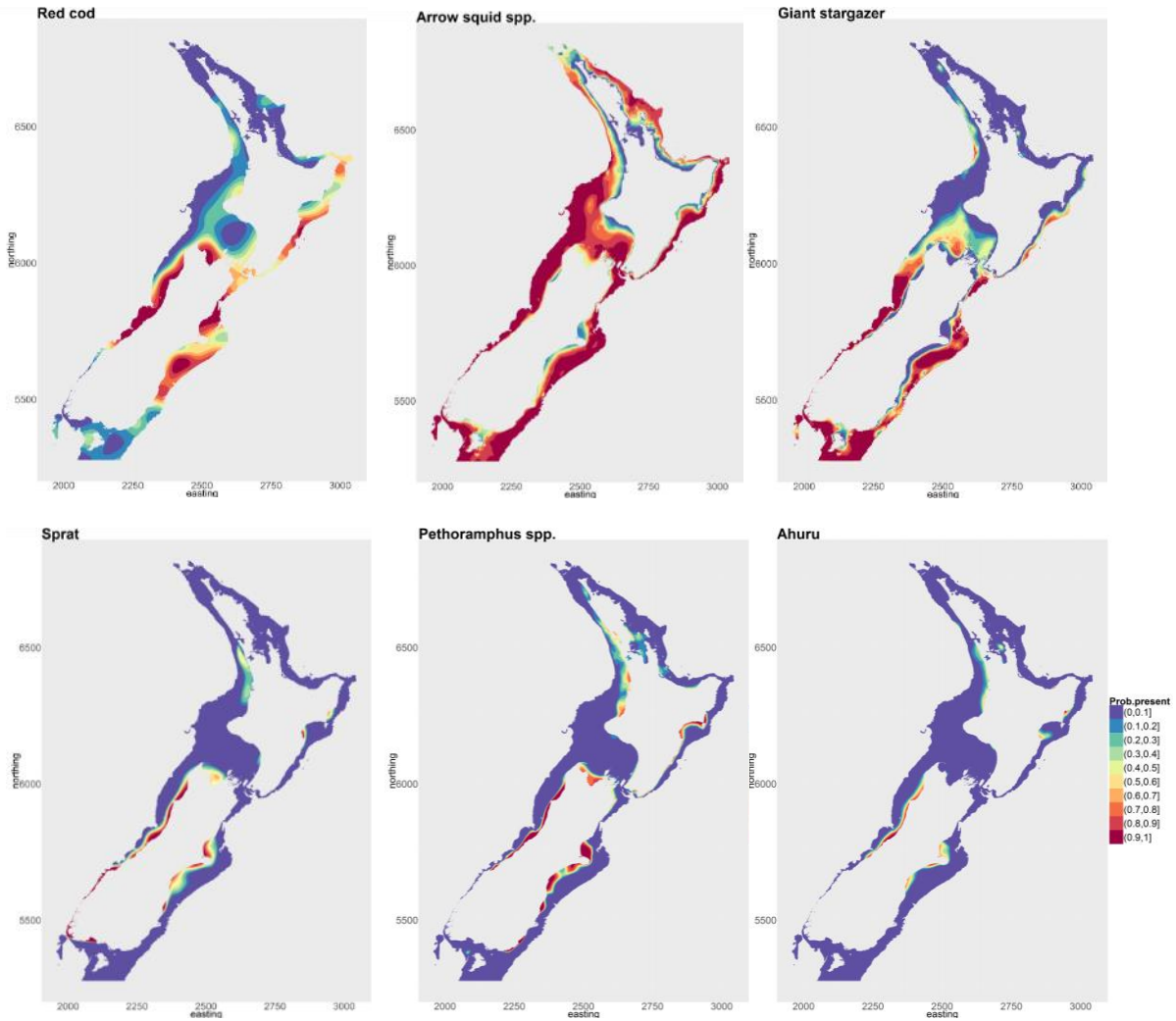
Figure A5-5: Model predicted proportion of *Kaharoa* and *Tangaroa* survey stations in which key prey species (Table A5-2) were present.

A multi-species exploration of the spatial distribution of raw (not modelled) data for top six prey taxa was also undertaken. Two spatial plots of raw data were produced:

1. The *mean count* of the top six prey taxa per trawl station (an integer between 0 and 6) aggregated by 0.1-degree grid cell; and
2. The *mean combined biomass (in kg)* of the top six prey taxa per trawl station aggregated by 0.1-degree grid cell.

No attempt was made to account for species-differences in catchability at this time.

These plots indicated that the key prey of Hector's and Māui dolphins were most diverse along the length of the west coast of the South Island to the north of Fiordland and, to a lesser extent, on the east coast of the South Island, particularly around Banks Peninsula (Figure A5-6, left-hand plot). Peak areas of survey catch biomass of the top six prey taxa included the west coast of the South Island, inshore Southland and the offshore region of the east coast South Island. The west of the North Island (where Māui dolphins occur), the South Taranaki Bight and the entire north coast of the North Island are notable for their low diversity and biomass of the key Hector's and Māui dolphin prey species, compared with the remainder of New Zealand (Figure A5-6, right-hand plot).
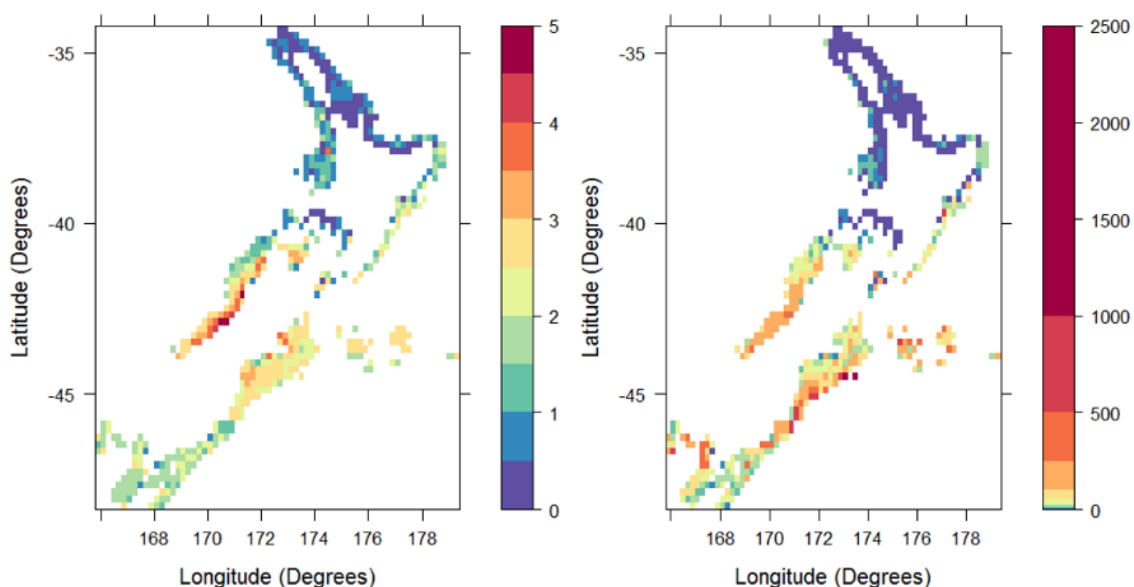
Figure A5-6: Unstandardised mean count of species (left) and combined biomass in kg (right) of the six key prey taxa (Table A5-2) for *Kaharoa* and *Tangaroa* survey stations aggregated by 0.2-degree grid. Note that no attempt was made to account for between-species variation in catchability.

Conclusions and risk assessment inputs

This analysis produced predicted spatial distributions of prey taxa (probability of presence in survey trawls) that were used by predictive models (along with physical/oceanographic habitat variables) to estimate the spatial abundance of Hector's and Māui dolphins. Dolphin abundance along aerial survey transects was used as a response variable (Section 5.1).

The estimated spatial distributions of sprat, sole and ahuru were all very similar with peak presence in high turbidity area of the east and west coast of the South Island. Red cod were present in most survey trawls. Patchy areas of moderate presence were also estimated for these species on the east and west coast of the North Island (Figure A5-5). An exploration of raw (not modelled trawl data) found that the diversity and biomass of key prey species was greatest on the west coast of the South Island, with regions of moderate diversity and biomass around the rest of the South Island and east coast of the North Island.

The west coast of the North Island where Māui dolphin occur was notable for low diversity and biomass of the key prey. The Māui dolphin sample for which dietary information was available was small ($N = 2$), although it did confirm that red cod, ahuru and sole are predated on by Māui dolphins (Miller et al. 2013).

Hector's dolphin habitat preference models predicted that the dolphins moved further off-shore in winter (Figure 17 and Figure 18). This off-shore movement was also noted by Miller (2015), although at a smaller spatial scale (around Banks Peninsula), potentially in response to seasonal prey movements. However, limiting trawl survey sampling in the post-1991 (standardised) period meant that seasonal prey distribution could not be estimated by our analysis, owing to insufficient spatial coverage for both summer and winter periods.

Future research to generate improved prey distribution layers may include:

- Consideration of prey species body length in survey trawls representative of small size fractions dominating Hector's/Māui dolphin diet (Miller et al. 2013);

- Model-based estimation of spatial prey species biomass, rather than probability of presence in a survey trawl;
- The estimation of seasonal (summer and winter) prey species distributions using catch information from surveys prior to 1991 (when survey methods were standardised). This analysis may also consider the use of observer catch records from commercial fishery operations; and
- Future trawl survey effort and dietary information for Hector's/Māui dolphin would be useful for assessing changes in prey distribution/availability through time.

In addition, some of the key prey species of Hector's and Māui dolphins are commonly important prey for other protected marine mammal and seabird species. For example, red cod are also key prey for New Zealand sea lions, New Zealand fur seals, and yellow-eyed penguins (Boren 2010; Lalas 1997; Moore & Wakelin 1997). As such predicted prey distributions using survey and/or commercial fishery data may have utility for estimating habitat-preference based distributions for these other species also.

References

Bagley, N.W.; Hurst, R.J. (1996). Trawl survey of middle depth and inshore bottom species off Southland, February-March 1996 (TAN9604). New Zealand Fisheries Data Report No. 77.

Beentjes, M.P.; Stevenson, M.L. (2000). Review of the east coast South Island winter trawl survey time series, 1991–96. *NIWA Technical Report 86*. 64 p.

Beentjes, M.P.; Stevenson, M.L. (2001). Review of east coast South Island summer trawl survey time series, 1996–97 to 1999–2000. *NIWA Technical Report 108*. 92 p.

Boren, L. (2010). Diet of New Zealand fur seals (*Arctocephalus forsteri*): a summary. DOC Research & Development Series 319. 19 p.

Currey, R.J.C.; Boren, L.J.; Sharp, B.R.; Peterson, D. (2012). A risk assessment of threats to Māui's dolphins. Ministry for Primary Industries and Department of Conservation, Wellington. 51 p. (Unpublished report held by Fisheries New Zealand, Wellington.)

Hurst, R.J.; Bagley; N., Chatterton, T.; Hanchet, S.; Schofield, K; Vignaux, M. (1992). Standardisation of hoki/middle depth time series trawl surveys. MAF Fisheries Greta Point Internal Report No. 194. 89 p. (Unpublished report held in NIWA library, Wellington.)

Lalas, C. (1997). Prey of Hooker's sea lions *Phocarctos hookeri* based at Otago Peninsula New Zealand. Pp. 130–136 in Hindell, M.; Kemper, C. (Eds): Marine mammal research in the Southern hemisphere, status, ecology and medicine, vol 1. Surrey Beatty and Sons, Chipping Norton.

MacKenzie, D.I.; Clement, D.M. (2016). Abundance and Distribution of WCSI Hector's dolphin. *New Zealand Aquatic Environment and Biodiversity Report No. 168*. 67 p.

Miller, E.J. (2015). Ecology of Hector's dolphin (*Cephalorhynchus hectori*): Quantifying diet and investigating habitat selection at Banks Peninsula (Thesis, Doctor of Philosophy). University of Otago. 168 p.

Miller, E.; Lalas, C.; Dawson, S.; Ratz, H.; Slooten, E. (2013). Hector's dolphin diet: The species, sizes and relative importance of prey eaten by *Cephalorhynchus hectori*, investigated using stomach content analysis. *Marine Mammal Science, 29*: 606–628.

Moore, P.J.; Wakelin, M.D. (1997). Diet of the Yellow-eyed Penguin *Megadyptes antipodes*, South Island, New Zealand, 1991–1993. *Marine Ornithology 25*: 17–29.

Morrison, M.; Stevenson, M.; Hanchet, S. (2001a). Review of Bay of Plenty trawl survey time series (1983-99). Final Research Report for Ministry of Fisheries Research Project MOF1999/04O. (Unpublished report held by Fisheries New Zealand, Wellington.)

Morrison, M.; Stevenson, M.; Hanchet, S. (2001b). Review of west coast North Island trawl survey time series (1986-96). *NIWA Technical Report 97*. 56 p.

Stevenson, M.L.; Hanchet, S.M. (1999). Review of the inshore trawl survey series of the east coast North Island, 1993–96. Final Research Report for Ministry of Fisheries Research Project INT9801. (Unpublished report held by Fisheries New Zealand, Wellington.)

Stevenson, M.L.; Hanchet, S.M. (2000). Review of the inshore trawl survey series of the west coast of the South Island and Tasman and Golden Bays, 1992–97. *NIWA Technical Report 82*. 79 p.

Stevenson, M.L.; MacGibbon, D.J. (2018). Inshore trawl survey of the west coast South Island and Tasman and Golden Bays, March-April 2017 (KAH1703). *New Zealand Fisheries Assessment Report 2018/18*. 92 p.

APPENDIX 6 – NON-PREY HABITAT LAYERS CONSIDERED FOR HECTOR'S/MĀUI DOLPHIN DISTRIBUTION MODELLING
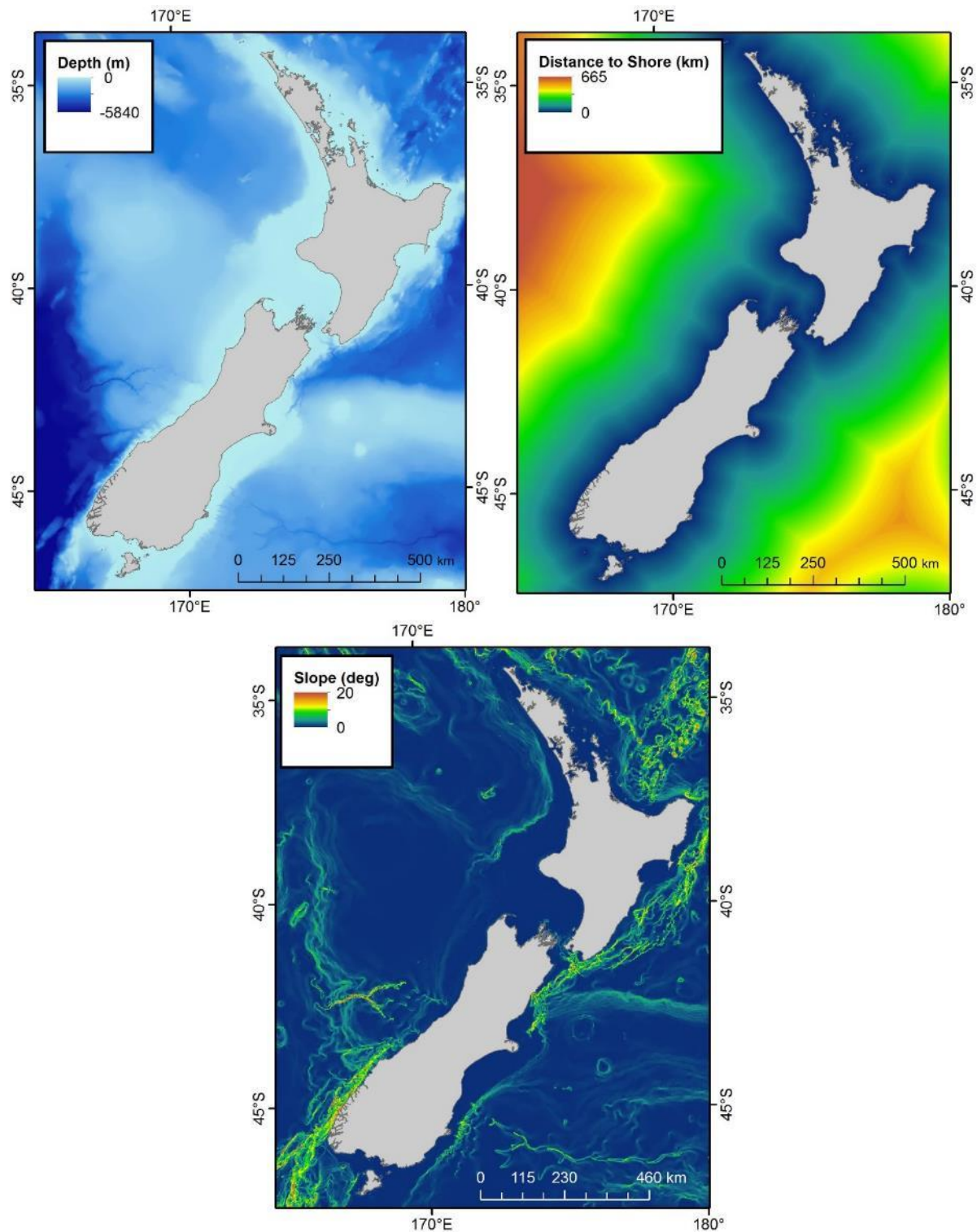
Figure A6-1: Static habitat variables used in Hector's/Māui distribution modelling.
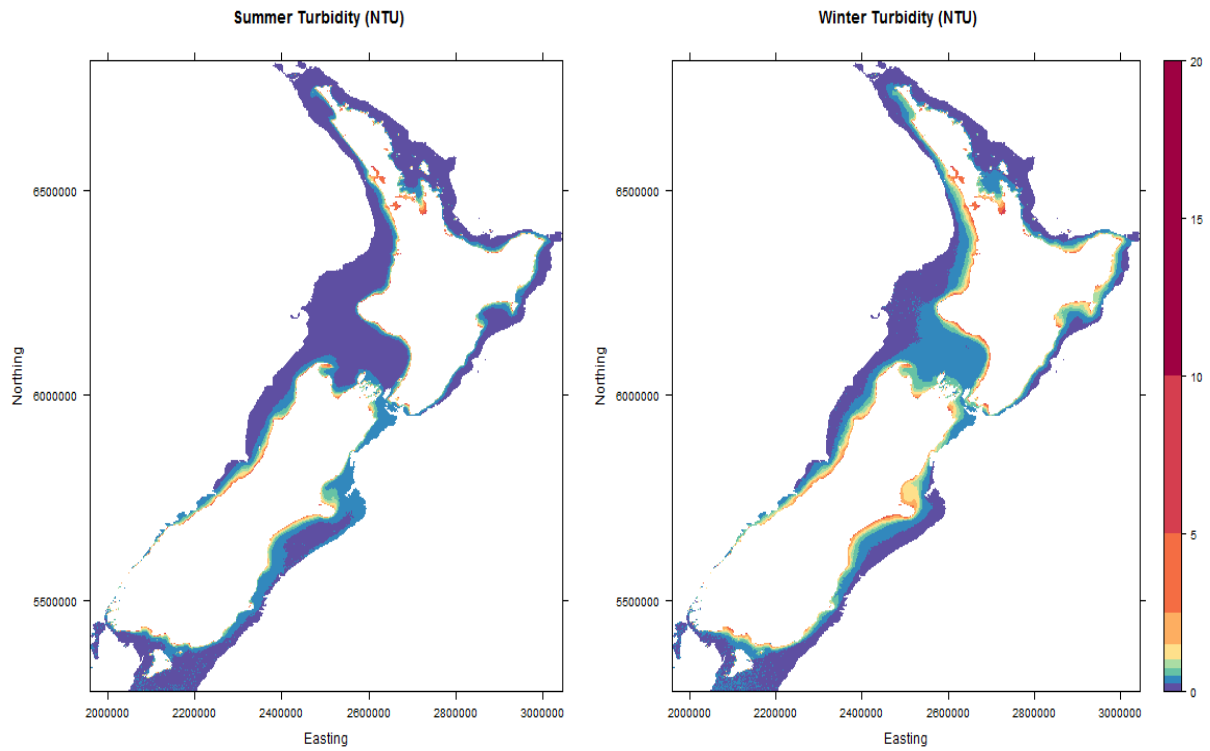
Figure A6-2: Seasonal turbidity – Nephelometric Turbidity Units (NTU), used in Hector's/Māui distribution modelling.
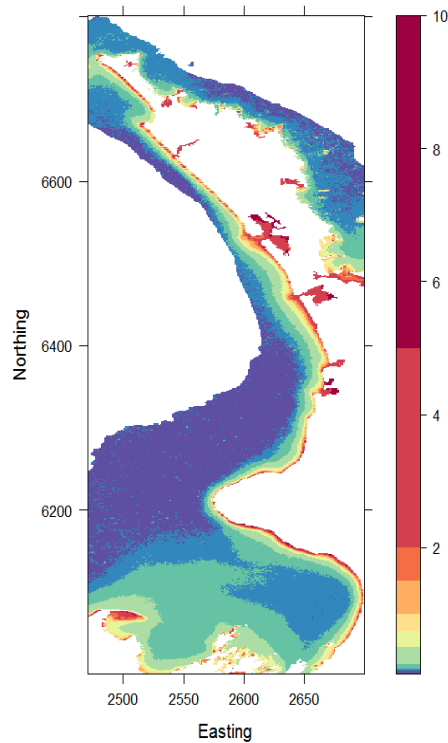

Figure A6-3: Summer turbidity - Nephelometric Turbidity Units (NTU), used in final model fitted to public sightings
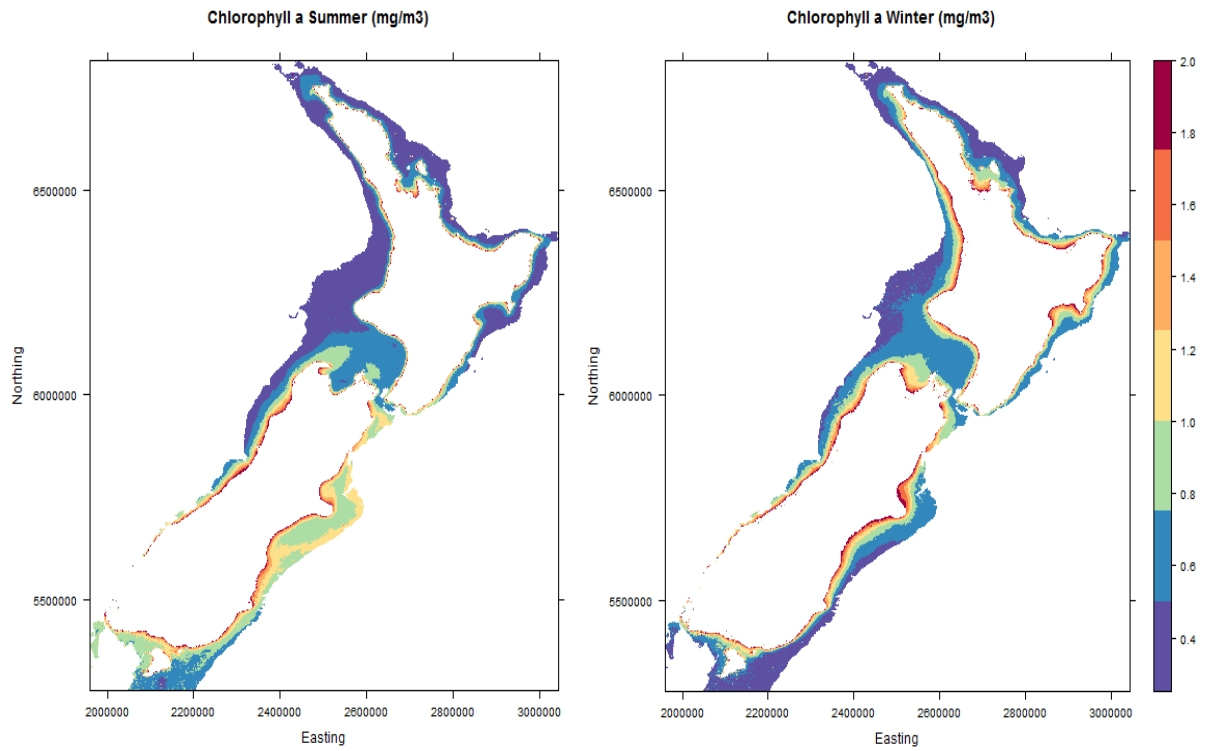
Figure A6-4: Seasonal Chlorophyll a (mg/m³), used in Hector's/Māui distribution modelling.
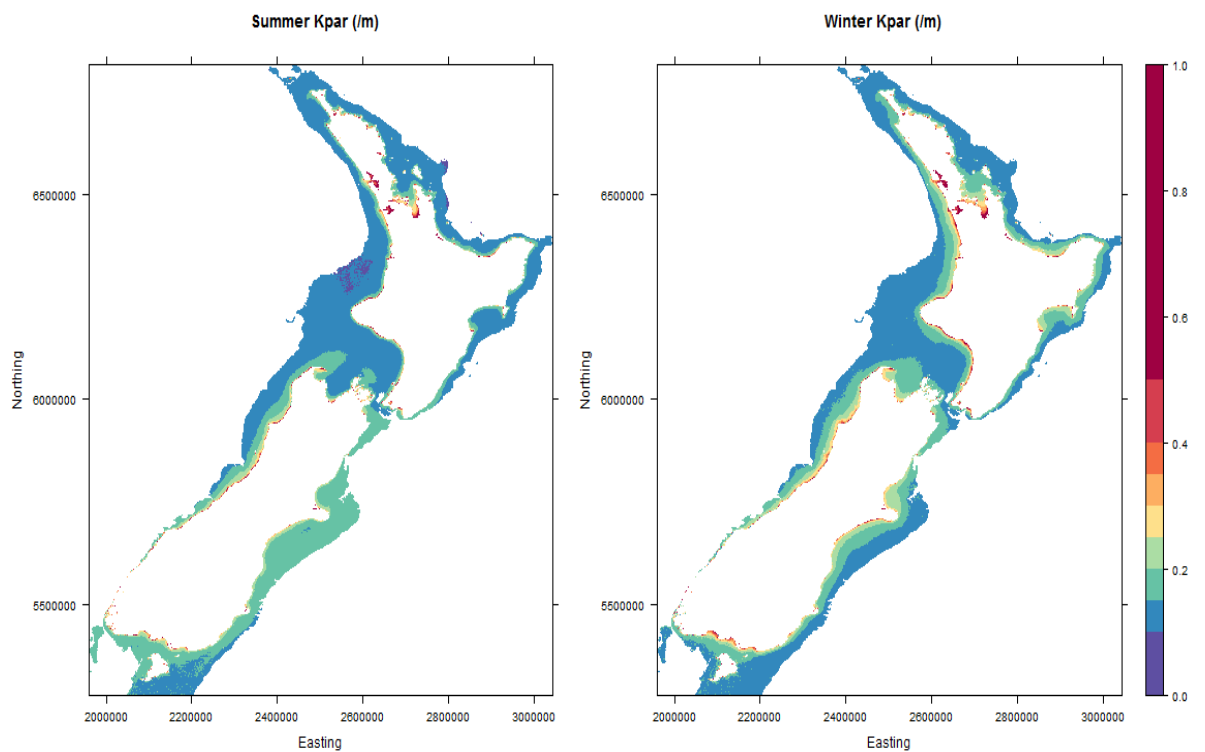
Figure A6-5: Seasonal downwelling light attenuation (K_{PAR} m⁻¹), used in Hector's/Māui distribution modelling.
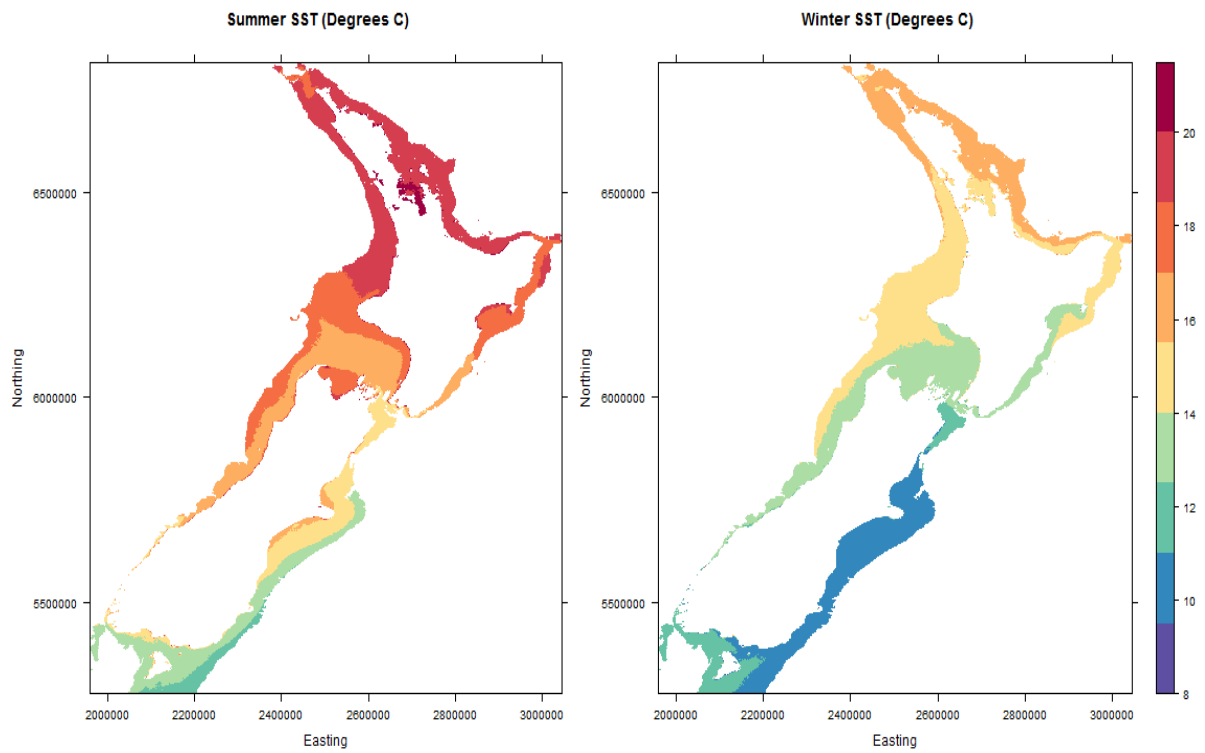
Figure A6-6: Seasonal sea surface temperature (Degrees-Celsius), used in Hector's/Māui distribution modelling.

APPENDIX 7 – SPATIAL DENSITY PREDICTION OF HECTOR'S & MĀUI DOLPHINS COMPARED WITH OTHER INFORMATION
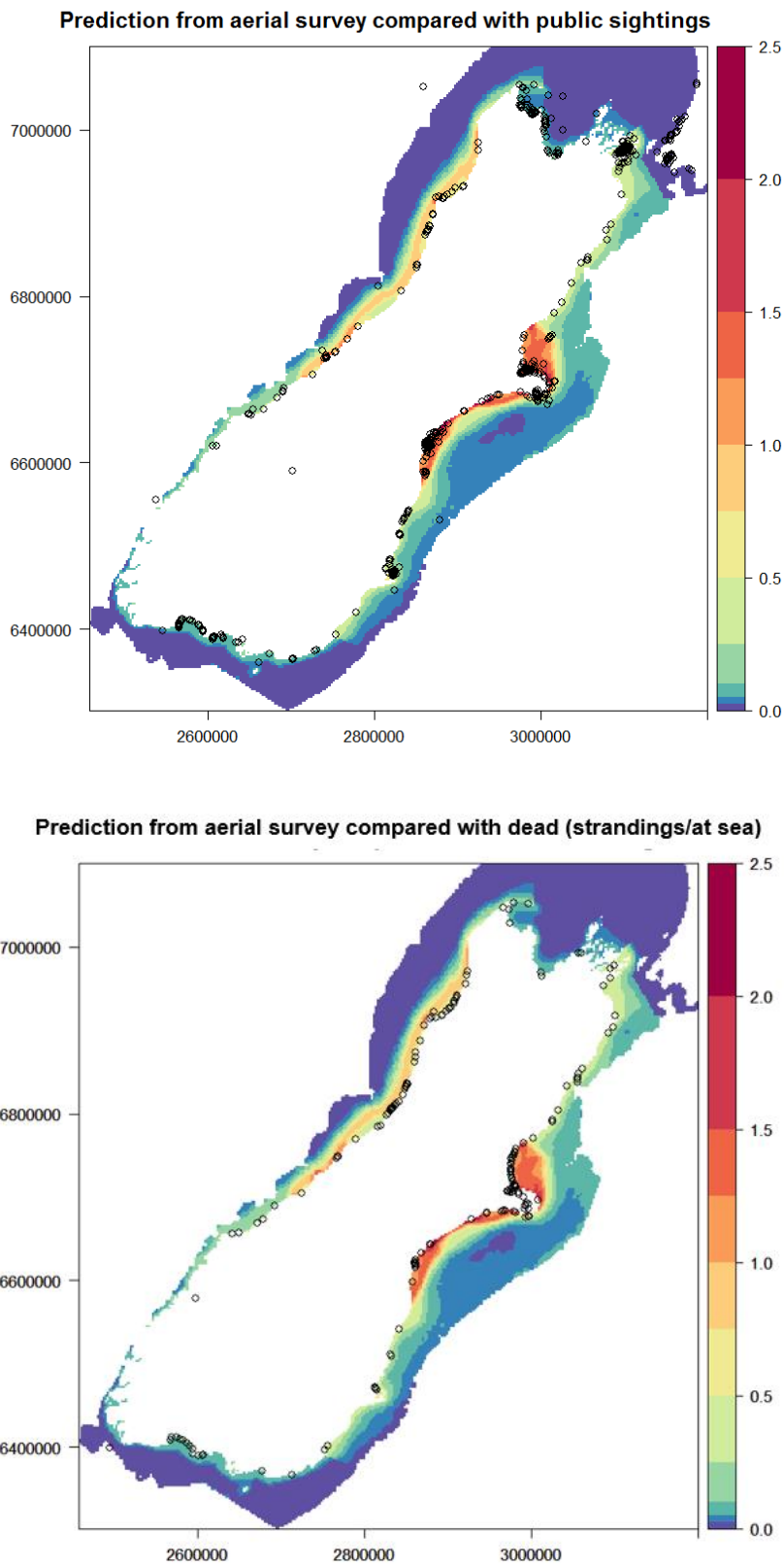

Figure A7-1: Final predicted spatial abundance of Hector's and Māui dolphins in summer used for the spatial risk assessment compared with the spatial distribution of public sightings of live animals, including unvalidated sightings (top) and sightings of dead animals (stranded and at-sea)—South Island.


Figure A7-2: Final predicted spatial abundance of Hector's and Māui dolphins in summer used for the spatial risk assessment compared with the spatial distribution of commercial fishery observer sightings (top) and commercial fishery-reported captures (set net and trawl)—South Island.
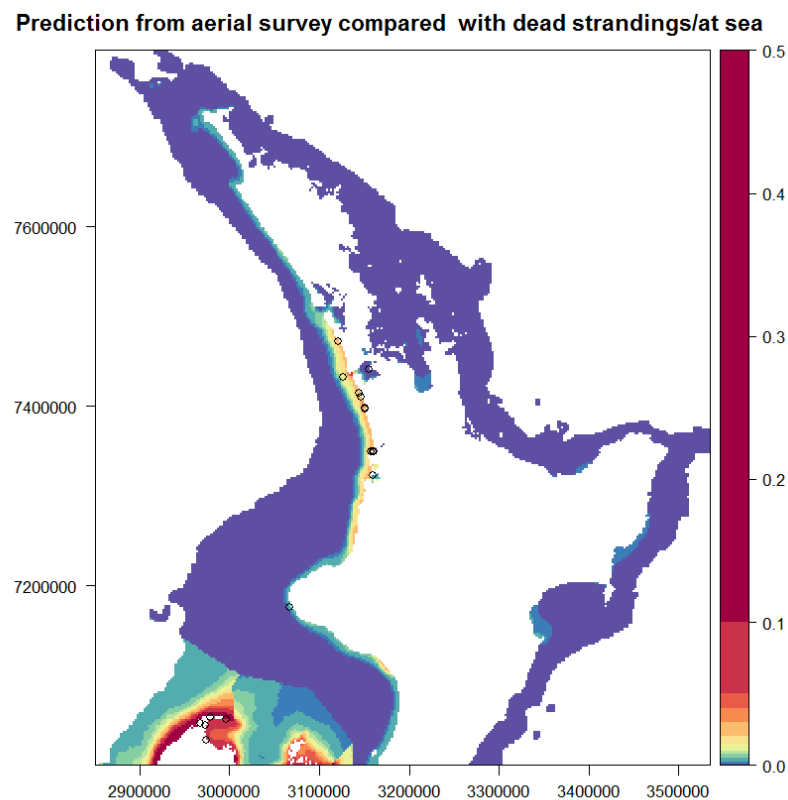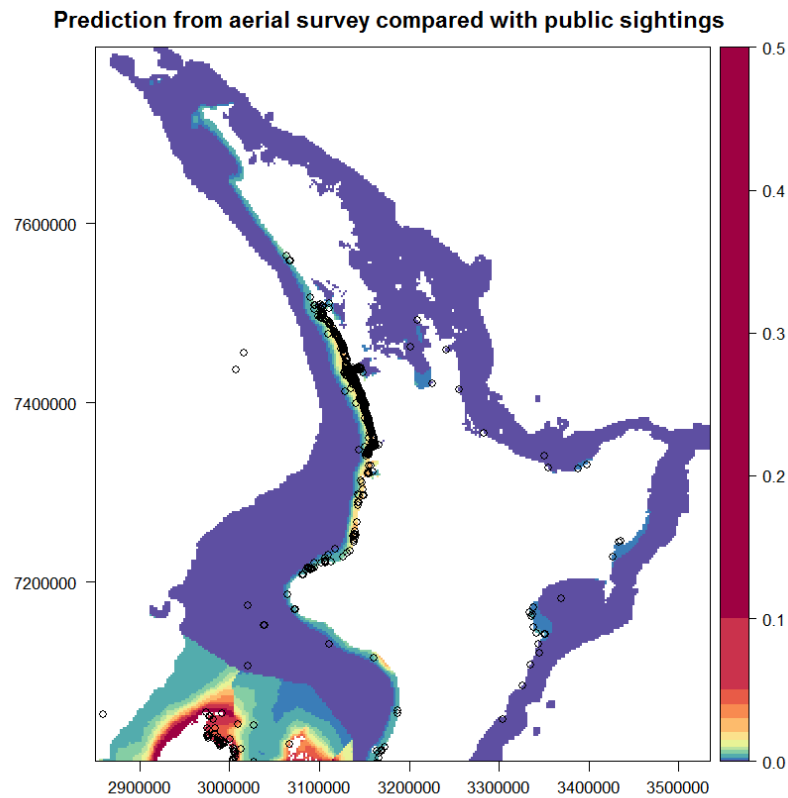
Figure A7-3: Final predicted spatial abundance of Hector's and Māui dolphins in summer used for the spatial risk assessment compared with the spatial distribution of public sightings of live animals, including unvalidated sightings (top) and sightings of dead animals (stranded and at-sea)—North Island.

Prediction from aerial survey compared with NOMAD fish. obs. sightings
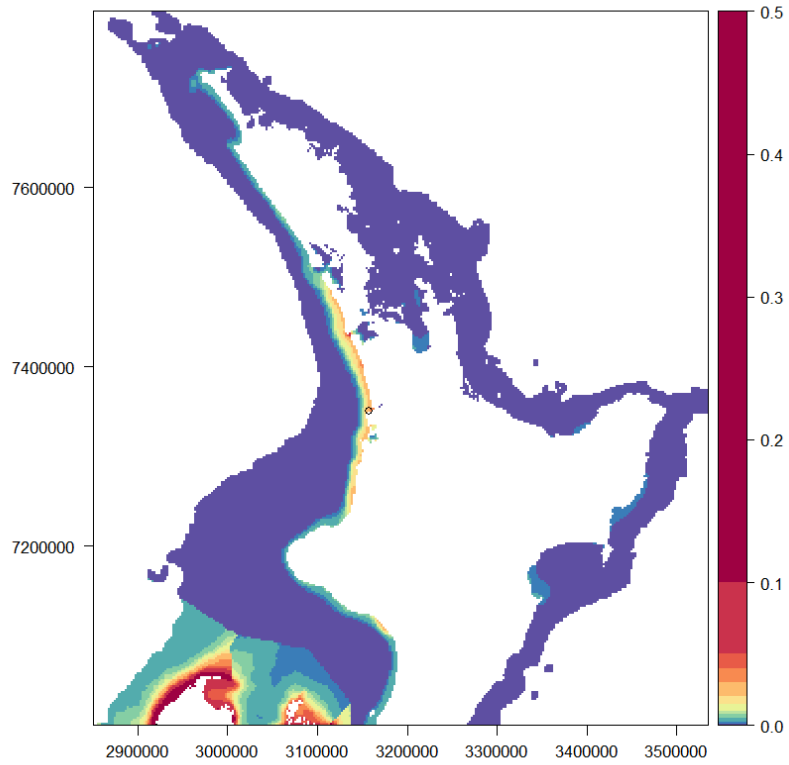
**Prediction from aerial survey compared with fishery-reported captures**
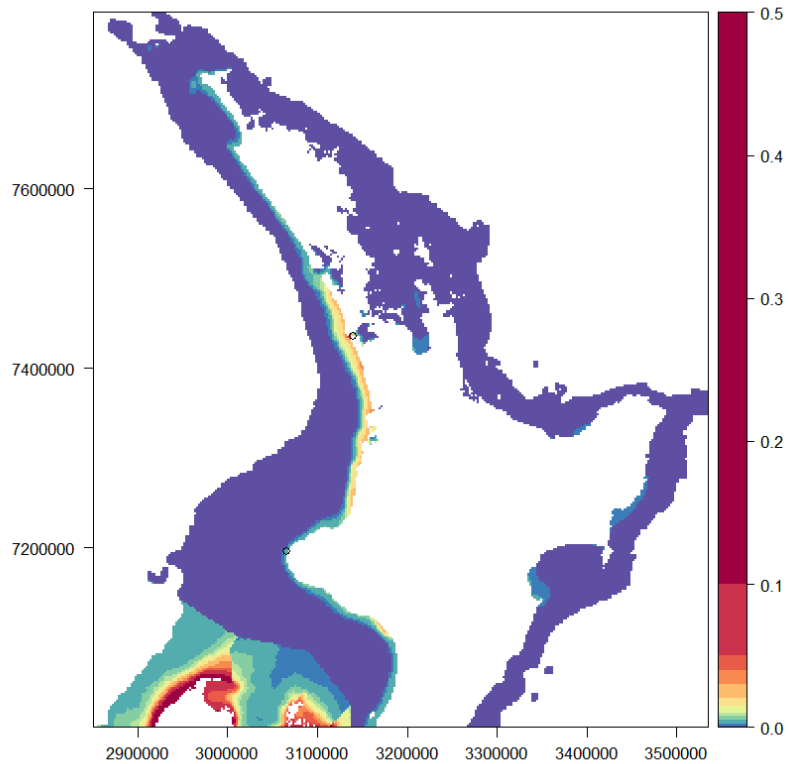
Figure A7-4: Final predicted spatial abundance of Hector's and Māui dolphins in summer used for the spatial risk assessment compared with the spatial distribution of commercial fishery observer sightings (top) and commercial fishery-reported captures (set net and trawl)—North Island.

APPENDIX 8 – BROADNOSE SEVENGILL SHARK (*NOTORYNCHUS CEPEDIANUS*) SPATIAL ABUNDANCE

Background

The spatial risk assessment of Hector's/Māui dolphin required spatial information on the abundance of their main shark predator species. Shark predation was attributed as the primary cause of death of two individuals during the period during which comprehensive, consistent necropsy methods were adopted, including a Hector's dolphin on the south coast of the South Island and a Māui dolphin on the west coast of the North Island (Table A4-4). The remains of Hector's/Māui dolphins have previously been found in the stomachs of the following shark species:

- Broadnose sevengill shark (*Notorynchus cepedianus*). Individuals captured in set nets have been found with the remains of Hector's dolphins in their stomachs (Cawthorn 1988);
- Great white shark (*Carcharodon carcharias*). An immature male captured in a set net had the remains of a new-born Hector's/Māui dolphin in its stomach (Malcolm Francis, unpub. data); and
- Blue shark (*Prionace glauca*) (DOC 1992);

Of these, the broadnose sevengill shark was deemed by the Aquatic Environment Working Group to be the most plausible main predator of Hector's/Māui dolphins. They are well-known to be frequent predators of coastal dolphins and porpoises globally (Heithaus 2001). For example, 12.5% of sevengill sharks from the Eastern Cape of South Africa contained dolphin remains, comprising 29.3% of prey mass, and this was deemed to be too high to be explained by scavenging alone (Ebert 1991b). Anecdotal evidence suggests that they are abundant and widespread around New Zealand's coastal waters and their preference for turbid water (Ebert 1991b) would be likely to increase their spatial overlap with Hector's/Māui dolphins.

Broadnose sevengill sharks were considered to have a medium level of susceptibility to capture in gillnets targeting shark species in Southeast Australia (Walker et al. 2008). This Appendix describes an analysis that uses commercial setnet catch effort data to estimate the relative spatial abundance of broad-nose sevengill sharks around New Zealand.

Methods

Generalised Additive Models (GAMs) were used for all predictive models, with a binomial error structure assumed for all models.

Data - subsetting

The primary data source for this analysis was vessel reported commercial set net catch effort records reported on set net (NCELR) forms (introduced 2006/07). The extract included NCE records up until the 2014/15 fishing season.

Fishing events were subsetted to eliminate values for candidate predictor variables for which effort was low. Fishing events were retained that met the following criteria:

- Total net length < 4,000 m; and
- Effort height < 8 m;
- Fishing seasons since 2006/07

Data - explanatory and response variables

A bivariate spline for station northing and easting was selected as the first model term (the smooth basis dimension "k" was set to 50 to allow complex surface smooths). In addition, candidate fishing operational predictor variables (univariate spline with "k" set to three for all terms) included:

- Total net length;
- Effort height; and
- Gear soak time (fishing duration).

Fishing year was not offered as a model term, since the proportion of positive fishing events was fairly consistent through time (Table A8-1). The response variable was the binomial presence/absence of broadnose sevengill shark in a set net fishing event.

Modelling approach

Model selection was based on model AIC. Standard diagnostics were used to compare models (model AIC; percentage of deviance explained) and to check that distributional assumptions were met (quantile-quantile plots).

Data – prediction

The optimal model was then used to produce a spatial prediction of the proportion of set net fishing events positive for sevengill shark captures for a grid of northing and easting values of a 1 km resolution.

Results

The temporal and spatial coverage of set net fishing events was generally representative (Table A8-1 and Figure A8-1, left). More than 7000 fishing events were undertaken in each fishing year with some coverage in areas of highest abundance for Hector's dolphin (comparing Figure A8-1 with figure 18 of MacKenzie & Clement 2016) and for Māui dolphin (comparing Figure A8-1 with figure 1 of Currey et al. 2012).

Table A8-1: Summary of total number of fishing events reported on NCE forms meeting the subset criteria above, and the number of events for which broadnose sevengill shark captures were reported.

| Fishing year	Total fishing events	Fishing events with broadnose sevengill shark captures
2006/07	8 441	98
2007/08	8 425	201
2008/09	7 752	177
2009/10	8 147	155
2010/11	8 369	151
2011/12	8 060	135
2012/13	8 081	128
2013/14	7 452	143
2014/15	7 287	141
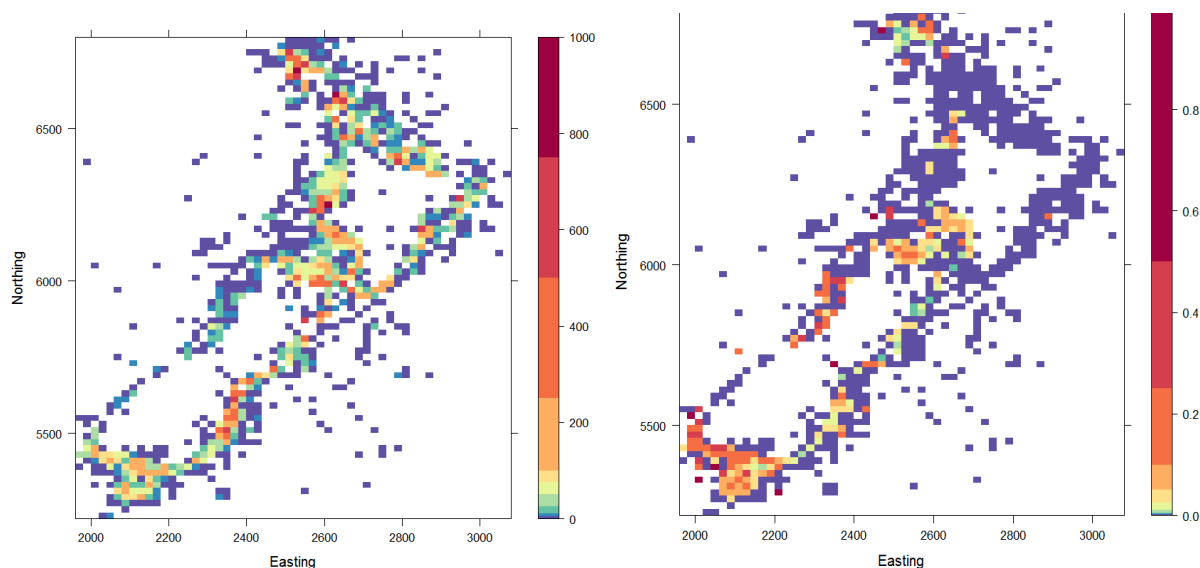
Figure A8-1: The spatial distribution of set net events reported on NCE forms meeting the subset criteria above, aggregated by 20 km grid cell (left); and the proportion of those events for which broadnose sevengill shark captures were reported, also aggregated by 20 km grid cell (right).

The GAM structure with the lowest model AIC (Model ID GAM1.2.1.1) retained all of the candidate splined terms (net length, net height and fishing duration), as well as the bivariate spline for northing and easting, which was fixed as the first model term (Table A8-2). For the optimal model, the percentage of deviance explained was moderate (26.2%). Quantile-Quantile plots were produced for model residuals and indicated a reasonable model fit (Figure A8-2). Prey taxa GAM splines are shown in Figure A8-3, which indicated the greatest probability of a positive fishing event with maximum net length and gear soak time and at an intermediate net height.

Table A8-2: Comparison of candidate GAMs for estimating the spatial probability of capturing broadnose sevengill sharks, in ascending order of model AIC.

| Model ID	Model structure	R^2	Deviance (% explained)	Delta-AIC
GAM1.2.1.1	Presence/absence ~ s(easting, northing, k = 50) + s(net length, k = 3) + s(fishing duration, k = 3) + s(effort height, k = 3)	0.094	26.2%	0
GAM1.2.1	Presence/absence ~ s(easting, northing, k = 50) + s(net length, k = 3) + s(fishing duration, k = 3)	0.094	25.6%	72
GAM1.2.2	Presence/absence ~ s(easting, northing, k = 50) + s(net length, k = 3) + s(effort height, k = 3)	0.090	25.6%	80
GAM1.2	Presence/absence ~ s(easting, northing, k = 50) + s(net length, k = 3)	0.090	25.0%	146
GAM1.1	Presence/absence ~ s(easting, northing, k = 50) + s(fishing duration, k = 3)	0.077	22.8%	442
GAM1.3	Presence/absence ~ s(easting, northing, k = 50) + s(effort height, k = 3)	0.070	22.8%	446
GAM1	Presence/absence ~ s(easting, northing, k = 50)	0.069	21.9%	565
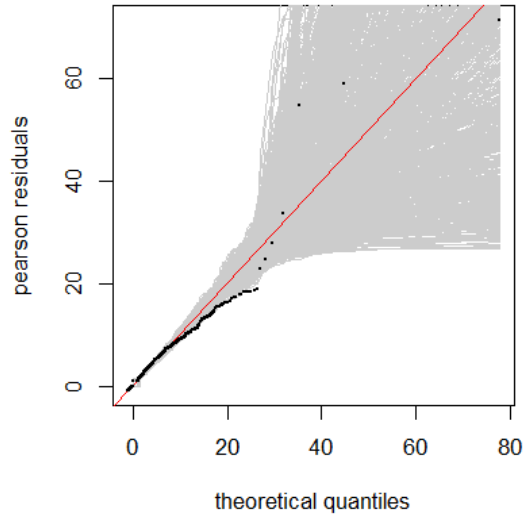
Figure A8-2: Simulation-based quantile-quantile plot for final broadnose sevengill shark GAM, with Pearson residuals and 1000 simulation replicates.
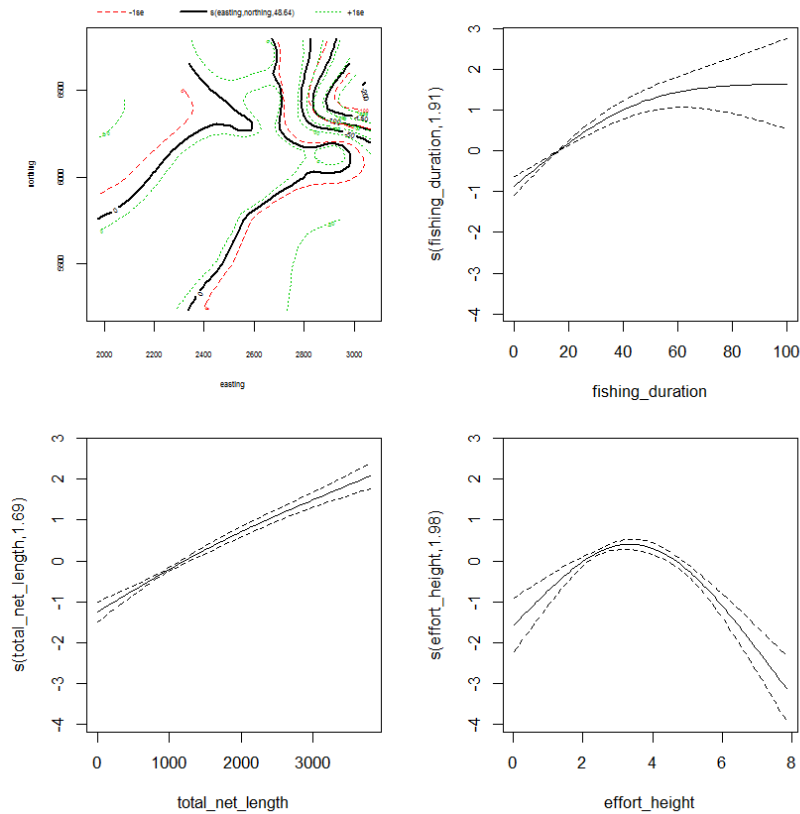

Figure A8-3: Final broadnose sevengill shark GAM splines for all splined terms.

Spatial model predictions generally agreed well with raw area grid-cell averaged values (comparing Figure A8-4 left and Figure A8-1 left). There was no evidence for spurious predictions in regions of low survey effort, except offshore on the east coast of the North Island (Figure A8-1). Coastal areas of relatively high sevengill shark capture probability (over 5% of set net events) from the model included: the west coast South Island; Southland, particularly near TeWaiwai Bay, Oamaru and Manakau to Raglan—all of which are high abundance areas for Hector's/Māui dolphins (Figure 17 and Figure 18). Areas with an intermediate catch rate (1 – 5% of set net events) included Banks Peninsula, Golden Bay/Tasman Bay, the Kapiti Coast and Northland (Figure A8-4). The coefficient of variation associated

with the spatial sevengill shark prediction was low (c.v. less than 0.3) around all of the South Island, the Kapiti Coast and Manakau region (Figure A8-4, right-hand plot). Spatial estimates for the east and north coasts of the North Island had a much greater coefficient of variation although both raw and model estimated positive fishing events were consistently low for these areas (Figure A8-1 and Figure A8-4).
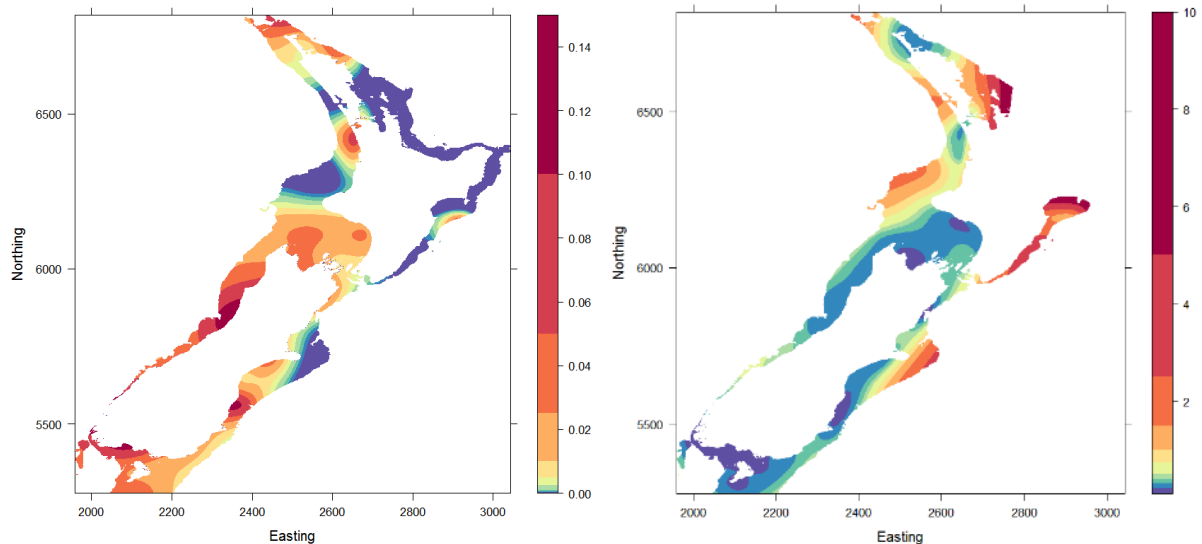

Figure A8-4: Model predicted spatial proportion of set net events in which sevengill sharks were captured (left); and spatial CV associated with the model prediction (right; grid cells of northeast of North Island with CV over 10 are not coloured so that graduations at the lower end of the axis are visible).

Conclusions and risk assessment inputs

This analysis produced the predicted relative spatial abundance of broadnose sevengill shark (probability of presence in commercial set net events) that was used to estimate annual deaths from predation events by the spatial risk model, given relative spatial overlap with Hector's/Māui dolphins (Section 5.2). Areas of high spatial overlap with Hector's/Māui dolphins include Southland, the west coast of the South Island and south of Manakau Harbour (Figure 19 and Figure A12-2). As such, the proportion of deaths associated with predation would be expected to be higher in these areas, depending on spatial overlap with other lethal threats.

Future research to generate improved broadnose shark distribution layers may include:

- Consideration of shark body size representative of size classes that would be likely to predate on Hector's/Māui dolphins;
- Model-based estimation of spatial sevengill shark counts per event, rather than probability of presence; and
- The estimation of seasonal (summer and winter) prey species distributions, which are known to be variable for this species (Barnett & Semmens, 2012).

In addition, catch rate information from commercial inshore set net and trawl fisheries could be used to assess for changes in relative abundance through time that may also be associated with changes in predation pressure.

It may be appropriate to offer broadnose sevengill shark density as a candidate predictor variable for Hector's/Māui abundance. This would be appropriate if predation pressure from this species was deemed sufficient to impact on the spatial abundance of Hector's/Māui dolphins.

References

Barnett, A.; Semmens, J.M. (2012). Sequential movement into coastal habitats and high spatial overlap of predator and prey suggest high predation pressure in protected areas. *Oikos, 121*: 882–890.

Cawthorn, M.W. (1988). Recent observations of Hector's dolphin *Cephalorhynchus hectori*, in New Zealand. *Report of the International Whaling Commission Special Issue, 9*: 303–314.

Currey, R.J.C.; Boren, L.J.; Sharp, B.R.; Peterson, D. (2012). A risk assessment of threats to Maui's dolphins. Ministry for Primary Industries and Department of Conservation, Wellington. 51 p.

DOC (1992). Banks Peninsula Marine Mammal Sanctuary Technical Report, 1992. Canterbury Conservancy Technical Report Series 4. Department of Conservation, Christchurch. 111 p.

Ebert, D.A. (1991a). Observations on the predatory behaviour of the sevengill shark *Notorynchus cepedianus*. *South African Journal of Marine Science, 11*: 455–465.

Ebert, D.A. (1991b). Diet of the sevengill shark *Notorynchus cepedianus* in the temperate coastal waters of southern Africa. *South African Journal of Marine Science, 11*: 565–572.

Heithaus, M.R. (2001). Predator-prey and competitive interactions between sharks (order *Selachii*) and dolphins (suborder *Odontoceti*): a review. *Journal of Zoological Society of London, 253*: 53–68.

MacKenzie, D.I.; Clement, D.M. (2016). Abundance and distribution of WCSI Hector's dolphin. *New Zealand Aquatic Environment and Biodiversity Report No. 168*. 67 p + supplemental material.

Walker, T.I.; Stevens, J.D.; Braccini, J.M.; Daley, R.K.; Huveneers, C.; Irvine, S.B.; Bell, J.D.; Tovar-Avila, J.; Trinnie, F.I.; Phillips, D.T.; Treloar, M.A.; Awruch, C.A.; Gason, A.S.; Salini, J.; Hamlett, W.C. (2008). Rapid Assessment of Sustainability for Ecological Risk of Shark and Other Chondrichthyan Bycatch Species Taken in the Southern and Eastern Scalefish and Shark Fishery. Queenscliff: Primary Industries Research Victoria. 355 p.

APPENDIX 9 –*TOXOPLASMA GONDII* OOCYST DENSITY IN THE COASTAL WATERS OF NEW ZEALAND

Jim Roberts; Christian Zammit; Julian Sykes (All NIWA); Glenn Aguilar (Unitec Institute of Technology); Wendi Roe (Massey University).

Background

Toxoplasmosis in marine mammals

Toxoplasmosis is a potentially fatal disease caused by infection with *Toxoplasma gondii* oocysts. The only known definitive hosts for *T. gondii* are members of the family Felidae including the domestic cat (*Felis catus*), which may shed more than 20 million *T. gondii* oocysts in its faeces following infection (Dubey 1995). Oocysts may remain viable and infective in soil and freshwater for more than one year (Dumetre & Darde 2003) and in seawater for at least six months (Lindsay et al. 2003). Intermediate hosts include birds and mammals, which become infected after ingesting soil, water, or plant material contaminated with oocysts, or by ingesting prey containing tissue cysts (Dubey 2002). In humans, infection with *T. gondii* may be asymptomatic, but can lead to illness and death in immune-compromised individuals, or through exposure to particular strains (Demar et al. 2012; Tenter et al. 2000). Toxoplasmosis is also a known cause of abortions in livestock and marine mammals (e.g. Dubey 2009; Shapiro et al. 2016).

Toxoplasmosis was relatively recently found to be the primary non-fishery cause of death of a necropsied sample of beachcast and bycaught Hector's and Māui dolphins (Roe et al. 2013), which was updated by this assessment (Section 5.1 and Appendix 4). A total of nine out of 31 non-fishery diagnoses for non-calves were attributed to toxoplasmosis (Table A4-4), of which seven were females and six were classified as mature (Table A4-6). Since 17 out of 28 (61%) individuals assessed by Roe et al. (2013) were found to be positive for *T. gondii* DNA, latent infections are likely to be much higher than mortality rates.

Of the nine confirmed toxoplasmosis mortalities in Hector's and Māui dolphins, five were recovered on the east coast of the South Island, two on the west coast South Island and two were Māui dolphins recovered on the North Island (Table A4-4), indicating that *T. gondii* is widespread in the coastal waters of New Zealand (also see Figure A9-1). The majority of confirmed toxoplasmosis deaths of Hector's and Māui dolphin deaths were of individuals recovered in October and November, indicating a potential seasonality in toxoplasmosis deaths or a seasonal bias in their stranding and/or recovery for necropsy (Figure A9-1).
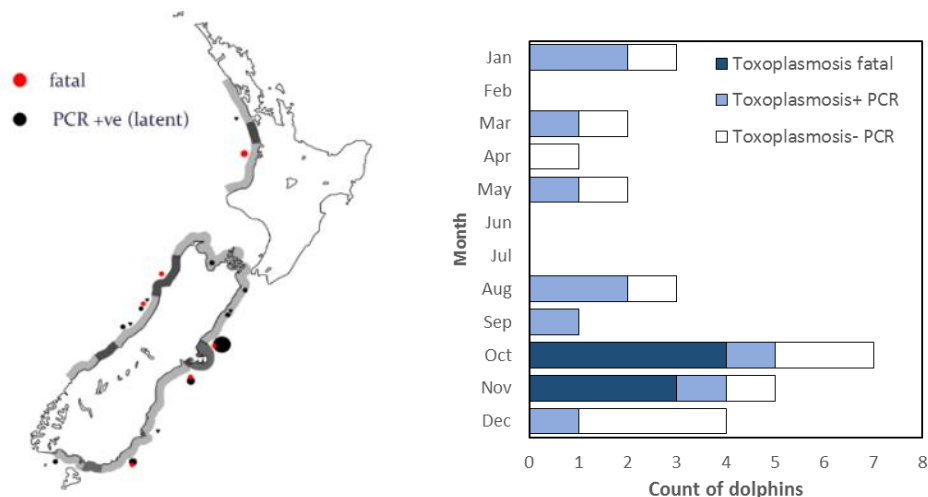
Figure A9-1: Spatial distribution of recovered Hector's and Māui dolphins corpses for which *Toxoplasma gondii* infection was the primary cause of death or were confirmed to have been infected with *T. gondii* (left); and seasonal distribution of Toxoplasmosis cases (right), including the total necropsied sample by month. See Roe et al. (2013) for details of necropsy records used to make these plots, which included Hector's and Māui dolphin recoveries from 2007 to 2011.

Toxoplasmosis has also been identified as a primary cause of death for some other marine mammal populations, including: southern sea otters (*Enhydra lutris nereis*) (Kreuder et al. 2003); northern sea otters (*Enhydra lutris* kenyoni) (White et al. 2018) and Hawaiian monk seals (*Neomonachus schauinslandi*) (Barbieri et al. 2016). With respect to southern sea otters, approximately half of newly dead individuals recovered along the California coast were found to have been infected with *T. gondii* (Conrad et al. 2005).

Toxoplasma gondii oocysts are thought to be transported from land to sea by runoff, as supported by research demonstrating that the seroprevalence of southern sea otters for *T. gondii* was spatially correlated with proximity to urbanised areas with substantial freshwater runoff (Conrad et al. 2005). Subsequent research by VanWormer et al. (2016) simulated the density of *T. gondii* oocysts for river catchments along the California coast using hydrological and felid oocyte loading models and obtained a good spatial agreement with *T. gondii* infection rates of sea otters. Watersheds with high infection rates were characterised by coastal development and higher densities of domestic cats (VanWormer et al. 2016).

Spatial Toxoplasma gondii in New Zealand coastal waters

The risk model developed for the spatial multi-threat risk assessment for Hector's and Māui dolphins (described in the main body of this report) required predictions of the relative threat intensity of toxoplasmosis that could be used to apportion toxoplasmosis and other non-fishery causes of death (e.g., predation and other) for different populations, based on spatial overlap.

Methods

Modelling approach

Potential risk factors other than spatial oocyst density (e.g., the relative virulence of *T. gondii* strains, or consideration of dietary pathway) were not addressed. Following the approach of VanWormer et al. (2016), we utilised an existing high resolution hydrological model and spatial information on unowned cat density (stray and colony) to simulate the seasonal (summer/winter) spatial density of *T. gondii* oocysts in the rivers and coastal waters of New Zealand.

Unowned cat presence

This assessment used a spatial prediction of unowned (stray and colony) cat habitat suitability by Aguilar et al. (2015) as a proxy for *T. gondii* oocyst density across New Zealand. Scenario B of Aguilar et al. (2015) was used (Figure A9-2). Scenario B prediction was based on Auckland-based records of unowned cats sourced from animal welfare organisations and human population density, from which cat occurrence/absence was determined for respective human census mesh blocks. Previous research has demonstrated that human population density is a major factor for the presence of unowned cats (Aguilar & Farnworth 2012). Maxent (Phillips et al. 2006) was then used to produce a habitat suitability prediction across New Zealand using the derived unowned cat occurrence locations related to Bioclim environmental variables (Hijmans et al. 2005). The maximum range estimates for feral cats across a review of home range studies was then used to spatially smooth the Maxent habitat suitability output, to account for un-owned cats becoming feral (Aguilar et al. 2015).
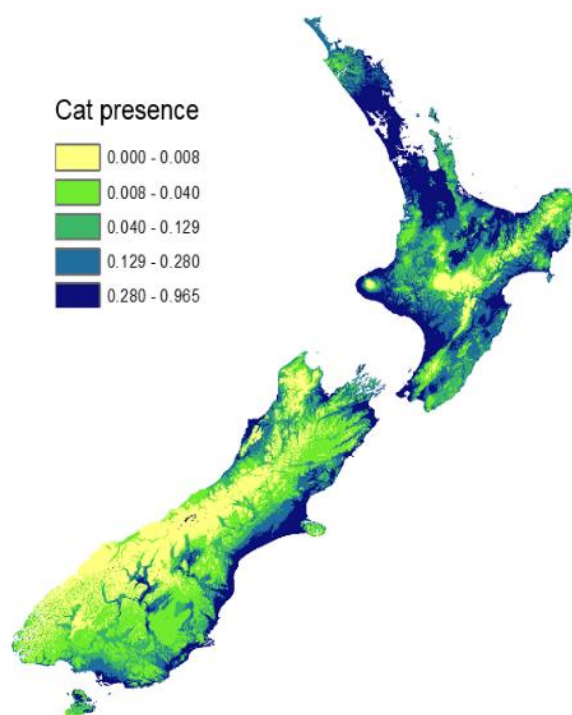
Figure A9-2: Predicted occurrence of unowned cats (stray and colony) around New Zealand. This was Scenario B from habitat suitability modelling by Aguilar et al. 2015.

TopNet hydrological model

The TopNet hydrological model is a spatially resolved, time-stepping model of water balance that is driven by a time series of precipitation and temperature data and additional weather elements. TopNet simulates water storage in snowpack, plant canopy, rooting zone, shallow subsurface, lakes and rivers and produces time series of modelled river flow throughout the modelled river network of New Zealand. TopNet has two major components: a basin module and a flow-routing module. The basic structure of the basin module is illustrated in Figure A9-3.

The TopNet model combines Topmodel hydrological model concepts (Beven et al. 1995) with a kinematic wave channel routing algorithm (Goring 1994; Clark et al. 2008) and a simple temperature based empirical snow model (Clark et al. 2008). Considerable effort was made during the development of TopNet to ensure that the model has a strong physical basis and that the dominant rainfall-runoff dynamics are adequately represented in the model (McMillan et al. 2010). TopNet model equations and information requirements are provided by Clark et al. (2008) and McMillan et al. (2013).

Spatial information in TopNet is provided by national datasets on catchment topography (i.e., 30 m digital elevation model), physical (Land Cover Database version 3-LCDB3, Land Resource Inventory, Newsome et al. 2012), soil (Fundamental Soil Layer- FSL, Wilson & Giltrap 1982) and hydrological properties (River Environment Classification, Snelder & Biggs 2002). In this application, the REC hydrological network was set to REC version 2 (NIWA 2012). The method for deriving TopNet initial parameter estimates from GIS data sources in New Zealand is given in table 1 of Clark et al. (2008).
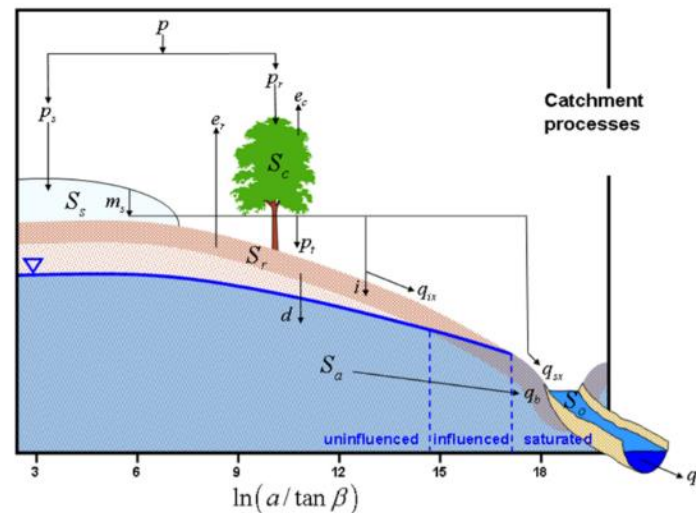

Figure A9-3: TopNet model structure within each sub-basin, showing modelled water fluxes and storages.

Climate information used to drive the hydrological model (precipitation, temperature, relative humidity, solar radiation, mean sea level pressure and wind speed) were generated using NIWA's Virtual Climate Station Network (VCSN) (Tait et al. 2006). The VCSN network represents daily interpolated climate information over a regular 0.05 degrees latitude/longitude grid interpolated over nearly 500 climate stations across New Zealand since 1972.

The land-based *T. gondii* load (see below) was generated during rainfall events, for which *T. gondii* oocytes are routed through river network to catchment outlets. The following methodology was used to generate the TopNet model:

- The model was run using a non-calibrated mode over 576 343 land-based sub-catchments across New Zealand (average size of 0.5 km^2);
- The TopNet model was generated over the period 1 Jan 1973–1 September 2017 to represent the long-term average hydrological loading;
- Catchment-based surface runoff fluxes time series (i.e., q_{ie} and q_{se} fluxes on Figure A9-3) were summarised for each monthly time step;
- Catchment-based surface runoff fluxes were aggregated at seasonal (Summer = 1 November to 31 April; Winter = 1 May to 31 October) and annual time steps.

Toxoplasma gondii *oocyst load*

Relative *T. gondii* loadings were generated for each catchment for a seasonal and annual time step through the combination of catchment-based runoff and catchment-averaged estimated cat occurrence (see above) using the simple equation

relative catchment load = catchment average cat occurrence * surface runoff

---

The value derived is considered a relative load (rather than absolute load of oocysts), since multiplying by surface runoff renders the resulting dimensions meaningless in a real-world context.

River catchment *T. gondii* load was then aggregated through the digital river network to the sea catchment outlet (i.e. the terminal point of discharge at the coast) for each time step. It was assumed that all oocysts remained viable through the simulation (i.e., there was no decay in *T. gondii* load with time).

Spatial Toxoplasma gondii *oocyst density in coastal waters*

For a given season (summer or winter), the spatial density of *T. gondii* oocysts was then estimated for coastal waters surrounding New Zealand, using the coastal river terminal load of oocysts from the TopNet model. ArcGIS was then used to generate seasonal kernel densities of *T. gondii* oocysts in coastal waters, specifying a 50 km search radius (the distance used for smoothing). This search radius was informed by a simulation of released propagules from coastal discharge points around New Zealand (Chiswell & Rickard 2011) and empirical evidence that suggests that between 20% and 70% of oocysts stay suspended in the marine water column, as opposed to sticking to surfaces or precipitating in sediment (Karen Shapiro, unpublished data).

Results

An example of the simulated routed annual average catchment relative *T. gondii* load for all modelled reaches is given for the Gisborne region in Figure A9-4. This figure illustrates the high spatial resolution of the TopNet model used to estimate seasonal *T. gondii* oocyst load at river discharge points around the coast of the New Zealand.

Plots illustrating the model estimated seasonal *T. gondii* load at river discharge points are shown in Figure A9-5 (values in this plot are the ratio of oocyst load relative to the annual average across all rivers). These plots illustrate the estimated seasonal pattern of increased *T. gondii* discharge in winter months, driven by increased surface runoff in winter. Exceptions to this include some rivers of the east and west coasts of the South Island which have elevated flow in summer months driven by glacial melting (Figure A9-5). River terminals with greatest estimated *T. gondii* oocyst load were located on the North Island (e.g., Waikato River and Wairoa River on the west coast and rivers of the South Taranaki Bight) or the northern west coast of the South Island (e.g., Buller and Grey Rivers) (Figure A9-5). The coastal density of *T. gondii* oocysts derived using the estimated river terminal loads is shown in Figure A9-6. This follows the general pattern of the terminal loads, with respect to seasonality and regions with high and low estimated *T. gondii* load/density.
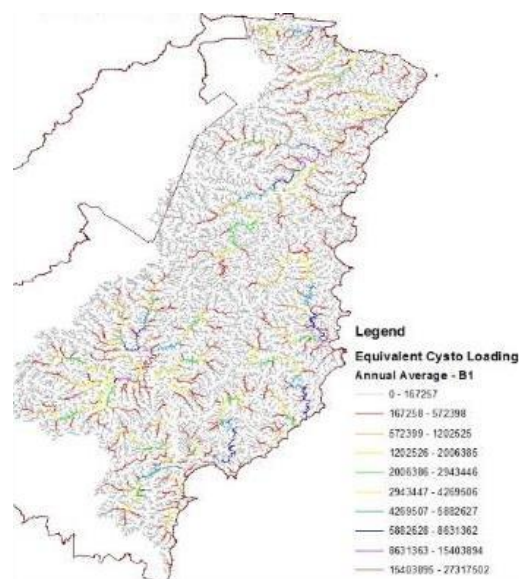
Figure A9-4: Routed annual average *T. gondii* catchment load for the Gisborne region.
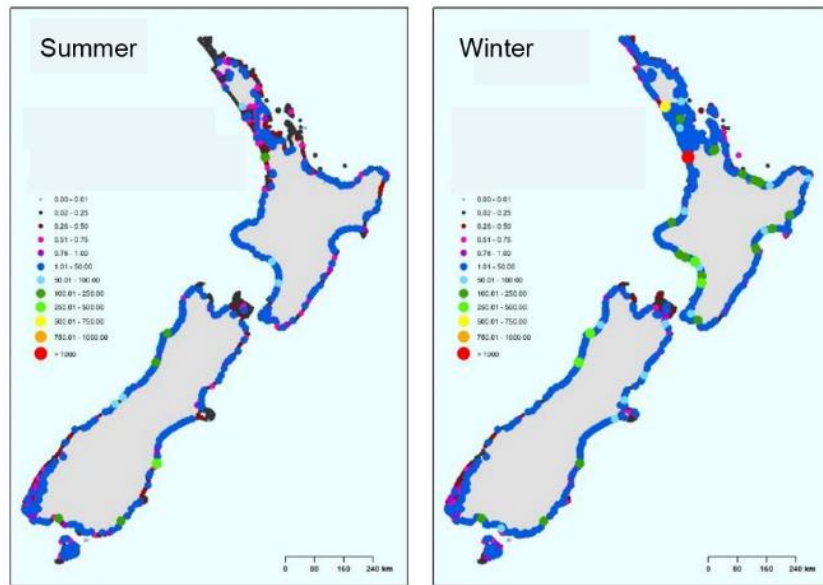
Figure A9-5: Estimated load of *Toxoplasma gondii* oocysts at terminal outflow points of New Zealand rivers in summer (left) and winter (right), relative to the annual mean across all terminal river outflows.
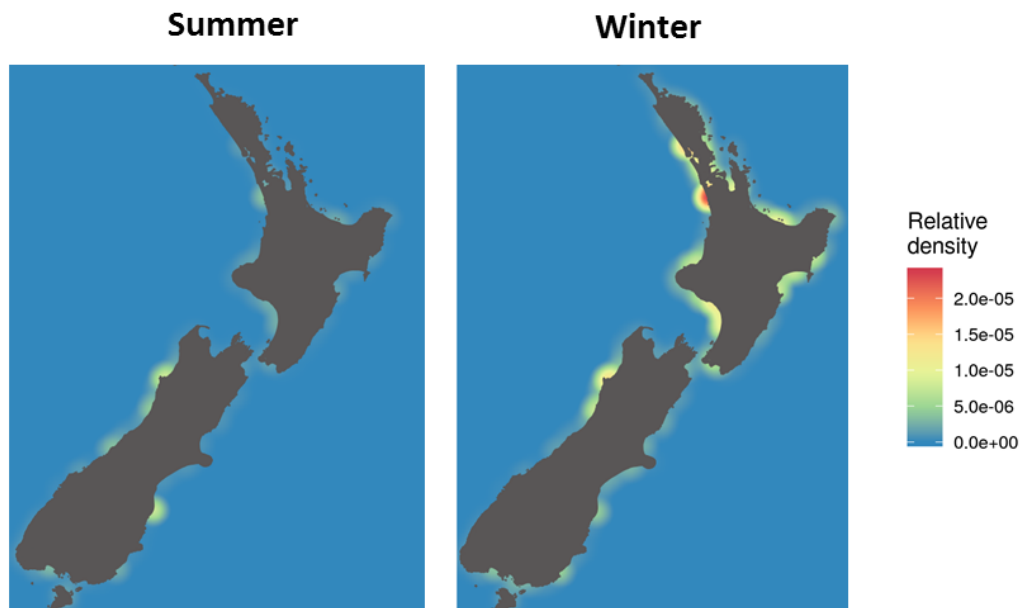
Figure A9-6: Estimated relative coastal water densities of *Toxoplasma gondii* oocysts in summer (left) and winter (right).

Conclusions and risk assessment inputs

This analysis produced seasonal predictions of the relative spatial density of *T. gondii* oocysts in the coastal water of New Zealand. These were then used by the spatial risk model to estimate annual deaths from Toxoplasmosis, given relative spatial overlap with Hector's/Māui dolphins (Sections 5.2 and 5.3).

This assessment made a number of simplifying assumptions that were required given data limitations. Future research to generate improved coastal toxoplasmosis threat intensity to Hector's and Māui dolphins could include:

- Validating/updating spatial cat habitat suitability models with field-based surveys of stray and feral cat density;
- Validation/updating coastal *T. gondii* oocyst density estimates by screening the tissues of filter-feeding species (e.g. mussels) collected from targeted locations;
- Using coastal hydrodynamic models to propagate river terminal *T. gondii* loads around coastal waters given current flows;
- Investigating the spatial prevalence of *T. gondii* in Hector's and Māui dolphins;
- Consideration of the infective strain of *T. gondii* for Hector's and Māui dolphins;
- Determination of the dietary pathway for the infection of Hector's and Māui dolphins with *T. gondii* (e.g. including species with dietary overlap) and the biological risk factors for infection to progress to toxoplasmosis.

Acknowledgements

References

Aguilar, G.D.; Farnworth, M.J. (2012). Stray cats in Auckland, New Zealand: discovering geographic information for exploratory spatial analysis. *Applied Geography, 34*: 230–238.

Aguilar, G.D.; Farnworth, M.J.; Winder, L. (2015). Mapping the stray domestic cat (*Felis catus*) population in New Zealand: Species distribution modelling with a climate change scenario and implications for protected areas. *Applied Geography, 63*: 146–154.

Barbieri, M.M.; Kashinsky, L.; Rotstein, D.S.; Colegrove, K.M.; Haman, K.H.; Magargal, S.L.; Sweeny, A.R.; Kaufman, A.C.; Grigg, M.E.; Littnan, C.L. (2016). Protozoal-related mortalities in endangered Hawaiian monk seals *Neomonachus schauinslandi*. *Diseases of Aquatic Organisms, 121*:85–95.

Beven, K.J.; Lamb, R.; Quinn, P.; Romanowicz, R.; Freer, J. (1995). TOPMODEL, in: Computer Models of Catchment Hydrology, edited by: Singh, V.P., Water Resources Publications, 627–668.

Chiswell, S.M.; Rickard, G.J. (2011). Larval connectivity of harbours via ocean currents: A New Zealand study. *Continental Shelf Research, 31*: 1057–1074.

Clark, M.P.; Rupp, D.E.; Woods, R.A.; Zheng, X.; Ibbitt, R.P.; Slater, A.G.; Schmidt, J.; Uddstrom, M. J. (2008). Hydrological data assimilation with the ensemble Kalman filter: Use of streamflow observations to update states in a distributed hydrological model, *Advances in Water Resour*ces *31*: 1309–1324, doi:10.1016/j.advwatres.2008.06.005.

Conrad, P.A.; Miller, M.A.; Kreudera, C.; James, E.R.; Mazeta, J.; Dabritza, H.; Jessup, D.A.; Gulland, F.; Grigg, M.E. (2005). Transmission of *Toxoplasma*: Clues from the study of sea otters as sentinels of *Toxoplasma gondii* flow into the marine environment. *International Journal for Parasitology, 35*: 1155–1168.

Demar, M.; Hommel, D.; Djossou, F.; Peneau, C.; Boukhari, R.; Louvel, D.; Bourbigot, A.M.; Nasser, V.; Ajzenberg, D.; Darde, M.L.; Carme, B. (2012). Acute toxoplasmosis in immunocompetent patients hospitalized in an intensive care unit in French Guiana. *Clinical Microbiology and Infection, 18*: E221–E231.

Dubey, J. (1995). Duration of immunity to shedding of *Toxoplasma gondii* oocysts by cats. *Journal of Parasitology, 81*: 410–415.

Dubey, J. (2002). A review of toxoplasmosis in wild birds. *Veterinary Parasitology, 106*: 121–153.

Dubey, J. (2009). Toxoplasmosis in sheep—The last 20 years. *Veterinary Parasitology, 163*: 1–14.

Dumetre, A.; Darde, M.L. (2003). How to detect *Toxoplasma gondii* oocysts in environmental samples? *FEMS Microbiology Reviews 27*: 651–661.

Goring D.G. (1994). Kinematic shocks and monoclinal waves in the Waimakariri, a steep, braided, gravel-bed river, Proceedings of the International Symposium on Waves: Physical and Numerical Modelling, University of British Columbia, Vancouver, Canada, 21–24 August, 1994, pp. 336–345.

Hijmans, R.J.; Cameron, S.E.; Parra, J.L.; Jones, P.G.; Jarvis, A. (2005). Very high resolution interpolated climate surfaces for global land areas. *International Journal of Climatology, 25*: 1965–1978.

Kreuder, C.; Miller, M.A.; Jessup, D.A.; Lowenstine, L.J.; Harris, M.D.; Ames, J.A.; Carpenter, T.E.; Conrad, P.A.; Mazet, J.A.K. (2003). Patterns of mortality in southern sea otters (*Enhydra lutris nereis*) from 1998–2001. *Journal of Wildlife Diseases 39*: 495–509.

Lindsay, D.S.; Collins, M.V.; Mitchell, S.M.; Cole, R.A.; Flick, G.J.; Wetch, C.N.; Lindquist, A.; Dubey, J.P. (2003). Sporulation and survival of *Toxoplasma gondii* oocysts in seawater. *Journal of Eukaryotic Microbiology, 50 (Suppl.)*: S687–S688.

McMillan, H.; Freer, J.; Pappenberger, F.; Krueger, T.; Clark, M. (2010). Impacts of uncertain river flow data on rainfall-runoff model calibration and discharge predictions. *Hydrological Processes 24(10):* DOI: 10.1002/hyp.7587: 1270–1284.

McMillan, H.K.; Hreinsson, E.O.; Clark, M.P.; Singh, S.K.; Zammit, C.; Uddstrom, M.J. (2013). Operational hydrological data assimilation with the recursive ensemble Kalman Filter. *Hydrology and Earth System Sciences 17*, 21–38.

Newsome, P.F.J.; Wilde, R.H.; Willoughby, E.J. (2012). Land Resource Information System Spatial Data Layers, Technical Report, Palmerston North, Landcare Research NZ Ltd., New Zealand, 2000, Updated in 2012.

NIWA (2012). River Environmental classification version 2.0 (https://www.niwa.co.nz/freshwater-and-estuaries/management-tools/river-environment-classification-0)

Phillips, S.; Anderson, R.; Schapire, R. (2006). Maximum entropy modeling of species geographic distributions. *Ecological Modelling, 190*: 231–259.

Roe, W.; Howe, L.; Baker, E.; Burrows, L.; Hunter, S. (2013). An atypical genotype of *Toxoplasma gondii* as a cause of mortality in Hector's dolphins (*Cephalorhynchus hectori*). *Veterinary Parasitology, 192*: 67–74.

Shapiro, K.; Miller, A.E.; Packham, A.E.; Aguilar, B.; Conrad, P.A.; Vanwormer, E.; Murray, M.J. (2016). Dual congenital transmission of *Toxoplasma gondii* and *Sarcocystis neurona* in a late-term aborted pup from a chronically infected southern sea otter (*Enhydra lutris nereis*). *Parasitology, 143*: 276–288.

Snelder, T.H.; Biggs, B.J.F. (2002). Multiscale River Environment Classification for water resources management, *Journal of the American Water Resources Association 38*, 1225–1239, doi:10.1111/j.1752-1688.2002.tb04344.x.

Tait, A.; Henderson, R.; Turner, R.; Zheng, X. (2006). Thin plate smoothing spline interpolation of daily rainfall for New Zealand using a climatological rainfall surface, *International Journal of Climatology 26*, 2097–2115, doi:10.1002/joc.1350.

Tenter, A.M.; Heckeroth, A.R.; Weiss, L.M. (2000). *Toxoplasma gondii*: from animals to humans. *International Journal of Parasitology 30*: 1217–1258.

VanWormer, E.; Carpenter, T.E.; Singh, P.; Shapiro, K.; Wallender, W.W.; Conrad, P.A.; Largier, J.L.; Maneta, M.P.; Mazet, J.A.K. (2016). Coastal development and precipitation drive pathogen flow from land to sea: evidence from a Toxoplasma gondii and felid host system. *Scientific Reports, 6*: 29252.

Wilson, A.D.; Giltrap, D.J. (1982). Prediction and mapping of soil water retention properties. New Zealand Soil Bureau District Office Report WN7. 15p.

White, C.L.; Lankau, E.W.; Lynch, D.; Knowles, S.; Schuler, K.L.; Dubey, J.P.; Shearn-Bochsler, V.I.; Isidoro-Ayza, M.; Thomas, N.J. (2018). Mortality trends in northern sea otters (*Enhydra lutris kenyoni*) collected from the coasts of Washington and Oregon, USA (2002–15), *Journal of Wildlife Diseases, 54*: https://doi.org/10.7589/2017-05-122

APPENDIX 10 – REVIEW OF CRYPTIC MORTALITY AND POST-RELEASE SURVIVAL

Background

Potential sources of cryptic commercial fishery-related mortality relating to direct interactions with fishing gear include (Gilman et al. 2013):

- Pre-catch losses, including dolphins that are caught, collide with the vessel or gear, and die but are not observed when the gear is retrieved. Pre-catch losses also include depredation events, dolphins that fall out of the net on hauling before they can be observed ('drop-offs') and pre-hauling escapes that result in mortality;
- Ghost fishing mortalities; and
- Post-release mortalities, including delayed collateral and cumulative effects, e.g., relating to stress resulting from capture, or the cumulative effects of capture-related stress and fishing effects on habitat.

The spatial risk model assumes commercial fishery-specific priors for the observable probability (the inverse of the cryptic multiplier) relating to a commercial fishing event that accounts for pre-catch losses and ghost fishing mortalities from the above list. In a previous marine mammal risk assessment also using the SEFRA method, the observable probability assumed a uniform prior between 0.33 and 1.00 for set-net fisheries, and between 0.50 and 1.00 for all other fisheries, corresponding to a cryptic multiplier of 1.65 (95% CI = 1.02 to 2.86) in set nets and 1.39 (95% CI = 1.01 to 1.95) in trawls (Abraham et al. 2017). These priors were suggested by Fisheries New Zealand, based on video observations of Hector's dolphins caught in set net fisheries (McElderry et al. 2007). With respect to post-release survival, Abraham et al. (2017) assumed a uniform prior between 0.00 and 1.00.

Ghost fishing mortality

Ghost fishing capture rates have been studied experimentally for target and bycatch species through the monitoring of deliberately lost gear, primarily gill nets and pots (see Uhlmann & Broadhurst 2015). The studies indicate that daily capture rates of fish and crustacean species in set nets decline markedly within 20 days of deployment along with net height/spread (Kaiser et al. 1996). However, these studies were generally not designed for marine mammals, presumably for ethical reasons. As such, we used information with respect to fish and invertebrate mortality rate from ghost-fishing gear. A review by Brown & Macfadyen (2007) estimated that from less than 1 to 7% of all landed catches in European and North American pot and static net fisheries were lost to ghost fishing, ranging from:

- 0.01–3.2% of Baltic Sea cod catches;
- 1.5% of Cantabrian monkfish (4.5% was the worst-case scenario);
- 0.3% of Cantabrian hake; and
- 0.27–0.54% of Mediterranean hake fisheries.

These estimates suggest that 1% would be an appropriate best estimate for the percentage of Hector's/Māui dolphin captures that would occur due to ghost fishing set net gear and that 5% would be a conservative upper limit (accounting for differences in the respective ghost fishing capture rate of fish and dolphin species and also regional differences in gear loss rate compared with New Zealand).

Pre-catch losses

Cawthorn (1988) reported that the remains of Hector's dolphins were found in each of five broad-nosed seven gill sharks (*Notorynchus cepedianus*), captured in set nets north of Banks Peninsula, apparently over a short time period in 1984. This species of shark is known to scavenge dead prey and to depredate prey from fishing gear (Ebert 1991). However, we could not find a study for estimating potential depredation rates, which would vary with the population density of predatory shark species (e.g. broad-nosed sevengill sharks), which is poorly understood around New Zealand. Likewise, cumulative effects are very poorly understood and we assumed the respective contribution to cryptic mortality of cumulative effects and shark depredation events to be zero.

Pre-catch losses on hauling gear have been estimated for other dolphin and porpoise species captured in gill nets. Kindt-Larsen et al. (2012) found 25/39 (64%) harbour porpoises registered from vessel records and video footage were recorded in vessel logbooks and 7/14 (50%) harbour porpoises observed in a sample of video footage only were deemed by video reviewers to have been seen by crew were recorded in vessel logbooks. Those that were recorded required disentangling from gear, whereas the remainder dropped out of the nets before they could be discovered by vessel crew. This agrees with Berrow et al. (1994), who estimated that 51% of 44 porpoises captured in gillnets were brought on-board. Another study noted that in 21 out of 36 porpoise bycatch events observers reported that individuals fell off the gear before reaching the deck, often sinking quickly (Bravington & Bisack 1996). This study also estimated an off-watch detection probability of 43% in one fishing year, attributed to lower detection probability when observers had other tasks.

Bravington & Bisack (1996) went on to note that on-watch observation periods (where the sole task is to monitor catch in gear as it is hauled from the water to the boat) could realistically be assumed to have a detection probability around 100% in the later years of the study, following improvements to observer instructions. Historically, the primary protected species-related task of Fisheries New Zealand observers aboard set netters has been to undertake deck-based estimates of seabird and marine mammal species abundance around the vessel, such that observers will only have spent part of their on-effort time monitoring gear between the water's surface and the side of the boat (Andy McKay, pers. comm.). Furthermore, safety requirements may preclude observers from viewing positions that would allow continuous observation of gear as it being retrieved. As such, it is likely that observers would not see a fraction of drop-offs, and, so, a modal observable probability of 0.5 was assumed for Hector's/Māui dolphins, approximating to vessel crew detection probability estimates from previous studies of other species (ranging from 0.43 to 0.51, see above).

This review could find no published study or other information for estimating sub-surface pre-catch losses with respect to commercial set nets or trawls. In lieu of any estimate of sub-surface pre-catch losses, we have chosen to account for this by assuming suitably broad bounds around a modal observable probability estimate of 0.5, based on drop-offs between the water's surface and landing on deck. With respect to set net fishing events, we assumed a beta distribution for the prior on observable probability, parameterised to give a 95% interval of 0.25 and 0.75 (corresponding to cryptic multipliers of 4 and 1.33, respectively). This interval contains the detection probability rates from previous studies (ranging from 0.43 to 0.51, see above) and was assumed to be sufficiently broad to account for sub-surface pre-catch losses and ghost fishing-related mortality.

Since the above studies were not informative for trawler-based observations, we assumed the same prior as used by Abraham et al. (2017) for trawl events, i.e. a uniform prior bounded at 0.5 and 1.0, which corresponds to cryptic multipliers of 2.0 and 1.0, respectively).

Post-release survival

Studies estimating the post-release survival of dolphins following capture in commercial fishing gear appear to be lacking, though analogous studies (e.g., Sharp et al. 2016; Wells et al. 2013) have been conducted on stranded dolphins in varying degrees of health. A study by Sharp et al. (2016) applied satellite tags to 34 stranded dolphins, including 23 individuals deemed to be healthy and 11 to be of "borderline" health, to assess their post-release survival. Of these, 8 dolphins transmitted for less than one day (either died or the tags failed) and the remaining 68% of dolphins were confirmed to have survived for more than one day, with no significant difference in the post-release survival characteristics of healthy versus borderline health individuals. The metric of 3-week transmission duration was used as an indicator of success by Sharp et al. (2014). Based on this metric, 18 out of 34 (53%) qualified as successful post-releases, though this figure would be biased low by tag failures.

A review of 69 post-release survival studies of small dolphin species (using a mixture of satellite tags, VHF transmitters or sighting information of identifiable individuals) found that 42% were "Successes"

(confirmed alive after 6-weeks; note different metric from above), 38% were "Unknown-Positives" (medical history and post-release data suggestive of successful release), 7% were "Unknown-Positives" (behavioural concerns prior to loss of contact), 10% were "Failures" (died or re-stranded) (Wells et al. 2013). The results of this study indicate a post-release survival between 42% and 83% of stranded individuals. Given that a larger percentage of those of uncertain fate were considered more likely to have survived and accounting for tag loss, 50–90% appears a reasonable estimate of post-release survival of Hector's and Māui dolphins from fishing events that would account for species differences (although Wells et al. 2013 found no obvious species effect across various species including dolphins, porpoises and pilot whales) and factors relating to capture in fishing gear versus stranding. These update the range of 0–100%, assumed by Abraham et al. (2017).

Studies of post-release survival relating to fishing events have been documented in numerous shark species, such as satellite-tagged whale sharks captured in purse seines (64% of 11 individuals survived at least 21 days after release) (Escalle et al. 2018); shortfin mako sharks captured by recreational fishing and marked with Survivorship Pop-up Archival Transmitting tags (90% of 30 individuals) (French et al. 2015). Despite clear differences in their biology compared with dolphins, these results are consistent with post-release survival after captures relating to fishing exceeding 50% and consistent with the 50–90% range proposed for Hector's/Māui dolphins.

Conclusions and risk assessment inputs

Based on the brief assessment above, the following priors were assumed by the spatial risk model for the estimation of annual incidental commercial fishery-related deaths:

- Observable probability prior:
  - Set-net events = Beta ($\alpha = 6.916$, $\beta = 6.916$); ~consistent with 95% CI of 0.25 and 0.75
  - Trawl events = U[0.5, 1.0]
- Post-release survival prior = U[0.5, 0.9]

References

Abraham, E.R.; Neubauer, P.; Berkenbusch, K.; Richard, Y. (2017). Assessment of the risk to New New Zealand marine mammals from commercial fisheries. *Aquatic Environment and Biodiversity Report 189*. 123 p.

Berrow, S.D.; Tregenza, N.J.C.; Hammond, P.S. (1994). Marine mammal bycatch on the Celtic Shelf. European Commission Document: DG XIV/C/1 Study Contract 92/3503.

Bravington, M.V.; Bisack, K.D. (1996). Estimates of harbor porpoise bycatch in the Gulf of Maine sink gillnet fishery, 1990–1993. *Reports of the International Whaling Commission 46*: 567–574.

Brown, J.; MacFadyen, G. (2007). Ghost fishing in European waters: Impacts and management responses. *Marine Policy, 31*: 488–504.

Cawthorn, M.W. (1988). Recent observations of Hector's dolphin *Cephalorhynchus hectori*, in New Zealand. *Reports of the International Whaling Commission Special Issue, 9*: 303–314.

Ebert, D.A. (1991). Observations on the predatory behaviour of the sevengill shark *Notorynchus cepedianus*. *South African Journal of Marine Science, 11*: 455–465.

Escalle, L.; Amandé, J.M.; Filmalter, J.D.; Forget, F.; Gaertner, D.; Dagorn, L.; Mérigot, B. (2018). Update on post-release survival of tagged whale shark encircled by tuna purse-seiner. *Collective Volumes of Scientific Papers of ICCAT, 74*: 3671–3678.

French, R.P.; Lyle, J.M.; Tracey, S.; Currie, S.; Semmens, J.M. (2015). Post-release survival of captured mako sharks: contributing to developing best-practise for catch and release game fishing. Report produced by Institute for Marine and Antarctic Studies, University of Tasmania. 27 p.

Gilman, E.; Suuronen, P.; Hall, M.; Kennelly, S. (2013). Causes and methods to estimate cryptic sources of fishing mortality. *Journal Fish Biology, 83*: 766–803.

Kaiser, M.J.; Bullimore, B.; Newman, P.; Lock, K.; Gilbert, S. (1996). Catches in 'ghost fishing' set nets. *Marine Ecology Progress Series, 145*: 11–16.

Kindt-Larsen, L.; Dalskov, J.; Stage, B.; Larsen, F. (2012). Observing incidental harbour porpoise *Phocoena phocoena* bycatch by remote electronic monitoring. *Endangered Species Research, 19*: 75–83.

McElderry, H.; McCullough, D.; Schrader, J.; Illingworth, J. (2007). Pilot study to test the effectiveness of electronic monitoring in Canterbury fisheries. *DOC Research and Development Series 264*.

Sharp, S.M.; Harry, C.T.; Hoppe, J.M.; Moore, K.M.; Niemeyer, M.E.; Robinson, I.; Rose, K.S.; Sharp, W.B. (2016) A comparison of postrelease survival parameters between single and mass stranded delphinids from Cape Cod, Massachusetts, *U.S.A. Marine Mammal Science, 32*: 161–180.

Sharp, S.M.; Knoll, J.S.; Moore, M.J.; et al. (2014). Hematological, biochemical, and morphological parameters as prognostic indicators for stranded common dolphins (*Delphinus delphis*) from Cape Cod, Massachusetts, U.S.A. *Marine Mammal Science, 30*: 864–887.

Uhlmann, S.; Broadhurst, M.K. (2015). Mitigating unaccounted fishing mortality from gillnets and traps. *Fish and Fisheries, 16*: 183–229.

Wells, R.S.; Fauquier, D.A.; Gulland, F.M.D.; Townsend, F.I.; DiGiovanni, Jr., R.A. (2013). Evaluating postintervention survival of free-ranging odontocete cetaceans. *Marine Mammal Science 29*: E463–E483.
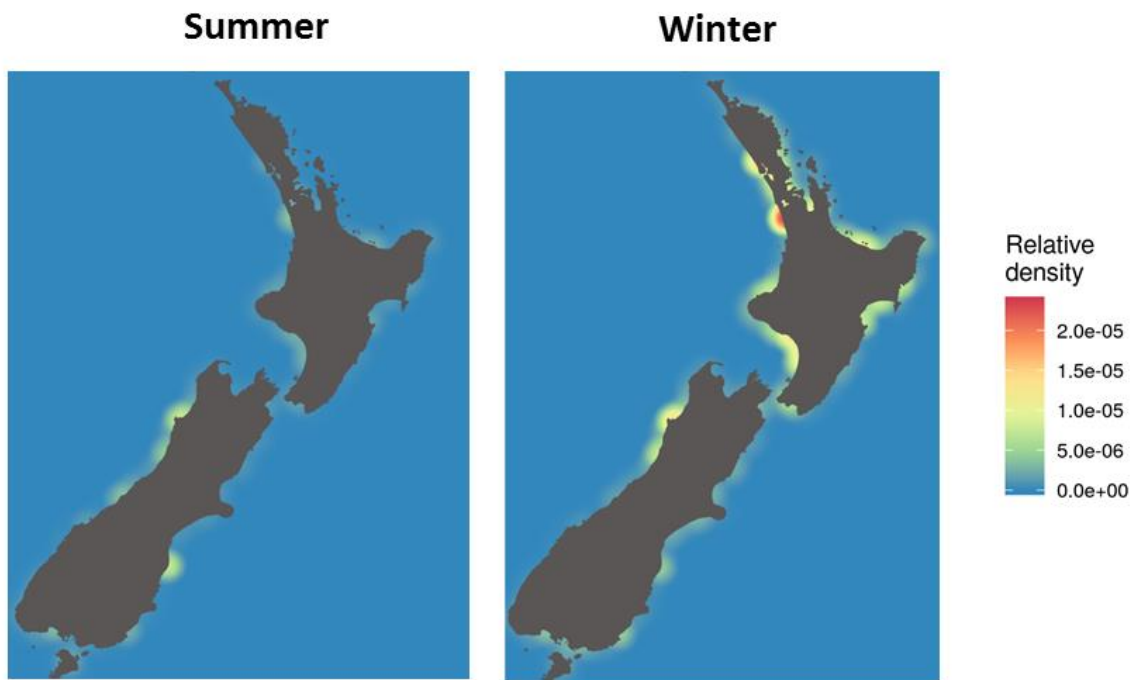
Figure A11-1: Toxoplasmosis estimated seasonal spatial threat intensity.
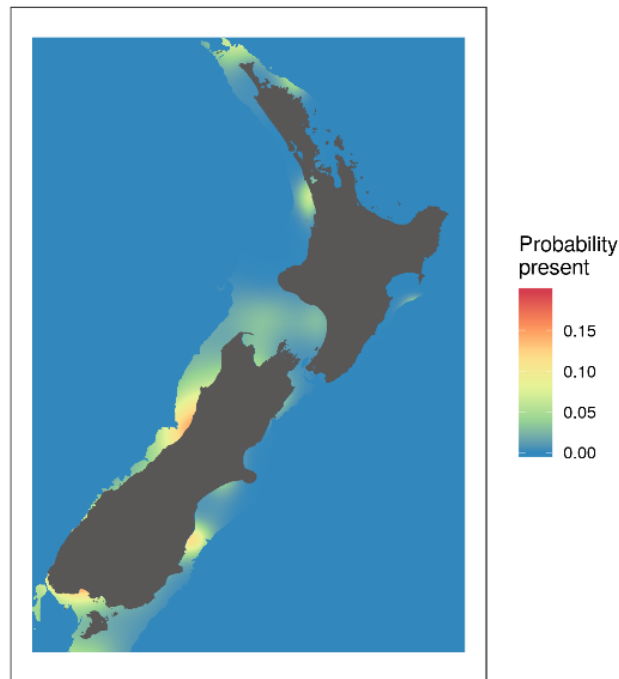
Figure A11-2: Predation (broadnose sevengill shark) estimated spatial threat intensity.

Figure A11-3: Recreational netting estimated spatial threat intensity.

Figure A11-4: Aquaculture estimated spatial threat intensity (current operations only)
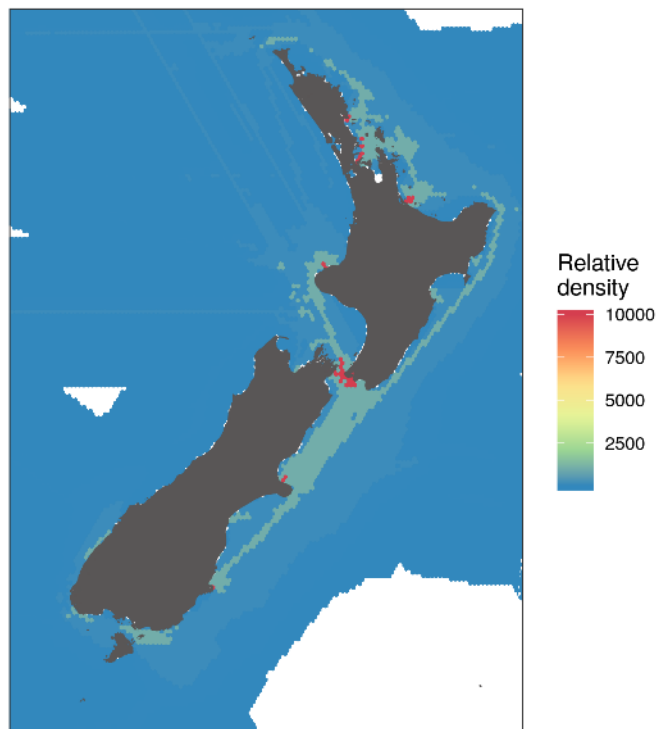
Figure A11-5: Oil spill risk estimated spatial threat intensity.
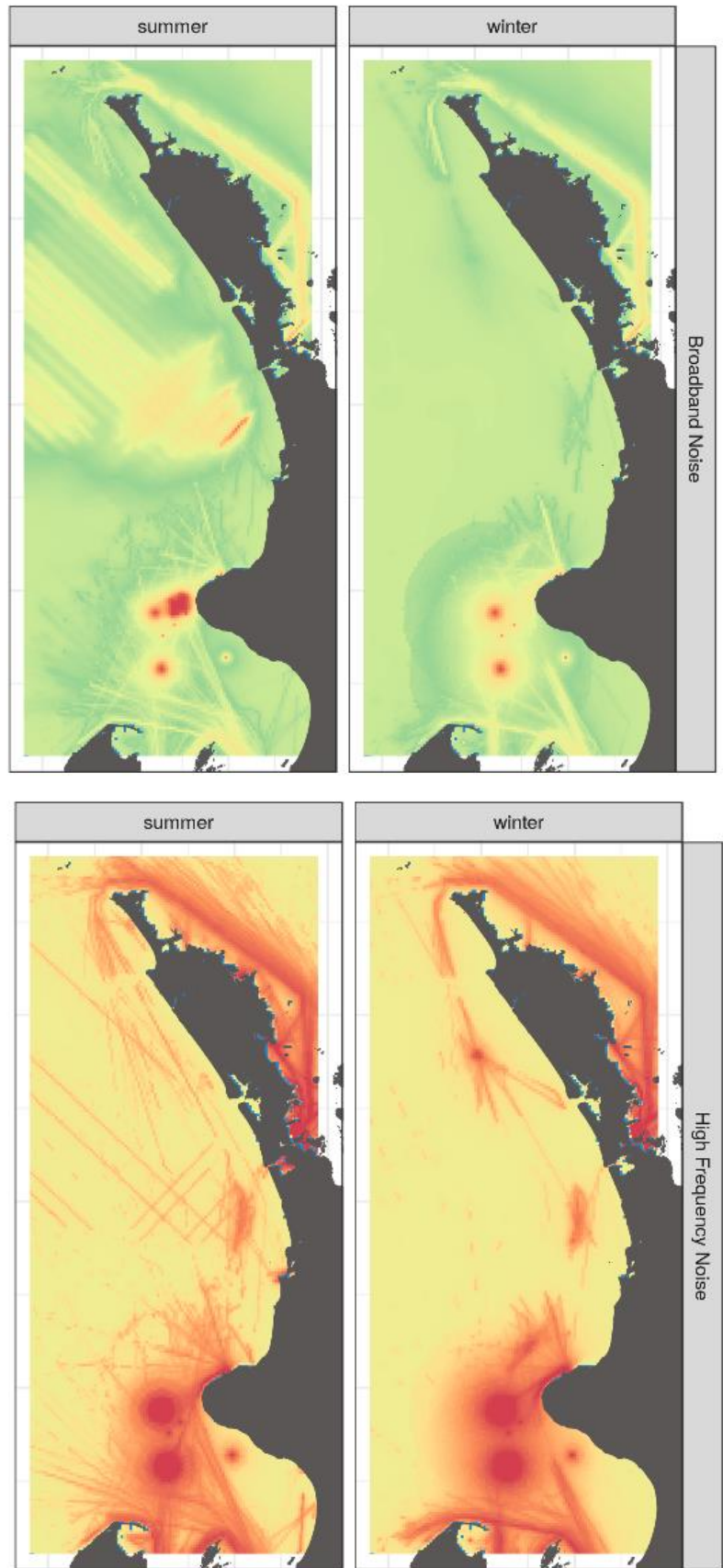
Figure A11-6: Estimated cumulative broadband noise (top) and high-frequency noise (bottom) in summer (left) and winter (right). Spatial estimates from noise modelling by McPherson et al. (2019).

APPENDIX 12 – SPATIAL OVERLAP WITH THREATS
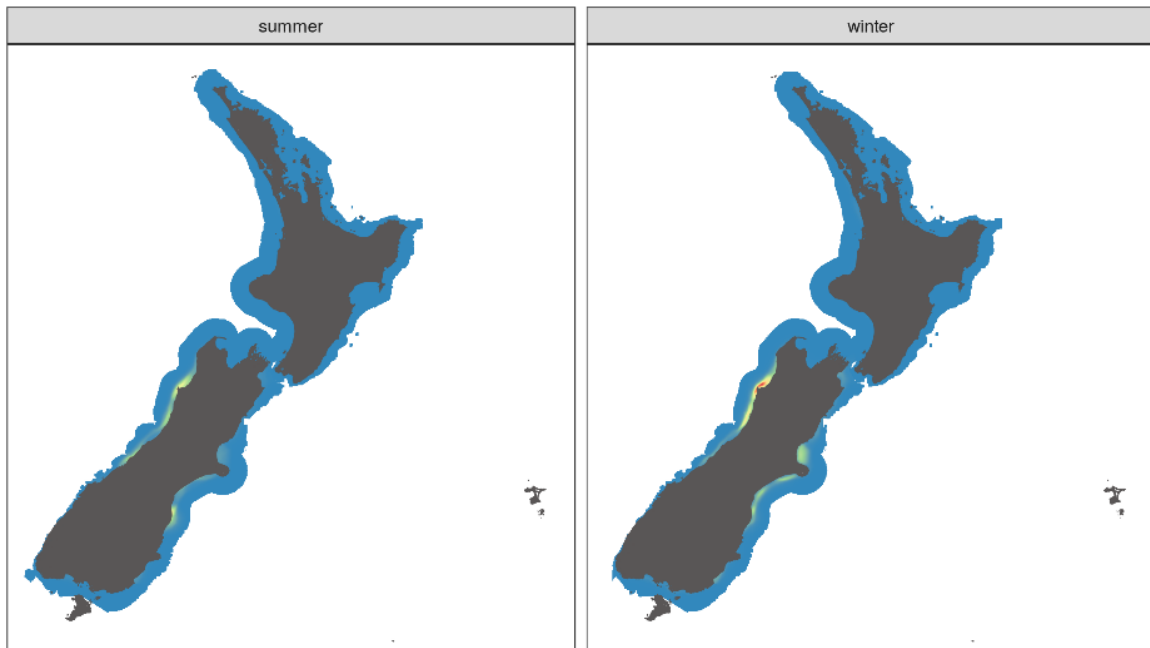
Figure A12-1: Toxoplasmosis estimated seasonal spatial overlap with Hector's and Māui dolphins.
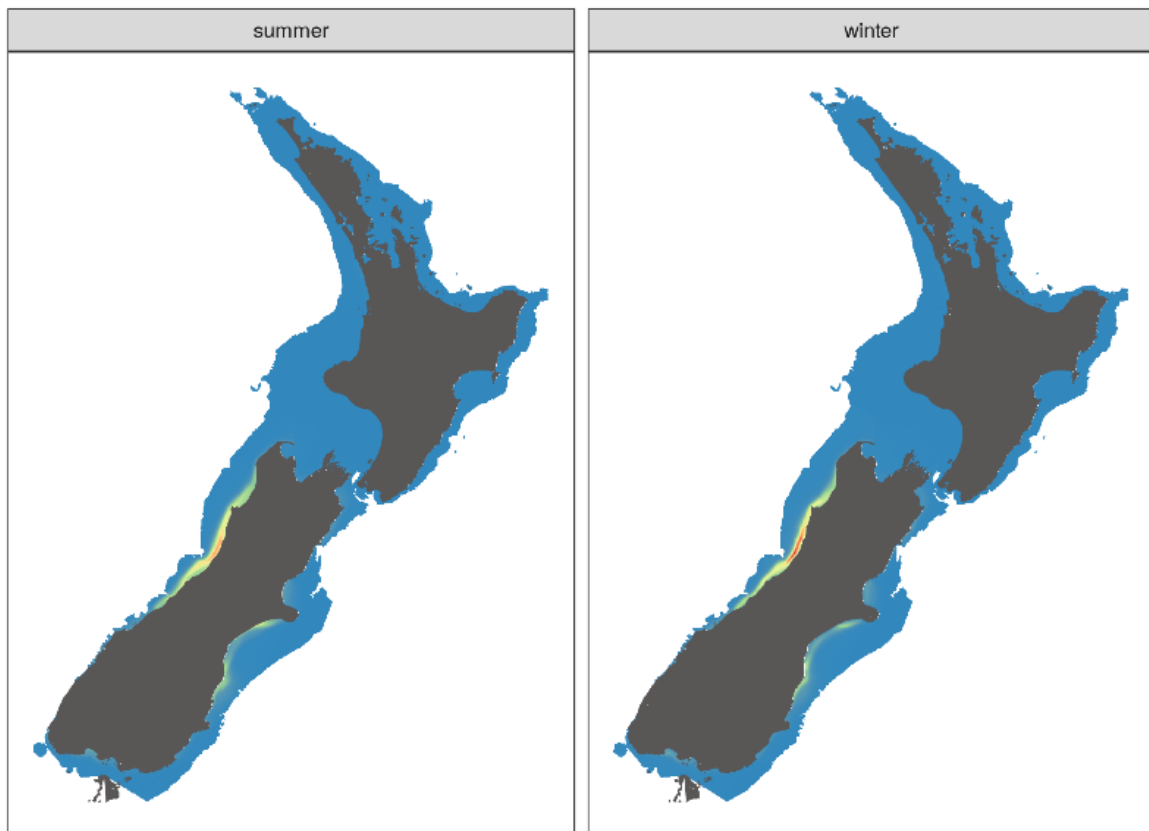
Figure A12-2: Predation (broadnose sevengill shark) estimated seasonal spatial overlap with Hector's and Māui dolphins.
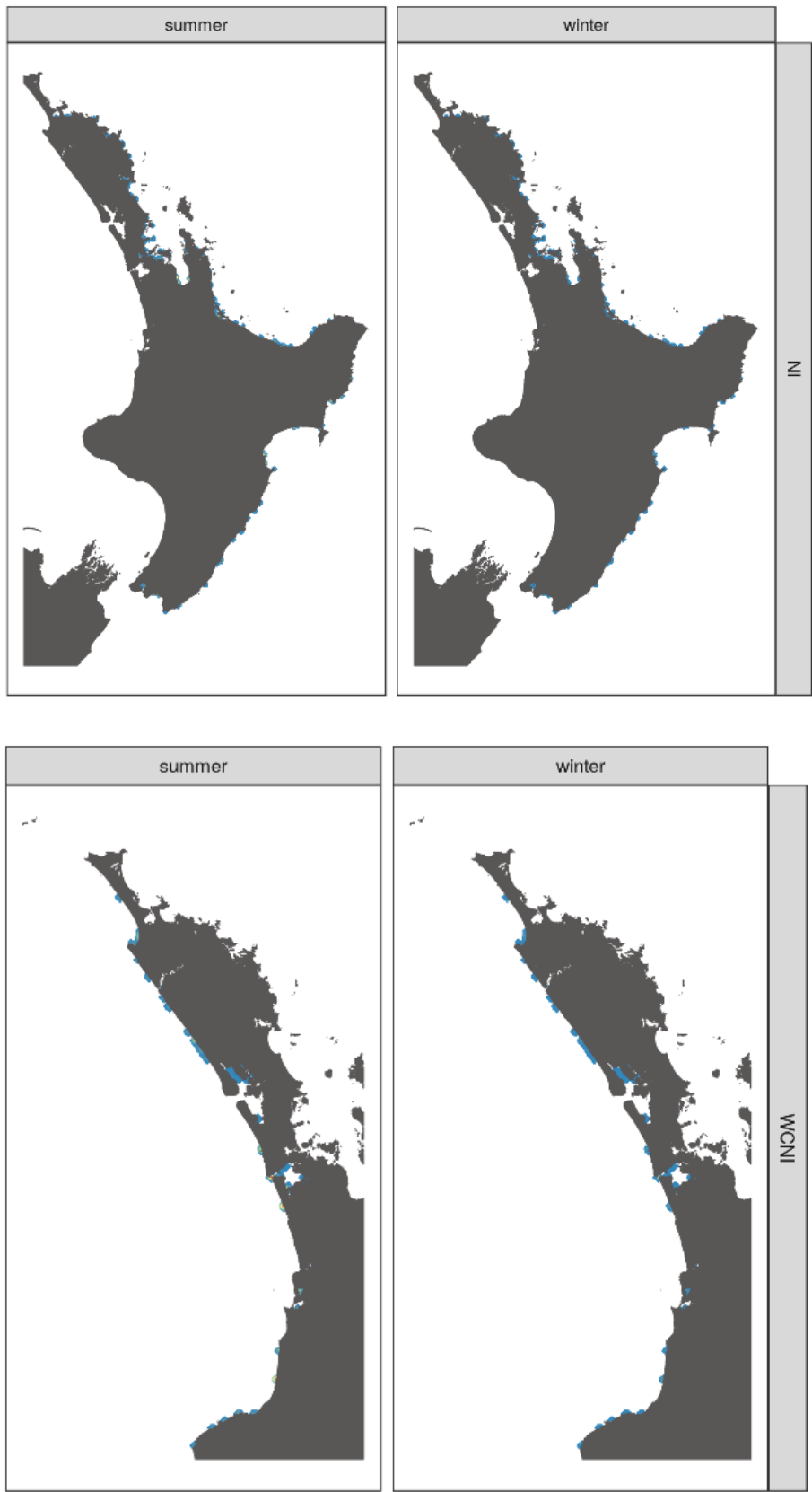
Figure A12-3: Recreational netting estimated seasonal spatial overlap with Hector's and Māui dolphins.
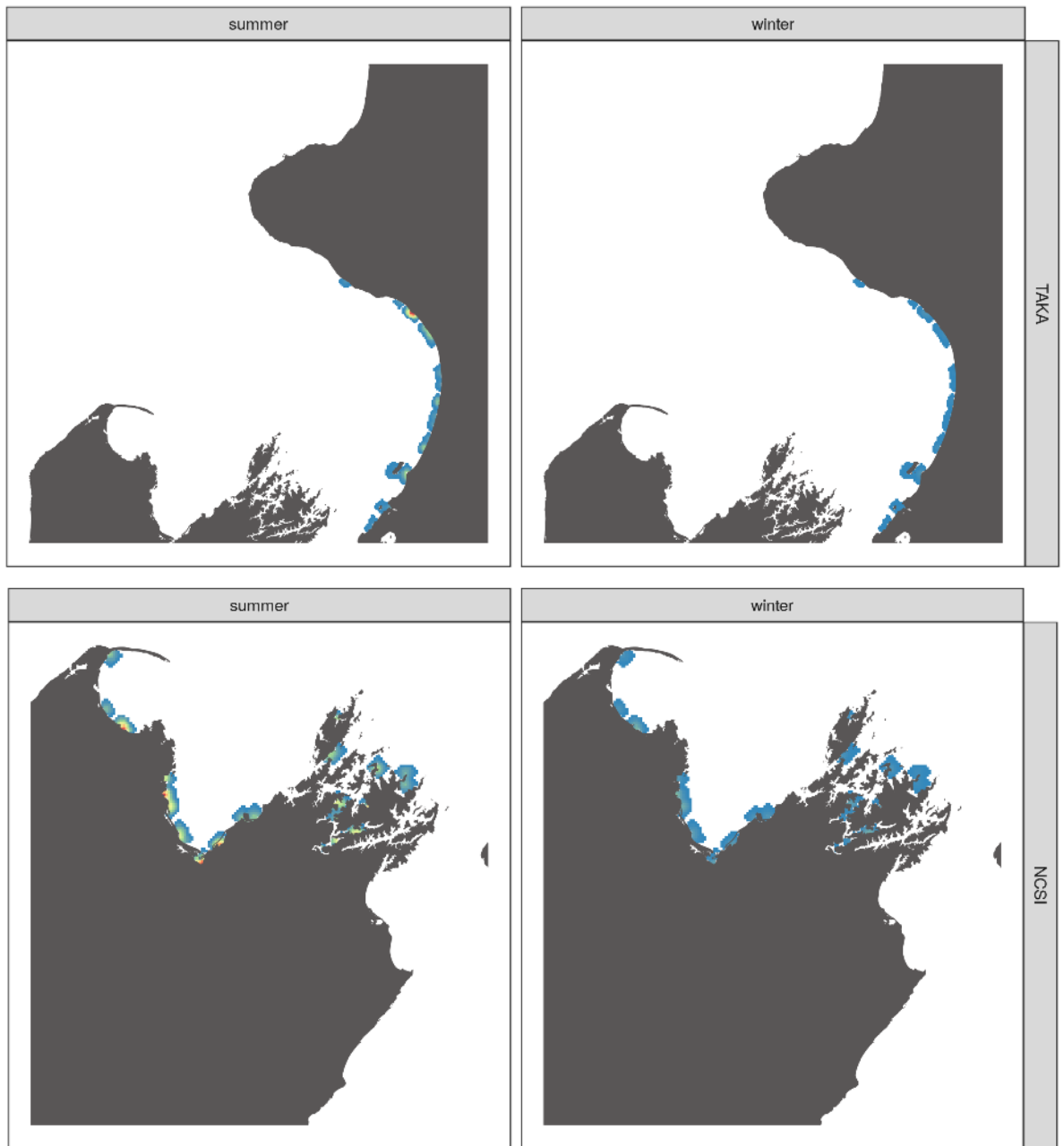
Figure A12-3: Recreational netting estimated seasonal spatial overlap with Hector's and Māui dolphins. Continued

Figure A12-3: Recreational netting estimated seasonal spatial overlap with Hector's and Māui dolphins. Continued
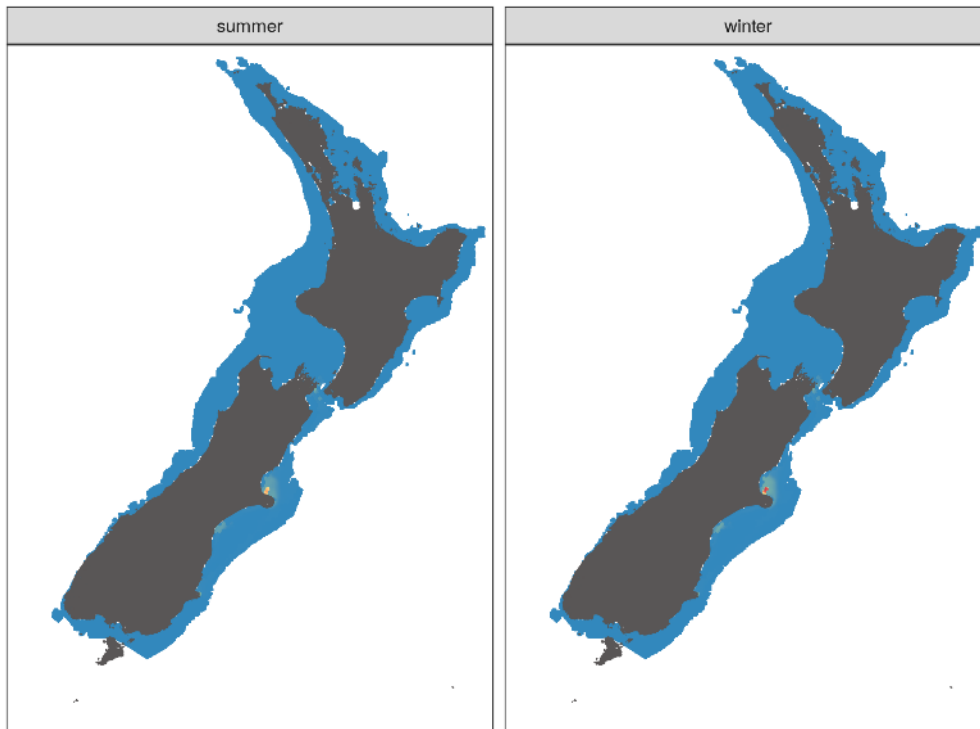
Figure A12-4: Oil spill risk estimated seasonal spatial overlap with Hector's and Māui dolphins.
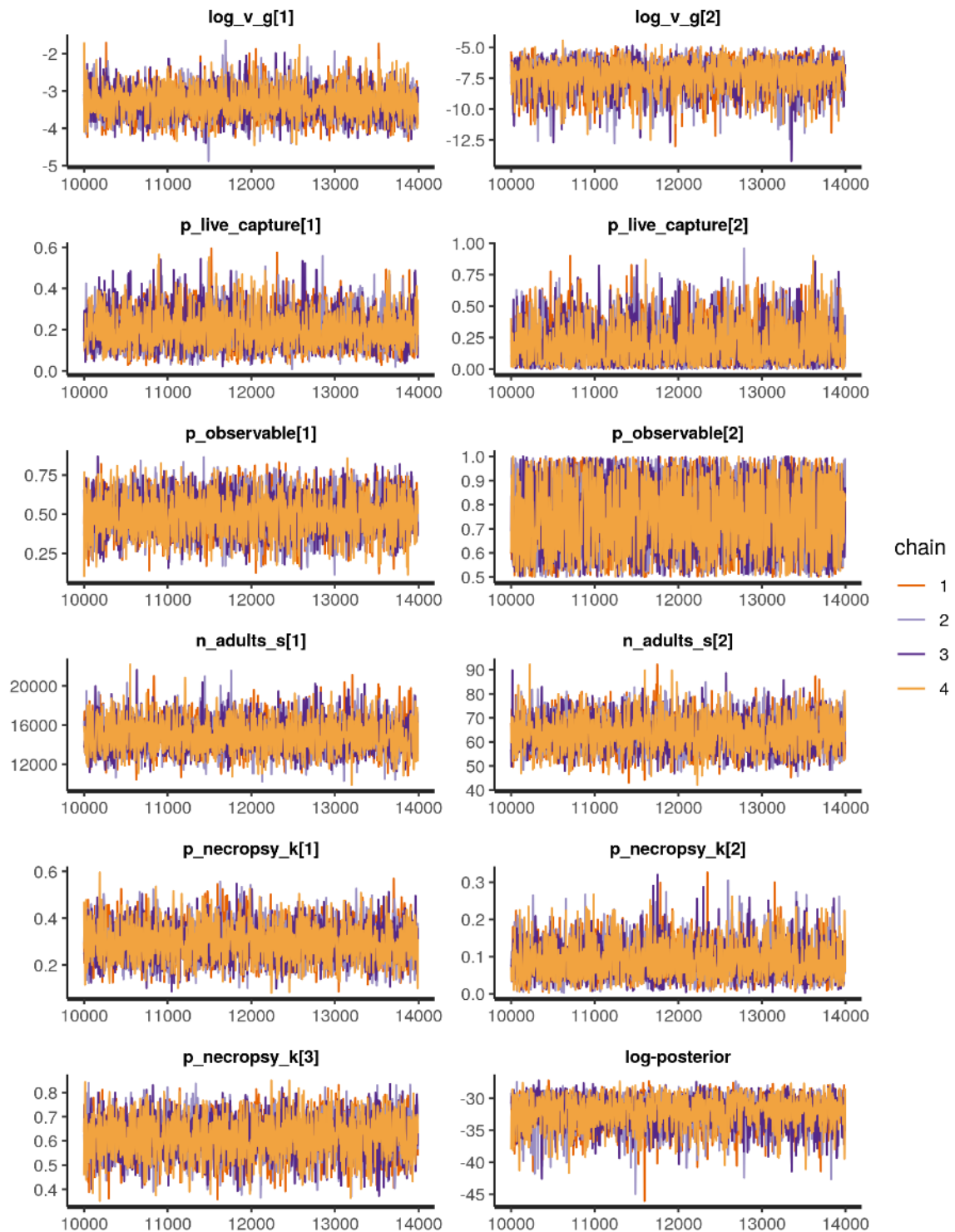
Figure A13-1: Markov chain Monte Carlo (MCMC) trace plots for all estimated model parameters and the log-posterior density (i.e. the objective function). This model run assumed a calibration coefficient (ϕ) of 0.2.
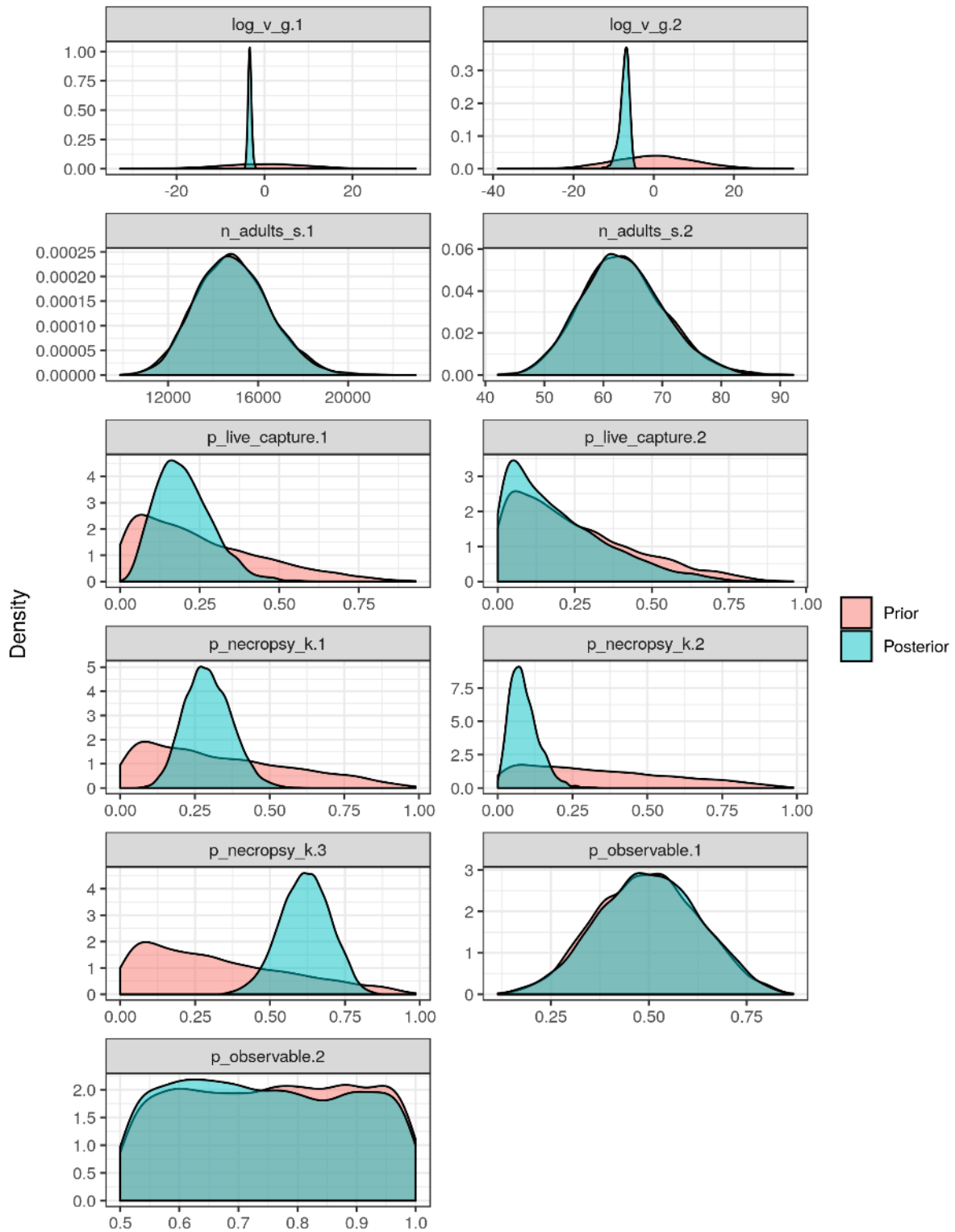
Figure A13-2: Prior and posterior distributions of all estimated model parameters. This model run assumed a calibration coefficient (ϕ) of 0.2.
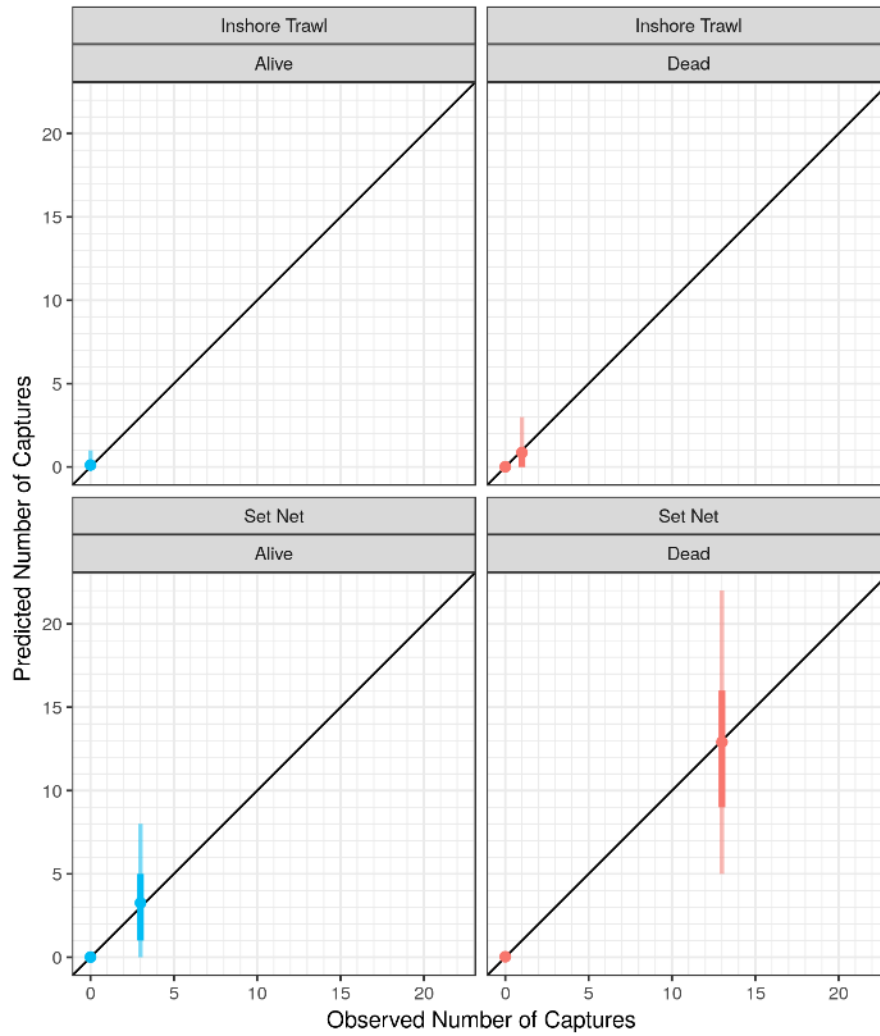
Figure A13-3: Observed vs. spatial risk model predicted number of Hector's/Māui dolphin captures that are alive (blue) or dead (red) in inshore trawl or set nets. This model run assumed a calibration coefficient (ϕ) of 0.2.

APPENDIX 14 – RISK MODEL PARAMETER ESTIMATES

Table A14-1. Quantiles (median and 95% credible interval) of parameters, random variables, and generated quantities in the spatial risk model for Hector's and Māui dolphins, assuming a calibration coefficient ϕ of 0.2. Estimated parameters and random variables above the line, derived quantities below.

| Parameter label	Parameter description	Equal detection probability			Predation sensitivity		
		50%	2.50%	97.50%	50%	2.50%	97.50%
n_adults_s[1]	Hector's population size	14 821	11 992	18 255	14 865	11 942	18 477
n_adults_s[2]	Māui population size	62.96	50.57	78.04	62.96	50.36	77.92
vulnerability_g[1]	Vulnerability set net	0.036	0.017	0.082	0.036	0.018	0.083
vulnerability_g[2]	Vulnerability trawl	0.001	0.000	0.004	0.001	0.000	0.005
p_observable[1]	Proportion set net captures observable	0.500	0.248	0.744	0.497	0.247	0.745
p_observable [2]	Proportion trawl captures observable	0.742	0.513	0.988	0.747	0.514	0.987
p_live_capture[1]	Probability live capture set net	0.191	0.062	0.396	0.190	0.062	0.391
p_live_capture[2]	Probability live capture trawl	0.155	0.007	0.602	0.156	0.007	0.614
p_necropsy_k[1]	Proportion necropsy toxoplasmosis	0.291	0.156	0.452	0.292	0.156	0.460
p_necropsy_k[2]	Proportion necropsy predation	0.081	0.017	0.200	0.080	0.019	0.199
p_necropsy_k[3]	Proportion necropsy other	0.618	0.449	0.771	0.620	0.448	0.768
p_survive_capture[1]	Probability survive release	0.696	0.509	0.891	0.701	0.510	0.890
adult_survival_s[1]	Non-calf survival Hector's	0.923	0.859	0.964	0.923	0.861	0.965
adult_survival_s[2]	Non-calf survival Māui	0.893	0.870	0.913	0.893	0.870	0.913
rmax_s[1]	r_s^{max} Hector's	0.050	0.028	0.071	0.050	0.029	0.071
rmax_s[2]	r_s^{max} Māui	0.045	0.025	0.067	0.045	0.022	0.067
captures_sg[1,1]	Hector's observable captures set net	23.450	13.399	37.201	23.475	13.499	36.750
captures_sg[1,2]	Hector's observable captures trawl	4.450	0.150	22.200	4.350	0.150	22.701
captures_sg[2,1]	Māui observable captures set net	0.050	0.000	0.200	0.050	0.000	0.150
captures_sg[2,2]	Māui observable captures trawl	0.000	0.000	0.050	0.000	0.000	0.050
deaths_sg[1,1]	Hector's deaths set net	40.800	20.149	91.954	41.100	20.199	94.211
deaths_sg[1,2]	Hector's deaths trawl	5.100	0.200	27.605	4.925	0.200	28.351
deaths_sg[2,1]	Māui deaths set net	0.100	0.000	0.300	0.100	0.000	0.300
deaths_sg[2,2]	Māui deaths trawl	0.000	0.000	0.050	0.000	0.000	0.050
total_deaths_s[1]	Hector's deaths total	1145.59	500.87	2158.78	1153.10	498.21	2159.54
total_deaths_s[2]	Māui deaths total	6.733	5.005	9.037	6.727	5.017	9.068
non_fishery_deaths_sk[1,1]	Hector's deaths toxoplasmosis	311.47	106.73	719.40	176.39	53.99	469.75
non_fishery_deaths_sk[1,2]	Hector's deaths predation	85.03	15.49	274.19	485.92	129.80	1149.03
non_fishery_deaths_sk[1,3]	Hector's deaths other non-fishery	667.12	267.99	1355.95	384.89	130.39	895.59
non_fishery_deaths_sk[2,1]	Māui deaths toxoplasmosis	1.901	0.964	3.274	1.105	0.442	2.310
non_fishery_deaths_sk[2,2]	Māui deaths predation	0.532	0.113	1.422	3.039	1.049	5.273
non_fishery_deaths_sk[2,3]	Māui deaths other non-fishery	4.059	2.645	5.987	2.354	1.154	4.273
non_fishery_risk_sk[1,1]	Hector's risk ratio toxoplasmosis	4.245	1.417	11.135	2.443	0.711	7.325
non_fishery_risk_sk[1,2]	Hector's risk ratio predation	1.174	0.205	4.168	6.646	1.742	17.637
non_fishery_risk_sk[1,3]	Hector's risk ratio other non-fishery	9.041	3.431	22.315	5.309	1.703	13.966
non_fishery_risk_sk[2,1]	Māui risk ratio toxoplasmosis	6.811	3.168	14.729	4.011	1.469	10.472
non_fishery_risk_sk[2,2]	Māui risk ratio predation	1.894	0.401	5.807	10.828	3.561	24.655
non_fishery_risk_sk[2,3]	Māui risk ratio other non-fishery	14.406	8.319	28.236	8.498	3.711	20.147
pst_s[1]	PST Hector's	74.097	40.556	114.209	73.469	41.373	112.861
pst_s[2]	PST Māui	0.283	0.148	0.444	0.282	0.136	0.447
risk_ratio_sg[1,1]	Hector's risk ratio set net	0.563	0.237	1.487	0.566	0.246	1.572
risk_ratio_sg[1,2]	Hector's risk ratio trawl	0.070	0.003	0.444	0.066	0.003	0.435
risk_ratio_sg[2,1]	Māui risk ratio set net	0.282	0.000	1.230	0.297	0.000	1.297
risk_ratio_sg[2,2]	Māui risk ratio trawl	0.000	0.000	0.295	0.000	0.000	0.294

Table A14-2. Estimated annual deaths by threat and subarea.

Cause of death	Sub-population	Deaths equal detection			Deaths predation sensitivity		
		50.0%	2.5%	97.5%	50.0%	2.5%	97.5%
Set net	MĀUI	0.10	0.00	0.30	0.10	0.00	0.30
Set net	NI	0.07	0.04	0.17	0.08	0.04	0.17
Set net	TAKA	0.06	0.03	0.13	0.06	0.03	0.13
Set net	NCSI	0.65	0.31	1.47	0.65	0.32	1.49
Set net	WCSI	0.32	0.15	0.74	0.33	0.16	0.75
Set net	ECSI	38.86	18.57	88.25	39.14	19.41	89.42
Set net	SCSI	0.80	0.38	1.81	0.80	0.40	1.84
Inshore trawl	MĀUI	0.00	0.00	0.05	0.00	0.00	0.05
Inshore trawl	NI	0.00	0.00	0.02	0.00	0.00	0.02
Inshore trawl	TAKA	0.00	0.00	0.00	0.00	0.00	0.00
Inshore trawl	NCSI	0.10	0.00	0.54	0.10	0.00	0.59
Inshore trawl	WCSI	1.84	0.08	9.40	1.77	0.07	10.29
Inshore trawl	ECSI	3.04	0.14	15.56	2.93	0.12	17.04
Inshore trawl	SCSI	0.11	0.00	0.56	0.11	0.00	0.62
Toxoplasmosis	MĀUI	1.90	0.96	3.27	1.11	0.44	2.31
Toxoplasmosis	NI	0.25	0.09	0.58	0.14	0.04	0.38
Toxoplasmosis	TAKA	0.40	0.15	0.93	0.23	0.07	0.61
Toxoplasmosis	NCSI	1.10	0.40	2.54	0.63	0.19	1.67
Toxoplasmosis	WCSI	187.03	67.86	432.09	106.80	32.69	284.43
Toxoplasmosis	ECSI	115.06	41.75	265.81	65.70	20.11	174.97
Toxoplasmosis	SCSI	5.05	1.83	11.67	2.88	0.88	7.68
Predation	MĀUI	0.53	0.11	1.42	3.04	1.05	5.27
Predation	NI	0.00	0.00	0.00	0.01	0.00	0.02
Predation	TAKA	0.03	0.01	0.11	0.19	0.05	0.44
Predation	NCSI	0.77	0.16	2.63	4.47	1.19	10.56
Predation	WCSI	62.64	12.72	214.41	363.62	97.13	859.84
Predation	ECSI	17.64	3.58	60.37	102.38	27.35	242.09
Predation	SCSI	2.63	0.53	9.00	15.26	4.08	36.08
Other	MĀUI	4.06	2.65	5.99	2.35	1.15	4.27
Other	NI	0.42	0.17	0.88	0.24	0.08	0.57
Other	TAKA	0.56	0.23	1.16	0.32	0.11	0.75
Other	NCSI	9.06	3.69	18.78	5.22	1.77	12.15
Other	WCSI	232.05	94.49	480.99	133.72	45.30	311.15
Other	ECSI	411.79	167.67	853.54	237.29	80.39	552.14
Other	SCSI	14.05	5.72	29.13	8.10	2.74	18.84

Table A14-3. Estimated annual risk ratio by threat and subarea when assuming a calibration coefficient (ϕ) of 0.2, consistent with population recovery to at least 90% of carrying capacity.

Cause of death	Sub-population	Risk ratio equal detection			Risk ratio predation sensitivity		
		50.0%	2.5%	97.5%	50.0%	2.5%	97.5%
Set net	MAUI	0.28	0.00	1.23	0.30	0.00	1.30
Set net	NI	1.61	0.68	4.23	1.63	0.72	4.57
Set net	TAKA	0.94	0.39	2.46	0.95	0.42	2.66
Set net	NCSI	0.65	0.27	1.72	0.66	0.29	1.85
Set net	WCSI	0.01	0.01	0.03	0.01	0.01	0.04
Set net	ECSI	0.86	0.36	2.27	0.87	0.39	2.45
Set net	SCSI	0.52	0.22	1.36	0.52	0.23	1.47
Inshore trawl	MAUI	0.00	0.00	0.30	0.00	0.00	0.29
Inshore trawl	NI	0.07	0.00	0.42	0.07	0.00	0.44
Inshore trawl	TAKA	0.01	0.00	0.05	0.01	0.00	0.05
Inshore trawl	NCSI	0.10	0.00	0.63	0.10	0.00	0.66
Inshore trawl	WCSI	0.07	0.00	0.43	0.07	0.00	0.45
Inshore trawl	ECSI	0.07	0.00	0.40	0.07	0.00	0.42
Inshore trawl	SCSI	0.07	0.00	0.43	0.07	0.00	0.45
Toxoplasmosis	MAUI	6.81	3.17	14.73	4.01	1.47	10.47
Toxoplasmosis	NI	5.38	1.87	14.21	3.14	0.91	9.41
Toxoplasmosis	TAKA	6.47	2.25	17.07	3.77	1.10	11.31
Toxoplasmosis	NCSI	1.10	0.38	2.90	0.64	0.19	1.92
Toxoplasmosis	WCSI	7.30	2.54	19.27	4.26	1.24	12.77
Toxoplasmosis	ECSI	2.53	0.88	6.68	1.48	0.43	4.43
Toxoplasmosis	SCSI	3.26	1.13	8.59	1.90	0.55	5.69

Table A14-4. Estimated annual risk ratio by threat and subarea when assuming a sensitivity calibration coefficient (ϕ) value of 0.5, consistent with population recovery to at least 75% of carrying capacity.

Cause of death	Sub-population	Risk ratio equal detection			Risk ratio predation sensitivity		
		50.0%	2.5%	97.5%	50.0%	2.5%	97.5%
Set net	MĀUI	0.12	0.00	0.50	0.12	0.00	0.50
Set net	NI	0.65	0.28	1.75	0.66	0.28	1.74
Set net	TAKA	0.38	0.16	1.02	0.38	0.16	1.01
Set net	NCSI	0.26	0.12	0.71	0.27	0.11	0.70
Set net	WCSI	0.01	0.00	0.01	0.01	0.00	0.01
Set net	ECSI	0.35	0.15	0.94	0.35	0.15	0.93
Set net	SCSI	0.21	0.09	0.56	0.21	0.09	0.56
Inshore trawl	MĀUI	0.00	0.00	0.12	0.00	0.00	0.12
Inshore trawl	NI	0.03	0.00	0.17	0.03	0.00	0.17
Inshore trawl	TAKA	0.00	0.00	0.02	0.00	0.00	0.02
Inshore trawl	NCSI	0.04	0.00	0.25	0.04	0.00	0.26
Inshore trawl	WCSI	0.03	0.00	0.17	0.03	0.00	0.17
Inshore trawl	ECSI	0.03	0.00	0.16	0.03	0.00	0.16
Inshore trawl	SCSI	0.03	0.00	0.17	0.03	0.00	0.17
Toxoplasmosis	MĀUI	2.74	1.23	5.98	1.56	0.59	4.09
Toxoplasmosis	NI	2.23	0.72	5.77	1.25	0.36	3.75
Toxoplasmosis	TAKA	2.68	0.87	6.93	1.51	0.44	4.51
Toxoplasmosis	NCSI	0.46	0.15	1.18	0.26	0.07	0.77
Toxoplasmosis	WCSI	3.03	0.98	7.83	1.70	0.49	5.09
Toxoplasmosis	ECSI	1.05	0.34	2.71	0.59	0.17	1.76
Toxoplasmosis	SCSI	1.35	0.44	3.49	0.76	0.22	2.27

APPENDIX 15 – RISK MODEL SPATIAL OUTPUTS

Where relevant, plots in this Appendix were generated using the SEFRA model assuming a calibration coefficient (ϕ) of 0.2**.**
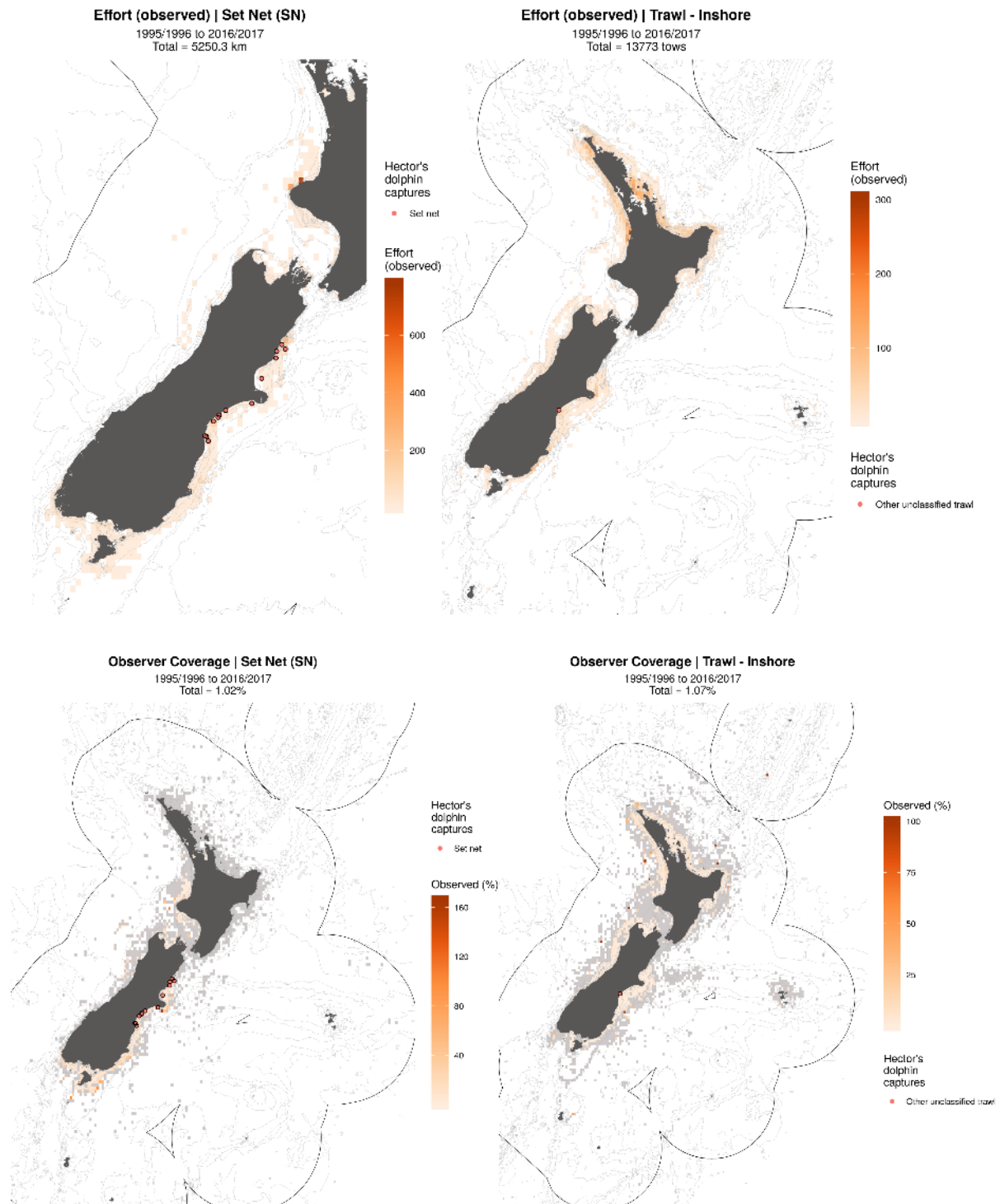
Figure A15-1: Total observed set net (top left) and inshore trawl (top right) fishing effort and observer coverage (bottom) in New Zealand from 1995/96 to 2016/17. Grey pixels represent cells where there was effort but no observer coverage. Observed Hector's dolphin captures in set nets and trawls between 1995/96 to 2016/17 are also shown as red points.

Figure A15-2: Observed Hector's dolphin overlap with set nets from 1995/96 to 2016/17. Observed Hector's dolphin captures in set nets between 1995/96 to 2016/17are also shown as red points.

Estimated Captures (observed) | Set Net (SN) | Hector's dolphin
1995/1996 to 2016/2017
Total = 15.9039
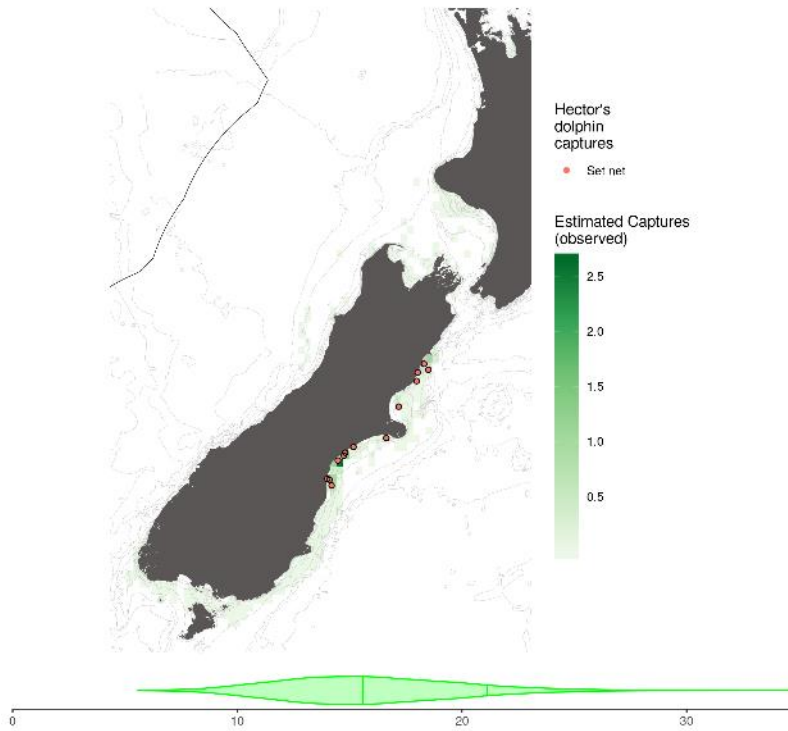
Estimated Captures (observed) | Trawl - Inshore | Hector's dolphin
1995/1996 to 2016/2017
Total = 1.0426
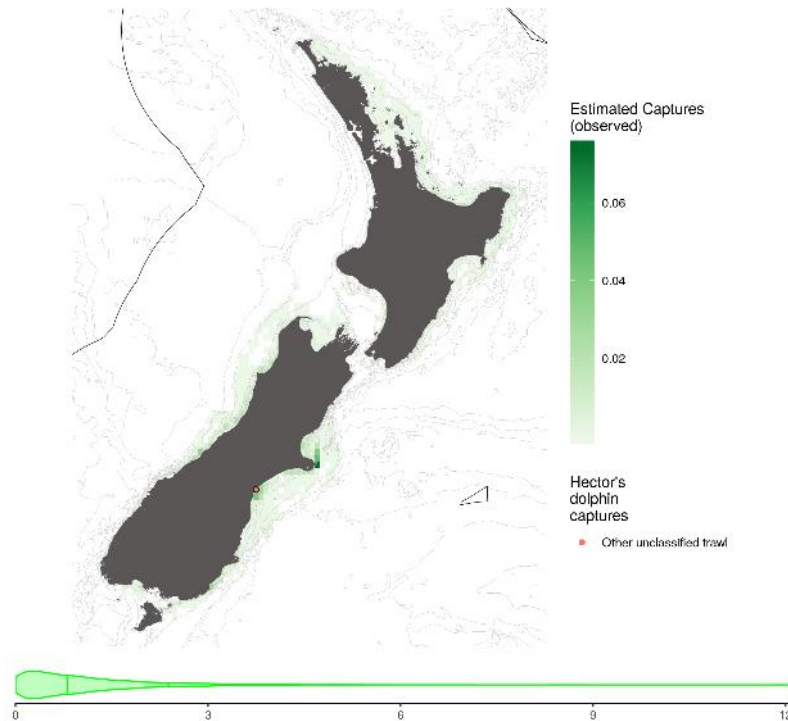
Figure A15-3: Predicted number of observed Hector's dolphin captures from 1995/96 to 2016/17. Observed Hector's dolphin captures in set nets between 1995/96 to 2016/17 are also shown as red points. The posterior distribution of the total estimated observed number of captures is also displayed as the violin along the bottom with the median and upper 90% quantile indicated by the vertical lines within the violin.

Estimated Captures (observed) | Set Net (SN) | Maui dolphin
1995/1996 to 2016/2017
Total = 0.0383
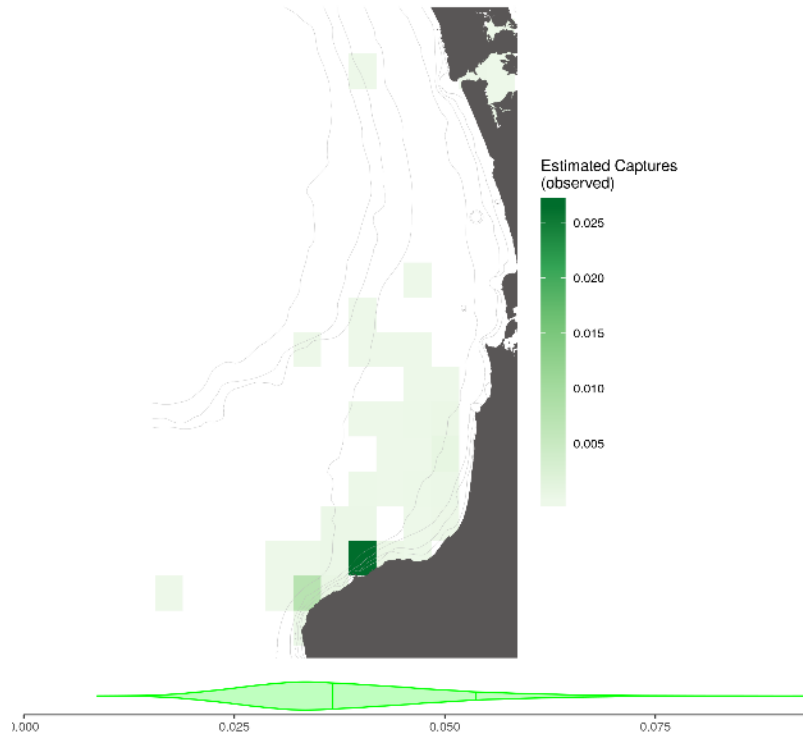
Estimated Captures (observed) | Trawl - Inshore | Maui dolphin
1995/1996 to 2016/2017
Total = 0.0119
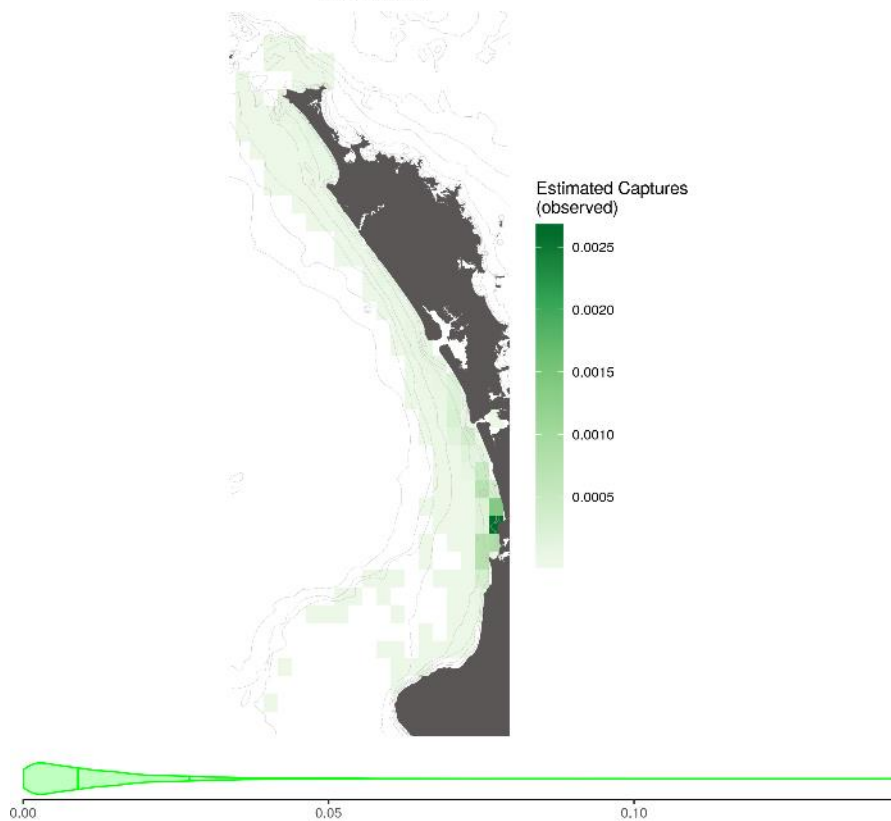
Figure A15-3: Continued
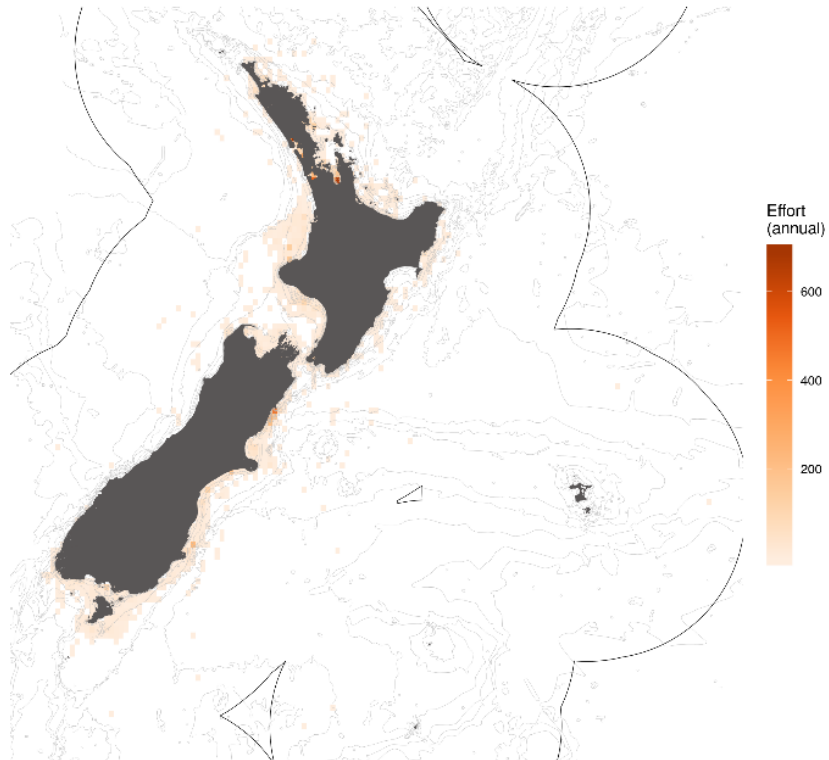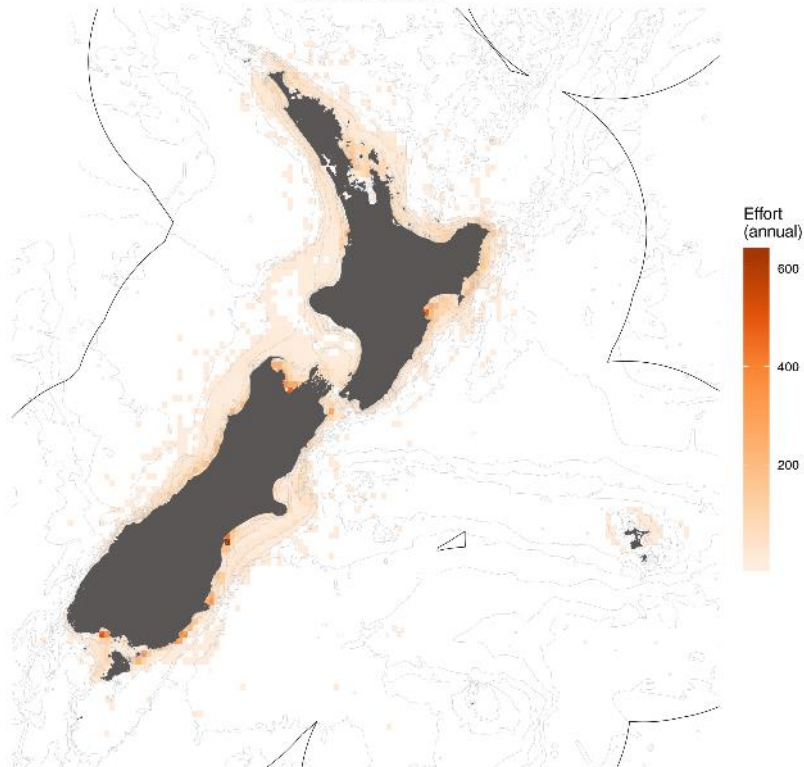
Figure A15-4: Total set net and inshore trawl fishing effort (observed and unobserved) in New Zealand from 2014/15 to 2016/17.
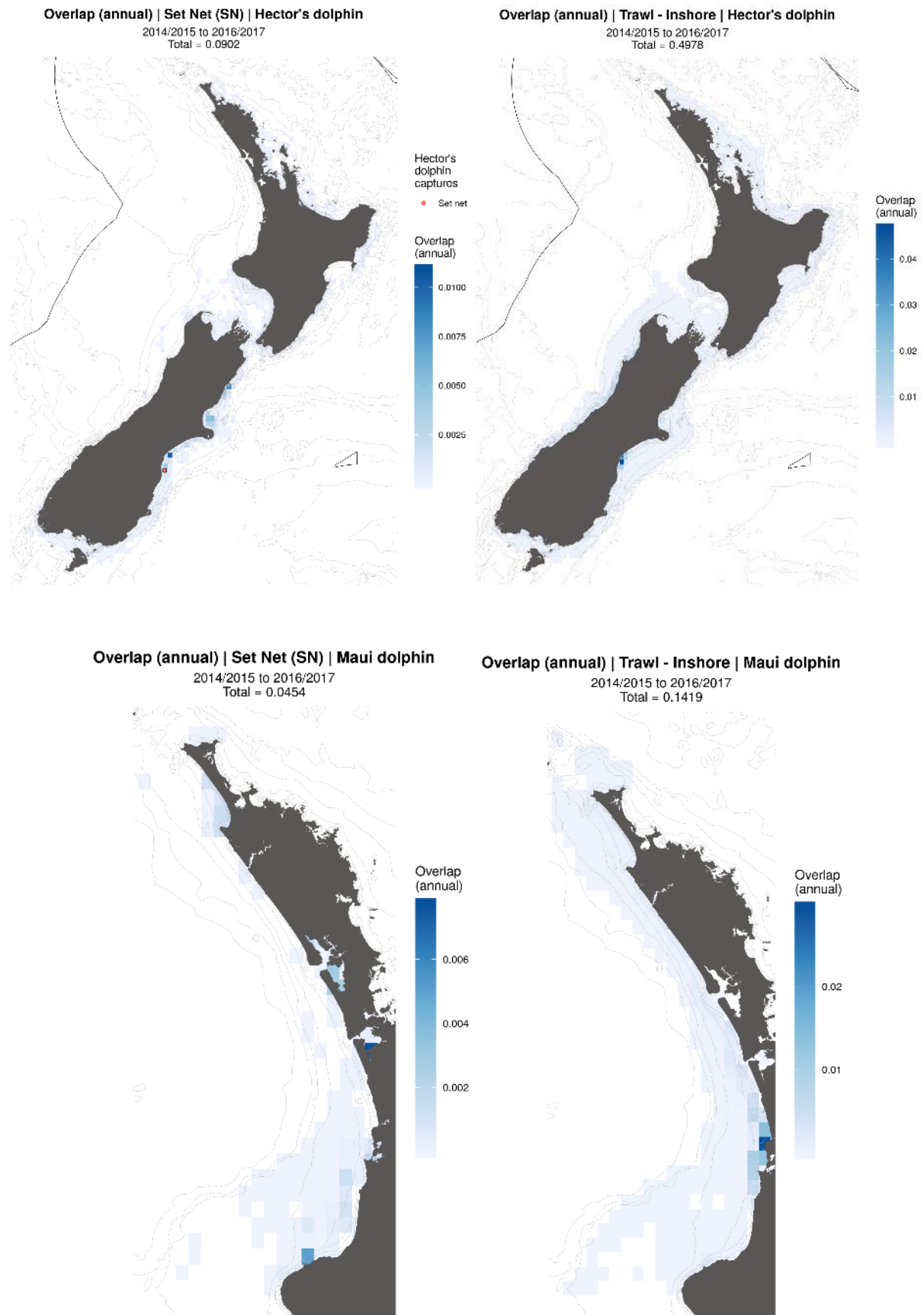
Figure A15-5: Total annual overlap (observed and unobserved) from 2014/15 to 2016/17. Observed Hector's dolphin captures in set nets between 2014/15 to 2016/17 are also shown as red points.

Estimated Deaths (annual) | Set Net (SN) | Hector's dolphin
2014/2015 to 2016/2017
Total = 44.4647
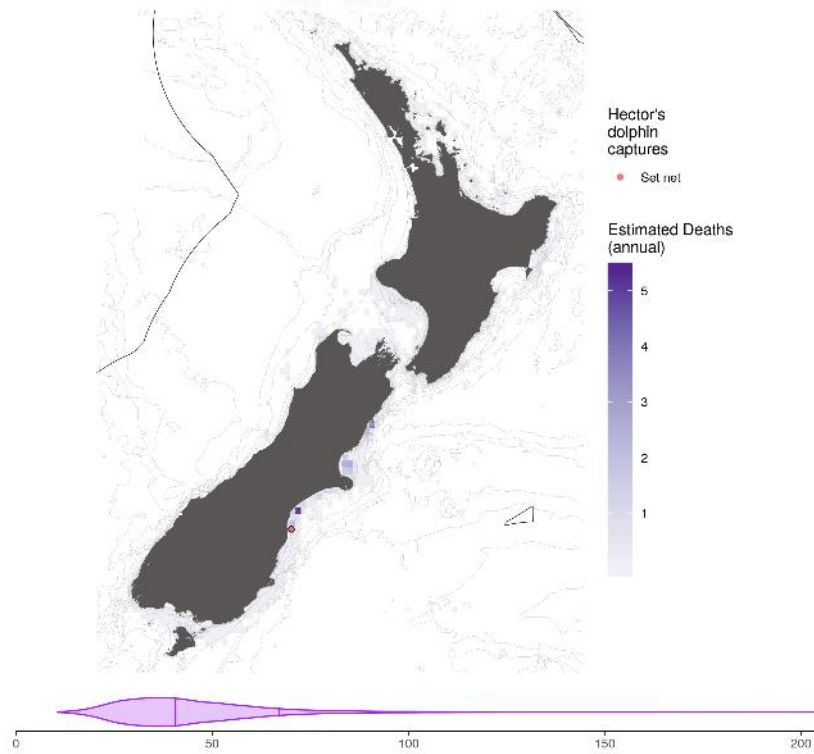
Estimated Deaths (annual) | Trawl - Inshore | Hector's dolphin
2014/2015 to 2016/2017
Total = 7.193
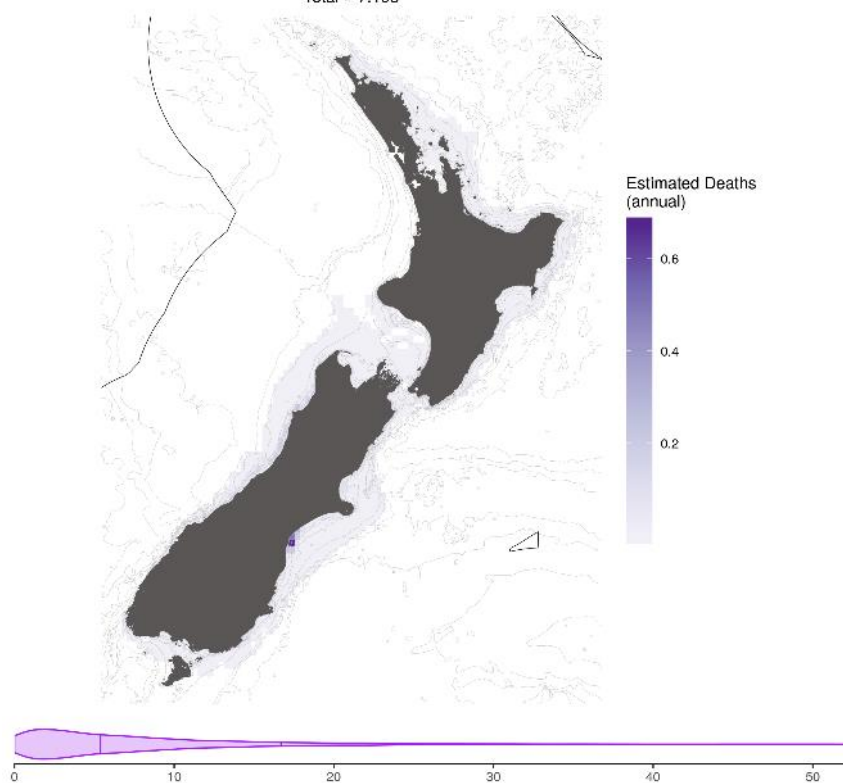
Figure A15-6: Total annual deaths (the mean from 2014/15 to 2016/17). Observed Hector's dolphin captures in set nets between 2014/15 and 2016/17 are also shown as red points. The posterior distribution of the number of deaths is also displayed as the violin along the bottom with the median and upper 90% quantile indicated by the vertical lines within the violin.

Estimated Deaths (annual) | Set Net (SN) | Maui dolphin
2014/2015 to 2016/2017
Total = 0.0957
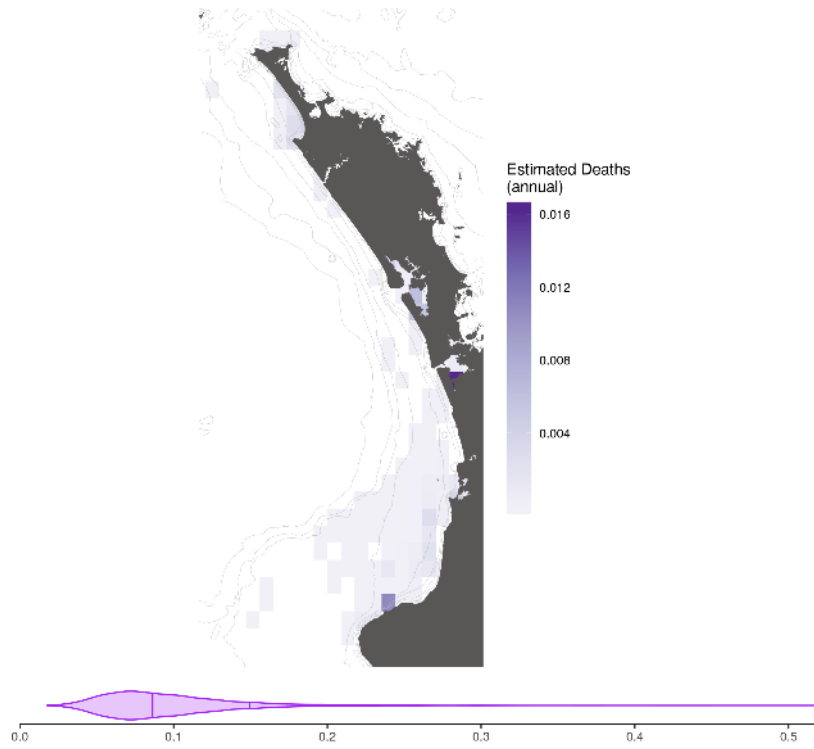
Estimated Deaths (annual) | Trawl - Inshore | Maui dolphin
2014/2015 to 2016/2017
Total = 0.0088
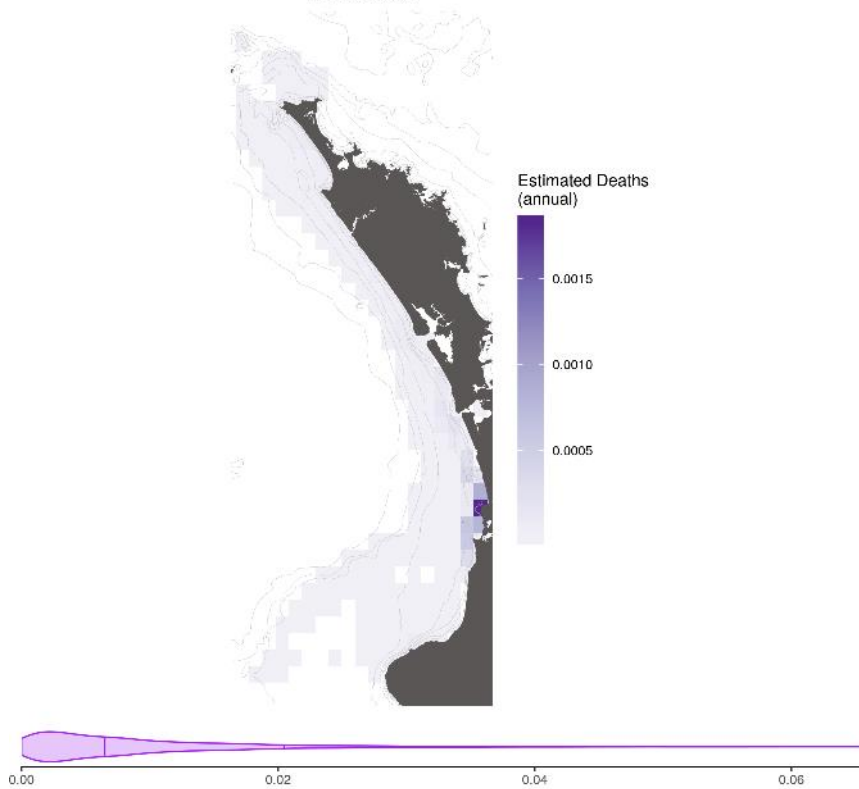
Figure A15-6 Continued.
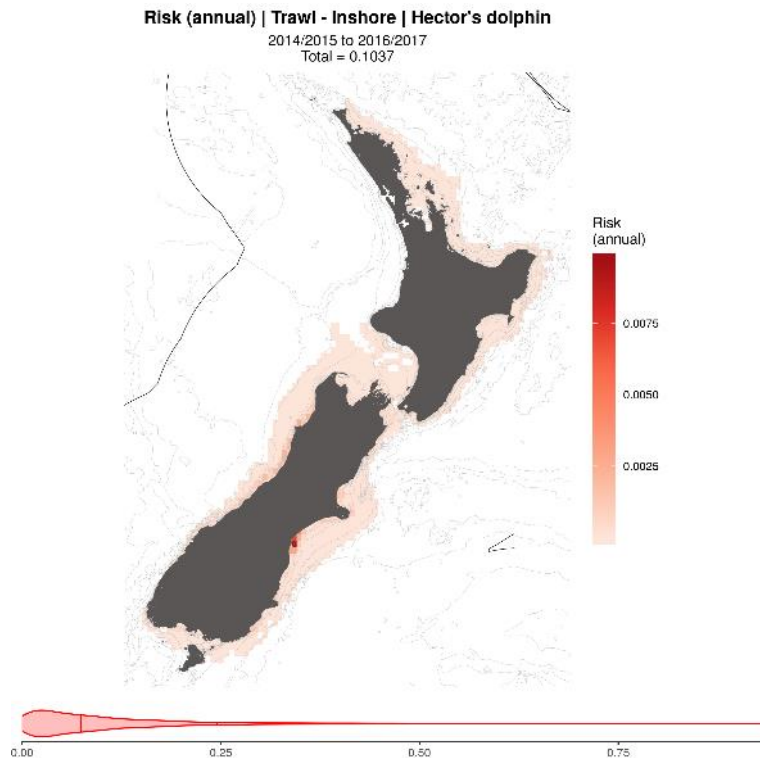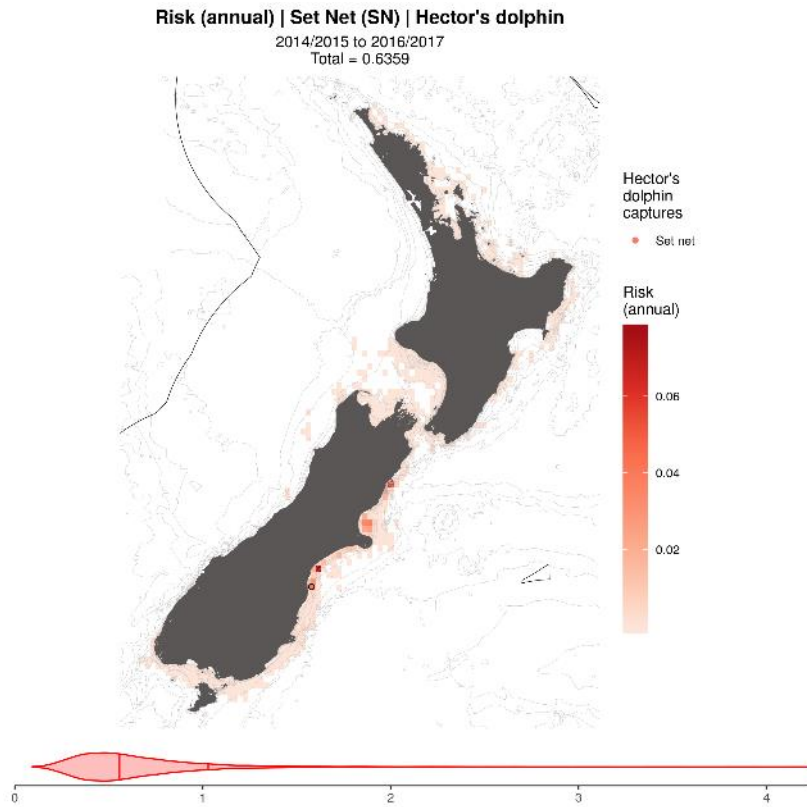
Figure A15-7: Total annual risk ratio (the mean from 2014/15 to 2016/17). Observed Hector's dolphin captures in set nets between 2014/15 and 2016/17 are also shown as red points. The posterior distribution of the risk ratio is also displayed as the violin along the bottom with the median and upper 90% quantile indicated by the vertical lines within the violin.

Risk (annual) | Set Net (SN) | Maui dolphin
2014/2015 to 2016/2017
Total = 0.3626
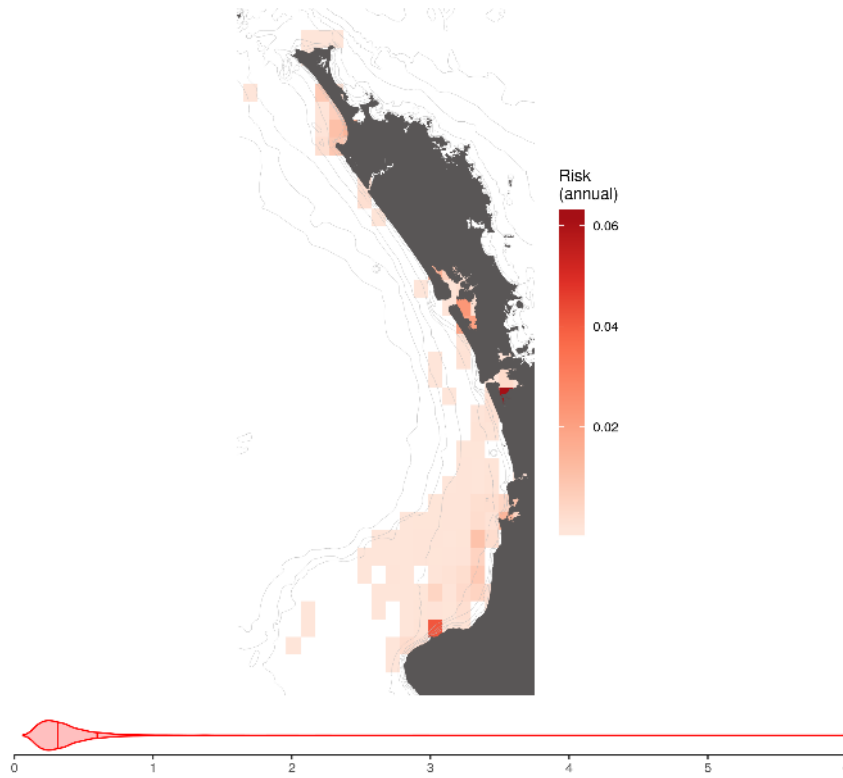
Risk (annual) | Trawl - Inshore | Maui dolphin
2014/2015 to 2016/2017
Total = 0.0336
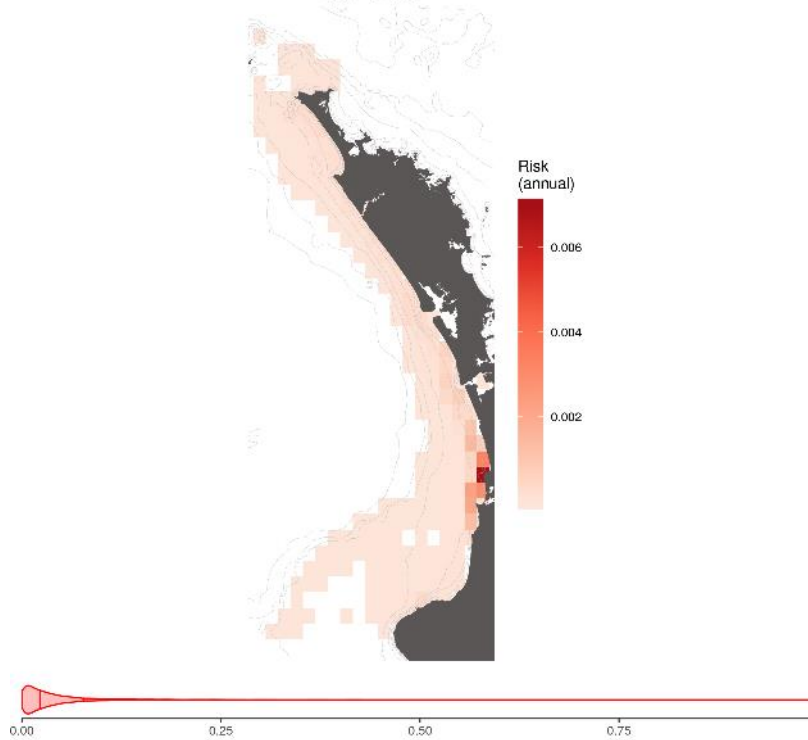
Figure A15-7: Continued
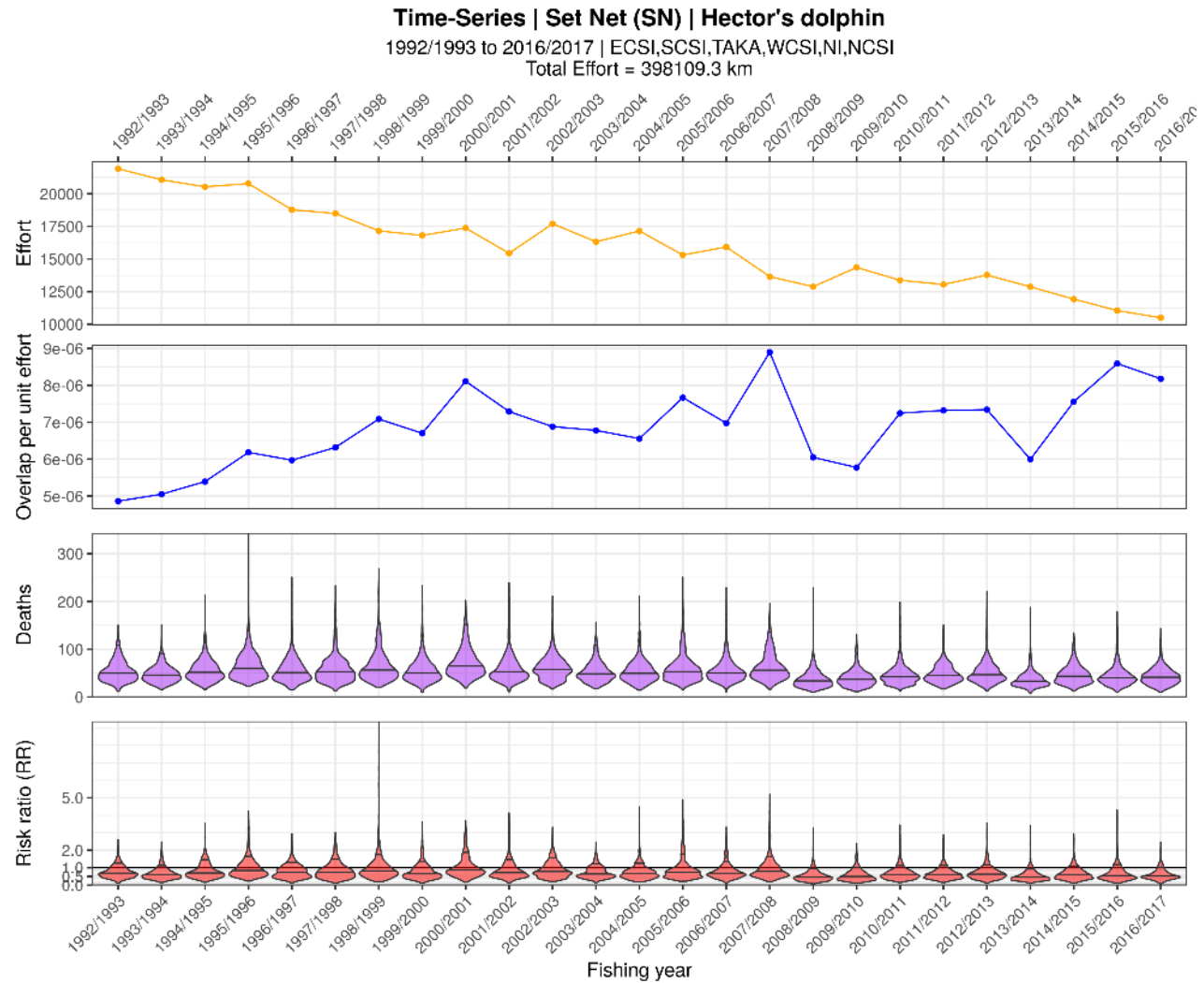
Figure A16-1: Commercial set net effort by fishing year (top) and spatial risk model outputs for Hector's dolphins also by fishing year: spatial overlap, annual deaths and risk ratio. This model run assumed a calibration coefficient (ϕ) of 0.2.
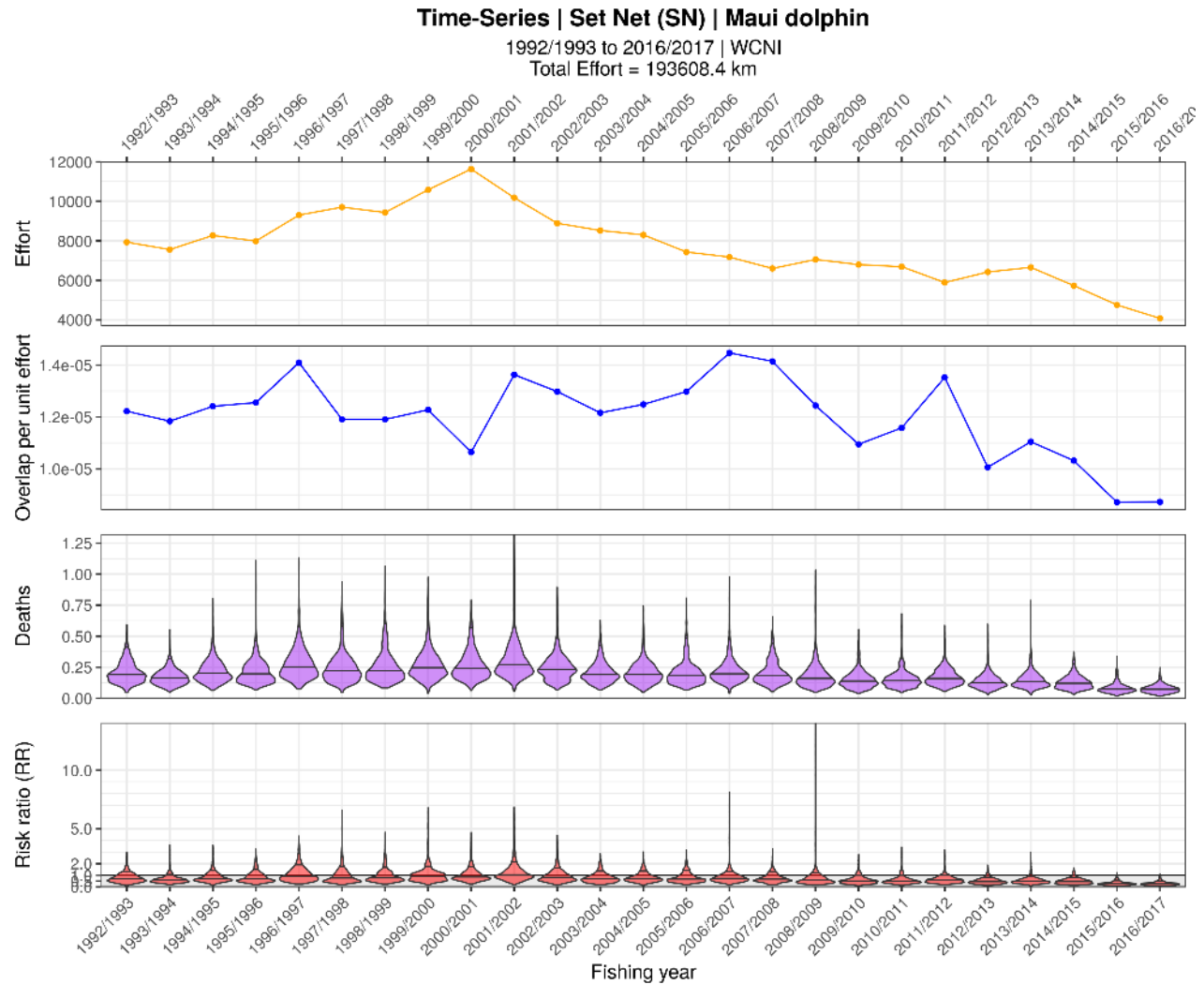
Figure A16-2: Commercial set net effort by fishing year (top) and spatial risk model outputs for Māui dolphins also by fishing year: spatial overlap, annual deaths and risk ratio. This model run assumed a calibration coefficient (ϕ) of 0.2.
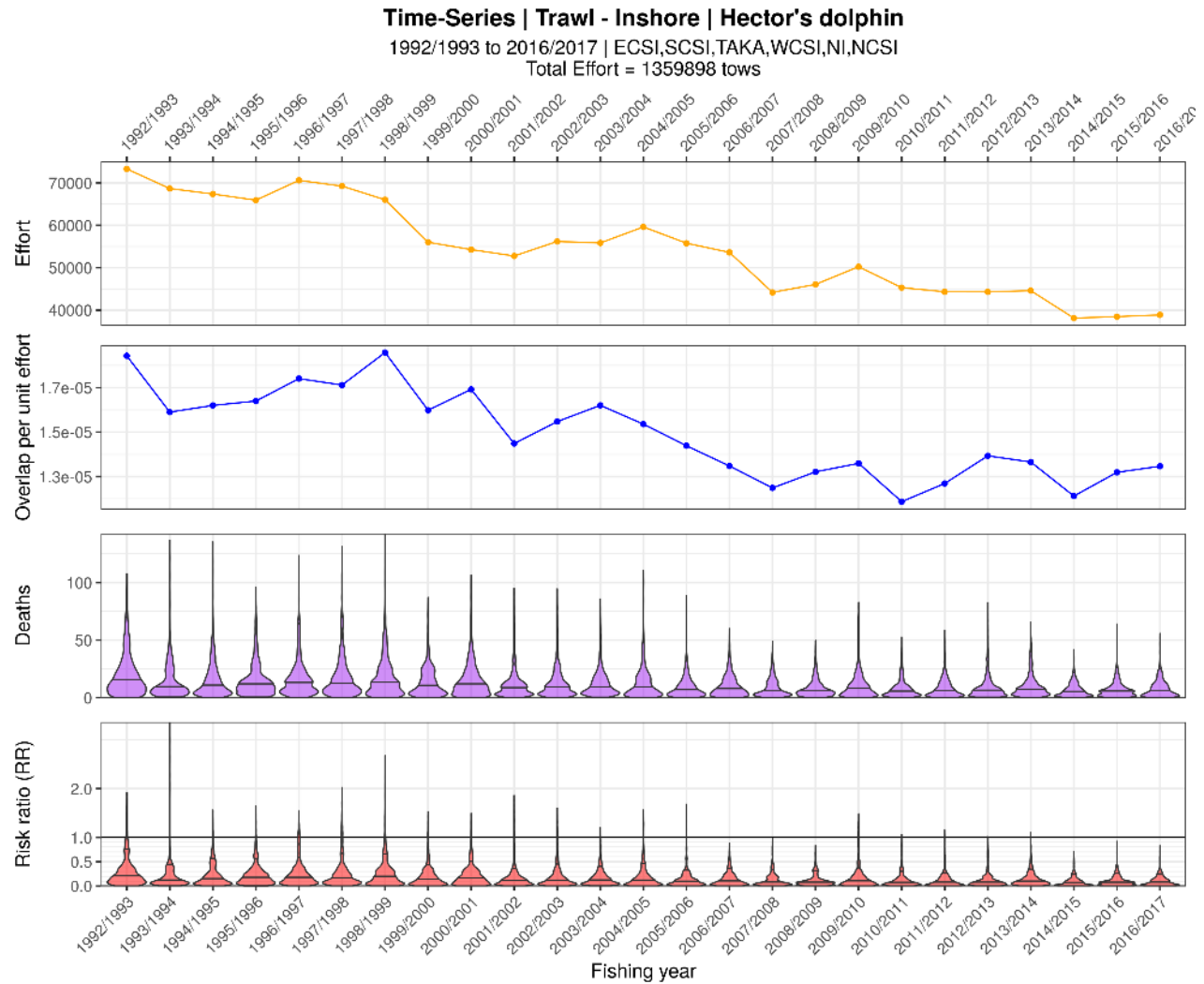
Figure A16-3: Inshore trawl effort by fishing year (top) and spatial risk model outputs for Hector's dolphins also by fishing year: spatial overlap, annual deaths and risk ratio. This model run assumed a calibration coefficient (ϕ) of 0.2.
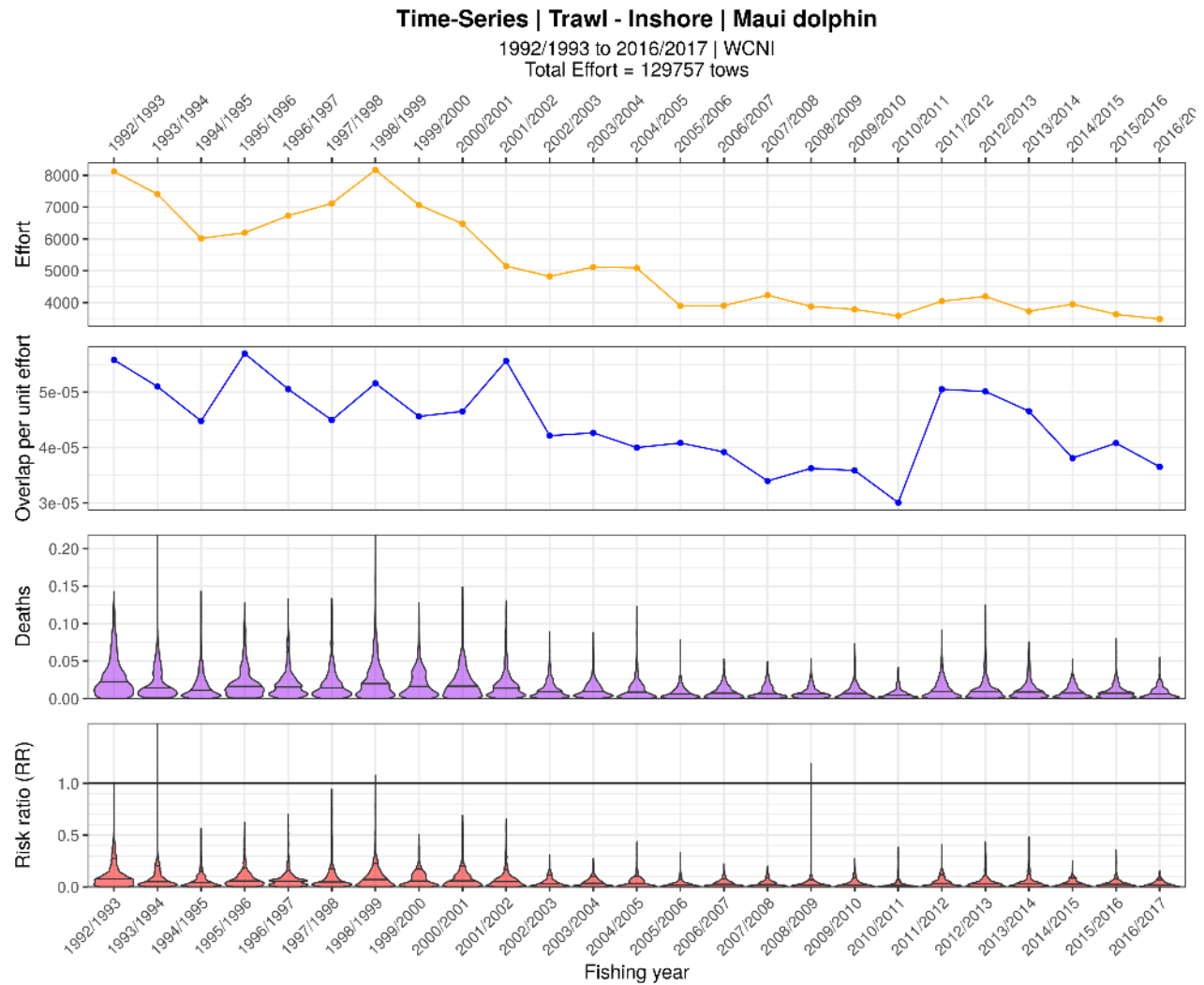
Figure A16-4: Inshore trawl effort by fishing year (top) and spatial risk model outputs for Māui dolphins also by fishing year: spatial overlap, annual deaths and risk ratio. This model run assumed a calibration coefficient (ϕ) of 0.2.

APPENDIX 17 – INSHORE TRAWL SENSITIVITY

Table 17-1: Sensitivity of risk model estimates of <u>annual deaths</u> by threat and sub-population to assuming that an average of two individuals were captured per positive inshore trawl fishing event. This affected a doubling of estimated annual deaths for inshore trawl fisheries, compared with estimates from models fitted to fisheries observer records (Table 15). This model run assumed a calibration coefficient (ϕ) of 0.2. The median and 95% credible intervals are shown for all estimates.

Cause of death	Sub-population	Deaths equal detection			Deaths predation sensitivity		
		50.0%	2.5%	97.5%	50.0%	2.5%	97.5%
Set net	MĀUI	0.10	0.00	0.30	0.10	0.00	0.30
Set net	NI	0.07	0.04	0.17	0.08	0.04	0.17
Set net	TAKA	0.06	0.03	0.13	0.06	0.03	0.13
Set net	NCSI	0.65	0.31	1.47	0.65	0.32	1.49
Set net	WCSI	0.32	0.15	0.74	0.33	0.16	0.75
Set net	ECSI	38.86	18.57	88.25	39.14	19.41	89.42
Set net	SCSI	0.80	0.38	1.81	0.80	0.40	1.84
Inshore trawl	MĀUI	0.00	0.00	0.10	0.00	0.00	0.10
Inshore trawl	NI	0.00	0.00	0.04	0.00	0.00	0.04
Inshore trawl	TAKA	0.00	0.00	0.00	0.00	0.00	0.00
Inshore trawl	NCSI	0.20	0.00	1.08	0.20	0.00	1.18
Inshore trawl	WCSI	3.68	0.16	18.80	3.54	0.14	20.58
Inshore trawl	ECSI	6.08	0.28	31.12	5.86	0.24	34.08
Inshore trawl	SCSI	0.22	0.00	1.12	0.22	0.00	1.24
Toxoplasmosis	MĀUI	1.90	0.96	3.27	1.11	0.44	2.31
Toxoplasmosis	NI	0.25	0.09	0.58	0.14	0.04	0.38
Toxoplasmosis	TAKA	0.40	0.15	0.93	0.23	0.07	0.61
Toxoplasmosis	NCSI	1.10	0.40	2.54	0.63	0.19	1.67
Toxoplasmosis	WCSI	187.03	67.86	432.09	106.80	32.69	284.43
Toxoplasmosis	ECSI	115.06	41.75	265.81	65.70	20.11	174.97
Toxoplasmosis	SCSI	5.05	1.83	11.67	2.88	0.88	7.68
Predation	MĀUI	0.53	0.11	1.42	3.04	1.05	5.27
Predation	NI	0.00	0.00	0.00	0.01	0.00	0.02
Predation	TAKA	0.03	0.01	0.11	0.19	0.05	0.44
Predation	NCSI	0.77	0.16	2.63	4.47	1.19	10.56
Predation	WCSI	62.64	12.72	214.41	363.62	97.13	859.84
Predation	ECSI	17.64	3.58	60.37	102.38	27.35	242.09
Predation	SCSI	2.63	0.53	9.00	15.26	4.08	36.08
Other	MĀUI	4.06	2.65	5.99	2.35	1.15	4.27
Other	NI	0.42	0.17	0.88	0.24	0.08	0.57
Other	TAKA	0.56	0.23	1.16	0.32	0.11	0.75
Other	NCSI	9.06	3.69	18.78	5.22	1.77	12.15
Other	WCSI	232.05	94.49	480.99	133.72	45.30	311.15
Other	ECSI	411.79	167.67	853.54	237.29	80.39	552.14
Other	SCSI	14.05	5.72	29.13	8.10	2.74	18.84

Table 17-2: Sensitivity of risk model estimates of <u>annual risk ratio</u> by threat and sub-population to assuming that an average of two individuals were captured per positive inshore trawl fishing event. This affected a doubling of estimated risk ratio for inshore trawl fisheries, compared with estimates from the model fitted to fisheries observer records (Table 16). This model run assumed a <u>calibration coefficient (φ) of 0.2</u>. The median and 95% credible intervals are shown for all estimates.

Cause of death	Sub-population	Risk ratio equal detection			Risk ratio predation sensitivity		
		50.0%	2.5%	97.5%	50.0%	2.5%	97.5%
Set net	MAUI	0.28	0.00	1.23	0.30	0.00	1.30
Set net	NI	1.61	0.68	4.23	1.63	0.72	4.57
Set net	TAKA	0.94	0.39	2.46	0.95	0.42	2.66
Set net	NCSI	0.65	0.27	1.72	0.66	0.29	1.85
Set net	WCSI	0.01	0.01	0.03	0.01	0.01	0.04
Set net	ECSI	0.86	0.36	2.27	0.87	0.39	2.45
Set net	SCSI	0.52	0.22	1.36	0.52	0.23	1.47
Inshore trawl	MAUI	0.00	0.00	0.60	0.00	0.00	0.58
Inshore trawl	NI	0.14	0.00	0.84	0.14	0.00	0.88
Inshore trawl	TAKA	0.02	0.00	0.10	0.02	0.00	0.10
Inshore trawl	NCSI	0.20	0.00	1.26	0.20	0.00	1.32
Inshore trawl	WCSI	0.14	0.00	0.86	0.14	0.00	0.90
Inshore trawl	ECSI	0.14	0.00	0.80	0.14	0.00	0.84
Inshore trawl	SCSI	0.14	0.00	0.86	0.14	0.00	0.90
Toxoplasmosis	MAUI	6.81	3.17	14.73	4.01	1.47	10.47
Toxoplasmosis	NI	5.38	1.87	14.21	3.14	0.91	9.41
Toxoplasmosis	TAKA	6.47	2.25	17.07	3.77	1.10	11.31
Toxoplasmosis	NCSI	1.10	0.38	2.90	0.64	0.19	1.92
Toxoplasmosis	WCSI	7.30	2.54	19.27	4.26	1.24	12.77
Toxoplasmosis	ECSI	2.53	0.88	6.68	1.48	0.43	4.43
Toxoplasmosis	SCSI	3.26	1.13	8.59	1.90	0.55	5.69

Table 17-3: Sensitivity of risk model estimates of <u>annual risk ratio</u> by threat and sub-population to assuming that an average of two individuals were captured per positive inshore trawl fishing event. This affected a doubling of estimated risk ratio for inshore trawl fisheries, compared with estimates from the model fitted to fisheries observer records (Table A14-4). This model run assumed a <u>calibration coefficient (φ) of 0.5</u>. The median and 95% credible intervals are shown for all estimates.

Cause of death	Sub-population	Risk ratio equal detection			Risk ratio predation sensitivity		
		50.0%	2.5%	97.5%	50.0%	2.5%	97.5%
Set net	MĀUI	0.12	0.00	0.50	0.12	0.00	0.50
Set net	NI	0.65	0.28	1.75	0.66	0.28	1.74
Set net	TAKA	0.38	0.16	1.02	0.38	0.16	1.01
Set net	NCSI	0.26	0.12	0.71	0.27	0.11	0.70
Set net	WCSI	0.01	0.00	0.01	0.01	0.00	0.01
Set net	ECSI	0.35	0.15	0.94	0.35	0.15	0.93
Set net	SCSI	0.21	0.09	0.56	0.21	0.09	0.56
Inshore trawl	MĀUI	0.00	0.00	0.24	0.00	0.00	0.24
Inshore trawl	NI	0.06	0.00	0.34	0.06	0.00	0.34
Inshore trawl	TAKA	0.00	0.00	0.04	0.00	0.00	0.04
Inshore trawl	NCSI	0.08	0.00	0.50	0.08	0.00	0.52
Inshore trawl	WCSI	0.06	0.00	0.34	0.06	0.00	0.34
Inshore trawl	ECSI	0.06	0.00	0.32	0.06	0.00	0.32
Inshore trawl	SCSI	0.06	0.00	0.34	0.06	0.00	0.34
Toxoplasmosis	MĀUI	2.74	1.23	5.98	1.56	0.59	4.09
Toxoplasmosis	NI	2.23	0.72	5.77	1.25	0.36	3.75
Toxoplasmosis	TAKA	2.68	0.87	6.93	1.51	0.44	4.51
Toxoplasmosis	NCSI	0.46	0.15	1.18	0.26	0.07	0.77
Toxoplasmosis	WCSI	3.03	0.98	7.83	1.70	0.49	5.09
Toxoplasmosis	ECSI	1.05	0.34	2.71	0.59	0.17	1.76
Toxoplasmosis	SCSI	1.35	0.44	3.49	0.76	0.22	2.27

APPENDIX 18 – SEFRA MODEL CODE

```
/**
 * Hector's/Maui dolphin spatially explicit fisheries risk assessment (SEFRA) model
 *
 * Darcy Webber
 * darcy@quantifish.co.nz
 *
 * December 2018
**/

data {

  // Dimensions
  int<lower=1> n_species;
  int<lower=1,upper=n_species> n_species_group;
  int<lower=1> n_method;
  int<lower=n_method> n_fishery_group;
  real<lower=1> n_years;

  // Which method each fishery group belongs to
  int<lower=1,upper=n_method> method_g[n_fishery_group];

  // Observed fishing events and observed captures (sum over 1 or more years)
  int<lower=1> n_i;
  int<lower=1,upper=n_species> species_i[n_i];
  int<lower=1,upper=n_species_group> species_group_i[n_i];
  int<lower=1,upper=n_method> method_i[n_i];
  int<lower=1,upper=n_fishery_group> fishery_group_i[n_i];
  vector<lower=0>[n_i] overlap_i;
  int<lower=0> live_captures_i[n_i];
  int<lower=0> dead_captures_i[n_i];

  // All fishing events (this includes observed and unobserved events and is the
mean over n_years)
  int<lower=1> n_j;
  int<lower=1,upper=n_species> species_j[n_j];
  int<lower=1,upper=n_species_group> species_group_j[n_j];
  int<lower=1,upper=n_method> method_j[n_j];
  int<lower=1,upper=n_fishery_group> fishery_group_j[n_j];
  vector<lower=0>[n_j] overlap_j;

  // Necropsies - there are l individuals that had necropsies and these were
assigned to 1,...,k categories
  int<lower=1> n_necropsy;
  int<lower=1> n_k;
  int<lower=1,upper=n_necropsy> necropsy_l[n_k];
  vector[n_necropsy] p_detection_k;

  // Priors for demographic parameters
  vector[n_species] mu_n_s;
  vector<lower=0>[n_species] sd_n_s;
  vector[n_species] mu_rmax;
  vector<lower=0>[n_species] sd_rmax;
  vector[n_species] mu_scurr_s;
  vector<lower=0>[n_species] sd_scurr_s;

  // PST calculation management target
  real<lower=0,upper=1> psi;

} // end of data
```

```
parameters {

  vector[n_fishery_group] log_v_g;
  vector<lower=0,upper=1>[n_method] p_live_capture;
  real<lower=0,upper=1> p_observable_sn;
  vector<lower=0.5,upper=1>[n_method-1] p_observable_other;
  vector<lower=0>[n_species] n_adults_s;
  simplex[n_necropsy] p_necropsy_k;

} // end of parameters

transformed parameters {

  vector[n_fishery_group] vulnerability_g;
  vector[n_method] p_observable;
  vector[n_i] mu_live_captures_i;
  vector[n_i] mu_dead_captures_i;

  for (g in 1:n_fishery_group) {
    vulnerability_g[g] = exp(log_v_g[g]);
  }
  p_observable = append_row(p_observable_sn, p_observable_other);

  for (i in 1:n_i) {
    real mu_captures = vulnerability_g[fishery_group_i[i]] *
p_observable[method_i[i]] * overlap_i[i] * n_adults_s[species_i[i]];
    mu_live_captures_i[i] = mu_captures * p_live_capture[method_i[i]];
    mu_dead_captures_i[i] = mu_captures * (1.0 - p_live_capture[method_i[i]]);
  }

} // end of transformed parameters

model {

  // Prior
  log_v_g ~ normal(0.0, 10.0);
  p_live_capture ~ beta(1.0, 3.0);
  p_observable_sn ~ beta(6.915929, 6.915929);
  for (s in 1:n_species) {
    n_adults_s[s] ~ lognormal(mu_n_s[s], sd_n_s[s]);
  }
  p_necropsy_k ~ dirichlet(rep_vector(1.0, n_necropsy));

  // Likelihood
  live_captures_i ~ poisson(mu_live_captures_i);
  dead_captures_i ~ poisson(mu_dead_captures_i);
  necropsy_l ~ categorical(p_necropsy_k);

} // end of model

generated quantities {

  // Outputs for observed and unobserved effort
  vector[n_j] mu_captures_j;
  vector[n_j] mu_deaths_j;
  vector[n_j] mu_risk_j;
  vector[n_j] captures_j;
  vector[n_j] deaths_j;

  // Prior and Posterior predictive checking
  vector[n_fishery_group] prior_log_v_g;
  vector[n_method] prior_p_live_capture;
  vector[n_method] prior_p_survive_capture;
  vector[n_method] prior_p_observable;
  vector[n_species] prior_n_adults_s;
  simplex[n_necropsy] prior_p_necropsy_k;
  vector[n_i] pred_live_captures_i;
  vector[n_i] pred_dead_captures_i;
```

```
  // Captures
  vector[n_species] captures_s;
  matrix[n_species,n_fishery_group] captures_sg;

  // Deaths
  vector[n_species] deaths_s; // Fishery related deaths
  matrix[n_species,n_fishery_group] deaths_sg; // Fishery related deaths
  vector[n_species] total_deaths_s; // Fishery and non-fishery related deaths
  vector[n_necropsy] non_fishery_deaths_sk[n_species]; // Non fishery related
deaths
  vector[n_necropsy] non_fishery_risk_sk[n_species]; // Non fishery related risk

  // Mortality check
  vector[n_species] mortality_in_bounds_s;

  // Outputs for Risk Atlas
  matrix[n_species,n_fishery_group] vulnerability_sg;
  matrix[n_species,n_fishery_group] p_observable_sg;
  matrix[n_species,n_fishery_group] p_live_capture_sg;
  matrix[n_species,n_fishery_group] p_survive_capture_sg;

  // rmax, PST, risk ratio
  simplex[n_necropsy] p_non_fishery_k;
  vector<lower=0,upper=1>[n_method] p_survive_capture;
  vector<lower=0,upper=1>[n_species] rmax_s;
  vector<lower=0,upper=1>[n_species] adult_survival_s;
  vector[n_species] pst_s;
  vector[n_species] risk_ratio_s;
  matrix[n_species,n_fishery_group] risk_ratio_sg;

  // Prior checking and simulated parameters
  for (m in 1:n_method) {
    prior_log_v_g[m] = normal_rng(0.0, sigma_v);
    prior_p_live_capture[m] = beta_rng(1.0, 3.0);
    prior_p_survive_capture[m] = uniform_rng(0.5, 0.9);
    p_survive_capture[m] = prior_p_survive_capture[m];
  }
  prior_p_observable[1] = beta_rng(6.915929, 6.915929);
  prior_p_observable[2] = uniform_rng(0.5, 1.0);
  for (s in 1:n_species) {
    prior_n_adults_s[s] = lognormal_rng(mu_n_s[s], sd_n_s[s]);
    rmax_s[s] = normal_rng(mu_rmax[s], sd_rmax[s]);
    adult_survival_s[s] = beta_rng(mu_scurr_s[s], sd_scurr_s[s]);
    pst_s[s] = 0.5 * psi * rmax_s[s] * n_adults_s[s];
  }
  prior_p_necropsy_k = dirichlet_rng(rep_vector(1.0, n_necropsy));

  // Posterior predictive checking
  for (i in 1:n_i) {
    pred_live_captures_i[i] = poisson_rng(mu_live_captures_i[i]);
    pred_dead_captures_i[i] = poisson_rng(mu_dead_captures_i[i]);
  }

  // Captures and deaths prediction
  for (g in 1:n_fishery_group) {
    for (s in 1:n_species) {
      captures_sg[s,g] = 0.0;
      deaths_sg[s,g] = 0.0;
    }
  }

  for (j in 1:n_j) {
    int sj = species_j[j];
    int mj = method_j[j];
    int gj = fishery_group_j[j];
```

```
    mu_captures_j[j] = vulnerability_g[gj] * p_observable[mj] * overlap_j[j] *
n_adults_s[sj];
    mu_deaths_j[j] = vulnerability_g[gj] * (1.0 - p_live_capture[mj] *
p_survive_capture[mj]) * overlap_j[j] * n_adults_s[sj];
    mu_risk_j[j] = mu_deaths_j[j] / pst_s[sj];
    captures_j[j] = poisson_rng(n_years * mu_captures_j[j]) / n_years;
    deaths_j[j] = poisson_rng(n_years * mu_deaths_j[j]) / n_years;
    captures_sg[sj,gj] += captures_j[j];
    deaths_sg[sj,gj] += deaths_j[j];
  }

  // Outputs as matrices by species and fishery group for Risk Atlas
  for (s in 1:n_species) {
    for (g in 1:n_fishery_group) {
      vulnerability_sg[s,g] = vulnerability_g[g];
      p_observable_sg[s,g] = p_observable[method_g[g]];
      p_live_capture_sg[s,g] = p_live_capture[method_g[g]];
      p_survive_capture_sg[s,g] = p_survive_capture[method_g[g]];
    }
  }

  // PST and risk ratio by population, species, and fishery group
  for (k in 1:n_necropsy) {
    p_non_fishery_k[k] = p_necropsy_k[k] * p_detection_k[k] / sum(p_necropsy_k .*
p_detection_k);
  }
  for (s in 1:n_species) {
    captures_s[s] = sum(captures_sg[s]);
    deaths_s[s] = sum(deaths_sg[s]);
    risk_ratio_s[s] = deaths_s[s] / pst_s[s];
    for (g in 1:n_fishery_group) {
      risk_ratio_sg[s,g] = deaths_sg[s,g] / pst_s[s];
    }
    total_deaths_s[s] = (1.0 - adult_survival_s[s]) * n_adults_s[s];
    mortality_in_bounds_s[s] = deaths_s[s] >= total_deaths_s[s] ? 0 : 1; // Check
mortality constraint
    non_fishery_deaths_sk[s] = (total_deaths_s[s] - deaths_s[s]) * p_non_fishery_k;
    non_fishery_risk_sk[s] = non_fishery_deaths_sk[s] / pst_s[s];
  }

} // end of generated quantities
```